EXCHANGE AND HYDROGENOLYSIS REACTIONS OF HYDROCARBONS ON RHODIUM - TITANIA AND PLATINUM - IRIDIUM - ALUMINA CATALYSTS

ARNALDO DA COSTA FARO, JR.

PHD THESIS

UNIVERSITY OF EDINBURGH

1984

VOLUME 1

PART I : INTRODUCTORY CHAPTERS

PART II: THEORETICAL AND DEUTERIUM N.M.R STUDY OF CYCLOPENTANE EXCHANGE WITH DEUTERIUM ON METAL CATALYST

ABSTRACT

A Monte Carlo method was developed which allows the calculation of theoretical cyclopentane exchange patterns for a mechanism involving interconversion between monoadsorbed and α,β-diadsorbed cyclopentane combined with rollover or α,α-diadsorption processes. Theoretical patterns were compared with experimental results for cyclopentane exchange on Rh, Ir, Pt, Pd and Ni catalysts. It was concluded that several parallel exchange processes have to be invoked in order to explain the experimental patterns. Samples obtained from exchange experiments on supported Rh, Ir and Pt catalysts were examined by deuterium-n.m.r. spectroscopy. Several resonances were observed in the spectra and the corresponding frequencies were interpreted in terms of isotopic shifts associated with deuterium atoms in different positions in the molecule. The values of the isotopic shifts were found to be α = -18 p.p.b., β_C = - 6 p.p.b., β_T = -9 p.p.b., γ_C = -3 p.p.b., γ_T = 0 p.p.b. (C = cis, T = trans). Special attention was given to the elucidation of the nature of the large d_2 component frequently found in cyclopentane exchange on Rh. It was concluded that the d_2 componente arises largely from cyclopentane - 1,2 - d_2.

A 0.6 wt % Rh/TiO_2 catalyst was prepared and characterized by pulse chemisorption/titration techniques. After reduction at 473 K (LTR treatment) the catalyst showed normal chemisorptive behaviour but after reduction at 773 K (HTR treatment) its chemisorption capacity was suppressed indicating that a strong metal-support interaction (SMSI) was induced by HTR. The activity of the catalyst after both LTR and HTR was measured for a number of reactions such as methane and cyclopentane exchange,neopentane hydrogenolysis and methylcyclopentane (MCP) reactions and compared to that of a 3 wt % Rh/SiO_2 catalyst subjected to the same pretreatments. Suppression

of activity after HTR was only found with Rh/TiO_2. Different reactions displayed different sensitivities to the SMSI effect, decreasing in the order: neopentane hydrogenolysis > cyclopentane exchange > MCP multiple hydrogenolysis > methane exchange ~ MCP ring-opening ~ MCP aromatization ~ MCP demethanation > MCP dehydrogenation. The results were discussed in terms of electronic, ensemble and structural effects and it was concluded that an ensemble effect correlates a greater number of results.

A series of Pt-Ir catalysts containing 0,5 wt % of metal supported on γ - Al_2O_3 was characterized by temperature-programmed reduction (TPR) and related techniques. The effect of pretreatments such as calcination at 523 K and 773 K was examined. The catalysts showed a high dispersion and gave evidence of having a single metallic phase although phase separation occurred on calcination at 773 K. In all cases two peaks were found during TPR: the first with a maximum at ca. 400 K was attributed to reduction of the metallic phase and the second, which was centred at 650-700 K was thought to result from reduction of hydroxyl groups on the surface of the support.

The exchange reactions of neopentane and benzene with D_2 and neopentane and MCP hydrogenolysis were examined on the series of Pt - Ir catalysts. Isobutane, isopentane and n-hexane hydrogenolysis were examined on the monometallic catalysts. The results suggested that Pt and Ir interact in the bimetallic catalysts and that little, if any, surface enrichment in Pt is likely to have occurred. The activity patterns observed with neopentane in the 480 K to 520 K temperature range are consistent with a model wereby 3-5 atom ensembles participate in the reaction and mixed Pt - Ir ensembles have an activity intermediate between those of pure Pt and pure Ir ensembles. Evidence was presented that cleavage of disecondary bonds involves intermediates different from

the ones involved in neopentane hydrogenolysis under the experimental conditions selected (ca. 480 K, 5-10 kPa total pressure, ca. 10:1 hydrogen to hydrocarbon).

I certify that, unless otherwise stated, all the work described in this thesis was performed by myself at the laboratories of the University of Edinburgh in the period from septempter 1979 to April 1982.

Arnaldo da Costa Faro Junior

Lectures attended in the period of September 1979 to April 1982:

Undergratuate lectures:

- Chemical Reactor Design
- Catalysis and its Uses
- Chemistry of the Solid State
- Physical Methods for Adsorption Studies

Postgraduate lectures:

- Aspects of Industrial Inorganic Chemistry
- Zeolites
- Mass Spectrometry
- Computers in Chemistry
- Chemical Applications of Synchrotron Radiation
- Lasers in Chemistry
- Meetings of the E.U. Catalytic Club

ACKNOWLEDGEMENTS

I would like to express my heartfelt thanks:

To Professor Charles Kemball for his erudite guidance, enlightening suggestions and constant encouragement.

To Petrōleo Brasileiro S.A. - PETROBRĀS who provided me with financial support for carrying-out this project.

To the many friends and colleagues at Edinburgh University who helped to make my stay in Edinburgh a pleasant and successful event and specially: to mr.Ronald Brown an invaluable hand whenever things needed to be built or to be fixed and to whom the synthesis of cyclopentane-1,1-d_2 is to be credited; to mr. John Broom, a true artist in the craft of glassblowing; to dr.Maureen E.Cooper, responsible for the design and construction of the TPR apparatus, for her valuable suggestions and help in performing TPR experiments; to dr. Ian H.Sadler for obtaining the deuterium-n.m.r. data and for many helpful suggestions on the interpretation of the results; to mr.Ian H.B.Haining who introduced me to the secrets of performing the catalytic experiments; to dr.Duncan Taylor for much practical advice during the course of this project; to dr. David A.Whan for all the help and assistance throughout my stay in Edinburgh.

To dr. Leonardo Nogueira from PETROBRĀS whose contribution to this project cannot be expressed in few words. A true friend and definitely someone to have at your side in a fight.

And last, but by no means least, to Maria Luisa, my wife, for her moral support, unselfishness and understanding, without which very little would have been achieved.

TO MARIA LUIZA, MARIA CLÁUDIA,
MARIA CECÍLIA AND EDUARDO

CONTENTS

VOLUME 1

CHAPTER 1

GENERAL INTRODUCTION

CHAPTER 1

GENERAL INTRODUCTION

1.1 - HYSTORICAL BACKGROUND[1,2]

Reactions which are today classed as catalytic have been known for many centuries. The production of alcoholic beverages and vinegar by fermentation processes, a typical case of a technological application of enzymatic catalysis, has its origins lost in the beginnings of civilization itself. The first man-made catalyst was put into use during the Dark Ages in the well known preparation of ethyl ether from ethanol with sulfuric acid as the catalyst.

It was not until the beginning of the 19th century, however, after work done in the previous century had lifted chemistry to the status of an exact science, that the first scientific observations of catalytic phenomena began to appear. Thus, Kirchhof (1812) reported on the hydrolysis of starch catalysed by dilute acids; Thénard (1818), on the decomposition of H_2O_2 in the presence of Mn, Au, Ag, Pt and fibrin; Davy (1820) on the Pt catalysed oxidation of ethanol; Döbereiner (1822), on hydrogen - oxygen combination on Pt sponge; Dulong and Thénard (1823), on the same reaction on Au, Ag and glass; Mitscherlich (1834) on the acid catalysed dehyration of ethanol; etc...

That was a very important and active period in the history of chemistry, when the fundamental laws of chemical combinations became clearly established in the minds of chemists and the atomic theory gained acceptance through the works of Dalton. This same period saw the emergence of electrochemistry and the consequent ideas about "electrochemical affinities" as an explanation for chemical reactivity and compound formation[3].

Catalytic reactions defied the concepts that were just being laid out, since they seemed to be brought about

by the mere presence of small amounts of certain substances which remained unchanged in the reacting system. It is to be credited to Jöns Jacob Berzelius to have grouped the widely scattered results in the literature under a common concept. Berzelius (1836) ascribed the action of bodies which induce in other bodies "decompositions of their elements and different recombinations of these same elements to which they themselves remain indifferent" to a "new force ... common to organic and inorganic nature" and called this force catalytic force and catalysis "the decomposition of bodies by this force in the same way that one calls by the name analysis the decomposition of bodies by chemical affinity" (after a translation given by Falk [1]).

The succeeding 60 years saw the discovery of a great number of new catalytic systems and the appearance of a variety of theories attempting to explain the mechanism of catalytic action. Catalysis, however, had to wait for the development of chemical thermodynamics and chemical kinetics during this period, before its essentially modern definition was given by Ostwald in 1894. Ostwald defined catalysis as the "acceleration of a slowly proceeding reaction by the presence of a foreign body" and catalyst as "a substance which, without appearing in the end products modifies its velocity". Ostwald also recognized that "the general energy relationships are not changed by the presence of a catalyst and, therefore, as in all natural transformations, the changes occur in the direction of decreasing the free-energy of the whole system" (after a translation given by Falk[1]).

The early mechanistic theories about catalysis can be divided in two broad groups: the ones that regarded catalysis as consisting merely of physical phenomena and those which invoked the formation of unstable intermediates during the course of the reaction.

The theory of intermediate compound formation can be

traced to the period before Berzelius definition, when Clement and Desormes (1806) proposed the intermediacy of nitrogen oxides as oxygen carriers in the lead chamber process for sulfuric acid manufacture. In many instances the intermediate could be directly observed, as in the dehydration of ethanol catalysed by sulfuric acid, where Williamson (1854) proved ethyl-sulfuric acid to be an intermediate. Also in heterogeneous systems, the formation of intermediate compounds could be sometimes unequivocally proposed, e.g. in the production of acetone from acetic acid over barium carbonate, with barium acetate as an intermediate, or in the disproportionation of carbon monoxide over Ni, where Ni carbonyls were identified as intermediates[4]. In other cases, however, intermediates could only be postulated without direct experimental evidence.

Many investigators did not believe that a direct combination between reactants and catalyst had to take place for catalytic action to occur. Nernst (1904) thought that the surface of a solid catalyst was covered by a condensed layer of appreciable thickness where chemical reactions were supposed to occur extremely rapidly, so that the observed rates of reaction were regulated by diffusion through this layer, an idea also supported by Bodenstein. The porous state of a solid catalyst was considered by Duclaux (1911) to be a sufficient condition for catalysis, because of the high compression and heating achieved inside the cavities of porous catalysts. These theories failed to account for the selective properties of catalysts and for the fact that very good adsorbents, such as charcoal, were catalytically inert, as pointed out by Sabatier[4].

Theories derived from the intermediate compound concept received strong support from the work of Irving Langmuir in the field of chemisorption[5,6].

Langmuir's pioneering work demonstrated that solids are capable of displaying two different kinds of adsorption, one occurring at temperatures in the vicinity of the boiling point of the adsorbate, easily reversible by evacuation and general to all solids, and the other occurring at higher temperatures, not easily reversible by evacuation and characteristic of only certain combinations of gases and solids[4]. This led Langmuir to suggest that the forces involved in the second type of adsorption were of the same nature as those occurring between atoms in typical chemical compounds. Langmuir regarded the surface of solids as a two dimensional array of atoms (checker-board concept) where adsorption could occur on definite points. Applying this concept, Langmuir was able to derive adsorption isotherms for a variety of cases, including simple chemisorption, dissociative chemisorption, competetive chemisorption and chemisorption on heterogeneous surfaces[4]. He then applied these isotherms to the investigation of the kinetics of reactions such as the oxidation of carbon monoxide and hydrogen - oxygen combination on Pt[5], thus inaugurating a new era in mechanistic studies of heterogeneous catalysis and promoting the unification of the adsorption and intermediate compound theories of heterogeneous catalysis.

1.2 - DEFINITION AND CONSEQUENCES

For a substance to be classed as a catalyst for a given reaction the following requirements must be met:

1 - Small amounts of the substance, as compared to the amount of reactants in the system, must be able to increase the rate of reaction relative to the rate of the uncatalysed reaction.

2 - The substance must not be consumed in the reaction.

3 - The final equilibrium state of the reaction must be unaltered by the presence of the catalyst. This is

actually a consequence of the two former requirements, imposed by the laws of thermodynamics.

From these requirements, the following definition of a catalyst has been given[7]:

"A catalyst is a substance which increases the rate at which a chemical reaction approaches equilibrium without being consumed in the process".

An important implication of this definition is that a catalyst can only be effective for a reaction that is thermodinamically feasible and any efforts to bring about a thermodinamically forbidden reaction by means of catalysis are bound to be fruitless. Another consequence, imposed by the principle of microscopic reversibility, is that if a substance catalyses a given reversible reaction in one direction it will also be a catalyst for the same reaction in the reverse direction.

1.3 - SOME BASIC CONCEPTS AND DEFINITIONS[8]

The ability of a catalyst to convert the reactants into products is called the activity of the catalyst. Activity may be expressed in a number of ways, such as the amount of reactant converted per unit time per unit amount of catalyst under a given set of experimental conditions. When activity is expressed in this way it is normally referred to as the specific activity of the catalyst. When solids are used as catalysts, activity is not generally associated with the whole surface of the solid, but is concentrated on certain points or regions of the surface called active sites or active centres[9]. If the concentration of active sites is known, activity may be expressed as a turnover frequency, meaning the number of molecules converted per unit time per active site.Activity may also be expressed as the temperature necessary to attain a given rate of reaction: the lower the temperature required to achieve the specified rate of conversion, the higher is the activity of the catalyst.

In general, at any set of reaction conditions, there are a number of thermodinamically possible reaction pathways for the reactants. It is a very important aspect of catalysis that different catalysts display widely different tendencies to select among the several possible pathways. This property is called the selectivity of the catalyst. Scheme 1.1 illustrates several of the products that may be obtained from ethanol using different catalysts[10].

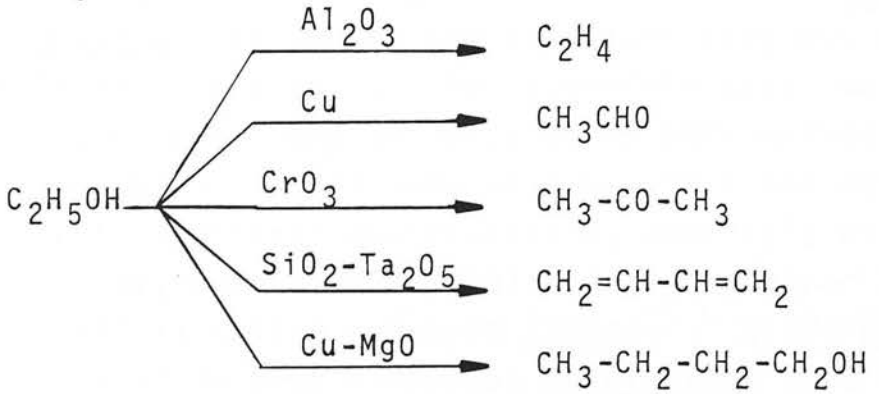

SCHEME 1.1

The term selectivity is also used to denote the ability of the catalyst to convert preferentially one of the components of a reaction mixture. For example, Pd catalysts have been found useful in the selective hydrogenation of dienes or acetylenes in an olefin stream[11].

A third type of selectivity refers to the ability of a catalyst to stop a sequence of consecutive reactions at the reaction stage which gives the desired product. Following Wheeler[12], the three types of selectivity may be classified as follow:

Type I selectivity - $A \rightarrow B$, $C \not\rightarrow D$

Type II selectivity - $A \rightarrow B$, $A \not\rightarrow C$

Type III selectivity - $A \rightarrow B \not\rightarrow C$

The requirement that a catalyst is not consumed in the reaction it catalyses applies strictly to the specific reaction considered. This is not to say that the activity of a catalyst may be mantained indefinitely. There may be impurities in the reacting system which combine with the catalyst changing its chemical nature with consequent loss of activity. This is called poisoning of the catalyst. Similarly, by-products of the reaction may combine with the catalyst and this process is known as self-poisoning or fouling. Poisoning and self-poisoning may be reversible or irreversible and in the reversible case the activity of the catalyst may be restored by some method of regeneration. It is also possible that the catalyst suffers structural modifications, generally of a permanent character, under the conditionsof reaction or regeneration and this is called catalyst ageing. Different catalysts in general display different stabilities towards all forms of deactivation. An ideal practical catalyst should ally adequate activity, selectivity for the desired reaction and stability.

1.4 - THE MECHANISM OF CATALYSIS

It is accepted nowadays that at some stage of a catalytic reaction one or more of the reactants combines chemically with the catalyst to give an unstable intermediate which subsequently decomposes to yield the products and to regenerate the catalyst which is then free to participate in a new reaction cycle. In order that a substance may function effectively as a catalyst it is necessary that the indirect route via an unstable intermediate is more favourable than the direct route from reactants to products. In terms of the thermodynamic formulation of reaction rates[13], the rate constant k of a reaction is given by expression (1.1):

$$k = \frac{k_\beta T}{h} e^{-\frac{\Delta G^{\ddagger}}{R_G T}} \qquad (1.1)$$

where k_B is Boltzman's constant, h is Planck's constant, $\Delta G^{\ddagger}$ is the free energy of activation, R_G is the ideal gas constant and T is absolute temperature. The free energy of activation is related to the entropy of activation ($\Delta S^{\ddagger}$) and to the enthalpy of activation ($\Delta H^{\ddagger}$) through expression (1.2):

$$\Delta G^{\ddagger} = \Delta H^{\ddagger} - T\Delta S^{\ddagger} \qquad (1.2)$$

The function of the catalyst must be to decrease the free - energy of activation. Since in a catalytic reaction the transition state looses translational freedom due to combination with the catalyst, the entropy of activation will generally be smaller than in the case of the uncatalysed reaction. Therefore, for $\Delta G^{\ddagger}$ to be smaller with the catalysed reaction, it is necessary that $\Delta H^{\ddagger}$ is also sufficiently smaller to overcompensate for the decrease in $\Delta S^{\ddagger}$. The enthalpy of activation is related to the energy activation E_a through expression (1.3)

$$E_a = \Delta H^{\ddagger} - (\Delta n^{\ddagger} - 1)\, R_G T \qquad (1.3)$$

where $\Delta n^{\ddagger}$ is the number of reacting species involved in the formation of the transition state.

It may then be predicted that the role of the catalyst is to provide an alternative reaction path to the uncatalysed reaction that proceeds with a smaller energy of activation. Experimental observation generally conforms to this prediction as shown in table 1.1 for a number of reactions[14]. The situation is illustrated in figure 1.1 for a simple transformation A → B, in terms of a potential energy diagram. If the activation energies for the formation and the decomposition of the unstable intermediate (AC) are both smaller than the activation energy for the uncatalysed reaction, catalysis will ensue. If the intermediate is too unstable with respect to the reactants, catalysis will not be very effective since the

activation energy for its formation will be large. If, on the other hand, it is too stable, the reaction becomes limited by the decomposition of the intermediate and the activity of the catalyst will again be small. There must be therefore an optimum degree of stability of the unstable intermediate for efficient catalysis to occur and this is known as the Principle of Sabatier[4]. This has been observed experimentally in a number of cases when catalyst activity is plotted as a function of some parameter related to the stability of the intermediate[15,16], as illustrated in figure 1.2 for the decomposition of formic acid on metal catalysts[15]. It has been suggested that this reaction proceeds via formation of surface metal formates and if catalyst activity (expressed as the temperature required to attain a rate of reaction of 0.16 molecules $site^{-1}$ sec^{-1}) is plotted as a function of the heat of formation of the metal formates, a maximum in activity is found for intermediate values of heat of formation. Curves such as the one shown in figure 1.2 are commonly referred to as "volcano-shaped"[17].

TABLE 1.1

ACTIVATION ENERGIES FOR CATALYSED AND UNCATALYSED REACTIONS

REACTION	E_u/kJmol^{-1} (1)	E_c/kJmol^{-1} (2)	Catalyst
$2HI \rightarrow H_2 + I_2$	184	104	Au
		58	Pt
$2N_2O \rightarrow 2N_2 + O_2$	244	121	Au
		136	Pt
$2NH_3 \rightarrow N_2 + 3H_2$	>320	163	W
		196	Os

(1) Uncatalysed reaction

(2) catalysed reaction

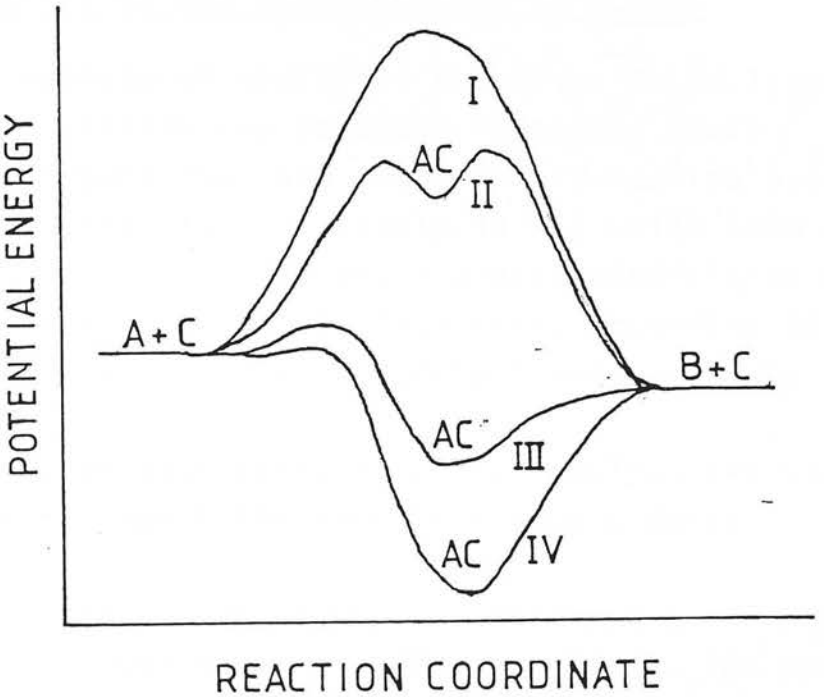

Figure 1.1 - Potential Energy Diagrams for Catalysed and Uncatalysed Reactions: I - Unacatalysed reactions; II - Poor Catalyst - intermediate too unstable; III - Good Catalyst; IV - Poor Catalyst-intermediate too stable

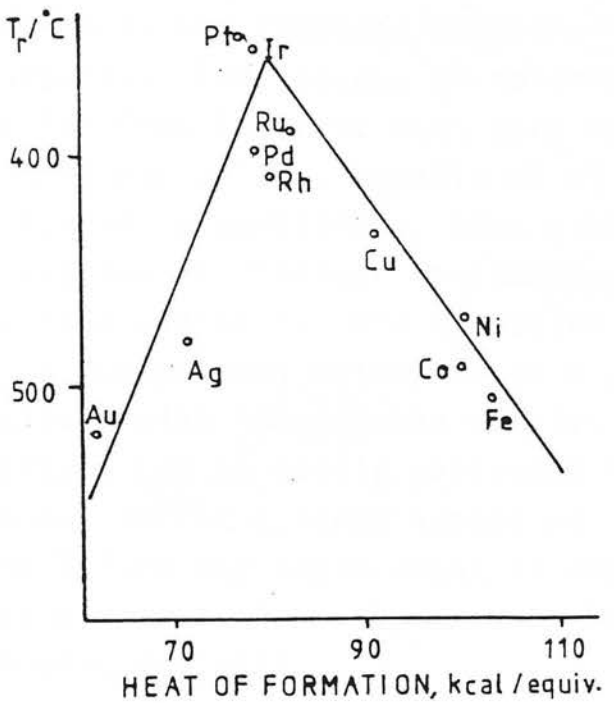

Figure 1.2 - Volcano Shaped Curve of Formic Acid Decomposition on Metals[15] (activity vs. heat of formation of the metal formate)

1.5 - HOMOGENEOUS AND HETEROGENEOUS CATALYSIS

The variety of catalytic reactions is so large that few generalizations are possible regarding their mechanisms beyond the ones presented in section 1.4. As a consequence, the study of catalysis has split into several more or less distinct fields, the main subdivision being made, appart from enzymatic catalysis, according to the phase relationship between catalyst and reactants.

In Homogeneous Catalysis, the catalyst and at least one of the reactants are part of a single phase.

In Heterogeneous Catalysis, catalyst and reactants are present in two or more different phases. The present work deals exclusively with heterogeneous catalysis and, in particular, with gas-solid systems. Examples of different phase combinations for both homogeneous and heterogeneous catalysis are given in table 1.2.

Heterogeneous catalysts have found much more widespread application in the chemical industry than their homogeneous counterparts. The success of heterogeneous catalysts stems partly from the fact that they are mostly thermally stable inorganic solids, capable of withstanding relatively severe operating conditions, thus giving access to some important classes of chemical reactions, such as alkane C-H and C-C bond activation and N_2 activation which remain unaccessed to homogeneous catalysts on a practical scale. Also in contrast with homogeneous catalysts, heterogeneous catalysts can be easily separated from the product stream and may suffer a large number of regeneration cycles before any replacement is needed, whereas homogeneous catalysts normally have to be resynthetized when deactivated[18].

TABLE 1.2

EXAMPLES OF HOMOGENEOUS AND HETEROGENEOUS CATALYTIC REACTIONS

	Catalyst(*)	Reactant(*)	
HOMOGENEOUS	G	G	$SO_2 + \frac{1}{2} O_2 + H_2O \xrightarrow{N_2O_3} H_2SO_4$
	L	L	$-\overset{|}{\underset{|}{C}}-\overset{|}{\underset{|}{C}}-OH \xrightarrow{H^+} \diagup C=C \diagdown + H_2O$
	L	L,G	$C=C + H_2 \xrightarrow[\text{complexes}]{\text{soluble}} -\overset{|}{\underset{H}{C}}-\overset{|}{\underset{H}{C}}-$
	S	S	$K\,ClO_4 \xrightarrow{MnO_2} KCl + 2O_2$
HETEROGENEOUS	L	G	$\diagup C=C \diagdown \xrightarrow{H_3PO_4} -C-C-C-C-$
	S	L	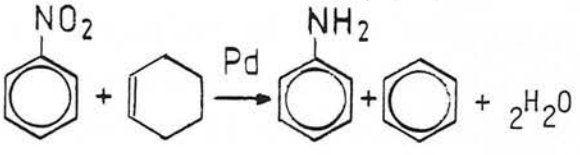
	S	G	$N_2 + 3H_2 \xrightarrow{Fe} 2NH_3$
	S	L,G	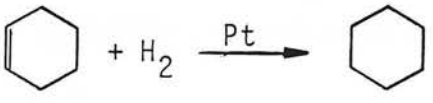

(*) S - Solid; L - Liquid; G- gas

1.6 - THE MECHANISM OF HETEROGENEOUS CATALYSIS

It is generally accepted that the "unstable intermediate" in heterogeneous catalysis is some form of complex formed by adsorption of reactant molecules on the surface of the solid. The main steps of the reaction may then be summarized as follows:

1 - Diffusion of the reactant(s) to the surface;
2 - Adsorption of the reactant (s);
3 - Reaction on the surface;
4 - Desorption of the product(s);
5 - Diffusion of the product(s) to the fluid phase

Depending on the reaction considered and on the experimental conditions, any of these steps may be considerably slower than the remaining ones in the sequence, and therefore be the rate-determining step of the reaction.

1.7 - ADSORPTION ON SOLID SURFACES

The surface of a solid is a region of high potential energy due to unbalance of the attractive forces responsible for the cohesion of the solid existing at this region. In order to minimize the free-energy of the system, molecules in the surrounding fluid are attracted to the surface to form a condensed layer in equilibrium with the fluid. This phenomenon is known as adsorption.

The forces which hold the adsorbed layer to the surface may vary greatly in nature. These forces may be relatively weak and similar to the attractive forces that hold molecules together in the liquid state (van der Waals forces) or they may be strong and of the same nature as the ones responsible for binding atoms in chemical compounds. The weak form of interaction is generally called physical adsorption or physisorption and the strong

form is known as chemical adsorption or chemisorption.

1.7.1 - Physical adsorption

Physical adsorption is a result of London dispersion forces (present in all systems) and of electrostatic attraction between ionic solids and polar or readily polarizable molecules[19]. Dispersion forces arise from interactions betweenrapidly fluctuating dipoles in molecules (or atoms) and dipole moments induced in surrounding molecules (or atoms) by the fleeting dipole in the central molecule[19]. Heats of physical adsorption are generally of the same order as the heat of condensation of the adsorbate so that physical adsorption is only substantial at near or below the boiling point of the adsorbate. Due to this fact, condensation of further molecules upon the first adsorbed layer may occur at sufficiently large pressures. No energy of activation is associated with physical adsorption processes. Since the heats of physisorption are small, little disturbance results in the structure of the adsorbate and physical adsorption is of little significance to catalysis. However, the non-specific nature of physical adsorption has been put into use for the experimental estimation of the surface area of solidswhich is of great importance to the characterization of solid catalysts[20].

This is usually achieved by measuring the adsorption isotherm of a chemically inert gas on the solid under consideration. The procedure involves measuring the amount of gas adsorbed as a function of pressure at a fixed temperature. The experimental points are then fitted to a suitable theoretical isotherm which contains the amount of gas adsorbed at monolayer coverage as a parameter. Knowing the area occupied by a molecule of adsorbate and the amount corresponding to monolayer coverage, the area of the solid may be determined. The adsorption isotherm equation derived by Brunauer, Emett

and Teller (BET isotherm)[21] is found to apply to a large number of cases and is commonly used in the determination of surface areas. The BET equation is of the form:

$$\frac{p}{x(p_o-p)} = \frac{1}{x_m c} + \frac{c-1}{x_m c} \cdot \frac{p}{p_o} \qquad (1.4)$$

where x is the amount of gas adsorbed at a pressure p, p_o is the vapour pressure of the adsorbate at the temperature of the isotherm, x_m is the amount adsorbed at monolayer coverage and c is a constant. If $p/x(p_o-p)$ is plotted against p/p_o, a straight line should result with slope α and intercept β. The monolayer amount may then be calculated from expression (1.5):

$$x_m = \frac{1}{\alpha + \beta} \qquad (1.5)$$

1.7.2 - Chemisorption

In the previous section some experimental criteria were given which characterize a given type of adsorption as physical. These criteria are compared in table 1.3 with the ones which characterize chemisorption[7].

TABLE 1.3

CRITERIA FOR DISTINGUISHING PHYSICAL AND CHEMICAL ADSORPTION[7]

CRITERION	CHEMISORPTION	PHYSISORPTION
Heat of adsorption	40-800 $kJmol^{-1}$	8-20 $kJmol^{-1}$
Activation Energy, E_a	small	zero
Temperature of occurrence	Depends on E_a	Depends on boiling point of the adsorbate
Number of layers adsorbed	one	More than on possible

The forces involved in chemisorption are of the same nature as the ones existing between atoms in typical chemical compounds. This implies that heats of chemisorption are of the same order of magnitude as the heats of chemical reactions. As a consequence, chemisorbed complexes may remain on the surface of solids at temperatures much in excess of the boiling point of the adsorbate and, although physical adsorption may occur upon the chemisorbed layer, saturation coverage by chemisorbed species occurs at much lower pressures than the ones required for physical adsorption to become significant. While physical adsorption depends little on the nature of the solid but mostly on the boiling point of the adsorbate, chemisorption is highly specific in character. For example, heats of carbon monoxide chemisorption on polycristalline metal surfaces varying from about 40 $kJmol^{-1}$ (Cu, Ag, Au) to about 630 $kJmol^{-1}$ (Ti, Zr) have been recorded[22]. Molecules frequently undergo dissociation upon chemisorption (dissociative chemisorption). This situation may be described with reference to the potential energy diagram shown in figure 1.3 for the case of a diatomic molecule adsorbing on a metal surface[23]. Curve A represents the potential energy of the system as a function of the distance between the surface and the molecule M-M. At infinite separation, the potential energy is taken as zero and a shallow energy minimum exists corresponding to physical adsorption of M-M. Curve B corresponds to chemisorption of two atoms M on two metal sites S. At infinite separation from the surface, the difference in energy between curves A and B is equal to the energy of dissociation of the molecule M-M. The point at which these two curves cross corresponds to the top of the activation barrier for dissociative chemisorption of M-M. In figure 1.3 , the two curves cross at a potential energy value greater than zero and the chemisorption process will proceed with a certain activation energy E_a (activated chemisorption). This situation applies, for example, to

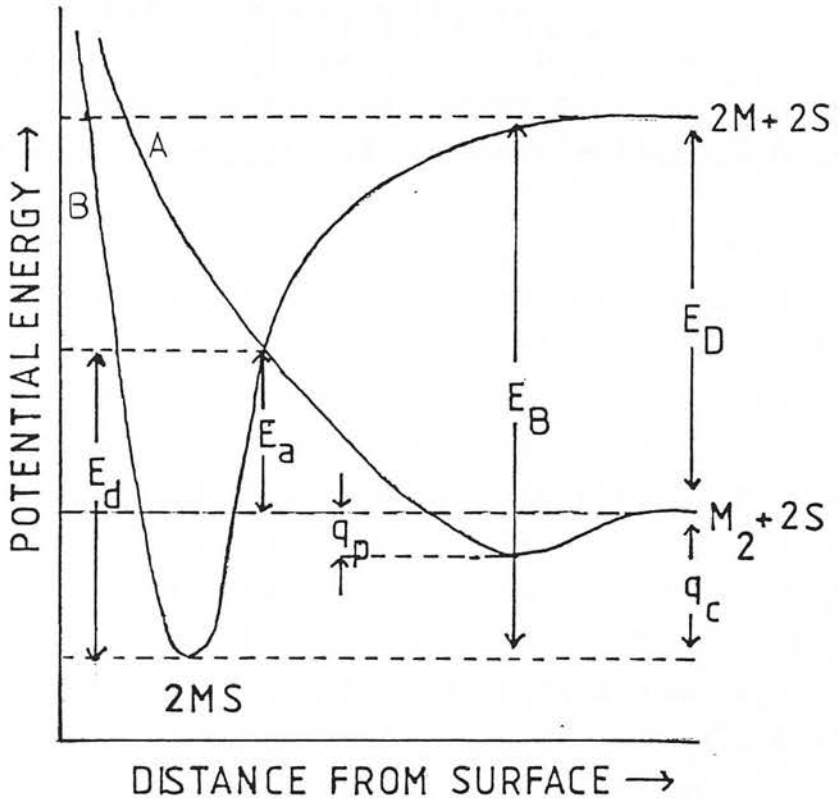

Figure 1.3 - Potential Energy Diagram for Dissociative Chemisorption: q_p - heat of physisorption; q_c - heat of chemisorption; E_a - activation energy for chemisorption; E_d - activation energy for desorption; E_D - dissociation energy for M_2

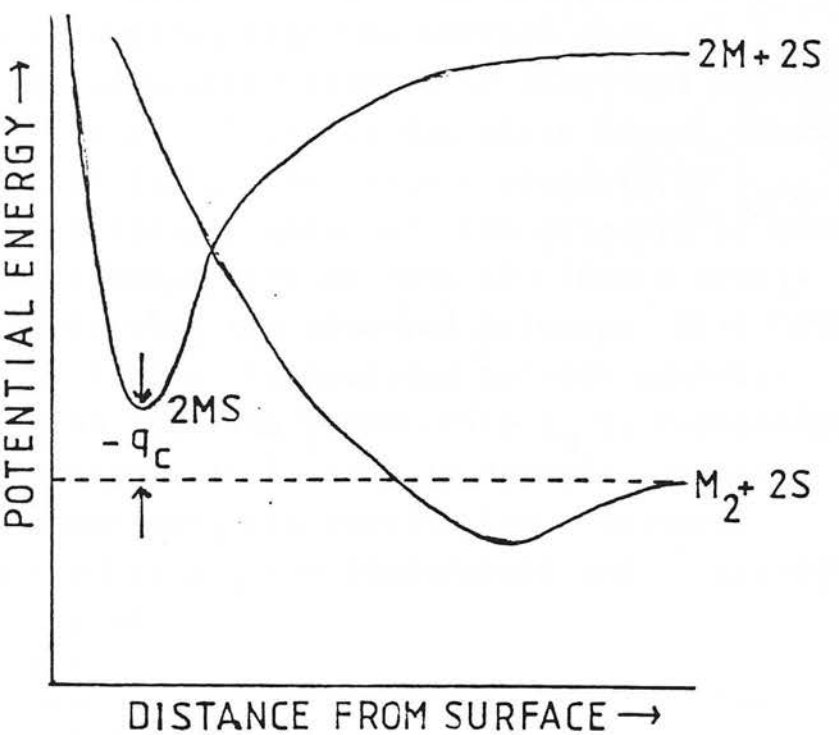

Figure 1.4 - Potential Energy Diagram for Endothermal Chemisorption

the dissociative chemisorption of hydrogen on Cu[24] and of nitrogen on Fe[25]. In many cases, however, the crossing point of the curves lies below the zero potential energy level and the dissociative chemisorption is non-activated.

Chemisorption is a process accompanied by a decrease in entropy due to the loss of translational degrees of freedom when the molecule becomes attached to the surface. Therefore, for chemisorption to be spontaneous it must be an exothermal process. Endothermal chemisorption may occur, however, if the molecule is dissociated in the gas phase and the surface is kept at a sufficiently low temperature to prevent mobility and consequent recombination of the chemisorbed atoms. A potential energy diagram corresponding to this situation is shown in figure 1.4 and applies, for example, to the chemisorption of hydrogen atoms on Au[26].

1.7.3 - Adsorption isotherms

The simplest model for chemisorption involves the assumption that the surface contains a fixed number of adsorption sites with identical adsorptive properties. Molecules from the gas phase become adsorbed on collision with empty sites with a probability s_o. When the site is already occupied, the molecule is back-scattered to gas phase with no loss of kinetic energy and without perturbing the adsorbed molecule. It is further assumed that no lateral interaction between adsorbed species exists so that the probability s_o is independent of surface coverage. It is easy to demonstrate that, with these assumptions, the equilibrium fractional surface coverage Θ at a given temperature and pressure may be expressed as:

$$\Theta = \frac{K_a P}{1 + K_a P} \qquad (1.10)$$

where K_a is a constant at a given temperature. The constant K_a represents the equilibrium constant for adsorption and is given as a function of temperature by:

$$K_a = e^{\frac{\Delta Sa}{R_G}} \cdot e^{\frac{q_a}{R_G T}} \qquad (1.11)$$

where ΔSa is the entropy of adsorption and q_a is the differential heat of adsorption. Expression (1.10) is the well-known Langmuir isotherm equation and modified versions may be written to account for complicating factors such as dissociative chemisorption or dual-site occupancy (associative chemisorption on a pair of sites) while keeping the remaining assumptions of the Langmuir model. For dissociative chemisorption on a pair of sites, for example, the Langmuir isotherm becomes:

$$\Theta = \frac{(K_a P)^{1/2}}{1 + (K_a P)^{1/2}} \qquad (1.12)$$

The Langmuir adsorption model represents an idealized situation and real chemisorption phenomena are much more complex in nature. An important deficiency of the Langumuir model is the assumption of the constancy of heats of chemisorption with increasing coverage (perfectly homogeneous surface with no interaction between adsorbed species). The fact that the surface of solids is topographically complex in a microscopic scale leads naturally to the concept of surface heterogeneity. Surface heterogeneity implies that species adsorbed at sites of different atomic environments will in general be bound to the surface with different energies. As sites associated with larger binding energies are preferentially occupied at lower equilibrium coverages, the result is that differential heats of chemisorption decrease with increasing coverage. The effect of surface heterogeneity on the binding energy of adsorbed species is illustrated in figure 1.5 with the thermal desorption

spectra of hydrogen on different Pt single-crystal planes[27]. On the smooth Pt (111) surface, one desorption peak is observed although the assimetry of this peak indicates that more than one adsorbed species contributes to the desorption spectrum. The Pt (557) surface contains monoatomic steps besides terraces with a (111) structure. In this case, a second desorption peak appears, corresponding to a higher binding energy. The Pt (12,9,8) surface contains kinks besides terraces and steps and a third desorption peak appears corresponding to adsorption on kink sites.

Even the very smooth surface of low-index single-crystal planes present some degree of heterogeneity since molecules may occupy sites with different coordination numbers and rotational symmetries. For example, carbon monoxide may adsorb on the Rh (111) surface both directly on top of the metal atoms or occupying a bridging position between two atoms. The former species is formed at lower coverages and remais longer on the surface during thermal desorption[28].

Surface heterogeneity is not the only reason for the variation of heats of adsorption with coverage. Lateral interactions between adsorbed species may also play an important role and since these interactions are generally of a repulsive character, a decrease in heats of chemisorption with increasing coverage results. Attractive interactions have also been observed, as in the chemisorption of CO on Pd (111) surfaces, leading to formation of adsorbed islands on the surface[29]. Therefore, besides an intrinsic heterogeneity, surfaces may present an induced heterogeneity due to the presence of adsorbed species.

From a macroscopic point of view, heats of chemisorption may often be described as simple functions of surface coverage. Thus, the assumption that heats of

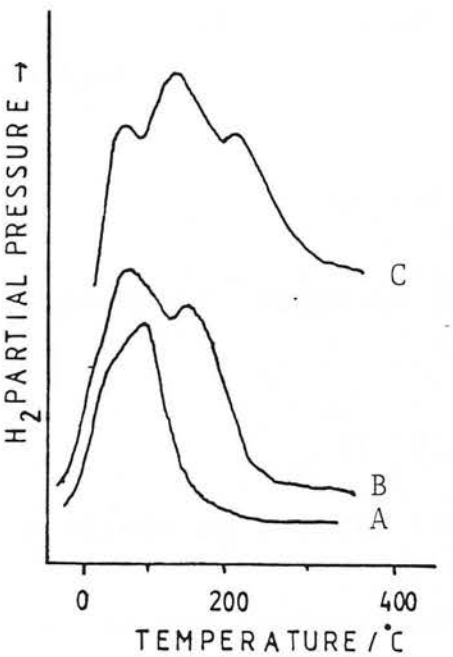

Figure 1.5 - Hydrogen Thermal Desorption Spectra from Pt Single Crystal Faces[27]: A - Pt (111); B - Pt (557); C - Pt (12, 9,8)

chemisorption decrease linearly with coverage leads to the Temkin isotherm, which has been used to describe the chemisorption of nitrogen on ammonia synthesis catalysts[30] and is of the form:

$$\Theta = a \ln bP \qquad (1.13)$$

where a and b are constants at a given temperature.

A logarithmic variation of heats of chemisorption of the type:

$$q = q_m \left(\ln \frac{\Theta}{\Theta_m}\right) \qquad (1.14)$$

where q_m and θ_m are constants, leads to the Freundlich isotherm[31]:

$$\Theta = aP^b \qquad (1.15)$$

where a and b are constants at a given temperature.

Despite its theoretical deficiencies, the Langmuir adsorption model is generally used in the derivation of kinetic expression for catalytic reactions when equilibrium between surface species and gaseous reactants is assumed. It has been suggested that, although a wide spectrum of adsorption energies may exist on the surface of solids, only a portion of this spectrum is of significance to catalysis, so that the Langmuir model may be used within good approximation[32]. Arguments have been presented, however, which show that even though there may exist an optimum adsorption stength for maximum catalytic activity, sites whose strength of adsorption deviate appreciably from the optimum value still contribute significantly to catalysis, but the analytical form of the kinetic expressions that take into account surface non-uniformity may be similar to the ones obtained assuming a Langmuir model[33].

1.8 - SURFACE REACTIONS[32]

The "unstable intermediate" in heterogeneous catalysis is some form of complex formed by chemisorption of reactant molecules on the surface of the catalyst. This complex may then decompose unimolecularly, it may undergo rearrangement to give isomerization products or it may react with another chemisorbed complex or with a molecule impinging from the gas phase.

The mechanism of bimolecular surface reactions which involves an interaction between chemisorbed molecules is generally referred to as the Langmuir-Hinshelwood mechanism. The alternative mechanism, involving a reaction between a chemisorbed species and a gas phase or physically adsorbed molecule is known as the Rideal-Eley mechanism.

A simple surface isomerization or unimolecular decomposition reaction may be represented as follows:

$$A + S \underset{k_{-1}}{\overset{k_1}{\rightleftharpoons}} AS \qquad (1)$$

$$AS \xrightarrow{k_2} \text{products} \qquad (2)$$

SCHEME 1.1

where A is a reactant, S is an empty adsorption site and AS is the chemisorbed complex.

The rate of reaction of the chemisorbed complex to give the products is given by:

$$r = k_2 \, \Theta_A \qquad (1.16)$$

where k_2 is the rate constant for step (2) of the reaction and Θ_A is the fractional surface coverage by

intermediate AS. Assuming that attainment of the adsorption equilibrium (step (1)) is much faster than step (2), it may be considered that the adsorption equilibrium is not disturbed by the occurrence of step (2). Assuming further that adsorption of A obeys the Langmuir isotherm, the fractional surface coverage Θ_A may be expressed as:

$$\Theta_A = \frac{K_A P_A}{1 + K_A P_A} \qquad (1.17)$$

and the rate of reaction is given by:

$$r = \frac{k_2 K_A P_A}{1 + K_A P_A} \qquad (1.18)$$

Two limiting cases may be distinguished for expression (1.18):

1 - Surface coverage is small, so that $K_A P_A << 1$. In this case the rate equation reduces to:

$$r = k_2 K_A P_A \qquad (1.19)$$

The reaction rate is then proportional to the first power of reactant pressure and the reaction is said to be of first order. The rate of reaction may be expressed as a function of temperature by:

$$r = A_2 e^{\frac{E_2}{R_G T}} \cdot e^{\frac{\Delta S_A}{R_G}} \cdot e^{\frac{q_A}{R_G T}} \qquad (1.20)$$

where A_2 and E_2 are, respectively, the pre-exponential factor and the activation energy for step (2) and ΔS_A and q_A are, respectively, the entropy and the heat of adsorption of reactant A. Expression (1.20) may be rearranged to give:

$$r = (A_2 \, e^{\frac{\Delta S_A}{R_G}}) \cdot (e^{-\frac{E_2 - q_A}{R_G T}}) \qquad (1.21)$$

The second term between brackets in (1.21) gives the apparent energy of activation for the reaction, E_a, which is expressed as:

$$E_a = E_2 - q_A \qquad (1.22)$$

2 - Surface coverage is large, so that $K_A P_A \ll 1$. The rate expression then reduces to:

$$r = k_2 \qquad (1.23)$$

In this case, the rate is independent of reactant pressure and the reaction is said to be of order zero and the apparent energy of activation is equal to the energy of activation for step (2).

For intermediate coverages, the Langmuir rate expression may be approximated over a limited range of reactant pressures by a power rate law of the type:

$$r = k_2 (K_A P_A)^{\alpha} \qquad (1.24)$$

where α is a number between 0 and 1.

A simple reaction of the Langmuir-Hinshelwood type between reactants A and B may be represented by:

$$A + S \underset{k_{-1}}{\overset{k_1}{\rightleftharpoons}} AS \qquad (1)$$

$$B + S \underset{k_{-2}}{\overset{k_2}{\rightleftharpoons}} BS \qquad (2)$$

$$BS + AS \xrightarrow{k_3} \text{products} \qquad (3)$$

SCHEME 1.2

According to this mechanism, the rate of reaction may be expressed as:

$$r = k_3 \Theta_A \Theta_B \qquad (1.25)$$

Assuming steps (1) and (2) to be at equilibrium, it is easy to show that fractional surface coverages by reactants A and B are given by expression (1.26a) and (1.26b), respectively:

$$\Theta_A = \frac{K_A P_A}{1 + K_A P_A + K_B P_B} \qquad (1.26a)$$

$$\Theta_B = \frac{K_B P_B}{1 + K_B P_B + K_B P_B} \qquad (1.26b)$$

The rate of reaction is then expressed as:

$$r = \frac{k_3 K_A K_B P_A P_B}{(1 + K_A P_A + K_B P_B)^2} \qquad (1.27)$$

In a series of experiments where P_B is held constant while P_A is varied, it is easy to show by differentiation of expression (1.29) with respect to P_A that a maximum in rate is obtained when:

$$K_A P_A = 1 + K_B P_B \qquad (1.28)$$

For large pressures of reactant A, or when A is strongly adsorbed so that $K_A P_A >> (1 + K_B)$, the rate expression reduces to:

$$r = \frac{k_3 K_B P_B}{K_A P_A} \qquad (1.29)$$

and the reaction becomes of negative order with respect to A.

For the Rideal-Eley mechanism, assuming B to be the gas phase molecule reacting with the AS chemisorbed complex and assuming further that B does not co-adsorb with A on the surface, the reaction mechanism may be written:

$$A + S \underset{k_{-1}}{\overset{k_1}{\rightleftharpoons}} AS$$

$$AS + B \xrightarrow{k_2} \text{products}$$

SCHEME 1.3

The rate expression is then given by

$$r = \frac{k_2 K_A P_A P_B}{1 + K_A P_A} \qquad (1.30)$$

It is easy to see from (1.30) that no maximum in rate is predicted as either P_A or P_B is varied while the pressure of the other reactant is kept constant. The existence of a maximum in reaction rate as the pressure (or, more generally, the surface coverage) of one of the reactants is varied is a distinguishing feature of the Langmuir-Hinshelwood mechanism with respect to the Eley-Rideal mechanism[32,34].

1.9 - DIFFUSION CONTROL

The transfer of reactant from the bulk of the fluid to the surface of the catalyst requires a driving force which is a concentration difference. For a porous catalyst which is used in powder or pellet form, it is

convenient to distinguish two types of reactant transfer:

1 - Transport of reactant from the bulk of the fluid to the external surface of the catalyst particle (external diffusion).

2 - Transport of reactant from the external surface to the interior of the catalyst particle through the porous structure of the solid where most of the catalytic activity usually resides (internal diffusion).

For a reaction which is carried-out under steady-state conditions, the rate of reaction at the external surface of a catalyst particle equals the rate of diffusion of the reactant from the fluid to the particle external surface.

For a first-order reaction involving a single reactant, the rate of reaction is given by:

$$r = k\, C_S = k_m(C_b - C_S) \qquad (1.31)$$

where k is the rate constant for the reaction, C_b and C_S are the reactant concentrations, respectively, at the bulk of the fluid and in the immediate vicinity of the catalyst surface and k_m is a constant, usually called the mass-transfer coefficient[35]. Solving equation(1.31) for C_S yields:

$$C_S = \frac{k_m C_B}{k + k_m} \qquad (1.32)$$

It is easy to see that, if $k_m >> k$, then $C_S \sim C_B$ and the rate of reaction is given simply by kC_B, in terms of bulk concentration of reactant. If $k >> k_m$, then $C_S = k_m C_B/k$ and the rate of reaction is given by $k_m C_B$. In this situation, the reaction is said to be diffusion controlled and kinetic parameters measured in terms of bulk concentration of reactant bear no relationship to

the intrinsic kinetics of the reaction.

The mass transfer coefficient depends on the degree of mixing of the fluid and on the diffusivity of the reactant. Thorough mixing of the fluid phase improves the transport of reactant to the catalyst surface. Since the diffusivity is approximately proportional to $T^{3/2}$ and k is proportional to $e^{-\frac{E_a}{R_G T}}$, it is easy to see that the apparent activation energy recorded for a reaction under diffusion controlled conditions will in general be smaller than the "true" activation energy. Therefore, the following experimental criteria may be given to recognize the transition from kinetic control to an external diffusion controlled regime[7]:

1 - The apparent energy of activation decreases with increasing temperature;

2 - The rate of reaction ceases to increase linearly with the amount of catalyst employed;

3 - The rate of reaction increases with increasing agitation of the fluid.

When packed-bed tubular flow reactors are employed transport of reactant to the catalyst occurs across a layer of stagnant fluid that surrounds the solid particles. The thickness of this layer decreases with increasing linear velocity of the fluid. Therefore, a fourth criterion may be given in the case of flow reactors, namely that the rate of reaction is expected to increase with increasing flow rate (while keeping the same ratio of reactant feed rate to amount of catalyst) if the reaction is limited by diffusion[36].

In the same way that a concentration gradient exists between the fluid phase and the external surface of catalyst pellets, a concentration gradient also exists between the surface of the pellet and its interior. The effect of internal diffusion limitation is to reduce the

rate of reaction to below the value that would be obtained in the absence of a concentration gradient. The size of the intrapellet diffusion effect is usually expressed in terms of an effectiveness factor η, defined as the ratio of the observed reaction rate per catalyst pellet, r_p, to the reaction rate, r_k, expected from the intrinsic kinetics of the reaction in the absence of a concentration gradient:

$$\eta = \frac{r_p}{r_k} \qquad (1.33)$$

Under diffusion controlled conditions, the effectiveness factor is approximately given by (first-order reaction, spherical pellets)[35]:

$$\eta = \frac{3}{R}\sqrt{\frac{D_e}{k\rho_p}} \qquad (1.34)$$

where ρ_p is the density of the pellet, D_e is the effective diffusivity of the reactant within the porous structure of the pellet and R is the radius of the pellet. From (1.33) and (1.34), the observed rate of reaction may be expressed as:

$$r_p = \frac{3}{R}\cdot\sqrt{\frac{D_e}{\rho_p}}\cdot k^{1/2} C_S \qquad (1.35)$$

From expression (1.35), two important conclusions may be drawn:

1 - Under conditions limited by intrapellet diffusion, the rate of reaction varies inversely with the radius of the pellet.

2 - Since the observed rate of reaction is proportional to the square-root of the intrinsic rate constant, the apparent energy of activation is one-half of the "true" value.

Furthermore, the pressure dependence of the effective diffusivity may vary from order zero (Knudsen diffusion) to negative first order (bulk diffusion) depending on the dominating diffusion mechanism. Hence, if the reactant concentration is changed by changing the reactant pressure, the observed reaction order may be smaller than the true value.

The heat consumed or produced at the catalyst surface during reaction is also subject to transport limitations. The difference in temperature between the bulk of the fluid and the surface is given approximately by[35]:

$$T_S - T_b = 0.7 \frac{-\Delta H}{C_p \rho} (C_b - C_S) \qquad (1.39)$$

where $-\Delta H$ is the heat of reaction, and C_p and ρ are, respectively, the heat capacity and the density of the fluid. If the reaction is limited by diffusion $C_b - C_S$ is large and consequently the difference $T_S - T_b$ may also be large, depending on the heat of reaction. Values of 200^o for $T_S - T_b$ have been measured for the hydrogenation of oxygen in a dilute gas stream on a Pt catalyst[37].

Temperature differences between the surface and the interior of catalyst pellets may also develop due to heat transport limitations. For exothermal reactions, such heating compensates the decrease in rate due to diffusion limitations and, under certain conditions, effectiveness factors in excess of unity may be observed[38].

1.10 - TYPES OF HETEROGENEOUS CATALYST

Solid catalysts may be classified according to their conductive properties into metals, semiconductors and insulators. Despite considerable fine structure within each class, this subdivision is convenient from

the point of view of the electronic theories which have been put forward to explain chemisorptive and catalytic phenomena with these materials.

Table 1.4 shows examples of typical reactions catalysed by the different types of solid[7]. Typical reactions on metals and semiconductors involve a change in the oxidation state of the reactants. Metals (in particular transition metals) are especially active for reactions involving hydrogen and hydrocarbons, since these substances can be reversibly chemisorbed on metal surfaces.

TABLE 1.4

CLASSIFICATION OF HETEROGENEOUS CATALYSTS

CLASS	REACTIONS	EXAMPLES
Metals	Hydrogenation Dehydrogenation Hydrogenolysis Oxidation	Fe, Ni, Pt, Pd
Semiconductors	Oxidation Dehydrogenation Desulphurization Hydrogenation	NiO, ZnO, MnO_2 Cr_2O_3, Bi_2O_3 - MoO_3, WS_2
Insulators	Dehydration Polymerization Isomerization Cracking Alkylation	Al_2O_3, SiO_2 - Al_2O_3, zeolites

Sulphur containing molecules and oxygen combine irreversibly with the surface of most metals,so that these materials are of limited usefulness for desulphurization and oxidation reactions. Many metal sulphides, however, are adequate for desulphurization reactions and metal oxides for oxidation reactions. Most

reactions catalysed by insulating oxides do not involve a change in oxidation state of the reactants and are typically of acid-base character.

1.10.1 - Acid-base Catalysis

The surface of many solids display chemical properties which satisfy the Lewis and Brönsted definitions of acids and bases. Surfaces which are able to donate protons or to accept an electron pair from a basic molecule behave as Brönsted acids or Lewis acids, respectively. Surfaces which show a tendency to accept protons or to donate electron pairs are Brönsted or Lewis bases, respectively. Most oxides of catalytic interest possess both acid and basic sites on their surfaces and are predominantly acidic or basic according to the acid or basic strength of these sites[39].

Estimation of the number and strength of acid sites on solid surfaces may be obtained from a number of experimental methods such as titration with amines using Hammet bases as indicators[40], adsorption and thermal desorption of volatile bases (pyridine, n-butylamine, ammonia, etc...)[39] and surface infra-red spectrometric measurements of adsorbed bases[41]. This last method is especially useful for the independent measurement of Lewis and Brönsted acidity, since protonated bases (i.e., bases adsorbed on Brönsted sites) display different adsorption bands from coordinated bases (i.e., bases adsorbed on Lewis sites).

Similarly, basic sites may be titrated with acids using appropriate indicators[42].

Important insulating oxides of catalytic interest are the aluminas, silica-aluminas and zeolites.

Transition aluminas (η- and γ- Al_2O_3) display strong surface acidity when heated at elevated temperatures[39] (500 - 1200 K). Infra-red measurements indicate that the acidity of aluminas is largely due to Lewis acidity and any Brönsted sites on the surface are not strong enough to protonate pyridine [41]. Lewis acid sites are visualized as incompletely coordinated aluminium atoms exposed at the surface during dehydration of the alumina[43]:

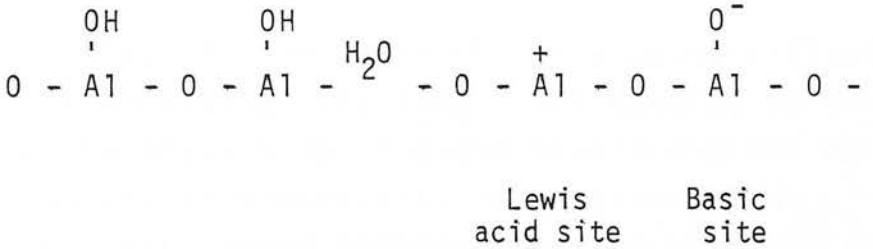

SCHEME 1.6

More detailed models of the alumina surface have been given by Peri[44] and by Knözinger and Ratnasamy[45].

Very pure silica gels display neither acidic nor basic properties. However mixed oxides containing both silica and alumina (silica-aluminas) display strong acidity. Infra-red spectra of amines indicate the presence of both Lewis and Brönsted acid sites[41]. Acidity is thought to arise from isomorphous substitution of tetravalent silicon by trivalent aluminium which creates a net negative charge at the point of substitution. This charge is neutralized by a proton which displays strong Brönsted acidity[46]:

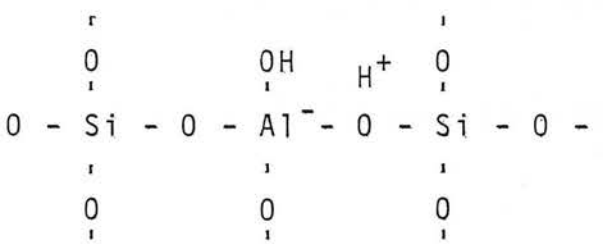

SCHEME 1.7A

Dehydration of the silica-alumina leaves aluminium atoms exposed at the surface which are Lewis acid sites[46]:

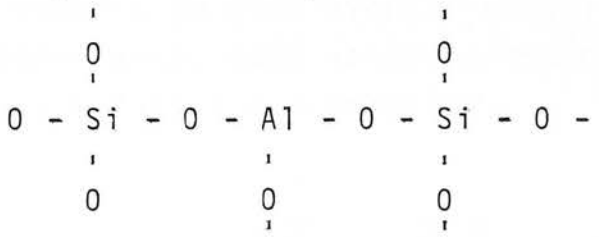

SCHEME 1.7B

Zeolites are crystalline alumino-silicates comprised of linked SiO_4^- and AlO_4^{5-} tetrahedra, so as to form a structure consisting of cages interconnected by channels of molecular dimensions. As a consequence, zeolites have a very large internal surface area but only molecules of appropriate size can penetrate the channels and gain access to this area. This leads to the molecular-sieve action of zeolites and to shape-selective catalysis whereby molecules of similar chemical nature (say, n-hexane and 3-methylpentane) display widely differring reactivities in the presence of the catalyst due to differences in their effective diameters[47].

Typical hydrocarbon reactions which occur on solid acid catalysts are those expected from carbonium ion mechanisms. Initial formation of the carbonium ion may occur by addition of a proton from a Brönsted acid site to an unsaturated compound (olefin or aromatic) or by hydride abstraction by a Lewis acid site from a saturated molecule[16]:

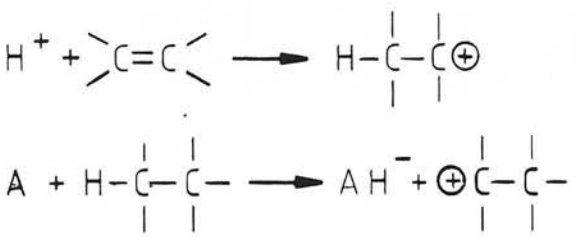

SCHEME 1.8

Typical reactions undergone by carbonium ions are illustrated in scheme 1.9[16]. These elementary reaction steps combine to give overall reactions of great technological importance, such as hydrocarbon isomerization, polymerization, alkylation and cracking.

Internal hydride transfer

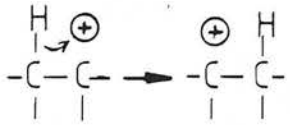

Intermolecular hydride transfer

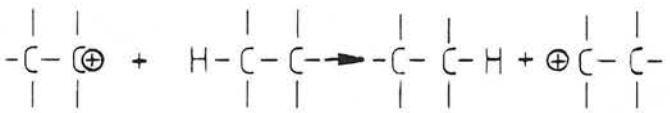

Rearrangement

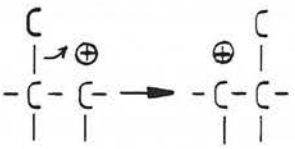

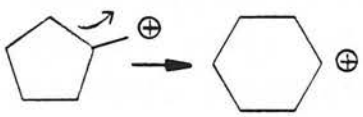

Double bond alkylation

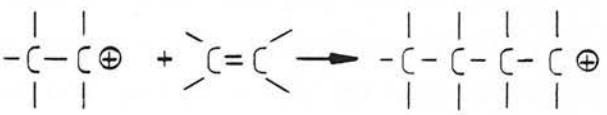

β - Scission

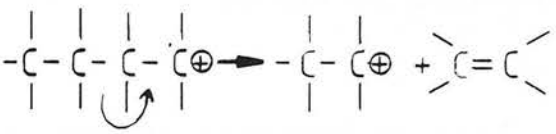

Proton Loss

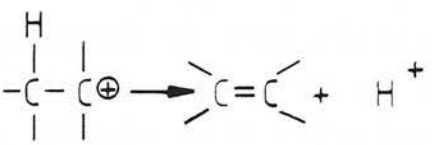

SCHEME 1.9

The dehydration of alcohols and its reverse reaction, olefin hydration, also occurs on acid catalysts and is thought to involve cooperation of acid and basic sites on the surface[48]:

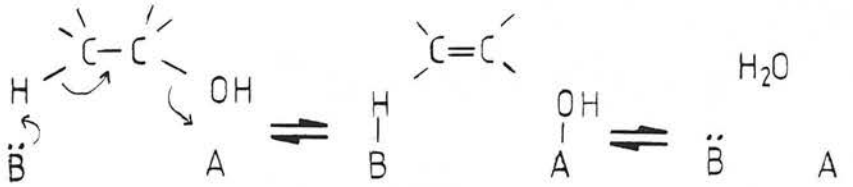

SCHEME 1.10

1.10.2 - Catalysis on semiconductors

Semiconductors of catalytic interest are generally metal oxides and sulphides whose semiconductivity is due to energy levels in the forbidden gap arising from non-stoichiometry or from the presence of foreign impurities[49]. Many semiconductors (e.g. ZnO, TiO_2, V_2O_5, Cr_2O_3, etc...)[50] display acid-base properties[39] and are thus capable of catalysing the types of reaction mentioned in the previous section. Apart from those, semiconductors may also participate in one-electron transfer processes with adsorbed molecules, which gives rise to oxidation-reduction reactions and homolytic cleavage of adsorbate bonds[50].

According to charge-transfer theories of catalysis on semiconductors[51,52], the activity of these materials is due to the presence of free-electrons on the conduction band (n-type semiconductors) or of positive holes in the valence band (p-type semiconductors). Reactions whose rate-determining step involves the transfer of electrons to the catalyst should proceed more easily with increasing p-type semiconductivity (donor reactions) and reactions which involve an electron transfer from the catalyst to the adsorbate are facilitated by increasing

n-type conductivity(acceptor reactions). A classic example is the decomposition of nitrous oxide (N_2O), which is thought to proceed through the following mechanism on p-type semi-conductors[52]:

$$N_2O(g) \xrightarrow{fast} N_2(g) + O^-(a) + p$$

$$2O^-(a) + 2p \xrightarrow{slow} O_2$$

SCHEME 1.11

In this scheme p refers to the creation of a positive hole in the valence band of the semiconductor due to the transfer of one electron from the catalyst to the adsorbed particle. On n-type semiconductors the reaction may be written[52]:

$$N_2O(g) + e^- \xrightarrow{fast} N_2(g) + O^-(a)$$

$$2O^-(a) \xrightarrow{slow} O_2 + 2e^-$$

SCHEME 1.12

where e^- stands for an electron transferred from the conduction band of the semiconductor to the chemisorbed particle. It has been shown that p-type semiconductors catalyse this reaction at much lower temperatures (473 - 673 K) than n-type semiconductors (>873 K)[53]. On n-type semiconductors, the conductivity of the catalyst drops during reaction, confirming that conduction electrons are trapped by chemisorbed oxygen. With p-type oxides, conductivity increases. Doping of the p-type semiconductor NiO with Li_2O increases p-type semiconductivity and also the catalytic activity for N_2O decomposition. Addition of In_2O_3, on the other hand, decreases both p-type conductivity and catalytic activity, in accordance with

the predictions of the theory[52].

Few other reactions can be so neatly explained by consideration of simple charge transfer theories and many other factors seem to influence the catalytic properties of semiconductors. Krylow[50] examined a large body of literature data on oxidation-reduction reactions on semiconductors and concluded that the ligand symmetry theory initially proposed by Dowden and Wells[54,55] seems to be in agreement with experimental observations in many oxidation, hydrogenation, dehydrogenation and decomposition reactions. According to this theory, which is derived from crystal-field theory, the driving force for many chemisorptions and catalytic reactions is the stabilization energy gained by restoration of octahedral symmetry around an exposed cation due to coordination with adsorbed species. From crystal-field theory, the stabilization energy is zero for transition metal cations containing 0, 5 or 10 d-electrons (equal occupancy of all d-levels) such as Ca^{2+}, Sc^{3+} (no d-electrons), Mn^{2+}, Fe^{3+} (5 d-electrons) Cu^{+} an Zn^{2+} (10 d-electrons). If the rate determining step of a reaction involves an increase in coordination number, catalytic activity minima should be expected for d^0, d^5 and d^{10} oxides. A striking example of a system which closely conforms to this prediction is the H_2-D_2 exchange reaction on oxides of the first transition period as illustrated in figure 1.6. Other reactions which display the expected minima are cyclohexane dehydrogenation H_2O_2 decomposition, and the O_2^{16} - O_2^{18} isotopic exchange.

1.10.3 - Catalysis on metals

The research to be described in succeeding chapters of the present dissertation belongs to the subject of catalysis on metals. This subject will be treated in somewhat more detail in the remainder of the present chapter.

1.11 FORMS OF METALLIC CATALYSTS[56,57]

Metals may be used as catalysts in either massive or dispersed form. Massive metals are specially suited to fundamental studies of chemisorption and catalysis, since they allow better opportunity for control of variables such as surface structure and surface contamination. Polycristalline forms of massive catalysts include wires and foils. Single crystals may be cut to expose selected crystallographic faces.

Dispersed forms of metal catalysts include powders, blacks (sponges), skeletal metals (Raney catalysts), evaporated metal films, colloidal metals and supported metals. Powders, blacks and colloidal metals are usually prepared by reduction of a suitable precursor compound. Raney catalysts are prepared by leaching out with alkaly the aluminium from metal-aluminium alloys. Evaporated metal films may be obtained in polycrystalline form or they may be deposited on crystalline supports (mica, rock-salt) so as to obtain oriented metal films. Ultrathin evaporated films have been prepared with particle sizes below 5 nm.

From a technical point of view, supported metal catalysts are by far the most important. In these catalysts, the metal is deposited under the form of small crystallites on the surface of a large surface-area support. Common supports are the silicas, aluminas, silica-aluminas, zeolites and carbon which may be prepared with surface-areas in the order of several hundred m^2 per gram. The dispersion of the metal is defined as the number of metal atoms exposed on the surface ratioed to the total number of metal atoms in the catalyst. Supported metal catalysts with dispersion equal to unity can be prepared. Although the main function of the support is usually to provide a

large surface-area so that the metal can be well dispersed, the support may interact with the metal modifying its catalytic properties (cf.chapter 2) or it may provide catalytic functions which are not present in the metal. For example, in catalytic reforming processes, where it is desired to transform straight-chain paraffins into branched hydrocarbons, cycloalkanes and aromatics, Pt supported on acidic transition-aluminas is commonly used as the catalyst. The metal peforms mainly the role of a hydrogenation-dehydrogenation agent, while isomerization carbonium ion reactions take place on the acidic sites of the support. Such catalysts are commonly referred to as dual- or bifunctional catalysts.

The metallic phase of a catalyst may be comprised of a single metal or bi- and multimetallic catalysts may be prepared with catalytic properties different from any of the metals alone. This provides an important way of controlling the activity, selectivity and stability of metallic catalysts.

1.12 REACTIONS ON METAL CATALYSTS

Table 1.4 summarized the main types of reactions catalysed by metals. It is out of the scope of the present chapter to discuss in any detail the patterns of activity of the different metals for each type of reaction. The following general trends, however, have been repeatedly noticed in the literature[16,19,56,58,59]:

1. The activity of metals for a given reaction depends both on the nature of the metal and,in many cases, on the method of catalyst preparation. In the absence of contamination of the metal, during preparation, this second factor may be generally related to differences in structure of the metal surface due to differences in catalyst

preparation method. Some reactions are insensitive to surface structure and these have been named "structure insensitive" or "facile" reactions . Reactions which are sensitive to surface structure are termed "structure sensitive" or "demanding" reactions[60]. In general, there are much larger differences in catalytic activity among different metals than among different preparations of a given metal[60,61].

2. For reactions involving hydrogen and hydrocarbons (hydrogenation, dehydrogenation, isotopic exchange with deuterium) the most active catalysts are to be found among the transition metals and specially among the metals of group VIII of the periodic table. Metals with a complete d-shell are less active than group VIII metals for these reactions as also are the metals located to the left of group VIII in the transition series. The same pattern of activity applies for other reactions, such as ammonia synthesis and decomposition and formic acid decomposition.

3. In oxidation reactions, activity may be attributed to the metal in the zero-valent state only in the case of the noble (Cu, Ag, Au) and the Pt group metals. In other cases, the active phase is the metal oxide rather than the metal. Both group $VIII_3$ and group IB elements display considerable activity in oxidation reactions.

1.13 CORRELATIONS BETWEEN CATALYTIC ACTIVITY AND PROPERTIES OF METALS.

In attempting to understand the mechanism of the catalytic action of metals, correlations have been sought between patterns of activity and properties of the metals.

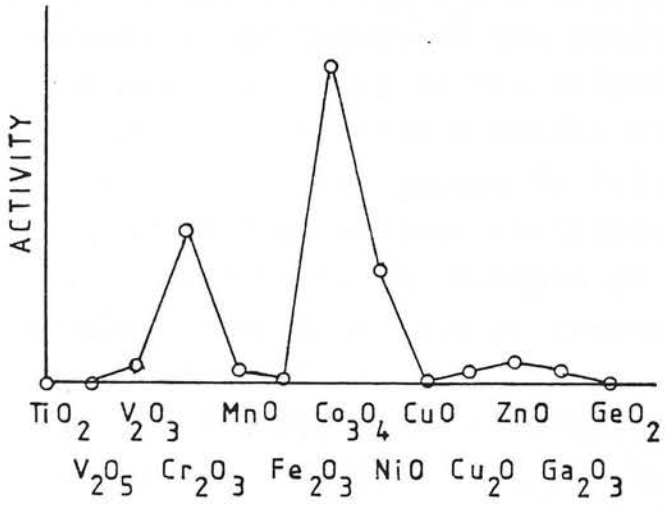

Figure 1.6 - Hydrogen - Deuterium Exchange on Oxides of the First Transition Period[55]

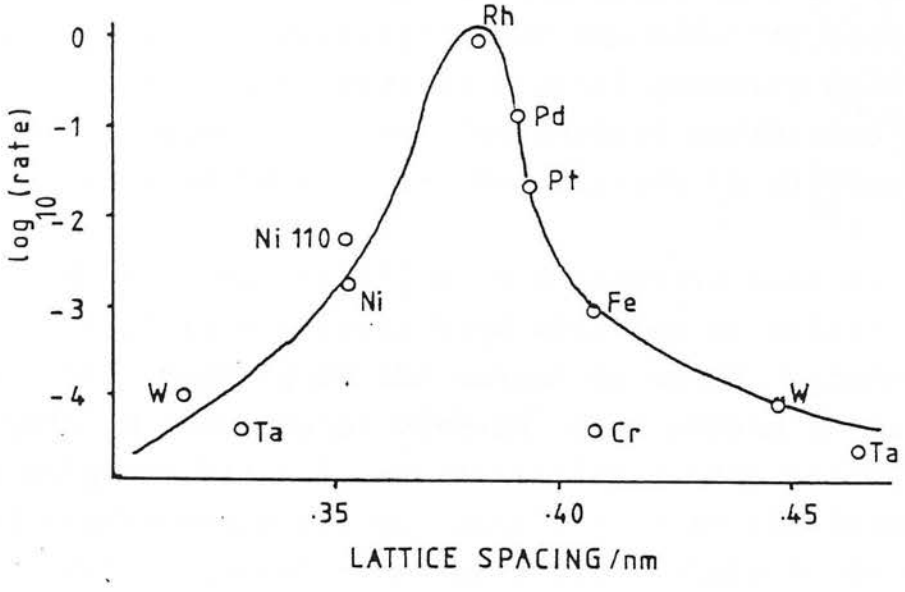

Figure 1.7 - Correlation Between Activity for Ethylene Hydrogenation at 273 K on Metal Films and Lattice Spacing[62]

Both geometric and electronic factors have been considered in these correlations.

As applied to the interpretation of patterns of activity as a function of nature of the metal, the geometric factor usually refers to the effect of lattice spacing on the energetics of chemisorption and surface reactions[62,63]. Other types of geometric factor appear when considering effects of surface structure on catalytic activity and alloying effects. An example of an apparently successful correlation between lattice spacing and catalytic activity of metals is given in the classical work of Beeck on the hydrogenation of ethylene on metal films[62]. As illustrated in figure 1.7, a relatively smooth curve can be fitted to the experimental points, with a maximum at Rh. It would seem that an optimum lattice spacing exists for catalysis of this reaction, possibly due to differring degrees of strain placed in the bonds of the reactive intermediate adsorbed on two or more neighbouring metal atoms. However, equally good correlations are obtained when catalyst activity is plotted against some parameter characteristic of the electronic structure of the metal (e.g. % d-character of the metallic bond-see below). This is clearly because crystal geometry and electronic structure are not independent parameters so that a distinction between the two factors is difficult.

The % d- character (δ) of the metallic bond as defined in Pauling's valence bond approach to metallic bonding[64] is a measure of the extent to which d-electrons participate in metal-metal bonding. This parameter is a maximum at group VIII of the transition series which is also the region where maximum catalytic activity is usually found. Therefore correlations have been attempted between δ and catalytic activity, with some measure of success in many cases[61,62] as illustrated in figure 1.8 for ethylene hydrogenation[62]. The theoretical significance of these correlations, however, is not at all clear. Beeck proposed

that % d-character is inversely related to the availability of unpaired d-electrons for bonding with the adsorbate and that thus heats of chemisorption would be expected to decrease with increasing δ[62]. It has been pointed out, however, that Pauling's treatment of % d-character does not lead to such relationship [65], but instead δ decreases approximately linearly with lattice spacing[19]. Gates et al. emphasize that the existence of a good correlation between δ and catalytic activity simply means that there is some relation between bulk-metal properties and catalytic activity[16].

The fact that group IB metals are capable of chemisorbing CO, olefins and pre-formed hydrogen atoms (cf. 1.7.2) casts some doubt on the idea that partially vacant d-orbitals are a necessary condition for chemisorption. It has been suggested that these orbitals are involved in the formation of a weakly chemisorbed precursor state (type C state)[66] which lowers the activation energy for formation of the final strongly chemisorbed state (cf. figure 1.9). The strong chemisorptive bond is then envisaged to be of the same type as the ones involved in metal-metal bonding, i.e., they are thought to involve unengaged hybrid dsp bonding orbitals emerging at the surface. Some correlation might then be expected between heats of chemisorption (and therefore catalysis) and the strength of metal-metal bonds as measured, for example, by the heat of sublimation of the metal (λ). Correlations of this type have been attempted for a number of reactions with no greater degree of success than obtained with δ correlations[56].

One principle, however, which seems to be of general validity is the principle of Sabatier, already mentioned under 1.4. Application of this principle to formic acid decomposition was already illustrated[15]. Tanaka and Tamaru observed that the heat of adsorption of various simple molecules is linearly correlated with the heat of

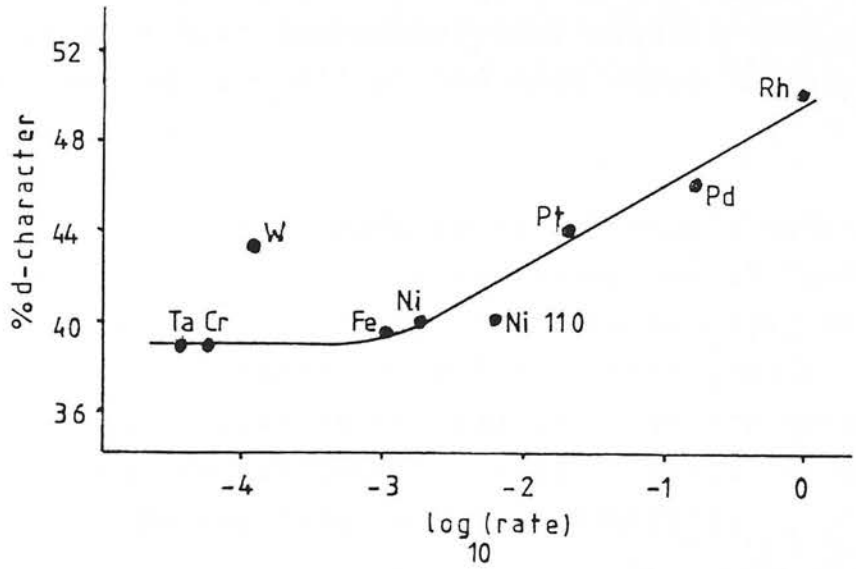

Figure 1.8 - Correlation Between Activity for Ethylene Hydrogenation at 273 K on Metal Films and % d - Character of the Metallic Bond[62]

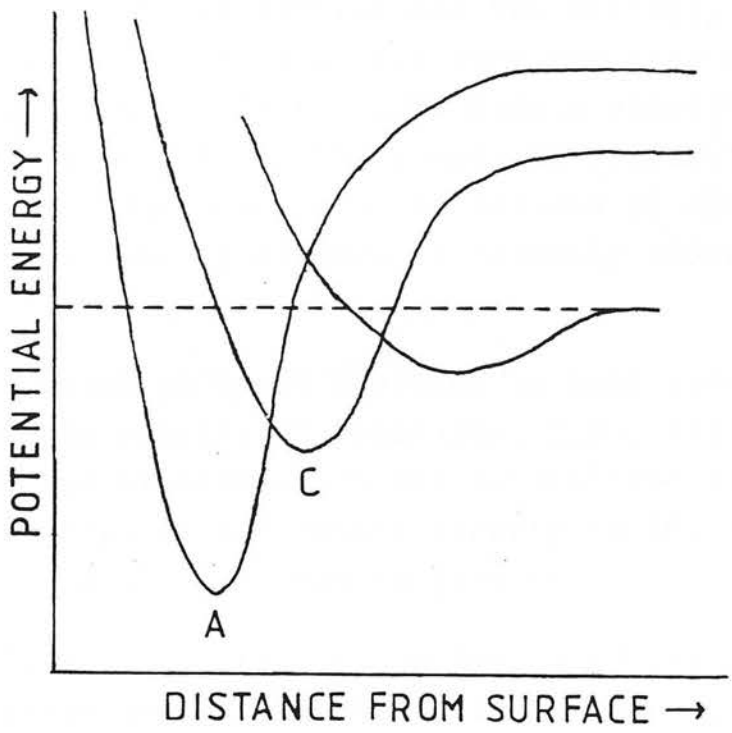

Figure 1.9 - Role of a Weakly Chemisorbed Precursor State (C) in Lowering the Activation Energy for Formation of the Strongly Chemisorbed State (A)

formation, $-\Delta H_f$, of the highest stable oxide of the metal[67]. Plots of catalytic activity for a number of simple reactions (ethylene hydrogenation, ammonia decomposition, ethane hydrogenolysis) against $-\Delta H_f$ result in volcano shaped curves[16] of the type shown for formic acid decomposition.

Initial heats of chemisorption of simple molecules (CO, H_2, O_2, N_2, CO_2) on polycrystalline metal surfaces are known to decrease steadily from left to right across any period of the transition series[22]. This simple experimental fact, when taken together with the principle of Sabatier provides an acceptable explanation for many activity patterns observed in metal catalysis.

1.14 FUNDAMENTAL APPROACHES

Ultimately, a theoretical understanding of chemisorption and catalysis on metals should arise from detailed quantum - mechanical calculations on the interactions of adsorbed species and the surface. The difficulties with this type of approach are many and results are only available for some highly simplified model systems. No attempt will be made to review this subject and only some important conclusions of the relevant studies will be stated, as recently summarized by Gates et al.[16]:

1. Adsorption on metal surfaces is most often a strongly localized phenomenon, i,e., electrons from the adsorbate are not delocalized over the whole crystal but remain largely in the vicinity of the atoms involved in bonding;

2. Differences in adsorption energy are due to differences in the immediate surroundings of the chemisorbed species and not to long-distance

induction effects;

3. The results support the idea of a "surface compound", whereby an atom or molecular fragment A adsorbed on a metal M may be envisaged as a pseudo-molecule, AM (or AM_x), weakly bound to the rest of the metal.

4. The d-orbitals of metals are highly localized in space and energy and therefore provide opportunity for strong mixing with orbitals of an adsorbing molecule. The lowering of activation energies for reaction requires that d-orbitals facilitate electron transitions, e.g., by receiving electrons from orbitals that are being raised in energy and donating electrons to orbitals being lowered in energy.

5. Calculations for the dissociative chemisorption of H_2 on Ni and Cu seem to confirm that unfilled d-orbitals are important in lowering the activation energy for chemisorption but do not materially affect the strength of the bond formed.

1.15 PARTICLE SIZE AND SURFACE STRUCTURE EFFECTS

The rates of many catalytic reactions are sensitive to the size of the metal particles and to the topography of the surface. This is not surprising when it is considered that on metal surfaces atoms with varying coordination numbers may occur which may be expected to display different catalytic properties. The importance of surface heterogeneity to the energetics of chemisorption was already emphasized in section 1.7.2.

The idea that metal atoms of low coordination number are endowed with special catalytic properties goes back a

long way in the past and is the basis of the "active site" concept first introduced by Taylor to explain the large sensitivity of some reactions to small amounts of added poisons[9]. Attempts to ascertain the possible role of active sites in metal catalysis have been actively pursued over the years, mainly by studying the effect of surface deffects created by rapid cooling of metal samples from high temperatures[68], ion[68] and radiation[69] bombardment and cold working of wires[70] on catalytic activity. Recently, methods have become available for the preparation and characterization of metal surfaces with controlled amounts of imperfections such as steps and kinks[71]. Studies of chemical reactions on these surfaces indicate that stepped and kinked Pt surfaces have a much higher activity for H-H (steps), C-H (steps) and C-C (kinks) bond breaking reactions than Pt low-index faces[72]. It has been suggested that low-coordination atoms are positively charged and the resulting electric field at corner sites helps to polarize incoming molecules and therefore facilitates bond cleavage[72]. Since small metal particles present a higher proportion of atoms of low-coordination number than large crystallites, a particle size effect results with dispersed catalysts.

Another way of looking at catalysis on metal surfaces involves the assumption that reactions take place on atoms of essentially uniform properties but that in general a certain number of neighbouring metal atoms, perhaps in a certain preferred arrangement, is required to promote a given reaction. This concept was first used by Herington and Rideal[73], who demonstrated that a single molecule of poison could render a large fraction of the surface inactive for catalysis if the reaction considered requires a large number of neighbouring metal atoms. The same concept forms the basis of Balandin's multiplet theory[17], of Kobosev's ensemble theory[74] and of many modern interpretations of catalysis on alloys (cf.chapter 3). Reactions which require a single metal atom may easily

take place on corner atoms of small metal particles but if the reaction occurs on a large ensemble (or multiplet or multiple site) a low index face may be required. In this fashion, the increase in selectivity for neopentane isomerization with increasing size of Pt crystallites has been rationalized by assuming that isomerization proceeds from a tripod-like intermediate bound to three neighbouring Pt atoms[75,76]:

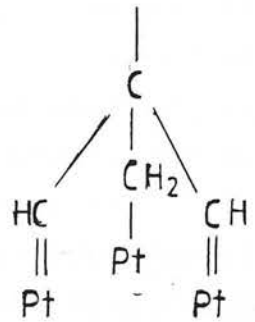

SCHEME 1.13

Five-atom sites with a step-like structure (B5 sites)[77] are thought to be present on metal crystallites larger than 1.5 nm, with a maximum relative concentration for particles of 2.0 to 2.5 nm, which is about the same range at which a maximum in catalytic activity is found for some reactions[61].

It has also been suggested that some particle size effects arise from differences in electronic properties between small and large metal particles. In particular, small Pt clusters of about six atoms have been shown to possess catalytic properties similar to those of Ir, suggesting that they are electron deficient[78].

Reactions which involve the cleavage or rearrangement of C-C bonds are frequently found to be structure sensitive[60,61,75] although sometimes a reaction appears to be structure sensitive on one metal but structure insensitive on the next[79,81]. Reactions which involve only

the cleavage and forming of H-H (H_2-D_2 exchange)[82,83] and C-H bonds (ethylene hydrogenation[84], benzene hydrogenation[85] cyclohexane dehydrogenation[83]) or labile C-C bonds (cyclopropane hydrogenation[86]) are generally found to be structure insensitive. Bearing in mind that it seems well established that the chemisorptive properties of metal atoms depend among other things on their coordination number, it is perhaps surprising that structure insensitive reactions do exist. It has been suggested that strong chemisorption of a reactant may lead to the formation of a surface substantially covered with surface molecules (corrosive chemisorption) which erase previously existing surface anisotropies[87,88]. It has also been suggested that carbonaceous layers deposited on the surface during the early stages of a reaction may be the active phase for hydrogenation-dehydrogenation reactions, thereby masking the effect of the underlying metal[89]. Kinetic compensation has been proposed to account for structure insensitivity[59]. Briefly, if it is assumed that the rate determining step of a reaction involves (or may be reduced to) the chemisorption of a reactant A on a multiple site with n atoms and that the most abundant surface intermediate B* is in equilibrium with gas phase B:

$$A + n* \xrightarrow{k} A(n_*)$$

$$B* \overset{K}{\rightleftharpoons} B + *$$

the rate expression for the reaction is given by:

$$r = \frac{kP_A}{(1 + KP_B)^n} \qquad (1.40)$$

If it is further assumed that a Brönsted type relation exists between k and K ($k \alpha K^{\alpha}$), it may be shown that large variations in K cause little change in r if n is equal to 1 (single site adsorption) but large changes

obtain if n is large. In other words, reactions which occur on small ensembles may be expected to be rather insensitive to changes in chemisorptive properties of the metal, the reverse being true for reactions which require a large ensemble. This simple concept could explain why structure insensitive reactions are also frequently less sensitive to other effects such as changes in nature of the metal and alloying effects[16,59,61].

1.16 - REFERENCES

1. K.G.Falk, Catalytic Action, Chemical Catalog Co., N.York, 1922.

2. A.J.B.Robertson, Catalysis of Gas Reactions by Metals, Springer-Verlag, N.York, 1970.

3. A.J.Ihde, The Development of Modern Chemistry, Harper and Row, N.York, 1964.

4. P.Sabatier, La Catalyse en Chimie Organique, 2nd ed., Ch.Beranger, Paris, 1920.

5. I.Langmuir, J.Am.Chem. Soc. 1917, 40, 1401

6. I.Langmuir, Trans. Faraday Soc., 1921, 17, 621

7. G.C.Bond, Heterogeneous Catalysis: Principles and Applications, Clarendon Press, Oxford, 1974.

8. R.L.Burwell, Jr., Adv.Catalysis, 1977, 26, 351

9. H.S.Taylor, Proc.Roy Soc. A, 1925, 108, 105

10. R.Ciola, Fundamentos da Catálise, Editora Moderna, São Paulo, 1981.

11. J.M.Winterbottom, in Catalysis and Chemical Processes, R.Pearce and W.R.Patterson eds., Blackie and Son, Glasgow, 1981, p.304

12. A.Wheeler, Adv.Catalysis, 1951, 4, 250.

13. K.J.Laidler, Chemical Kinetics, Tata McGraw-Hill, New Delhi, 2nd ed., 1973.

14. K.J.Laidler, in Catalysis, P.H.Emmett ed., Reinhold, N.York, 1954, v.1, p.195.

15. W.M.H. Sachtler, J.Fahrenfort, in Actes du Deuxieme Congress International de Catalyse, Technip, Paris, 1960, v.1, p.831.

16. B.C.Gates, J.R.Katzer, G.C.A.Schuit, Chemistry of Catalytic Processes, Mc-Graw-Hill, N.York, 1979.

17. A.A.Balandin, Adv.Catalysis, 1969, 19, 1

18. C.Masters, Homogeneous Transition-metal Catalysis, Chapman and Hall, London, 1981

19. A.Clark, The Theory of Adsorption and Catalysis, Academic Press, N.York, 1970

20. P.H.Emmett, in Catalysis, P.H.Emmett ed., Reinhold, N.York, 1954, v.1, p.31

21. S.Brunauer, P.H.Emmett, E.Teller, J.Am.Chem.Soc.,1938, 60, 309.

22. G.A.Somorjai, Chemistry in Two Dimensions: Surfaces, Cornell University Press, Ithaca, 1981

23. J.E.Lennard-Jones, Trans.Faraday Soc., 1932, 28, 333.

24. J.Pritchard, Trans.Faraday Soc., 1963, 59, 437

25. M.Grunze, in The Chemical Physics of Solid Surfaces and Heterogeneous Catalysis, D.A.King, D.P.Woodruff eds., Elsevier, Amsterdam, 1982.

26. J.Pritchard, F.C.Tompkins, Trans.Faraday Soc. 1960, 56, 540.

27. S.M.Davis, G.A.Somorjai, Surf.Sci, 1980, 91, 73.

28. L.H.Dubois, G.A.Somorjai, Surf.Sci, 1980, 91, 514

29. H.Conrad, G.Ertl, J.Koch, E.E.Latta, Surf.Sci, 1974, 43, 462

30. P.H.Emmett, in The Physical Basis for Heterogeneous Catalysis, E.Drauglis and R.I.Jafee eds., Plenum Press, N.York, 1975, p.1.

31. F.C.Tompkins, Chemisorption of Gases on Metals, Academic Press, London, 1978

32. K.J.Laidler, in Catalysis, P.H.Emmet ed., Reinhold, N.York, 1954, v.1, p.119.

33. M.Boudart, Kinetics of Chemical Processes, Prentice-Hall, Englewood Cliffs, 1968.

34. N.Pacia, J.A.Dumesic, J.Catalysis, 1976, 41, 155; T.Engel, G.Ertl, J.Chem. Phys., 1978, 69, 1267

35. J.M.Smith, Chemical Engineering Kinetics, 2nd Ed., Mc Graw-Hill Kogakusha, Tokyo, 1970.

36. R.B.Anderson, in Experimental Methods in Catalytic Research, R.B.Anderson ed., Academic Press, N.York, 1968, p.1

37. J.Maymo, J.M.Smith, A.I.Ch.E.J., 1966, 12, 845.

38. P.B.Weisz, J.S.Hicks, Chem. Eng. Sci., 1962, 17, 265.

39. K.Tanabe, Solid Acids and Bases, Kodansha, Tokyo, 1970.

40. H.A.Benesi, J.Phys.Chem., 1957, 61, 970

41. E.P.Parry, J.Catalysis, 1963, 2, 271

42. K.Tanabe, T.Yamaguchi, J.Res.Inst. Catalysis, Hokkaido Univ.,1964, 11, 179.

43. S.G.Hindin, S.W.Weller, J.Phys.Chem.,1956, 60, 1501

44. J.B.Peri, J.Phys. Chem., 1965, 69, 220.

45. H.Knözinger, P.Ratnasamy, Catalysis Rev.,1978, 17, 31.

46. R.C.Hansford, Adv.Catalysis, 1952, 4, 17

47. P.B.Weisz, V.J.Frillette, R.W.Maatman, E.B.Mower, J.Catalysis, 1962, 1, 307.

48. H.Pines, J.Manassen, Adv.Catalysis, 1966, 16, 49.

49. A.Clark, The Chemisorptive Bond, Academic Press, N.York, 1974.

50. O.V.Krylov, Catalysis by Non-Metals, Academic Press, N.York, 1970.

51. F.F.Vol'kenshtein, The Electronic Theory of Catalysis on Semiconductors, Pergamon Press, Oxford, 1963.

52. K.Hauffe, Adv.Catalysis, 1955, 7, 213

53. R.M.Dell, F.S.Stone, P.F.Tiley, Trans.Faraday Soc., 1953, 49, 201

54. D.A.Dowden, D.Wells, Actes du Deuxieme Congres International de Catalyse, Technip, Paris, 1960, v.2, p.1499

55. D.A.Dowden, Catalysis Rev., 1971, 5, 1.

56. G.C.Bond, Catalysis on Metals, Academic Press, London, 1962.

57. J.R.Anderson, Structure of Metallic Catalysts, Academic Press, London, 1975

58. J.H.Sinfelt, Catalysis Rev., 1973, 9, 147

59. M.Boudart, Proceedings of the Sixth International Congress on Catalysis, G.C.Bond, P.B.Wells, F.C. Tompkins eds., The Chemical Society, London, 1976, v.1, p.1.

60. M.Boudart, Adv.Catalysis, 1960, 20, 153

61. J.H.Sinfelt, Adv.Catalysis, 1973, 23, 91.

62. O.Beeck, Disc.Faraday Soc., 1950, 8, 118.

63. Z.Paal, P.Tetenyi, Nature, 1977, 267, 234.

64. L.Pauling, J.Am. Chem. Soc., 1947, 69, 542.

65. M.McD.Baker, G.I.Jenkins, Adv.Catalysis, 1955, 7, 1.

66. D.A.Dowden, in Chemisorption, W.E.Garner ed., Butterworths, London, 1957, p.3.

67. K.Tanaka, K.Tamaru, J.Catalysis, 1963, 2, 366

68. H.E.Farnsworth, R.F.Woodcock, Adv.Catalysis, 1957, 9, 3

69. E.H.Taylor, Adv.Catalysis, 1968, 18, 11.

70. I.Uhara, S.Kishimoto, T.Hikino, Y.Kageyama, H.Hamada, Y.Numata, J.Phys.Chem., 1963, 67, 996

71. B.Lang, R.W.Joyner, G.A. Somorjai, Surf.Sci, 1972, 30, 440.

72. G.A.Somorjai, Adv.Catalysis, 1977, 26, 1.

73. E.F.G.Herington, E.K.Rideal, Trans.Faraday Soc., 1944, 40, 505.

74. E.I. Gil'debrand, Int. Chem.Eng., 1966, 6, 449.

75. M.Boudart, A.W.Aldag, L.D.Ptak, J.E.Benson, J.Catalysis, 1968, 11, 35.

76. J.R.Anderson, N.R.Avery, J.Catalysis, 1966, 5, 446.

77. R.van Hardeveld, A.van Montfoort, Surf. Sci, 1966, 4, 1966.

78. R.A.Dalla Betta, M.Boudart, Proceedings of the Fifth International Congress on Catalysis, North-Holland, Amsterdam, 1973, p.1329.

79. K.Foger, J.R. Anderson, J.Catalysis, 1979, 59, 325.

80. J.Barbier, P.Marecot, Nouv. J.Chim., 1981, 5, 393.

81. S.Fuentes, F. Figueras, J.Catalysis, 1980, 61, 443.

82. K.E.Lu, R.R.Rye, Surf. Sci, 1974, 45, 667.

83. O.M.Poltorak, V.S.Boronin, Int. Chem. Eng., 1967, 7, 452.

84. J.C.Schlatter, M.Boudart, J.Catalysis, 1972, 24, 482.

85. P.Ratnasamy, J.Catalysis, 1973, 31, 466.

86. M.Boudart, A.Aldag, J.E.Benson, N.A.Dougharty, C.G.Harkins, J.Catalysis, 1966, 6, 92.

87. M.Boudart, J.Vac. Sci. Technol., 1975, 12, 329.

88. F.V.Hanson, M.Boudart, J.Catalysis, 1978, 53, 56.

89. S.J.Thomson, G.Webb, J.C.S.Chem. Comm., 1976, 526.

CHAPTER 2

STRONG METAL - SUPPORT INTERACTIONS

Chapter 2

STRONG METAL - SUPPORT INTERACTIONS

2.1 INTRODUCTION

The primary role of the support in catalysis over supported metals is to provide a large surface where the metal is deposited as small crystallites so that the largest possible active area may be obtained for a given amount of metal.

It has been known for a long time, however, that the support may influence the course of catalytic reactions either directly, by providing active sites which are not present on the metal[1], or indirectly by modifying the properties of the metal[2-6]. An important example of the former type of support effect is that of hydrocarbon reforming reactions on platinum dispersed on acidic supports, such as chlorided γ-alumina, where the metal acts mainly as a hydrogenation-dehydrogenation agent and the acidic sites on the support are primarily responsible for skeletal rearrangement processes[1]. Such catalysts are commonly referred to as dual- or bi-functional catalysts.

The semiconductive character of a support has been proposed to influence the electronic properties of small metal particles[2]. In short, the adjustment of the Fermi level of the metal particles to that of the underlying support is expected to alter the electron concentration within the metal particles thereby modifying their catalytic properties. There are many examples in the literature of reactions whose energy of activation changes in the direction expected from this theory when the semiconductive properties of the support are modified by adequate doping[2].

Differences in acid-base character of supports have also been proposed to modify the electronic properties of

metal particles. For example, the selectivity for production of alcohols in CO hydrogenation over supported Rh catalysts was found to increase with increasing support basicity[3]. This was attributed to the electron donating properties of basic supports which are thought to force Rh to acquire a Pd - like behaviour. Conversely, the methanation activity of Pd catalysts was considerably enhanced when acidic oxides were used as supports[4]. The strong electrostatic fields existing inside zeolite cages have been proposed to cause Pt particles to become electron deficient and therefore acquire a catalytic behaviour similar to Ir[5].

Interaction with the support may cause modifications in particle morphology so that certain crystal planes become preferentially exposed[6]. Reactions which are sensitive to particle structure will be also sensitive to this type of interaction.

Despite the fact that order of magnitude variations are sometimes found with respect to catalyst activity and selectivity for different supports, the gross adsorptive properties of the metal generally remain unaltered, as is clear from the good agreement that is commonly found among metal surface area determinations by chemisorptive and other methods (X - ray diffraction, transmission electron microscopy, etc...).

Recently, however, a new type of metal - support interaction has been disclosed[7], which is characterized by a strong suppression of the adsorptive capacity of the metal towards common adsorbates such as CO or H_2 when metals supported on reducible oxides[8] are reduced in hydrogen at high temperatures. Such drastic changes in adsorptive properties are generally accompanied by changes in catalytic activity and selectivity. Different reactions are suppressed to different degrees[9-12] and it has been proposed that some reactions such as CO hydrogenation may

be enhanced[13,14]. These interactions have been named "strong metal-support interactions" (SMSI)[7]. In the present chapter, recent knowledge about SMSI behaviour is reviewed.

2.2 CHEMISORPTION RESULTS

Table 2.1 summarizes a number of hydrogen and CO chemisorption results taken from several sources in the literature for TiO_2 supported catalysts. For comparison, average particle sizes determined by other methods are included, whenever available.

It is apparent from these data that, as first reported by Tauster and coworkers[7], attempts to reduce TiO_2 supported catalysts at temperatures higher than c.a. 700 K result in a more or less marked suppression of hydrogen and CO chemisorption, as compared to the same catalysts reduced at lower temperatures. Particle size determinations for these high temperature reduced (HTR) catalysts by independent methods, such as X-ray line broadening or transmission electron microscopy, indicate much smaller particle sizes than the ones derived from H_2 chemisorption measurements (examples 2-7, 11A, 12A, 13A, 14B, 14D, 15A, 17A, 18A, 19A and 21B in table 2.1). On the other hand, good agreement is found between H_2 chemisorption and other methods for catalysts reduced at temperatures below ca. 500 K (examples 12, 14, 14C, 15 and 20). For the intermediate range of reduction temperatures (500 - 700K) some discrepancy seems to exist, since Tauster and Fung[8] report a marked suppression of H_2 chemisorption for Ir/TiO_2 already at 523 K (example 21A), while large chemisorbed hydrogen to metal ratios were reported by Anderson[12] for Pt/TiO_2 reduced at 573 K (example 13). Also Fung[17] has reported suppression of H_2 chemisorption for Pt/TiO_2 reduced at 523 K (example 14A).

It seems clear that TiO_2 supported catalysts reduced at below 500 K (LTR catalysts) display normal chemisorptive

TABLE 2.1

CHEMISORPTION ON TiO_2 SUPPORTED CATALYSTS

Example[1]	Metal	% Weight	Tr/K[2]	t/h[3]	H/M[4]	CO/M[5]	d/nm[6]	Method	Reference
1	Ni	2.8	725	16	0,11	-	8.7	HC	19
							5.5	TEM	
2	Ni	15	725	16	0.043	-	23	HC	15
							10	TEM	
3	Ni	7	773	1	0.041	0.053	25	HC	16
							8	TEM	
4	Ni	12.3	773	1	0.05	0.045	20	HC	16
							9	TEM	
5	Ni	10	723	1.5	0.056	0.076	18	HC	13
							7.5	XR	
6	Ni	10	773	3	-	-	26.8	COC	10
							6.8	FMR	
7	Ni	1	773	3	-	-	8.7	COC	10
							1.9	FMR	
8	Rh	2	473	2	0.71	1.15	1.6	HC	7
8A	Rh	2	773	1	0.01	0.02	114	HC	7
9	Rh	0.95	473	4	0.98	2.17	1.1	HC	3

Example[1]	Metal	% Weight	Tr/K[2]	t/h[3]	H/M[4]	CO/M[5]	d/nm[6]	Method[7]	Reference
9A	Rh	0.95	673	?	0.24	1.71	4.5	HC	3
10	Rh	2	573	?	0.33	-	3.3	HC	9
10A	Rh	2	773	?	0.01	-	100	HC	9
11	Rh	3.2	473	2	0.25	-	4.4	HC	11
							2.3	OC	
							2.5	TEM	
11A	Rh	3.2	793	2	0.05	-	22	HC	11
							2.3	OC	
							2.3	TEM	
12	Pt	4.8	473	2	0.25	-	4.5	HC	11
12A	Pt	4.8	770	2	0.06	-	19	HC	11
							4.4	OC	
13	Pt	1	573	?	0.97	-	1.2	HC	12
							< 1	TEM	
13A	Pt	1	723	?	0.02	-	57	HC	12
							< 1	TEM	
14	Pt	2	423	1	0.63	-	1.8	HC	17
							< 5	XR	
14A	Pt	2	523	1	0.17	-	6.7	HC	17
14B	Pt	2	773	1	0	-	-	-	17
							< 5	XR	

Example	Metal	% Weight	Tr/K	t/h	H/M	CO/M	d/nm	Methods	Reference
14C	Pt[8]	2	383	1	0.08	-	14.2	HC	17
							10	XR	
14D	Pt[9]	2	773	1	0	-	-	-	16
							10	XR	
15	Pt	2	425	1	0.61	0.41	1.9	HC	18
							< 5	XR	
15A	Pt	2	875	1	0	0	-	-	18
							< 5	XR	
15B	Pt[10]	2	423	1	0.13	0.09	8.7	HC	18
15C	Pt[11]	2	423	1	0.39	0.26	2.9	HC	18
16	Pt	2	473	2	0.88	0.05	1.3	HC	7
16A	Pt	2	773	1	0	0.03	3	HC	7
17	Pd	1.86	448	1	0.18	0.23	6.2	HC	19
17A	Pd	1.86	773	1	0.03	0.07	37	HC	19
							< 5	XR	
18	Pd	2	448	2	0.93	0.53	1.2	HC	7
18A	Pd	2	773	2	0.05	0.02	22	HC	7
							< 1	TEM	
18B	Pd[12]	2	448	1	0.89	-	1.2	HC	7
19	Ir	2.7	473	2	0.61	-	1.7	HC	11
							2.3	TEM	

Example	Metal	% Weight	Tr/K	t/h	H/M	CO/M	d/nm	Methods	Reference
19A	Ir	2.7	793	2	0.06	-	17.5	HC	11
							2.3	TEM	
20	Ir	0.8	473	?	1.04	-	-	-	12
							< 1	TEM	
20A	Ir	0.8	723	?	0.04	-	28	HC	12
							< 1	TEM	
21	Ir	2	393	1	1.17	-	-	-	8
21A	Ir	2	523	1	0.32	-	3.2	HC	8
21B	Ir	2	773	1	0.02	-	52	HC	8
							< 1	TEM	
22	Ir	2	473	2	1.6	1.19	-	-	7
22A	Ir	2	773	1	0	0	-	-	7
23	Ru	2	473	2	0.23	0.64	5.8	HC	7
23A	Ru	2	773	1	0.06	0.11	22.1	HC	7
24	OS	2	473	2	0.21	-	6.4	HC	7
24B	OS	2	773	1	0.11	-	12.2	HC	7

(1) Examples with the same number correspond to different treatment of the same catalyst preparation.

(2) Reduction temperature

(3) Reduction time

(4) Hydrogen/metal ratio by hydrogen chemisorption

(5) CO/metal ratio by CO chemisorption

(6) Average particle diameter

(7) HC-Hydrogen chemisorption; XR - X- ray diffraction line broaduring; TEM - Transimision electron microscopy; COC-CO chemisorption; FR - Ferromagnetic resonance spectoscopy; OC-Oxygen chemisorption.

(8) 14B exposed to air at 773K and re-reduced at 383K.

(9) 14C re-ereduced at 773K.

(10) 15A exposed to water vapour at 525K and re - reduced at 423K.

(11) 15A exposed to oxygen at 875K and re-reduced at 423K.

(12) 18A exposed to oxygen at 673K and re-reduced at 448K.

behaviour and that the suppression of chemisorption observed for catalysts reduced at higher temperature is not due to metal particle growth.

Careful experimentation by Tauster and coworkers[7] has also established that this effect cannot be attributed to metal encapsulation due to sintering of the support, since no difference in BET surface area was found for catalysts reduced at 473 and 773 K and since the suppression effect was reversible by oxidation at 673 K. Also repetition of the HTR treatment after reoxidation resulted in reproduction of the chemisorption suppression efect , which renders it unlikely that the effect could be due to diffusion of support impurities,such as sulfur, to the metal surface.

No water could be observed in the gas phase when a HTR Ir/TiO_2 catalyst was exposed to oxygen at 773 K[20]. This indicates that the suppression effect is not caused by formation of a strongly chemisorbed form of hydrogen that cannot be removed by evacuation at 773 K.

CO and H_2 adsorption isobars obtained for a 7% Ni/TiO_2 catalyst subjected to HTR showed that activated chemisorption cannot be responsible for the small chemisorption uptakes observed at room temperature[16]. In the temperature range from 300 to 600 K, only a shallow hydrogen adsorption maximum could be observed, which was not large enough to account for the suppression effect. CO uptakes were considerably larger at 300 K than at higher temperatures.

It is well established that a reoxidation treatment is capable of restoring normal chemisorptive behaviour to HTR catalysts. This may be achieved by exposing the HTR catalysts either to air[7,17,18] or to water[18] at elevated temperatures (examples 14B, 15B, 15C and 18B in table 7.1). Interestingly, however, Meriaudeau and coworkers[11]

found that exposure to oxygen even at 293 K is capable of substantially restoring the normal chemisorptive properties of HTR catalysts. These investigators also report that particle sizes determined from oxygen chemisorption measurements on Pt/TiO_2 and Rh/TiO_2 HTR catalysts were in good agreement with those determined from TEM measurements. This is in agreement with Smith and coworkers[16] findings regarding Ni/TiO_2 catalysts, although in this case a different O/Ni stoichiometry had to be assumed from the one prevalent for Ni/SiO_2 and Ni/Al_2O_3.

SMSI behaviour is not limited to TiO_2 supported catalysts. Tauster and Fung[8] investigated the hydrogen chemisorption properties of Ir supported on several oxides from groups IIA to VB. Reducible supports (V_2O_3, Nb_2O_5, Ta_2O_5) led to hydrogen chemisorption suppression similarly to TiO_2, while normal chemisorptive behaviour was observed for Ir on non-reducible supports (MgO, Sc_2O_3, Y_2O_3, ZrO_2, HfO_2) when reduced at temperatures up to 973 K. It should be noticed, however, that some suppression of H_2 chemisorption has been reported for Pt/Al_2O_3 reduced at temperatures above 773 K[21] and for Ni/SiO_2 at above 1100K[22], which has been attributed to metal - support interactions due to support reduction.

Resasco and Haller[23] found that SMSI Rh/TiO_2 is capable of chemisorbing nitrogen at 523 K, a property that is not exhibited by LTR Rh/TiO_2 or by Rh supported on other materials, unless promoted by alkali metals. This was attributed to electron donation from reduced Ti cations to Rh, similarly to the proposed explanation for the promoting effect of alkalis. Burch and Flambard[24], however, have shown that TiO_2 itself, when subjected to HTR treatment adsorbs a considerable amount of nitrogen at 273 K, the effect being merely enhanced by the presence of Ni. The amount of adsorbed nitrogen was independent of the metal content in the range 1 to 5% Ni. It was thus

proposed that nitrogen adsorbs on exposed Ti^{3+} cations produced in larger amounts in the presence of Ni.

Bor-Her Chen and White[25] prepared a series of Pt catalysts supported on lower oxides of titatium (TiO, Ti_9O_{17}). These oxides were shown to suffer only surface oxidation when exposed to air. When Pt was deposited on these oxides and reduced at low temperature chemisorptive properties typical of SMSI catalysts resulted. It was concluded that SMSI behaviour is determined by the bulk semiconductive properties of the support and not by specific interactions between Pt and reduced cations on the support surface.

Wang Hongli and coworkers[26] studied SMSI phenomena with Pt/TiO_2 catalysts using hydrogen chemisorption and temperature programmed desorption (TPD) techniques. The measurements consisted in reducing the catalysts samples at a selected temperature, cooling the sample under hydrogen to room temperature and obtaining the TPD profile using argon as the carrier-gas. Repeated TPD profiles were obtained with or without exposure of the samples to hydrogen at room temperature before performing the TPD run. When the catalysts were reduced at 573 K, two desorption peaks were obtained with maxima at 403 and 563 K and hydrogen chemisorption at room temperature was observed. When the catalysts were reduced at 773 K no hydrogen chemisorption at room temperature could be measured but profuse desorption of hydrogen was observed at above 473 K during the TPD run up to the highest temperature used in the experiments (823 K). When successive TPD runs were performed with the same HTR catalyst sample without intermediate exposure to hydrogen at room temperature, progressively smaller amounts of hydrogen were desorbed at high temperature. After a few TPD cycles the sample recovered its capacity for hydrogen chemisorption and a TPD run performed after exposing the sample to hydrogen at room temperature revealed the two

TPD peaks characteristic of LTR Pt/TiO_2. It was proposed that during high temperature reduction hydrogen is stored on the surface of the support or perhaps diffused into the bulk. During a single TPD run part of this stored hydrogen migrates back to the metal surface and is desorbed. As the sample is cooled to room temperature after the TPD run, hydrogen continues to migrate from the support to the metal so that a subsequent attempt to measure hydrogen chemisorption will find the metal surface already occupied and no hydrogen uptake will be recorded. After a number of TPD cycles without intermediate exposure to hydrogen the support becomes depleted of hydrogen and normal chemisorptive properties are restored to the metals. Thus, in the view of Wang Hongli and coworkers[26], there is no loss in chemisorptive capacity of the metal but instead the metal surface becomes saturated with hydrogen before hydrogen chemisorption can be measured.

2.3 ACTIVITY AND SELECTIVITY OF TIO_2 SUPPORTED CATALYSTS

As mentioned before,the drastic modifications in chemisorptive properties characteristic of SMSI behaviour are accompanied by changes in catalytic activity and selectivity. A number of reactions, including CO hydrogenation[3,13,14,24,27-32],cyclohexane dehydrogenation[10,33] and hydrogenolysis[10,33], benzene and styrene hydrogenation[11] and ethane[10,33,34], neopentane[12] and n-butane[11] hydrogenolysis and isomerization have been studied in this respect. Some of the most important results from these studies are reviewed below.

It should be noticed that choosing an adequate basis for expressing catalyst activity is a problem in SMSI studies. It is not clear whether turnover frequencies should be expressed in terms of metal surface area or in terms of the number of active sites counted from hydrogen chemisorption measurements on HTR catalysts. In the discussion that follows, comparison of catalyst activity are made on a metal surface are basis (determined, e.g.,

from H_2 chemisorption measurements on the corresponding LTR catalyst), regardless of the criteria used by the authors of the relevant papers.

2.3.1 - Hydrocarbon Reactions

The hydrogenolysis of ethane was studied by Ko and Garten[34] over TiO_2 supported group VIII metals subjected to the HTR treatment. Suppression of hydrogenolysis activity at 478 K, relative to SiO_2 supported metals, was found to accompany SMSI generation. Assuming 100% dispersion for the TiO_2 supported catalysts (which should be approximately true, since no metal X - ray diffraction peaks were observed after the HTR treatment),hydrogenolysis suppression factors (suppression factor = rate on the SiO_2 metal relative to the rate on the TiO_2 supported metal) varied from nearly 1 (Ru) to > 10^6 (Fe), lying in the range from 10 to 10^4 for the remaining metals. In most cases, activation energies were similar for TiO_2 and SiO_2 supported metals, with exception of Ni and Ir, where the activation energies were, respectively, considerably lower (130 vs. 171 K J mol^{-1}) and considerably higher (217 vs. 150 K J mol^{-1}) for the TiO_2 supported metal. Due to their very low activity, no energies of activation were reported for HTR Pt/TiO_2 and Fe/TiO_2. Reaction orders with respect to hydrogen and ethane, used in conjunction with Sinfelt's kinetic analysis for ethane hydrogenolysis[35], indicated that the hydrogen deficient surface species, C_2H_x, thought to be involved in the carbon-carbon bond scission step, was less dehydrogenated on TiO_2 supported than on SiO_2 supported Ni, Pd and Os. With Ru and Rh, for which hydrogenolysis suppression was smallest, x values were the same for the metals supported on both carriers. It should be noticed that the less negative ordersin hydrogen observed by Ko and Garten[34], may simply mean that ethane competes more favourably with hydrogen for the surface of SMSI catalysts, since Sinfelt's analysis neglects competition effects.

Engels and coworkers[33] studied the hydrogenolysis of ethane and the reactions of cyclohexane over Al_2O_3 and TiO_2 supported Ni. Large suppression factors for ethane hydrogenolysis on Ni/TiO_2 relative to Ni/Al_2O_3 are apparent from the results presented. It was necessary to increase reaction temperature by 100 K, in the case of a moderately dispersed sample (7nm average particle size), and by more than 180 K, in the case of a well dispersed sample (2nm average particle size), in order to obtain on HTR Ni/TiO_2 activities comparable to those of Ni/Al_2O_3 catalysts of similar dispersion. In cyclohexane dehydrogenation, suppression was only found for the well dispersed Ni/TiO_2 catalyst. With Al_2O_3 supported Ni,a deep hydrogenolysis reaction, leading to complete degradation of the carbon skeleton to methane, was important for particle sizes larger than ca. 2nm during cyclohexane dehydrogenation, but was absent on the Ni/TiO_2 catalysts. Hydrogenolysis seemed to be, therefore, more susceptible to the SMSI effect than dehydrogenation. Engels and coworkers explained their results from the point of view of an ensemble dilution effect, caused by contamination of the Ni surface by titanium ions during the HTR treatment.

Similar results were obtained by Haller and coworkers[9], who studied ethane hydrogenolysis and cyclohexane dehydrogenation on Rh/SiO_2 and Rh/TiO_2. The suppression factors for a 2% Rh/TiO_2 catalyst reduced at 773 K, relative to the same catalyst reduced at 573 K,was in the order of 10^5 for ethane hydrogenolysis and near to 1.3 for cyclohexane dehydrogenation. At the same time, the ratio of cyclohexane dehydrogenation to cyclohexane hydrogenolysis increased from 14 to 60 in moving from the LTR to the HTR Rh/TiO_2 catalyst. Cyclohexane hydrogenolysis appears, therefore, to be less sensitive than ethane hydrogenolysis to SMSI. When LTR Rh/TiO_2 was compared with Rh/SiO_2, larger turnover frequencies (by about one order of magnitude) were found in ethane hydrogenolysis on highly dispersed Rh/TiO_2,while, with decreasing dispersion,

the activity of Rh/TiO_2 approached that of Rh/SiO_2. These LTR Rh/TiO_2 samples had been subjected to an oxidation, treatment at 673 K before reduction at 573 K. Haller and coworkers suggested that a support effect opposite to that of SMSI was responsible for the higher activity of pre-oxidized LTR Rh/TiO_2 relative to Rh/SiO_2. It was also proposed that the different sensitivities of different reactions towards SMSI reflect the extent to which these reactions occur on particles of different sizes. Thus, reactions which occur preferentially on small metal particles would suffer a larger degree of suppression when the catalyst is in the SMSI state, due to a selective deactivation of the smallest particles in the particle size distribution.

Anderson[12] studied the hydrogenolysis of neopentane on Pt/TiO_2 and Ir/TiO_2 catalysts. The LTR 473 K) TiO_2 supported catalysts were found to behave very similarly to the corresponding SiO_2 supported metals. Suppression factors in the order of 10^2 or more were found for HTR (723 K) catalysts, relatively to LTR samples. In the case of Pt/TiO_2, a threefold increase in isomerization selectivity was found to accompany generation of the SMSI state. Both the activity and the selectivity effects were attributed to a common factor, namely the decreased hydrogen concentration on the surface of SMSI catalysts. A hydrogen poor surface would tend to favour the formation of irreversibly chemisorbed carbonaceous residues, with a consequent decrease in catalyst activity. At the same time, according to a mechanism previously proposed by the author[36], the chance of isomerization relatively to hydrogenolysis increases.

Meriaudeau and coworkers[11] investigated the hydrogenation of benzene (228 K), ethylene (196 K) and styrene (288 K), the dehydrogenation of cyclohexane (523 K) and the hydrogenolysis of n-butane (503-623 K) on TiO_2 supported Rh, Ir and Pt. Suppression factors in the range of 2 to 20 were found for most hydrogenation - dehydrogenation reactions ,

with the exception of the partial hydrogenation of styrene to ethylbenzene, for which complete suppression was reported with all HTR catalysts. Reaction rates were, however, comparatively small in this last case, even for LTR catalysts, so that it is difficult to evaluate, from the data presented, the meaning of a zero reaction rate. Suppression factors in the order of 10^2 were observed for n-butane hydrogenolysis on HTR Pt/TiO_2 relative to the corresponding LTR catalysts. With Ir/TiO_2, complete suppression of this reaction was reported. Contrary to Anderson's findings in the reactions of neopentane[17], n-butane isomerization was more susceptible to the SMSI effect than n-butane hydrogenolysis on Pt/TiO_2. While isobutane accounted for more than 45% of the reaction products on the LTR catalyst, no isomerization products were found on HTR Pt/TiO_2. Filling of the d-band of the metal caused by electron transfer from the reduced support to the metal particles was proposed to account for the observed SMSI effects.

2.3.2 - Hydrogenation of Carbon Monoxide

There is currently a considerable interest in CO hydrogenation reactions due to their possible application in obtaining liquid fuels from coal, either directly from synthesis gas (Fischer-Tropsch process) or via methanol using high-silica zeolites[37]. Much interest in TiO_2 supported systems has been prompted by the discovey by Vannice and Garten[13] that TiO_2 supported Ni is one or two orders of magnitude more active for CO hydrogenation reactions than Ni supported on other materials and with a distinct shift in selectivity for production of higher molecular weight products. At atmospheric pressure and in the 490 to 530 K temperature range, unsupported Ni or Ni supported on alumina, silica and graphite produced methane with more than 80% selectivity on a % mole basis.Selectivity for methane on Ni/TiO_2 was 50 to 60%, corresponding to nearly 80% of the CO being converted to higher hydrocarbons,

mainly in the C_2 to C_4 range. Titania supported Ni was found to be more resistant to surface carbiding and to display a much smaller tendency for nickel carbonyl formation. The fact that increased activity for methanation was observed on Ni/TiO_2 indicated that the shift in selectivity was due to an enhancement of carbon-carbon bond making reactions rather than to a suppression of methanation. It was proposed that the CO chemisorption bond is weaker on the TiO_2 supported catalyst, resulting in less dissociative chemisorption of CO and consequently in a higher ratio of molecularly adsorbed CO to reactive surface carbon[27]. This was thought to enhance chain growth reactions over methanation. It was also proposed that a weaker chemisorption of CO could be associated with the increased overall activity of Ni/TiO_2[13].

Bartholomew and coworkers[14] also found much increased overall activities and selectivities for C_{2+} production on Ni/TiO_2 relative to those of Ni/SiO_2, unsupported Ni and poorly dispersed Ni/Al_2O_3. Highly dispersed Ni/Al_2O_3, however, displayed large selectivities for C_{2+} production ($C_{2+}/CH_4 \sim 5$ for 60% Ni dispersion), a fact that was correlated with the increasing ratio of adsorbed CO to adsorbed hydrogen with increasing metal dispersion observed in chemisorption experiments. Thus, in the view of Bartholomew and coworkers, large CO/H chemisorption ratios are to be associated with large C/H ratios in the hydrocarbon products. A particular sample of Ni/Al_2O_3, which was prepared by a controlled precipitation method rather than by impregnation, had a total activity approaching that of Ni/TiO_2 and nearly two orders of magnitude higher than impregnated Ni/Al_2O_3. These facts were explained by assuming increased metal - support interaction with Ni/TiO_2 and precipitated Ni/Al_2O_3 accompanied by electron transfer from the metal to the support, resulting in a behaviour similar to that of cobalt, which is more active and selective for C_{2+} production than nickel.

Burch and Flambard[24,38] studied the hydrogenation of benzene, the hydrogenolysis of n-hexane, the hydrogenolysis of ethane and CO hydrogenation on Ni/TiO_2 and Ni/SiO_2 containing ca. 10wt% of Ni. Samples reduced in hydrogen at 573 K and 723 K were investigated. It was observed that 10% Ni/TiO_2 reduced at either temperature had normal behaviour for all of the hydrocarbon reactions investigated, but that Ni/TiO_2 reduced at 723 K was nearly 40 times more active than Ni/SiO_2 in CO hydrogenation. No results were presented for Ni/TiO_2 reduced at 523 K for this reaction. It was concluded that the sites responsible for CO hydrogenation are distinct from the ones involved in hydrocarbon reactions and are located at the metal-support interface, since only CO hydrogenation sufferred a strong influence from the support.

Although pretreatment conditions in the CO hydrogenation work cited so far were such that development of the SMSI state would be expected, it is not clear that the effects reported were due to SMSI behaviour, since no comparison with LTR catalysts were made. Thus, it may not be excluded that the enhanced activity of Ni/TiO_2 for CO hydrogenation is related to the nature of the support rather than to its state of reduction.

Katzer and coworkers[3] studied CO hydrogenation on Rh supported on several oxides (TiO_2, Al_2O_3, CaO_2, SiO_2 and MgO). The activity of Rh/TiO_2 reduced at 473 K was more than one order of magnitude larger than that of Rh on any other support. Futhermore, there was reportedly no significant change in rate, on a gram metal basis, when Rh/TiO_2 was reduced at 673 K, despite the fact that significant suppression of H chemisorption was observed (see example 9 in table 2.1). It was proposed, therefore, that in this case it was the nature of the support which determined the enhancement of the rate of CO hydrogenation. This rate enhancement was related to the number of active sites available and not to changes in the energetics of

the reaction, since the activation energy for methanation was the same on all catalysts. As in the case of Ni/TiO_2[14], Rh/TiO_2 produced more C_{2+} products than Rh on other supports, but most of the C_{2+} hydrocarbons appeared as olefins on Rh/TiO_2, while on other supports only saturated hydrocarbons were observed. Methanol and small amounts of ethanol were also present in the reaction products. The selectivity for alcohol formation increased in the order: $Rh/TiO_2 < Rh/Al_2O_3 < Rh/CeO_2 < Rh/SiO_2 < Rh/MgO$.

On Rh/MgO, methanol was the main reaction product, methane being the only other product reported. The observed order for increasing alcohol selectivity was similar to the decreasing order of support acidity ($Al_2O_3 > TiO_2 > CeO_2 > SiO_2 > MgO$). The only inversion occurred for the Al_2O_3- TiO_2 pair. Accordingly, it was proposed that with basic oxides electron transfer occurs from the support to the metal particles forcing Rh to behave as Pd, which is methanol selective in CO hydrogenation. On more acidic supports, Rh displays a Fischer - Tropsch behaviour.

Qualitatively similar results were obtained by Solymozi and coworkers[28] for CO hydrogenation on Rh supported on TiO_2, Al_2O_3, SiO_2 and MgO. The selectivities for C_{2+} formation were similar with Rh/TiO_2 and Rh/Al_2O_3 and higher than those obtained with Rh/SiO_2 and Rh/MgO. No alcohols were reported as reaction products. Dissociation of CO was found to decrease in the order $Rh/TiO_2 > Rh/Al_2O_3 > Rh/SiO_2 > Rh/MgO$ and was held responsible for the large amount of carbon deposited on Rh/TiO_2 during the reaction. Considering that methanol formation on Rh has been shown to occur by a non-dissociative mechanism, the order of increasing CO dissociation reported by Solymozi et al. is in agreement with the one observed by Katzer and coworkers[3] for decreasing selectivity for alcohol production. Also in agreement with Katzer et al[3]. it was reported that catalyst reduction

temperature exerted little influence on the results. In the related CO_2 hydrogenation reaction[39], the same order of activities for Rh on different supports was found to apply.

Solymozi and coworkers[28] attributed the observed effects to electron transfer from the n - type semiconductor TiO_2 to the Rh crystallites,which increases electron backdonation to the π antibonding orbital of CO with a consequent strengthening of the carbon-metal bond and weakening of the carbon-oxygen bond.

In contrast with Rh, Vannice and Garten[29] found a lower activity for Ru/TiO_2 as compared to Ru supported on SiO_2, carbon or unsupported Ru. Similar C_{2+}/methane ratios were obtained for Ru/TiO_2,Ru/Al_2O_3 and unsupported Ru,but olefin formation increased in the order $Ru < Ru/Al_2O_3 < Ru/TiO_2$. Ruthenium supported on SiO_2 and on carbon produced more methanation and less olefin formation than the remaining catalysts. The increased olefin production on Ru/TiO_2 was attributed to electron transfer from the metal crystallites to the support, with a consequent decrease in the rate of olefin hydrogenation due to the reduced % d - character of Ru. Since no data were reported for LTR Ru/TiO_2 it is not clear that the SMSI state of the HTR Ru/TiO_2 catalyst was responsible for the observed effects.

Vannice and coworkers[30] studied CO methanation on Pt supported on TiO_2, Al_2O_3, SiO_2 - Al_2O_3 and SiO_2. Results for both LTR and HTR Pt/TiO_2 were reported and the ratio of rates on HTR to LTR catalysts under identical reaction conditions (101 kPa and 548 K) ranged from 0.7 to 4. The Pt/TiO_2 catalyst was from 7 to 20 times more active than Pt/Al_2O_3 or Pt/Al_2O_3 - SiO_2 and these catalysts in their turn were about 10 times more active than Pt/SiO_2. Therefore, as in the case of Rh, the nature of the support was the dominant factor in determining the relative

activities for CO hydrogenation and not its state of reduction.

Similar observations are valid for supported Pd catalysts in the CO methanation reaction[31]. Both LTR and HTR catalysts had an activity similar to that of Pd/Al_2O_3 and Pd/SiO_2- Al_2O_3, but more than one order of magnitude larger than that of Pd/SiO_2. Activation energies covered a range from 80 to 110 kJ mol^{-1} with apparently no correlation with particle size or support. Approximate reaction orders relative to hydrogen and CO were, respectively, 0.5 and 0 on Pd/TiO_2 and 1 and 0 on Pd supported on the other materials. It was proposed that the rate determining step on Pd/TiO_2 involves a reaction of adsorbed CO with hydrogen atoms while, on other supports, reaction with hydrogen molecules is favoured. This would be consistent with the observation that hydrogen was found to be capable of displacing adsorbed CO from Pd/TiO_2, but not from Pd on other supports[19]. As in the case of Rh and Pt, the state of reduction of the support exerted little influence on the results when turnover frequencies were expressed on a basis of metal surface area.

Vannice[32] studied CO methanation over several group VIII metals supported on TiO_2 and Al_2O_3. Since it was not possible to estimate metal surface areas for the TiO_2 supported catalysts from the data presented, comparison of intrinsic activities is difficult. On a gram metal basis, however, relatively large activity enhancements for TiO_2 supported metals relative to the metals supported on Al_2O_3 were found only with Ni and Ir. With Ru, Rh, Pd, Pt and Co, activities per gram of metal were similar for TiO_2 and Al_2O_3 supported catalysts with comparable metal loadings. Alumina supported Fe was more active than Fe/TiO_2 by several orders of magnitude. Since only HTR catalysts were studied, it is difficult to evaluate the influence of the SMSI state of the catalysts on their performance.

In summary, a clear support effect exists in CO hydrogenation reactions on group VIII metals affecting both catalyst activity and selectivity. The effects observed with TiO_2 do not seem to be related to the SMSI state induced after a HTR reatment. This fact is intriguing, bearing in mind the marked influence of catalyst reduction conditions on the chemisorptive properties of TiO_2 supported metals as well as on their performance in reactions of hydrocarbons. This may be due[40] to the fact that water is produced during CO hydrogenation and it has been shown that exposure of SMSI catalysts to water at elevated temperatures destroys the metal-support interaction[18].

2.4 - PHYSICAL CHARACTERIZATION OF SMSI CATALYSTS

A number of physical caracterization methods have been used in SMSI studies, including transmission electron microscopy (TEM), electron spin resonance (ESR), X - ray photoelectron spectroscopy (XPS),ultraviolet photoelectron spectroscopy (UPS) and Mössbauer spectroscopy.

Transmission electron microscopy was first used in SMSI studies by Baker and coworkers[41] who investigated the behaviour of Pt deposited under vacuum on thin films (ca. 35 nm) of TiO_2, Al_2O_3, SiO_2 and carbon. Particles of similar sizes and shapes were obtained on all supports after reduction in hydrogen at 425 K. Reduction of the Pt/TiO_2 specimen at 825 K and higher temperatures resulted in the formation of thin (ca.2nm thickness), flat pill-box structures of uniform thickness. Simultaneously,reduction of the TiO_2 support to the crystallographic shear phase Ti_4O_7 was observed from electron diffraction measurements. In the absence of Pt, only crystallization of the initially amorphous TiO_2 to a rutile structure could be observed after exposure to H_2 at 1075K. Little growth of the metal particles was apparent for the Pt/TiO_2 sample for reduction temperatures between 825 and 1075K, contrary to the case

of Pt on the other supports.

Subsequent work by the same authors[18] demonstrated that exposure of the HTR Pt/Ti_4O_7 film to water at 525 K led to appreciable increase in thickness of the metal particles, while the support was converted back to TiO_2. Globular Pt particles were obtained after exposure of the HTR sample to oxygen at 875 K.

The formation of raft-like metal particles under SMSI conditions has been confirmed by several investigators on Ni/TiO_2[14-16] and Pt/TiO_2 powders[41] and on Fe/TiO_2 films[42]. Meriaudeau and coworkers[11], however, failed to detect raft-like structures on Ir/TiO_2 and Rh/TiO_2 under SMSI conditions but observed such structures on Pt/TiO_2 even after mild reduction (ca.573 K). Also Huizinga and Prins[43] have reported raft-like Pt crystallites on Pt/TiO_2 reduced at 573 K. Raft-like particles have also been observed with Rh supported on carriers other than TiO_2[44].

The fact that SMSI behaviour is characteristic of metals deposited on reducible oxides strongly suggests that the effect is associated with partial reduction of the support. Since the Ti^{3+} ion is paramagnetic, it is possible to follow the reduction of TiO_2 by ESR spectroscopy. A strong Ti^{3+} ESR signal has been reported for pure TiO_2 reduced at temperatures as low as 473 - 573 K[11,43,45]. Interestingly this signal has been found to be absent from TiO_2 reduced at 673 K[45], although conflicting reports exist regarding this point[11].

Huizinga and Prins[43] found that reduction of a Pt/TiO_2 sample at 573 K, followed by evacuation a 293 K, resulted in a Ti^{3+}/Ti^{4+} ratio about 30 times larger than the one observed with pure TiO_2 treated under the same conditions. Subsequent evacuation of the Pt/TiO_2 sample at 573 K led to a suppression of the Ti^{3+} signal by a factor of 100. Reduction of Pt/TiO_2 at 773 K produced a

Ti^{3+}/Ti^{4+} ratio similar to the one found with the sample reduced at 573 K and evacuated at 293 K, but the Ti^{3+} signal was suppressed by a factor of only 2 after evacuation at 573 K. It was proposed that reduction at 573 K leads to spillover of hydrogen atoms from the metal surface to the support with production of hydroxyl anions and Ti^{3+} cations. Upon evacuation at 573 K hydrogen migrates back to the metal and Ti^{3+} is oxidized back to the 4 + state. When reduction is carried-out at 773 K, hydroxyl groups are eliminated as water from the support and the mechanism available for back migration of hydrogen is removed. In the view of Huizinga and Prins[43] dehydration of reduced TiO_2 leads to formation of Ti_4O_7, as reported by Baker and coworkers[41]. Interaction between the metal and this lower oxide of titanium was proposed to be responsible for the SMSI state.

Similarly to Huizinga and Prins[43], Meriaudeau and coworkers found a 10 times larger Ti^{3+} concentration in Pt/TiO_2 and Ir/TiO_2 reduced at 473 K as compared to pure TiO_2 reduced at the same temperature. However, no marked increase in Ti^{3+} concentration could be observed when the catalysts were reduced at 773 K.

The interaction between Pt and TiO_2 was studied by Fung[17] using XPS. A 1.6 eV decrease in binding energy (B.E.) of $Pt4f_{7/2}$ electrons was found after reduction at 623 K of a vacuum deposited Pt/TiO_2 film sample relative to a sample which received no hydrogen treatment. No further change in B.E. occurred after reduction at 873 K, which was close to that of bulk metallic Pt. A 2% Pt/TiO_2 powder reduced at 423 K produced a broad emission in the Pt 4f region which was attributed to a superposition of the low and high B.E. bands observed for the Pt/TiO_2 film sample. After reduction at 473 K, the high B.E. state started to disappear and was largely suppressed after reduction at 823 K. A vacuum deposited Pt/SiO_2 film sample did not display any significant shift in B.E, before and

after reduction at 573K. The B.E. energy for the Pt/SiO_2 film was 0.6 e V higher than that of bulk Pt.

Upon reduction at 873 K, a signal ascribed to Ti^{3+} appeared as a shoulder on the Ti^{4+} $2P_{3/2}$ line. It was proposed that the high B.E. Pt species is the one responsible for hydrogen chemisorption while the low B.E. species is the one in strong interaction with the support due to electron transfer from Ti^{3+} ions to Pt. It is interesting,however, that sintering of the HTR Pt/TiO_2 powder in air at 773 K, followed by reduction in hydrogen at 383 K resulted in the appearance of a Pt species with a $Pt4f_{7/2}$ B.E. value 1.2 e V lower than the one obtained when the sample was first reduced at 473 K. Reduction at 773 K led only to a further 0.1 e V decrease in B.E. The small value of the B.E. shift for the sintered HTR catalyst as compared to the sintered LTR catalyst was attributed to a decrease in electron transfer per Pt atom due to particle growth. It is then difficult to understand why suppression of hydrogen chemisorption was observed with the sintered HTR Pt/TiO_2 powder. This, plus the fact that extra-atomic relaxation effects, which may cause particle size dependent shifts in B.E., were not quantitatively taken into account seems to render Fung's results somewhat inconclusive.

Kao and coworkers[46] studied the Ni/TiO_2 system using a combination of XPS, UPS, LEED and Auger electron spectroscopy. Nickel was vacuum deposited on both unsputtered and argon - sputtered TiO_2 surfaces. The relevant findings of this study may be summarized as follows:

- Sputtering of the rutile (110) surface resulted in a decrease of the O/Ti surface ratio,which was further reduced by subsequent annealing at 673 K;

- This was accompanied by the appearance of reduced Ti cations (3 + or lower) that disappeared upon Ni deposition, indicating electron transfer from Ti^{3+} to the metal;

- Annealing of the Ni deposited sample for 5 minutes at 573 K or higher temperature resulted in Ni diffusion into the TiO_2 crystal. The diffusion length with the 573 K treatment was estimated in ca. 0.8 nm;

- The amount of charge transferred to Ni was found to be 0.13 electrons per Ni atom for the unsputtered surface and decreased with decreasing O/Ti ratio, implying that charge transfer to Ni may arise from Ni - O^{2-} interactions.

Although it is doubtful to what extent creation of defect centres on the TiO_2 surface through argon ion sputtering correctly simulates the high temperature reduction in hydrogen of TiO_2 supported catalysts, it is interesting that the effect observed by Kao and coworkers is opposite to that reported by Fung[17], i.e., there was less electron transfer to the metal on the surface which is more deficient in oxygen.

Tartachuck and Dumesic[42 47 48] investigated the Fe/TiO_2 system using a combination of TEM, XPS and Mössbauer spectroscopy. In their experiments, a Fe overlayer of 2.5 to 5nm thickness was deposited under vacuum on a ca. 50 nm thick rutile film, created by oxidation of a Ti foil, and subjected to various reduction treatments. Their results indicated that, as in the case of Ni, Fe diffusion into the support occurs upon reduction at 773 K or higher temperature. Reduction of the support assisted by Fe was observed at or above 875 K leading to formation of Ti^{3+} cations or lower Ti oxidation states. Simultaneously, a new Fe containing phase was created which was attributed to γ - Fe or to Fe_x Ti clusters and which was not present at lower reduction temperatures. Oxidation of this metallic species occurred only at 674 K with formation of mixed Fe - Ti oxides.

Herrmann and coworkers[40], studied the changes in electrical conductivity of Pt/TiO_2 and of pure TiO_2

(anatase) which accompany reduction in hydrogen at different temperatures. The effects of hydrogen chemisorption at room temperature and of titration of chemisorbed hydrogen with oxygen on electrical conductivity were also measured. The conductivity of Pt/TiO_2 after reduction at 473 K was two orders of magnitude higher than that of pure TiO_2, which was taken as evidence for the Pt catalysed reduction of TiO_2 at this temperature. Subsequent evacuation at 673 K increased the conductivity of TiO_2 by two orders of magnitude and decreased the conductivity of Pt/TiO_2 by a factor of 2 if conductivity was measured at 673 K. When the measurements were made at room temperature still under vacuum, the conductivity of Pt/TiO_2 decreased by three orders of magnitude but that of pure TiO_2 decreased by less than one order of magnitude. The increase in the conductivity of TiO_2 upon high-temperature evacuation was attributed to loss of oxygen from the surface with consequent creation of positively ionized anion vacancies. When platinum is present on the surface of TiO_2 electrons migrate to the metal crystallites and conductivity decreases. The small conductivity of Pt/TiO_2 at room temperature (three orders of magnitude smaller than the conductivity at 673 K) was related to the high energy of activation for conduction with this catalyst. Admission of hydrogen at room temperature to the Pt/TiO_2 catalyst reduced at 473 K and evacuated at 673 K caused the conductivity at room temperature to increase by two orders of magnitude. This was attributed to spillover of hydrogen from the metal to the support with consequent formation of hydroxyl anions and liberation of conduction electrons. No change in conductivity was observed on admission of hydrogen to TiO_2 reduced at 473 K.

Reduction at 773 K caused a marked increase in conductivity of all catalyst and little difference was found between TiO_2 and Pt/TiO_2, indicating that at this temperature the reduction of TiO_2 is not catalysed by Pt. There was little change in conductivity upon subsequent

evacuation at 773 K and when the measurements were made at room temperature the conductivity of Pt/TiO_2 decreased by only one order of magnitude. The relative insensitivity of conductivity values to the changes in experimental conditions following 773 K reduction was related to the large number of conduction electrons in the TiO_2 due to its high reduction degree. Upon hydrogen admission at room temperature to HTR Pt/TiO_2, the conductivity increased only slightly,whichis consistent with the loss in hydrogen chemisorption capacity of metals in the SMSI state.

Admission of oxygen to TiO_2 or Pt/TiO_2 reduced at both temperatures caused the conductivity to decrease by several orders of magnitude.

The model proposed by Herrmann et al.[40] to account for the results is illustrated in figure 2.1.. Reduction of the TiO_2 support causes the Fermi level of the support to be lifted to a higher energy. As a consequence the Schottky barrier at the metal-semiconductor interface is decreased, facilitating migration of electrons from the support to the metal. This causes the d orbitals of Pt to be filled with consequent loss of capacity of the metal for hydrogen chemisorption. When oxygen is adsorbed on the surface of the support electrons are pumped back from the Pt crystallites partially restoring their normal chemisorptive properties.

2.5 THEORIES ON SMSI BEHAVIOUR

The SMSI phenomenon originally described by Tauster and coworkers[7] is characterized by a strong suppression of H_2 and CO chemisorption when group VIII metals are deposited on the surface of reducible oxides and reduced at elevated temperatures.

The fact that the SMSI phenomenon is characteristic of reducible oxides[8] suggests that the effect involves an

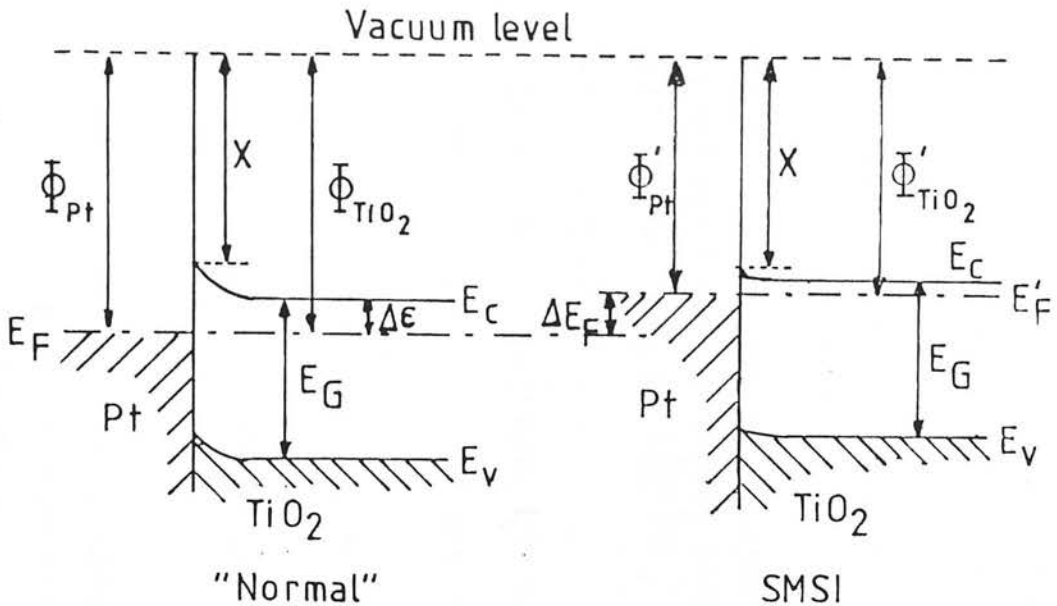

Figure 2.1 - Metal - Semiconductor Contact Model for SMSI:
ϕ : work function; X: electron affinity of TiO_2
E_G: band gap; E_F: Fermi level; ΔE_F: increase in E_F due to SMSI conditions.

interaction between the metal and some reduced form of the oxide support. This is substantiated by several reports which indicate that support cations of low oxidation state are produced under the reduction conditions that induce SMSI behaviour[11,43].

Several phenomena have been found to accompany generation of the SMSI state, including:

1) Changes in metal particle morphology. The metal particles tend to spread over the support and to acquire a raft-like or pill-box structure[14,16,41,42].
2) Diffusion of the metal into the support, at least in the case of TiO_2 supported Ni[46] and Fe[42,47,48].
3) Formation of metal-Ti clusters or changes in character of the metal-metal bond due to growth within a support matrix, at least in the case of Fe[47,48];
4) Reduction of TiO_2 to Ti_4O_7[41].
5) Increase in n-type semiconductivity of the support[16,40];
6) Changes in electronic properties of the metal particles[17];
7) Storage of large amounts of hydrogen by the support[26].

The detailed nature of the interaction, however, remains largely unknown.

Tauster and coworkers[7] original proposition involved an interaction of the type found in hexagonal barium titanates[49] where occupied d-orbitals of a transition metal cation overlap with vacant d-orbitals of Ti^{4+}. Although this type of interaction could conceivably occur between Ti^{3+} cations and zero-valent noble metal atoms, there is no firm basis to believe that it does indeed occur.

The possibility of Brewer[50] type intermetallic compound formation has also been considered[7]. Formation of these compounds involves donation of electrons from the

noble metal to Ti and is thermodinamically feasible under SMSI generating conditions. The fact that Ti intermetallic compounds are prepared at temperatures in excess of 1000 K from powdered reactants does not seem to pose insurmountable difficulties, since the high degree of dispersion of the metal on the support is likely to facilitate the reaction. Meriaudeau and coworkers[11] criticized this view considering that exposure of a SMSI system to oxygen at room temperature partially restores normal chemisorptive and catalytic properties to the metal but would not be expected to decompose the alloy. In the case of the Fe-Ti system, however, results consistent with alloy formation have been obtained[47,48].

Bonding through electron transfer from reduced Ti cations to Pt atoms has also been proposed. Horsley[51] reported a theoretical study of the Pt-$(TiO_5)^{7-}$ system, which was choosen as a model for a Pt atom interacting with a Ti^{3+} cation across an oxygen vacancy. The calculations indicated that the Ti 3d electron is largely transferred to Pt. Fung[17] claims direct evidence from XPS for electron transfer from Ti^{3+} to Pt in SMSI Pt/TiO_2. Meriaudeau et al[11] criticized this mechanism on the basis that LTR catalysts also contain Ti^{3+} cations but display normal chemisorptive behaviour. Furthermore it was argued that Rh atoms placed in close proximity to Ti^{3+} cations inside Y-zeolite supercages displayed normal chemisorptive and catalytic behaviour, irrespective of the temperature used during catalyst reduction[11].

Several investigators[11,25,40] have favoured a metal-semiconductor contact model, whereby the electron concentration in the metal particles increases due to the lift in the Fermi level of the support which accompanies high temperature reduction.

The mode whereby SMSI influences the course of catalytic reactions is correspondingly uncertain, since

changes in particle morphology, contamination of the metal surface due to alloy formation and changes in electronic properties of the metal may cause alterations in catalyst activity and selectivity. Irrespective of the cause of the SMSI effect, the simple fact that the chemisorptive properties of the metal are modified may lead to changes in the relative concentrations of reactive species and therefore influence the course of the reaction[17]. Also the selective deactivation of the smallest metal particles in the particle size distribution has been proposed to account for many of the results reported in the literature[9].

2.6 - REFERENCES

1 - F.G. Ciapetta, D.N. Wallace, Catalysis Rev., 1971, 5, 67.

2 - G. M. Schwab, Adv. Catalysis, 1978, 27, 1;F.Solymosi, Catalysis Rev., 1967, 1, 233.

3 - J. R. Katzer, A.W. Sleight, P. Gajardo, J. B. Michel, E. F. Gleason, S. McMillan, Faraday Discussions, 1981,72,preprint to paper # 8.

4 - Vannice, M. A., J. Catalysis, 1975, 40, 129.

5 - R. A. Dalla Betta, M. Boudart, Proceedings of the Fifth International Congress on Catalysis, Miami, 1972, p. 1329.

6 - A. G. Burden, R. B. Moyes, P. B. Wells, J. Catalysis, 1980, 65, 31.

7 - S. J. Tauster, S. C. Fung, R.L. Garten, J.Amer. Chem. Soc., 1978, 100, 170.

8 - S. J. Tauster, S.C. Fung, J. Catalysis, 1978, 55, 29.

9 - G.L. Haller, D.E. Resasco, A.J. Rouco, Faraday Discussions, 1981, 72, preprint to paper # 7.

10 - S. Engels, W. Mörke, M. Wilde, W. Roschke, B.Freitag, Z. Anorg. Allg. Chem., 1981, 472, 162.

11 - P. Meriaudeau, O.H. Ellestad, M. Dufaux, C.Naccache, J. Catalysis, 1982, 75, 243.

12 - J.R. Anderson, Am. Chem. Soc., Div. Pet. Chem. Prep., 1981, 26, 361.

13 - M.A. Vannice, R.L. Garten, J. Catalysis, 1979, 56, 236.

14 - C.H. Bartholomew, R. B. Pannell, J.L. Butler, D.G. Mustard, Ind. Eng. Chem. Prod. Res. Dev., 1981, 20, 296.

15 - D.G. Mustard, C.H. Bartholomew, J. Catalysis, 1981 67, 186.

16 - J. S. Smith, P.A. Thrower, M.A. Vannice, J.Catalysis, 1981, 68, 270.

17 - S.C. Fung, J. Catalysis, 1982, 76, 225.

18 - R.T.K. Baker, E.B.Prestridge, R.L. Garten, J. Catalysis, 1979, 59, 293.

19 - M.A. Vannice, S-Y. Wang, S.H. Moon, J. Catalysis, 1981, 71, 152.

20 - S.J. Tauster, S.C. Fung, R.T.K. Baker, J.A. Horsley, Science, 1981, 211, 1121.

21 - G.J. den Otter, F.M. Dautzenberg, J.Catalysis, 1978, 53, 116.

22 - H. Praliaud, G.A. Martin, J. Catalysis, 1981, 72, 394.

23 - D.Resasco, G. Haller, J. Chem. Soc., Chem. Commun. 1980, 1151 .

24 - R. Burch, A.R. Flambard, J. Chem. Soc., Chem. Commun., 1981, 965.

25 - Bor-Her Chen, J.M. White, J. Phys. Chem., 1982, 86, 3534.

26 - W. Hongli, T. Sheng, X. Maosong, X. Guoxing, G. Xiexian, in Metal-Support and Metal-Additive Effects in Catalysis, B. Imelik, C. Naccache, G. Coudurier, H. Praliaud, P; Meriaudeau, P. Gallezot, G.A. Martin, J.C. Vedrine eds., Elsevier, Amsterdam, 1982, p. 19.

27 - M.A. Vannice, R.L. Garten, J. Catalysis, 1980, 66, 242.

28 - F. Solymosi, M. Koczis, J. Catalysis, 1982, 75, 78.

29 - M.A.Vannice, R.L. Garten, J. Catalysis, 1980, 63, 255.

30 - M.A. Vannice, S.H. Moon, C.C.Two, Am.Chem. Soc. Div. Pet. Chem. Preps., 1980, 23, 303.

31 - S-Y. Wang, S.H. Moon, M.A. Vannice, J. Catalysis, 1981, 71, 167.

32 - M.A. Vannice, J. Catalysis, 1982, 74, 199.

33 - S. Engels, B. Freitag, W. Mörke, W. Roschke, M.Wilde, Z. Anorg. Allg. Chem., 1981, 474, 209.

34 - E.I. Ko, R.L. Garten, J. Catalysis, 1981, 68, 233.

35 - J.H. Sinfelt, Advan. Catalysis, 1973, 23, 91;

36 - K. Foger, J. R. Anderson, J. Catalysis, 1980, 64, 448.

37 - R. Pearce, M. V. Twigg, in Catalysis and Chemical Processes, R. Pearce & W. R. Patterson eds., Leonard Hill, Glasgow, 1981, p. 114.

38 - R. Burch, A. R. Flambard, in Metal-Support and Metal - Additive Effects in Catalysis, B. Imelik et al. eds., Elsevier, Amsterdam, 1982, p. 193.

39 - F. Solymosi, A. Erdöhlyi , T. Bánsági, J. Catalysis, 1981, 68, 371.

40 - J. - M. Herrmann, J. Disdier, P. Pichat, in Metal - Support and Metal - Additive Effects in Catalysis, B. Imelik et al. eds., Elsevier, Amsterdam, p. 27.

41 - R. T. K. Baker, E.B. Prestridge, R.L. Garten, J. Catalysis, 1979, 56, 390.

42 - B. J. Tatarchuk, J.A. Dumesic, J. Catalysis, 1981, 70, 308.

43 - T. Huizinga, R. Prins, J. Phys. Chem., 1981, 85, 2156.

44 - D.J.C. Yates, L.L. Murrell, E.B. Prestridge, J. Catalysis, 1979, 57, 41.

45 - T.M. Apple, P. Gajardo, C. Dybowski, J. Catalysis, 1981, 68, 103.

46 - C.C. Kao, S.C. Tsai, M.K. Bahl, Y.W. Chung, Surface Sci, 1980, 95, 1.

47 - B.J. Tatarchuk, J. A. Dumesic, J. Catalysis, 1981, 70, 323.

48 - B.J. Tatarchuk, J. A. Dumesic, J. Catalysis, 1981, 70, 335.

49 - J.G. Dickson, L. Katz, R. Ward , J. Amer. Chem, Soc. 1961, 83, 3026.

50 - L. Brewer, Science, 1968, 161, 115.

51 - J.A. Horsley, J. Amer. Chem. Soc., 1979, 101, 2870.

CHAPTER 3

ASPECTS OF CATALYSIS ON BIMETALLIC SYSTEMS

CHAPTER 3
ASPECTS OF CATALYSIS ON BIMETALLIC SYSTEMS

3.1 INTRODUCTION

The present chapter is adressed to the question of what happens when two (or more) metals are brought together to produce a catalyst. A short answer to this question is that in many cases materials are produced with catalytic properties very different from those of either metal alone, sometimes with distinct advantages in terms of activity, selectivity and/or stability. Practical realization of these advantages has been achieved in many instances, particularly in the field of hydrocarbon reforming[1-3].

Appart from their industrial interest, the importance of bimetallic catalysts for fundamental research in catalysis has long been recognized.

A great surge of interest in catalysis on bimetallic systems started in the early fifties with the development of the electronic theories of catalysis on metals[4-8]. These theories emphasized the importance of collective properties of metals and alloys, such as the concentration of d-band holes or the density of states at the Fermi level, as a determining factor in many catalytic reactions. According to the "rigid-band" model of alloys these properties could be controlled by appropriately mixing metals with different electron to atom ratios[9].

From the late-sixties onwards it became apparent that the local environment of individual surface metal atoms are of greater relevance to catalysis than the collective properties of the bulk material[10-16]. Most modern discussions of the electronic factor in alloy catalysis are made in terms of the "ligand-effect"[17,18], which takes into account the modifications of the properties of a surface metal atom caused by changes in

nature of its neighbours. At the same time evidence gathered[19-22] that many catalytic reactions require the simultaneous participation of several neighbouring metal atoms (multiplets or ensembles) so that some non-linear variations in catalytic activity observed when an unactive metal is added to an active one could be interpreted as arising from dilution of the active ensembles[14-16,23]. Athough the operation of both "ensemble" and "ligand" effects is generally considered to be possible, the relative importance of the two types of effect is still subject to much dispute[18,24].

The concept of the individual surface atom brought to the foreground the question of the surface composition of alloys which is known to differ in many cases from the bulk composition[17,25].

3.2 THE STRUCTURE OF BIMETALLIC PARTICLES

3.2.1 - Bulk thermodynamic considerations[26]

A solid solution is obtained when atoms of different elements are able to share together various sites of a common lattice. It is generally recognized that all metals show some solubility in the solid state but the extent of the solubility varies greatly from system to system. Some pairs of metals appear to be soluble in all proportions and are said to form a "continuous series of solid solutions" (e.g. Pd-Ag, Pd-Au, Pt-Rh, Pd-Pt)[27]. In other cases (e.g. Ni-Cu[28], Pd-Rh[29], Ni-Au[27], Rh-Ag[27], Ru-Cu[27], etc...), solubility is restricted to the composition regions near to the pure elements below a certain critical temperature and the resulting solutions are called "primary" or "terminal" solid solutions. The composition region corresponding to phase separation is known as the miscibility gap. The phase diagram for a system of catalytic interest which displays a miscibility

gap (Pt-Au) is illustrated in figure 3.1[27].

Other much more complicated phase diagrams are possible, characterized by the presence of several "intermediate phases". If the domain of existence of such phases is restricted around a stoichiometric composition these phases may be called "intermetallic compounds" or "valence compounds". One important system of catalytic interest which gives rise to intermetallic compound formation is the Pt-Sn system ($PtSn$, $PtSn_2$, $PtSn_3$)[27].

Solid solubitily may be analysed from a thermodynamic standpoint in terms of the free-energy of mixing ΔG_m which may be decomposed into an enthalpy and an entropy of mixing, ΔH_m and ΔS_m, respectively:

$$\Delta G_m = \Delta H_m - T\Delta S_m \qquad (3.2)$$

A necessary condition for solid solubility is that the free-energy of mixing is negative at a given temperature T. The enthalpy of mixing is related to the strength of interaction between the atoms in the bimetallic system. A large negative ΔH_m denotes a strong attraction and large positive values denotes a strong repulsion between unequal atoms. Negative enthalpies of mixing are associated with a tendency for ordering and positive values with a tendency for the formation of clusters where atoms of a given type tend to agglomerate.

The entropy term is a measure of the randomness of the alloy and has a maximum positive value for a completely disordered system. Assuming that ΔH_m and ΔS_m are approximately independent of temperature, it is easy to see from expression (3.2) that the free-energy of mixing becomes negative at sufficiently high temperature even when $\Delta H_m > 0$. The entropy of mixing is comprised of a configurational and of vibrational, magnetic and electronic

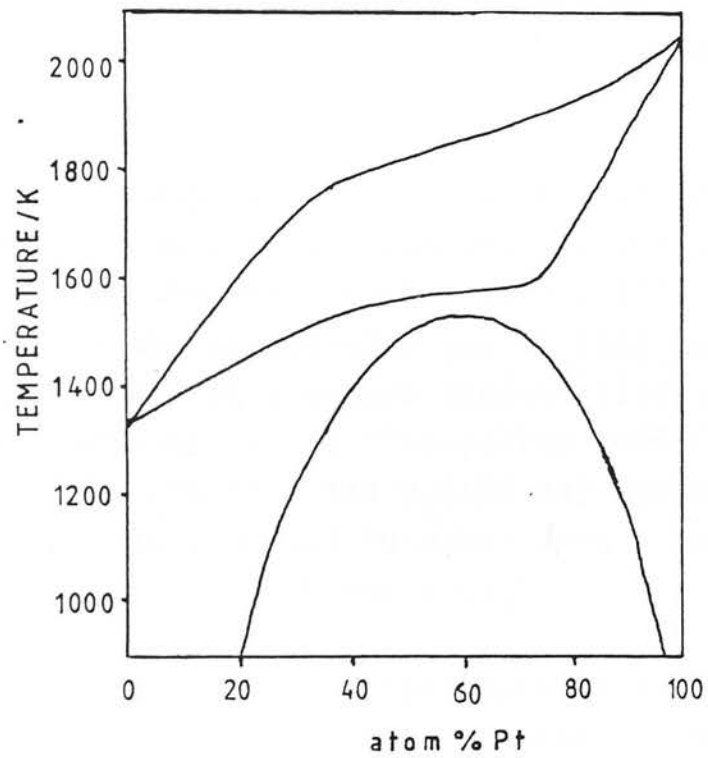

Figure 3.1 - Phase Diagram for the Pt - Au system[27]

terms:

$$\Delta S_m = \Delta S_c + \Delta S_v + \Delta S_m + \Delta S_e \qquad (3.3)$$

In the absence of short range ordering, the configurational term is given by expression (3.4) for a mixture of components A and B:

$$\Delta S_c = -R_G (X_A \ln X_A + X_B \ln X_B) \qquad (3.4)$$

where X_A and X_B are the atom fractions of components A and B, respectively.

The general features of a free-energy vs. composition graph at constant temperature are illustrated in figure 3.2 for the Ni-Cu system at 473 K[28]. The region corresponding to the miscibility gap at this temperature may be found by drawing a common tangent (line B-C) to the two negative portions of the free-energy curve. Within the region defined by compositions x_1(~0% Cu) and x_2(~82% Cu), phase separation is expected to occur into a nearly pure Ni phase (x_1) and a Cu-rich phase (x_2).

In theoretical thermodynamic studies of solid solutions, two model systems are frequently considered, namely ideal solution and regular solutions. With ideal solutions, ΔH_m is taken as zero and ΔS_m is expressed only by the configurational term expression (3.4). Regular solution theory goes a step further and considers $\Delta H_m \neq 0$ but retains the ideal approximation to ΔS_m. Although it may not be expected that solid solutions behave in a "regular" fashion, the regular solution model is the simplest one which predicts the possibility of a miscibility gap. In regular solution theory, use is frequently made of the "broken-bond" or "quasi-chemical" approximation which considers only pairwise interactions between nearest neighbours. In a solid solution of components A and B, the energy of interaction between a pair of A atoms is given a value, H_{AA}, between a pair of B atoms a value H_{BB} and between A-B atom pairs a value of H_{AB}, all values being composition independent, so

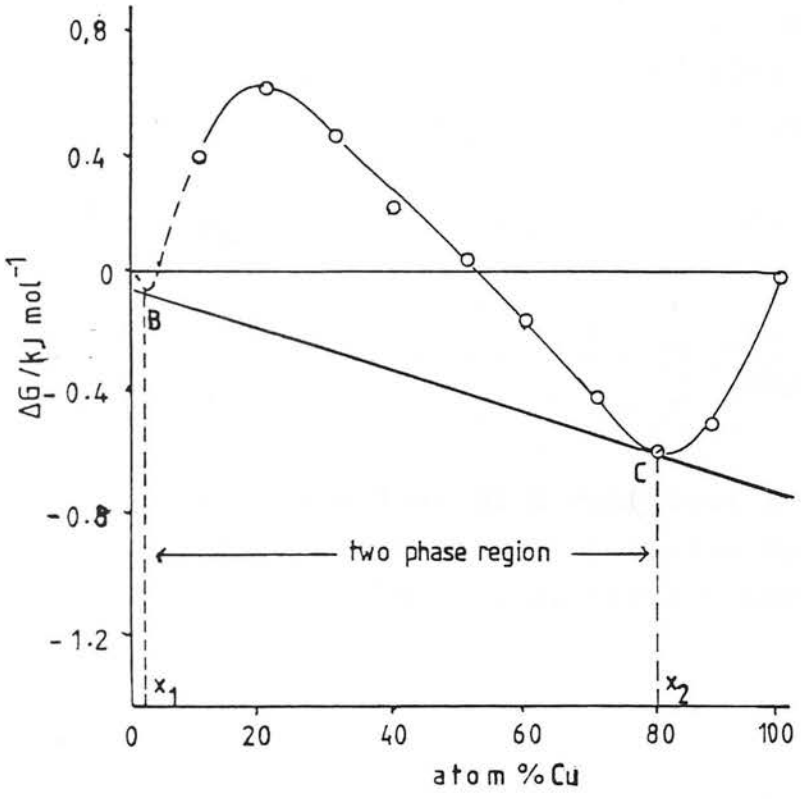

Figure 3.2 - Free - Energy vs. Composition Diagram for the Ni - Cu System at 473 K[28]

that H_{AA} and H_{BB} may be estimated from the properties of the two pure components.

With this assumption, it may be shown that the enthalpy of mixing for a regular solution is given by:

$$\Delta H_m = X_A X_B \, Z \, N_o \left[H_{AB} - 1/2(H_{AA} + H_{BB}) \right] \qquad (3.5)$$

where Z is the coordination number for an atom in the solution (e.g. 12 for an f.c.c. crystal), assumed to be equal for both components, and N_o is the total number of atoms. A quantity Ω may be defined by expression (3.6)

$$\Omega = Z N_o \left[H_{AB} - 1/2(H_{AA} + H_{BB}) \right] \qquad (3.6)$$

so that

$$\Delta H_m = X_A \, X_B \, \Omega \qquad (3.7)$$

Negative values of Ω represent an attractive interaction between A and B while a positive value denotes a repulsive interaction. For $\Omega = 0$, ideal behaviour is observed.

3.2.2 - Particle size effects

So far, we have ignored the presence of a surface. Usually, however, catalytic reactions are carried-out on small metal particles which may have a large surface/volume ratio and therefore surface energy effects become important. When an initially homogeneous bimetallic particle separates into two phases, an interface is created with an associated interfacial tension and the resulting increase in surface free-energy may be large enough to compensate the decrease in bulk free-energy obtained from phase separation. This problem was considered in detail by Ollis from the standpoint of regular solution theory[30]. Using realistic assumptions about interfacial tension values, Ollis estimated that the critical solution temperature could be decreased by several hundred degrees

for particles as large as 10 nm. In the particular case of Ni-Cu at 425 K, which should display immiscibility over more than 90% of the composition range with basis on bulk thermodynamics only, it was predicted that a continuous series of solid solutions should be obtained for particles of 10 nm diameter.

Hoffman proposed that small metal particles could be stable towards phase separation due to kinetic rather than to thermodynamic reasons[31]. Briefly, the nucleation and growth mechanism of phase segregation is thought to be blocked in small metal particles. Phase separation is then limited to the so-called "spinodal" mechanism which operates only at temperatures smaller than the one predicted by thermodynamics for a given composition. Especially large undercoolings are expected when there is a large difference in atomic size between the components of the solid solution.

There is a large body of experimental evidence that metals which have very limited mutual solubility interact strongly when in dispersed form[15,28,33-36]. It is doubtful, however, that the ideas exposed by Ollis and Hoffman have much bearing to many of these cases of bimetallic interaction. It has been found in some systems (Ni-Cu[28], Pt-Au[33]) that, although phase separation occurs, the metals still interact strongly since a phase with lower surface energy envelops a second phase with a higher surface energy (see 3.2.3 b). With very small metal particles, a similar situation arises, since sometimes a kernel strongly depleted in one of the components of the mixture is found to be enveloped by a layer strongly enriched in this same component[35,36]. With these very small metal particles, such as found in highly dispersed catalysts, it is perhaps inadequate to speak about single or separate metal phases, as characterized, for example, by the presence or absence of separate X-ray diffraction lines. In these cases the denomination "bimetallic cluster"

introduced by Sinfelt[15] seems to be more appropriate.

In some systems, phase separation seems to be limited by a restricted mobility of the metal atoms. For example, in the Pd-Rh[29] and Pt-Ir[37] systems a miscibility gap is predicted for temperatures normally used during catalyst preparation. For these systems however, it is reported that phase separation is very slow for bulk samples quench cooled from high temperatures, indicating very slow rates of interdiffusion. If the metal particles are initially formed so that the metals are in intimate contact, phase separation may then be inhibited during subsequent heat treatment. Moss and Gibbens prepared homogeneous Pd-Rh alloy films within the miscibility gap by simultaneous deposition of the metals onto a substrate held at 273 K followed by annealing at 673 K[38]. Many different forms of Pt-Ir catalysts have been prepared (supported, powders, skeletal, cf. chapter 8) with good bulk homogeneity and also in this case the particle size effect seems to be of little importance. Anderson and coworkers, however, reported the preparation of homogeneous SiO_2 supported Pt-Au alloy particles within the miscibility gap with particle sizes near to 1.5 nm[39] while with films particles comprised of a Pt-rich kernel surrounded by a Au-rich envelope have been reported[33] and in this case the particle size effect may be relevant.

3.2.3 - The surface composition of bimetallic particles[17,25,40]

This problem may be more convenienty analysed if miscible (solid solutions), immiscible and ordered systems are separately considered. Furthermore, complications due to particle size effects, influence of the gaseous environment and carrier effects in supported systems have to be taken into account.

3.2.3a - Miscible systems

It is a well established experimental fact that the surface composition of alloys may be considerably different from the bulk composition. The driving force for setting-up this concentration difference is, as usual, to minimize the free-energy of the system either by decreasing the surface free-energy or by relieving internal strain.

The extent of segregation of a component B to the surface of an A-B alloy is conveniently characterized by a surface enrichment factor F such that:

$$F = \frac{Y_B}{Y_A} \cdot \frac{X_A}{X_B} \qquad (3.8)$$

where X_i and Y_i are the atom fractions of component i in the bulk and at the surface, respectively. To the enrichment factor F, there is associated a certain free-energy of segregation, ΔG_S, given by:

$$\Delta G_S = -R_G T \ln F \qquad (3.9)$$

The simplest model for surface enrichment involves the assumption of ideal solution behaviour, with enrichment limited to the outermost atomic layer and determined only by surface energy considerations.With these assumptions, the free-energy of segregation ΔG_S is simply equal to the enthalpy of segregation ΔH_S and it can be demonstrated that

$$\Delta H_S = (\gamma_B - \gamma_A)a \qquad (3.10)$$

where γ_A and γ_B are the surface tensions of the solvent and of the solute, respectively, and a is the surface area covered by one mole of either component (atomic sizes assumed to be equal). By combining expressions (3.8) to (3.10) it is easy to see that the component with the smallest surface tension is expected to segregate to the

surface and furthermore surface enrichment is expected to decrease with increasing temperature.

Using a simple broken-bond approximation it may be demonstrated that.

$$\gamma_A \cdot a = \frac{\Delta Z}{Z} \cdot \Delta H_{VA} \qquad (3.11)$$

where ΔZ is the number of nearest neighbours that must be removed from an atom in a subsurface layer in order to produce a surface atom and ΔH_{VA} is the enthalpy of vapourization of metal A. For example, an atom in a face-centred cubic (f.c.c.) crystal has twelve nearest neighbours and three next neighbours must be removed before this atom becomes exposed at a (111) surface.

The $\Delta Z/Z$ factor which appears in expression (3.1) indicates that different crystal faces are expected to display different degrees of surface enrichment. For example, $\Delta Z/Z$ for the (110) face of an f.c.c. crystal is 5/12 and therefore surface enrichment is predicted to be larger with this face than with the (111) face. Even larger $\Delta Z/Z$ values are obtained for atoms located at edge and corner sites of stepped and kinked surfaces, so that segregation of the most volatile component is expected to occur preferentially to these positions[41]. This point is of high relevance to catalysis, since many reactions seem to occur preferentially on these sites of low coordination[42]. Different degrees of Cu segregation to different crystal faces have been observed experimentally with the Ni-Cu system[43].

A further elaboration of the theory of surface segregation involves the use of the regular solution model in order to account for solvent-solute interactions[44,45].

The effect of considering a heat of mixing for the alloy is to enhance surface enrichment with the most volatile component in systems with a tendency for clustering ($\Omega > 0$) and to decrease surface enrichment in systems with a tendency for ordering ($\Omega < 0$)[45].

Even more refined models have been built, still within the framework of regular solution theory, which take into account that surface enrichment may not be limited to the first atomic layer, but may extend through several layers before the bulk composition is reached[41,45,46].

Surface energy considerations do not always lead to correct prediction of the segrefating element in an alloy and when there is a large difference in atomic size between the alloy components, relief of internal strain may become the dominating factor[44,46-50]. An expression for the energy released when a solute atom B segregates to the surface of the solvent A has been given[40]:

$$\Delta G_S = - \frac{24\ KGr_A\ r_B(r_A - r_B)^2}{3Kr_B + 4Gr_A} \qquad (3.12)$$

where K is the bulk module of the solute, G is the shear modulus of the solvent and r_A and r_B are the atomic radii for solvent and solute atoms. Notice that, according to this expression, the solute will always segregate to the surface of the solvent regardless of the sign of the $(r_A - r_B)$ term. It has been remarked, however, that only oversized atoms are preferentially segregated to the surface[50] and good agreement with experiment is only obtained when expression (3.12) is applied to solute atoms that are larger than solvent atoms.

The neglect of the entropy of segregation implied in the regular solution model has been shown to

lead to serious erros in the quantitative estimation of surface segregation in some cases[47]. Seah has proposed a semi-empirical equation of the type[44]:

$$\ln F = \left[24(T_B - T_A) + 1.86\Omega + M.4.64.10^7\, r_B(r_A - r_B)^2\right] / R_G T \pm 1.29 \quad (3.13)$$

where T_B and T_A are the melting points of the alloy components in Kelvin units, Ω is in Joules per gram atom and r_B and r_A are in nm units and M = 1 for $r_A > r_B$ and M = 0 for $r_A < r_B$. This relation has a standard deviation of 8.7 $kJmol^{-1}$ over the range of free-energies of segregation from -80 to 20 $kJmol^{-1}$.

3.2.3b - Immiscible systems

Three situations may be distinguished when phase separation occurs during catalyst preparation, as illustrated in scheme 3.1[41].

SCHEME 3.1

In situation A, separate particles corresponding to the two phases are formed; B corresponds to the model used by Ollis[30] and Hoffman[31] in their studies of the influence of particle size on phase separation; C is the so-called "cherry-model", initially proposed by Sachtler and Jongepier to explain observations on the Ni-Cu system and corresponds to particles comprised of a kernel enriched in the least volatile component of the alloy enveloped by a skin enriched in the other component [28].

Burton and coworkers analysed this problem

from the standpoint of regular solution theory and concluded that situations B and C are the ones predicted from thermodynamics but that B should only arise when $\Omega/ZN_o >> H_{AA} - H_{BB}$ (see expression 3.6), which is not to be expected for most simple alloys[41].

Experimental evidence that some systems conform to the cherry model (e.g. Ni-Cu[10,11,28], Pt-Au[33] and Pd-Rh[38] films) comes from studies where the surface properties (e.g. work-function, chemisorptive capacity, catalytic activity)are found to remain constant over a wide composition range. In cases where the miscibility of the components is very small (e.g. Ru-Cu[35,36] Os-Cu[36], Rh-Ag[34]), the interaction between the metals is likened to that which would exist in the chemisorption of the most volatile metal on the least volatile one. In the Rh-Ag/SiO_2 system it was proposed that Ag can chemisorb on Rh to monolayer coverage and surplus Ag atoms segregate to form a separate Ag phase[34,51].

One question of considerable importance regards the arrangement of the overlayer of B atoms on the surface of an A metal particle. If the B-B bond is stronger than the B-A bond it may be expected that B atoms tend to form clusters on the surface of the A particles. When B-A bonds are stronger than B-B bonds it is probable that B atoms are more or less randomly distributed on the A surface. It has been suggested that the former situation applies to Rh-Ag/SiO_2[34] while the latter seems to prevail with the Ru-Cu system [52,53].

3.2.3c - Ordered systems

Systems which have $\Omega < 0$ become ordered at sufficiently low temperatures. In the Pt-Sn system, which is of great catalytic interest, the ordering region extends up to the melting point of the alloys (Pt, Pt_3Sn, PtSn, $PtSn_2$)[27]. There is an interplay of two opposing

effects in determining the surface composition of ordered alloys:

1. The tendency to maximize the number of bonds between unequal atoms;
2. The tendency of the most volatile component to segregate to the surface.

Therefore, increasing negative values of Ω oppose surface segregation while increasing difference between the surface tensions of the pure components favours segregation of the component with lowest surface tension.

From a theoretical analysis using a broken-bond model, it has been suggested that surface enrichment in ordered systems involves an interchange of atoms between the surface layer and the layer immediately below giving rise to strong depletion of the segregating component from the second layer[54]. Good consistency between chemisorptive (sensitive only to the outermost layer) and Auger electron spectroscopy (sensitive to several surface layers) could only be obtained by assuming this concentration inversion for Pt-Sn alloys where surface enrichment with Sn occurs[55].

Nakamura and coworkers studied the Fe-Co system which exhibits the formation of ordered b.c.c. phases (Fe_3Co, FeCo, $FeCo_3$)[56]. Theoretical calculations for the FeCo alloy indicated that no surface enrichment should occur at temperatures lower than the order -disorder transition temperature. However, AES studies suggested that the alloy was surface enriched in Fe and the degree of enrichment was consistent with an ideal solution model, indicating that the ordered b.c.c structure of the bulk alloy did not extend to the surface.

3.2.3d - Particle size effect

For small metal particles, surface enrichment may be limited by depletion of the segregating component in the bulk. The surface coverage by component B, Y_B, may be calculated as a function of the concentration of B in the interior of the particle from expression (3.8). For a certain fractional metal dispersion D, the following relation is valid:

$$X'_B = DY_B + (1-D)\, X_B \qquad (3.14)$$

where X'B is the atom fraction of B in the whole particle. Combining (3.8) and (3.14) gives[57]:

$$D(F-1)Y_B^2 - \left[(F-1)(D + X'_B) + 1\right] Y_B + X'_B F = 0 \qquad (3.15)$$

which allows the calculation of the fraction of B on the surface for an overall composition X'_B dispersion D and enrichment factor F. Williams and Nason considered this problem in detail for an ideal solution model[45].

As might have been anticipated (fig. 7 from reference [45]) the effect of dispersion becomes more pronounced with increasing heat of segregation and with decreasing overall concentration of the segregating component. Burton et al. remarked that even for very high dispersions, when essentially all atoms are exposed at the surface, some kind of segregation occurs, in the sense that the most volatile component tends to occupy sites of low coordination[41].

The expected influence of particle size on the degree of surface segregation has been experimentally observed in the Pt-Cu system[58].

3.2.3e - Influence of the gaseous environment

The influence of the surrounding gas atmosphere has been singled out as the most important factor in determining surface composition when the gas is strongly adsorbed on only one of the alloy components[25]. In this case, strong chemical bond formation between a surface metal atom and the adsorbate is the driving-force for segregation. This effect is expected to be especially pronounced with group VIII - group IB alloy combinations where the IB component is generally the most volatile and tends to segregate to the surface. However, since gases such as CO or H_2 chemisorb predominantly on the group VIII component, an attenuation of this tendency is expected to occur. This phenomenom is well documented experimentally[59-62]

3.2.3f - Influence of the support

Interactions between the metals and the support may modify the structure of bimetallic particles. For example, in the Ru-Au system very little mutual solubility of the metals is reported[27]. Since Au (ΔH_V = 345 kJmol^{-1})[63] is more volatile than Ru Ru(ΔH_V = 670 kJmol^{-1})[63] one would expect Ru-Au particles to be comprised of a Ru kernel covered by Au atoms. Catalytic and XPS measurements performed on supported Ru-Au/SiO_2 suggested only a limited degree of interaction between the metals[32,64]. When the metals were supported on MgO, however, enrichment of the surface with Ru was observed, instead of the expected Au enrichment[32,64,65]. It was suggested that Au interacts strongly with the MgO support and is therefore prevented from migrating to the surface of the bimetallic particles.

As already mentioned, Ag islands are thought to be formed on the surface of Rh in Rh-Ag/SiO_2 catalysts[34]. When the metals are supported on TiO_2, however, evidence was obtained that Ag becomes randomly dispersed on the Rh surface, which was attributed to a modification of the

Rh-Ag energetics due to interaction with the TiO_2 support[66].

3.2.4 - Influence of catalyst preparation method

The theories reviewed in previous sections allow some predictions to be made about the bulk and surface equilibrium composition of bimetallic particles. Whether an equilibrium structure is actually attained, however, depends strongly on the detailed method of catalyst preparation and pretreatment, since rates of equilibration may be very slow under the conditions selected.

The problem of restricted rates of interdiffusion of the metals was already commented under 3.2.2. The examples cited served to emphasize that in some cases where phase separation is predicted from the bulk phase diagram it is not actually observed even after annealing at moderate temperatures. Conversely, the preparation of homogeneous Pd-Ag films, for which no miscibility gap seems to exist, requires a deposition temperature and subsequent annealing temperature of 670 K under normal vacuum conditions (ca. 10^{-4} Pa). Under ultra-high vacuum, however, a temperature of 273 K is adequate for equilibration[67]. This serves to demonstrate the sort of preparative detail that may influence alloy homogeneization.

With supported systems there is the added complication of interactions of the carrier with the precursors of the metals and with the metals themselves. Furthermore metal atoms may have to move over fairly large distances in an atomic scale, in order that equilibration may be achieved.

In general it may be expected that methods which lead to the formation of well mixed precursor phases

and simultaneous reduction of the metals facilitate the equilibration of supported bimetallic particles. A few examples suffice to illustrate these points.

De Jongste and coworkers studied the preparation of Pt-Cu and Pt-Au supported on SiO_2[68]. Coimpregnation of the support with a solution of the metals in agua-regia followed by drying and reduction in hydrogen at 623 K led to alloying with the Pt-Cu system but no evidence for alloying was found with the Pt-Au system even after prolonged sintering at 883 K. It was proposed the Cu migrates more easily than Au on the surface of the SiO_2 which makes alloying possible under relatively mild conditions.

Simultaneous reduction of Pt and Au by addition of hydrazine to a suspension of SiO_2 in a solution of the metal chlorides yielded homogeneous alloys after completion of the reduction with hydrogen at 623 K.

Moss and coworkers studied the preparation of SiO_2 supported Pd-Ag catalysts[69].This system is expected to form a continuous series of solid solutions but it was shown that direct reduction of impregnated nitrates with hydrogen up to 873 K or reduction preceeded by calcination at temperatures up to 873 K were unsatisfactory for alloy equilibration. Satisfactory results were only obtained when the nitrates were impregnated on a SiO_2 sample prefired at 1073 K, then calcined at 1073 K and reduced at 723 K. Reasonable homogeneization was achieved by coreducing the nitrates at room temperature with hydrazine, followed by a treatment in nitrogen at 1023 K. Interestingly, the same treatment performed with hydrogen resulted in phase separation. It was proposed that a strong interaction between Pd and the SiO_2, caused by Pd-aided reduction of the silica followed by formation of a Pd-Si intermetallic compounds at temperatures in excess of 873 K, was responsible for

inhibiting the migration of Pd atoms necessary for alloy homogeneization. Simultaneous reduction of the metals with hydrazine again seemed to favour alloy formation as in the Pt-Au case.

In other cases, calcination of the precursors before reduction seems to be detrimental to alloy formation. Shiflett and Dumesic prepared Pt-Re catalysts supported on Al_2O_3 both by direct reduction of the precursors with hydrogen and with an intermediate calcination step[70]. Results obtained in the ammonia synthesis reaction with the catalysts which were directly reduced indicated that bimetallic particles were formed. On the other hand, catalysts which were subjected to a previous calcination behaved similarly to a physical mixture of Pt/Al_2O_3 and Re/Al_2O_3. Similar observations have been made with Pt-Ir catalysts (cf. chapter 8). It seems that in these cases growth of separate oxide phases during calcination works against homogeneization of the metals in the subsequent reduction stage.

3.3 - CHARACTERIZATION METHODS

The importance of characterizing bimetallic catalysts as closely as possible cannot be overemphasized, since only then is it possible to attempt a meaningful interpretation of their catalytic behaviour. There are two central questions to be answered in the characterization of bimetallic catalysts. The first one relates to the phase distribution of the metals (single phase, separate non-interacting phases, separate interacting phases). The second relates to the surface composition of the bimetallic particles.

With unsupported metals and with supported catalysts of low dispersion of the metals (particle diameter > ∿ 5nm) X-ray diffraction is usually the method employed to assess the extent of alloying. With smaller particle sizes, broadening of the X-ray signals and the possible interference of reflections from the support limits the usefulness of the method[71].

Mössbauer spectroscopy has been used in the characterization of highly dispersed bimetallic cluster catalysts, particularly those containing Fe and Sn[72]. Although the method applies best to Fe and Sn containing catalysts examination of other metals is feasible (e.g. Ru, Au[73]). Addition of a ^{57}Fe probe isotope to highly dispersed Pt-Ir/Al_2O_3 has been used to assess the degree of mixing of the metals[74].

Temperature-programmed reduction is a simple and inexpensive method which has been used successfully in characterizing the extent of interaction of the metals in highly dispersed catalysts. A review on the principles and applications of this technique is presented in chapter 8.

Extended X-ray Absorption Fine Structure (EXAFS) is

a recent technique that can furnish very detailed information on the structure of metallic particles[2]. The method is applicable to highly dispersed catalysts but its use is limited by the need of a source of intense and highly colimated X-rays such as produced by synchrotron X-ray radiation. The EXAFS technique has been used in the study of SiO_2 supported Ru - Cu clusters[75] and MgO supported Ru - Au clusters[65].

Auger Electron Spectroscopy (AES) is a technique suitable for quantitative analysis of the surface composition of unsupported alloys[40,76]. Different elements emit Auger electrons with different energies and this is the basis for the analytical applications of the technique. Auger electrons have a certain escape depth so that the electrons emmited from the subsurface layers (2-3 layers minimum) contribute to the Auger signal. Corrections are necessary if quantitative information on the composition of the surface layer is required[77].

X-ray Photoelectron Spectroscopy (XPS) relies on the emission of electrons from inner-shells due to absorption of X-ray photons[72]. The technique is surface sensitive but the escape depth of the XPS electrons is larger than that of Auger electrons. XPS is also suitable for the examination of supported catalysts[34,65,78,79].

Selective chemisorption of gases, mainly CO and H_2, is the most commonly used method for the estimation of the surface composition of dispersed bimetallic catalysts (e.g. references 11, 14, 15, 34, 39, 55). The method is specially useful in studies of bimetallic catalysts comprised of a group VIII metal and a B subgroup metal since the latter can only adsorb CO and H_2 weakly and reversibly. It is then assumed that it is possible to count the number of group VIII metal atoms at the surface from the amount of strongly chemisorbed gas[11,14,15]. This assumption seems to be justified in some cases. For

example, van der Plank and Sachtler compared the amount of hydrogen chemisorbed at room temperature on Ni-Cu films with the total surface area determined by xenon physisorption and obtained a surface composition consistent with thermodynamic predictions[11]. Gerberich and coworkers assumed the surface composition of their Pd - Au powders to be the same as the bulk composition and found the same stoichiometry of adsorbed CO molecules per surface Pd atom (0.6 - 0.7) for pure Pd and all alloy powders[80].

There are many limitations in the selective chemisorption method which have to be carefully taken into account. Care should be taken in the interpretation of results obtained with adsorbates, such as CO, which can be chemisorbed in more than one form[81]. The CO molecule may occupy a position on top of a metal atom (linearly chemisorbed CO) or a bridging position between two atoms (SCHEME 3.3).

SCHEME 3.3

Since the bridge-bonded species requires a two-atom site, its concentration on the surface decreases more rapidly than the concentration of the linear species on alloying (assuming a random arrangement of the metals on the surface) and a non-linear dependence of surface coverage with surface composition may result. Also with hydrogen, it is not clear that an isolated group VIII atom is capable of effecting chemisorption[55]. Shimizu and coworkers observed that as little as 5% of a Cu monolayer on the Ru (0001) surface reduces the saturation coverage with

hydrogen by about 50%, which indicates that a large Ru ensemble is necessary for H_2 chemisorption[82]. Anderson and coworkers demonstrated that using the amount of "strongly chemisorbed" hydrogen on Pt-Au/SiO_2 catalysts underestimated the surface concentration of Pt as compared to the predictions of the regular solution model[39]. On the other hand, the "total" amount of chemisorbed hydrogen, obtained by extrapolation of the linear portion of the adsorption isotherms to zero pressure, was in good agreement with the model calculations. Anderson and coworkers also concluded that hydrogen atoms can become chemisorbed on isolated Pt atoms. It seems that some care is necessary in extrapolating the chemisorptive behaviour of hydrogen from one bimetallic system to the next. An added complication in the interpretation of chemisorption results is the possibility of chemisorption induced surface segregation.

Chemisorptive methods have also been used to estimate the surface composition of bimetallic catalysts comprised of two group VIII metals[79,83,84]. Use has been made of the fact that the stoichiometries for H_2 and CO chemisorption vary from metal to metal so that the following system of simultaneous equations may be solved, assuming that the stoichiometries valid for the pure metals are also valid for the metals in the bimetallic system[79]:

$$\begin{aligned} D\,(C_A y_A + C_B y_B) &= C \\ D\,(H_A y_A + H_B y_B) &= H \end{aligned} \qquad (3.15)$$

where y_i is the fractional concentration of component i on the surface, D is the dispersion of the bimetallic catalyst (surface atoms/total atoms), C_i and H_i are, respectively, the stoichiometries for CO and H_2 chemisorption on pure metal i and C and H are, respectively, the CO/metal ratio and the H/metal ratio obtained from chemisorption measurements on the bimetallic catalyst. Using equations (3.15), both the dispersion and the surface composition of

the bimetallic catalyst may be estimated from CO and H_2 chemisorption measurements. In a similar line, the surface composition of Pt-Ru/Al_2O_3 catalysts has been estimated from H_2 and O_2 chemisorption measurements[84]. Also with respect to the Pt-Ru system, it has been observed that a Pt surface saturated with one volume of O_2 requires four volumes of CO before saturation coverage with CO is obtained[83]. With Ru this ratio is 1:1 and therefore titration of chemisorbed oxygen with CO was used to estimate the surface composition of Pt-Ru/SiO_2 catalysts[83].

3.4 - THE INTERPRETATION OF CATALYTIC PROPERTIES OF BIMETALLIC SYSTEMS

When a given metal A is modified by addition of a second metal B the observed changes in chemisorptive and catalytic properties may ultimately be traced to one or more of the effects shown schematically in figure 3.3.

Figure 3.3A represents a situation where the strength of the adsorbate-metal bond is modified by changes in nature of the atoms surrounding the adsorption site. These modifications are caused by changes in the electronic structure of the metals upon alloying and both long-range and localized effects may be envisaged. Older theories emphasized interactions between the adsorbate and collective electronic states of the metal crystal[4-8]. More recent theories emphasize the localized nature of the chemisorptive bond and the importance of the immediate surroundings of the adsorption site[17,18,85]. While both collective and short-range effects of this type are normally referred to as "electronic", the short-range alloying effects have been named "ligand effects" by analogy with similar phenomena in organometallic chemistry[17].

The situation depicted in figure 3.3B arises when the adsorbate is bonded to more than one surface atom, i.e.

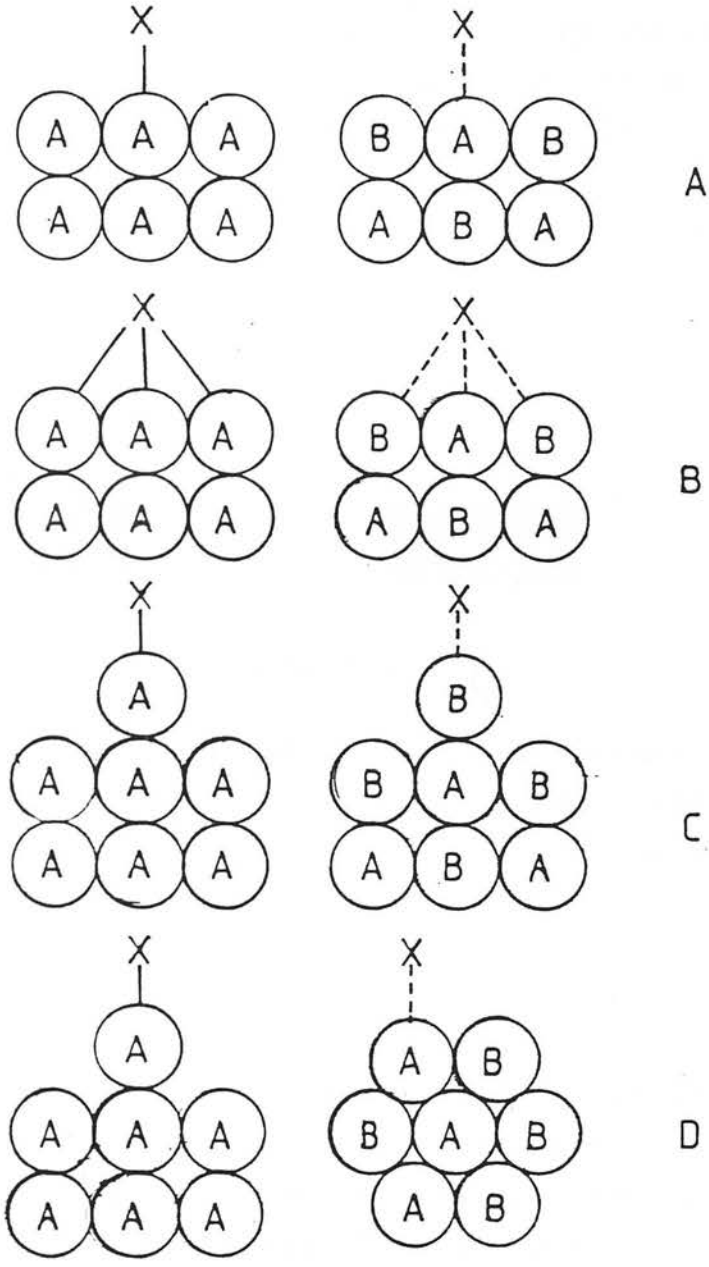

Figure 3.3 - Common Alloying Effects in Chemisorption and Catalysis: A - Ligand Effect; B - Ensemble Effect; C and D - Structural Effects

to a multiple site or ensemble. In this case it is reasonable to expect that the properties of a surface species bonded to an adsorption site comprised only of A atoms will be different from those of another species bonded to mixed-metal adsorption sites or pure B metal sites. One extreme situation occurs when the substitution of an A atom in a pure A-metal ensemble renders the whole adsorption site inactive and the activity of the catalyst is then dictated by the concentration of A-atom ensembles of the required size on the surface. Superimposed on a simple ensemble dilution effect, a ligand effect may also be envisaged for multi-site adsorption as illustrated in scheme 3.4.

SCHEME 3.4

In this case, adsorption of X can only occur on pure A-atom ensembles but the strength of the chemisorptive bond is modified by the presence of B atoms around the adsorption site[18,82,86].

In figure 3.3C, adsorption of X occurs preferentially on a site of low coordination. As mentioned under 3.3.3a, segregation of the most volatile component in an alloy is expected to occur preferentially to these sites and in this fashion marked alterations of catalytic properties may result from small additions of an alloying component[87-89]. It is also possible in some cases that alloying modifies the crystal structure of the bimetallic particles, so that cortain crystal faces become preferentially exposed[90]. The effects illustrated in figures 3.3C and D may be termed structural effects. In the next sections, each of these effects will be described in somewhat more detail.

3.4.1 - The electronic factor in catalysis on bimetallic systems

In trying to evaluate the electronic effects of alloying on chemisorption and catalysis it is crucial to understand how metal atoms of different natures interact with each other in the alloy and to this end chemists make frequent use of concepts derived from solid state theories of metals.

There is no room in the present work to describe in any detail the band theories which have been used to interpret the properties of pure metals, and their alloys.

It will be simply recalled that the band structure of pure metals is usually calculated by solving the wave equations for nearly free valence electrons moving in the periodic field created by positively ionized cores held in fixed positions of the metal lattice[91]. When disordered alloys are considered, the calculations are complicated due to the fact that the periodicity of the lattice is broken by the presence of impurity atoms. Several approximations have been used to deal with this problem[92].

The rigid-band model assumes that alloying leaves the lattice potential unaltered and that one can, therefore, consider the density of states (DOS) curve to be unaltered by the solute and alloying need only be considered in terms of changes in the position of the Fermi level[9]. For example, as a group IB metal is added to a group $VIII_3$ metal, the extra electron possessed by the group IB element is assumed to enter the collective valence band so that the Fermi level is shifted to a higher energy as illustrated in a highly schematic form in figure 3.4. This theory was much used in the past to rationalize catalytic phenomena on alloys but was gradually abandoned from the

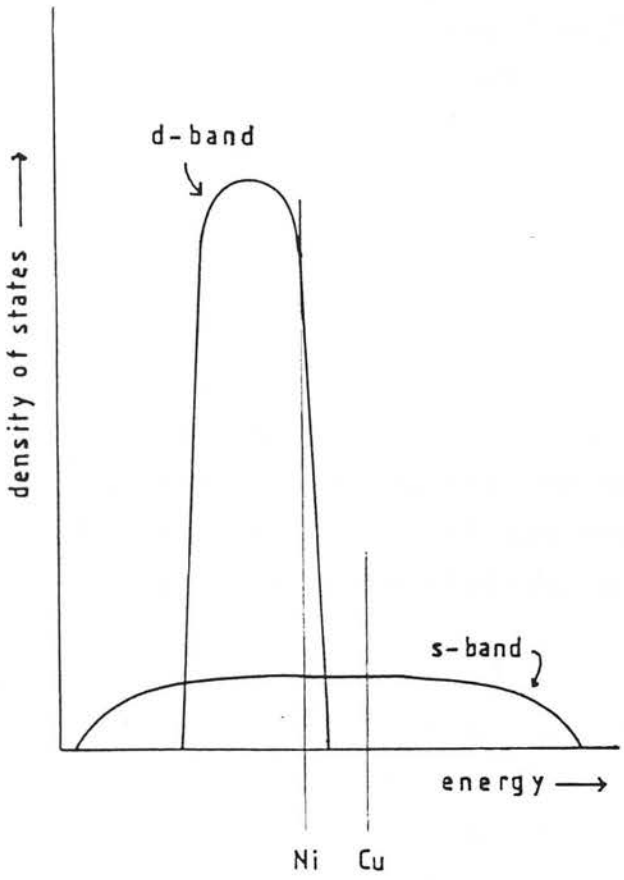

Figure 3.4 - Schematic Representation of the Valence Band Structure of Group VIII and Group IB Metals: The vertical lines show the position of the Fermi levels for Ni and Cu. According to the Rigid-Band approximation, the Fermi levels of Ni - Cu alloys lie between the positions corresponding to pure Ni and pure Cu

late sixties onwards, mainly due to the following reasons:

1 - the rigid-band theory predicts that all sites in the lattice become equivalent upon alloying while chemisorption studies clearly indicated that adsorbates such as CO and H_2 can distinguish between metal atoms active for chemisorption and atoms inactive for chemisorption even on alloys which according to the theory should have a completely filled d-band[10-15].

2 - Results from photo-electron spectroscopic measurements, which can directly probe the shape of the valence band of alloys, indicated that in alloys between group VIII and group IB metals no common d-band exists but instead features characteristic of each individual metal appear in the DOS curve[93]. This indicates that atoms of different elements keep much of their individuality in the alloy, which is contrary to the predictions of the rigid-band theory but is in agreement with the findings of chemisorption experiments.

Other models, such as the coherent potential approximation (CPA)[94], take into account the perturbation of the lattice potential due to the presence of foreign ions and the scattering of electron waves around impurity centres. These theories predict that there is little change either in shape or in the position of the bands of the host metal upon addition of even fairly large amounts of a foreign metal and that virtual bound states (i.e., broadened atomic levels) corresponding to the impurity atoms may develop within the DOS curve[95,96]. These features are illustrated in figure 3.5A which shows the development of a Ni state in a 13% Ni - 87% Cu alloy according to CPA calculations. Also shown in this figure is the optical density of states obtained from photoemission studies[93]. Corresponding results for a 81% Ni - 19% Cu alloy are shown in figure 3.5B. What these results indicate is that a Ni atom does not become indistinguishable from a Cu atom in a Ni - Cu alloy, but

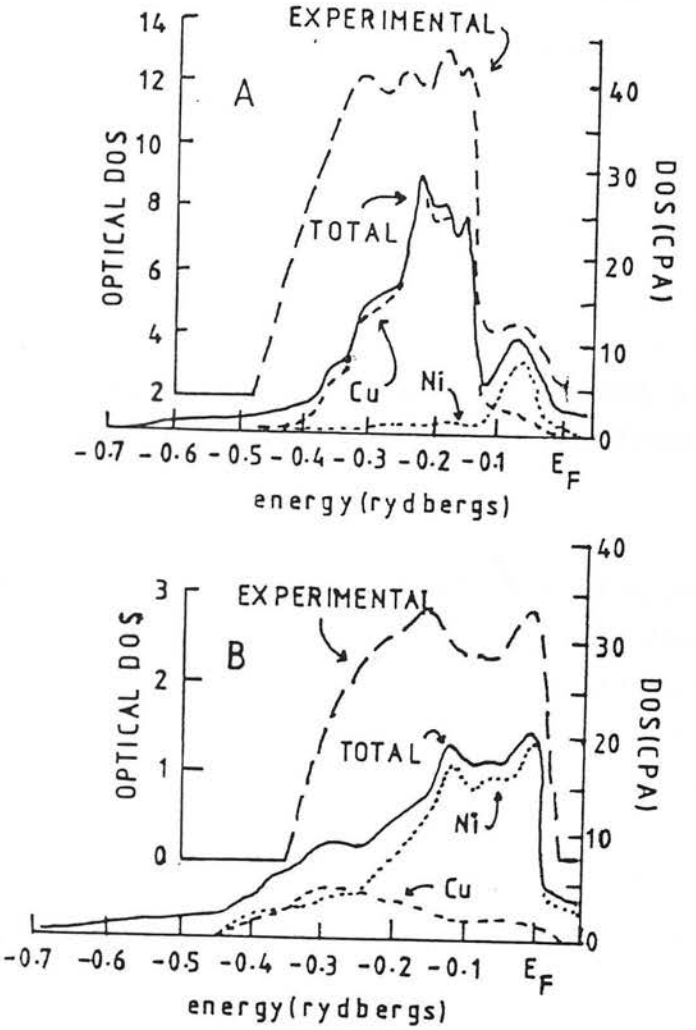

Figure 3.5 - Density of States Curves for Ni - Cu Alloys Calculated from CPA Theory: A - 87% Cu - 13% Ni; B - 81% Ni - 19% Cu. Also shown are optical DOS curves determined from photoemission studies[93]

the local electron density for a Ni atom in a Cu moiety is quite different from that of a Ni atom in a Ni environment[18]. In particular, the d-band of the transition metal becomes narrower with increasing dilution (meaning less interaction with like near-neighbours) and may eventually slip below the Fermi level, at which point the d-band becomes completely full[18] and catalytic activity (at least for reactions involving hydrogen and hydrocarbon) should become very small. The behaviour of different alloys with respect to transition metal d-band filling seems to be different: while in Ni - Cu d-band holes persist up to high Ni dilutions, Pd-Ag alloys have a completely filled d-band for Pd contents smaller than 35%[97]. More substantial interactions are expected with intermetallic compounds. For example in ordered β-brass (Cu - Zn) a downward shift in the position of the Cu d-band with respect to the Fermi level has been observed from UV - photoemission studies[98].

Once it is accepted that the electronic properties of metal atoms are sensitive to the environment, it remains to be established what the relevance of this conclusion might be for chemisorption and catalysis, i.e., whether a ligand effect in catalysis on alloys needs to be considered.

Evidence for the ligand effect is commonly searched from three sources:

1 - temperature - programmed desorption (TPD) of simple adsorbates (H_2, CO) from alloy sufaces[39,55,81,82,99-103];

2 - infrared spectra of adsorbed CO[81,89,104-110];

3 - chemical reaction studies.

In the first case one expects to see changes in the temperatures corresponding to the desorption peak maxima as a function of alloy composition, arising from changes in chemisorptive bond strength.

In the second case, one looks for changes in frequency of the CO streching vibration which should decrease with increasing d-electron density due to increased backdonation of electrons to antibonding π-orbitals of the adsorbed CO molecule[108].

In chemical reaction studies, the occurrence of synergistic effects (maxima[14,111-116] in catalytic activity as a function of alloy composition) have been frequently associated with an electronic effect. Sudden changes in activation energies[7,90] or the observation of very small reaction rates[117-119] (as compared to the unalloyed group VIII metal in group VIII - IB metal alloys) at alloy composition where the d-band is expected to be filled are also taken as evidence for an electronic effect.

TPD studies of CO[99,100] or H_2[39,101,103] from Pt-Au[39,101,103] and Ni - Cu[99,100] alloys have generally suggested that variations of chemisorptive bond strength with alloying are small in these systems, although the relative populations of different adsorbed states vary. An interesting study was reported recently by Sachtler and Somorjai on the TPD spectra of CO from Pt-Au single crystals[103]. These authors found that the temperatures of the peak maxima <u>increased</u> with increasing Au content, which is contrary to the predictions of a band filling effect. It was proposed that increasing Au contents caused decreasing repulsive interactions between adsorbed CO molecules due to isolation of Pt sites. With other alloys such as Pt-Sn[55], Ru - Cu[82] and Ir - Au[102] substantial changes in peak positions have been observed. The former case is not really surprising since Pt and Sn form exothermal alloys and the interaction between the metals is expected to be large but results obtained with the Ru-Cu and Ir-Au systems seem to counter some recent suggestions that the ligand effect is of little importance

with endothermal or weakly exothermal alloys[108].

The interpretation of infrared spectra of CO adsorbed on alloys is complicated due to several reasons. First, CO may adsorb in several forms involving different degrees of coordination with surface atoms and this may lead to changes in the infrared spectra due to geometric (ensemble effect) rather than to electronic reasons[104]. Second, lateral and through-bond interactions between adsorbed species may lead to changes in infrared absorption frequency, the main mechanism being the coupling of vibrating dipoles of identical frequencies which causes an upward shift in absorption frequency with increasing coverage of the surface with adsorbed CO molecules[108]. Therefore, reducing the concentration of CO on the surface of a transition metal either by exposure to a smaller CO pressure or by alloying with a group IB metal should lead to downward shifts in absorption frequency which have little to do with changes in the electronic properties of the transition metal by alloying. Up to recently, it was generally found with many alloys of catalytic interest (Ni - Cu[106], Pd - Ag[105], Pd - Au[107]) that the effects of alloying were larger than could be accounted for simply by a decrease in surface CO concentration and therefore a ligand effect has been invoked. Toolenaar and coworkers, however, using an isotope dilution method ($^{12}CO + {}^{13}CO$) demonstrated that the dipole coupling effect is enough to explain the observed frequency shift of CO adsorbed on Pt-Cu[108]. The reason for the discrepancy with former results seems to arise from the tendency of CO of form islands on the surface of the transition metal so that adsorbate-adsorbate interactions are already large at low surface coverages[108]. Sachtler has found with the Pd - Ag system[81], and Grill and coworkers with the Pt - Pd system[109], that the decrease in intensity of the band arising from the bridge-bonded form of CO adsorbed on Pd is larger than expected from simple dilution of Pd ensembles. It was suggested that a ligand effect operates, so that the bridge-bonded form is

disfavoured even though Pd ensembles of appropriate dimensions for adsorption of bridge-bonded CO may persist on the surface. Ponec suggested, however, that at least in the case of Pd - Ag uncertainties related to the surface composition of the alloy and the extinction coefficient of the different forms of adsorbed CO may lead to erroneous conclusions[120].

Clear evidence for ligand effects is difficult to obtain from chemical reaction studies. There is first the question that in many cases, particularly in the older literature, the surface composition of the alloys is not known in detail, which makes the interpretation of activity patterns very difficult. Secondly, it is generally accepted nowadays that ensemble effects will always be important if multiple adsorption sites are involved in the kinetically significant steps of a reaction and thus the possible contribution of a ligand effect becomes difficult to evaluate. Evidence for the ligand effect should be searched among the reactions classed as structure insensitive, which are thought to take place on single metal atoms or at most on small ensembles of neighbouring atoms[121]. Even in these cases interpretation of activity patterns is seldom straightforward. For example, maxima in catalytic activity are found for some reactions across a series of bimetallic catalysts[14,111-116]. These maxima are in principle difficult to rationalize from the standpoint of ensemble effects, but in some cases an indirect ensemble effect may be invoked, which causes the suppression of side reactions such as cracking and carbon residue formation. Thus, when benzene hydrogenation is performed at low temperatures (423 K) on Ni - Cu alloys, the activity is seen to drop markedly when Cu is added to Ni[11]. When the reaction is performed at 572 K, however, the alloys are more active than pure Ni[122]. A similar observation has been made regarding cyclohexane dehydrogenation on Pt - Sn or Pt - Pb: at 588 K activity

decreases continounsly with addition of the "inactive" metal (Pb, Sn) but at 773 K a maximum in activity is observed[123]. In these cases it is almost certain that at the higher temperatures side reactions occur which are suppressed by alloying possibly by an ensemble effect[122,123].

With Pd alloys the added complication exists that hydrogen dissolved in the metal may cause poisoning of the catalyst and since alloying may result in a decrease in the solubility of hydrogen, an increase in activity may be observed. In this way, the maximum in activity for ethylene hydrogenation on Pd - Ni alloys has been interpreted[124]. Also in cyclopentane exchange with deuterium on Pd - Au films a maximum in the ratio of one-set to two-set exchange (cf. chapter 5 for definition of these terms) is observed when the reaction is carried-out under ca. 8 torr of D_2 (large solubility of D_2) but not when the D_2 pressure is ca. 1 torr (small solubility of D_2)[125].

With Pd - Ag and Pd - Au alloys it is observed that activity for many reactions involving hydrogen (CH_4 exchange with D_2[117,118], ethylene hydrogenation[126], benzene hydrogenation[119]) drops to very small values for Pd contents smaller than about 40 - 60%. In other cases (e.g. ortho-para hydrogen conversion[7], formic acid decomposition[90]) a marked increase in activation energy is observed. Since it is known that the Pd d-band becomes filled in these alloys at about the same composition range, it is difficult to escape the conclusion that a ligand effect is important in these cases.

In some other hydrogenation reactions (e.g. but-2-yne hydrogenation)[16] no break in activity corresponding to d-band filling of Pd - Au alloys can be observed and it is possible that strong adsorption of the reactant overrides the bimetallic interaction.

We end-up this section by reviewing some recent results which have been interpreted in terms of a ligand effect. Renouprez and coworkers studied the isomerization and hydrogenolysis of neopentane on Pt-Ni/Al_2O_3 catalysts[116]. A maximum in activity for hydrogenolysis (ca. 2 orders of magnitude relative to pure Ni) was found with 10% Pt - 90% Ni and a similar maximum in isomerization activity was found with 85% Pt - 15% Ni. Maxima for the density of states at the Fermi level are expected at these approximate compositions from X-ray absorption measurements[116].

Becaud and coworkers studied the hydrogenation of benzene on Pt - Sn alloys and found the activity to drop to zero for Pt contents lower than 68%[127]. Evidence from Mössbauer spectroscopy was claimed for s-electron transfer from Sn to Pt.

Shimizu and coworkers observed that 5% of a monolayer of Cu on Ru reduces the saturation amount of chemisorbed hydrogen by about 50% but have little influence on the heat of hydrogen chemisorption[82]. Interpretation of this result from the standpoint of ensemble theory would lead to the conclusion that an ensemble of about seven Ru atoms is necessary for hydrogen chemisorption. A ligand effect of the type described in scheme 3.4 was proposed to account for this result. The same type of model has been recently proposed by Burch[18] to explain the very large ensemble sizes the are sometimes deduced from activity patterns on alloys[86,128] and was also adopted by Dalmon and Martin to explain why CO methanation on Ni - Cu/SiO_2 catalysts apparently requires a 12 atom ensemble[86].

Some catalysts which may be described as consisting of a layer of an active metal adsorbed on the surface of a second metallic phase display a catalytic behaviour rather different from that of the pure active

metal. Thus, Somorjai and coworkers studied the dehydrogenation of cyclohexane on Pt deposited on a Au (100) surface. The activity was found to increase with increasing Pt content and constant activity was only found after deposition of two or more Pt layers[129]. Furthermore the Pt bilayer was six times more active than a Pt (100) surface. Anderson and Mainwaring observed that supported Co - Rh catalysts prepared by decomposition of bimetallic carbonyls ($CO_2Rh_2(CO)_{12}$) had a markedly larger selectivity for hydrocarbon isomerization and cyclization reactions than either supported Co or Rh alone[130]. There was evidence that the surface of the bimetallic catalysts was strongly enriched in Co and it was proposed that the catalytic behaviour was characteristic of a Co monolayer on a Rh matrix. Both the Pt - Au and the Co - Rh results were explained from the standpoint of an electronic effect.

3.4.2 - The ensemble effect

Evidence for ensemble effects in catalysis on metals comes from several sources:

1 - From hydrogen pressure dependence studies, it was observed that many hydrocarbon reactions, such as hydrogenolysis, proceed from dehydrogenated intermediates[19]. It is then natural to assume that several neighbouring metal atoms are required to bind the dehydrogenated intermediate and to accomodate the hydrogen atoms split off the hydrocarbon molecule.

2 - It was realized, as explained before, that metal atoms keep much of their identity upon alloying, so that adsorbates are capable of distinguishing between "active" and "inactive" atoms[10-15].

3 - A precipitous decrease in catalytic activity is observed with some reactions upon adding an "inactive" to an "active" metal with no corresponding change in

activation energy, which suggests that it is the number rather than the quality of the active sites which is being changed[15,34,102,128].

If two reactions proceeding on the same metal A require ensembles with different numbers of metal atoms, it is easy to see[85] that the reaction which requires the largest ensemble will be more sensitive to addition of an inactive metal B, provided that the presence of one or more atoms of B in the ensemble renders the whole reaction site inactive. This may result in important selectivity effects in alloy catalysis and a much quoted example is that of the results obtained by Sinfelt and coworkers with the reactions of ethane and cyclohexane on Ni - Cu catalysts, illustrated in figure 3.6[14]. It is clear that the activity for ethane hydrogenolysis decreases precipitously upon Cu addition while the activity for cyclohexane dehydrogenation is hardly affected and in fact increases slightly. These results may be qualitatively understood if ethane hydrogenolysis requires a larger Ni ensemble than cyclohexane dehydrogenation. As explained in the previous section, the increase in activity for the cyclohexane reaction may be also understood from the standpoint of ensemble theory if side reactions such as hydrogenolysis and carbon deposition are suppressed due to alloying.

There is a large body of evidence in the literature that destructive reactions such as hydrogenolysis are more sensitive to alloying than non-destructive reactions such as hydrogenation-dehydrogenation, cyclization and isomerization reactions (e.g. references[13,15,23,87,88,103,122,123,128,131,132]).

Several mechanisms working in parallel are thought to contribute to each of these reactions[24,133] and since different mechanisms may have different ensemble requirements, rather complex activity patterns may result.

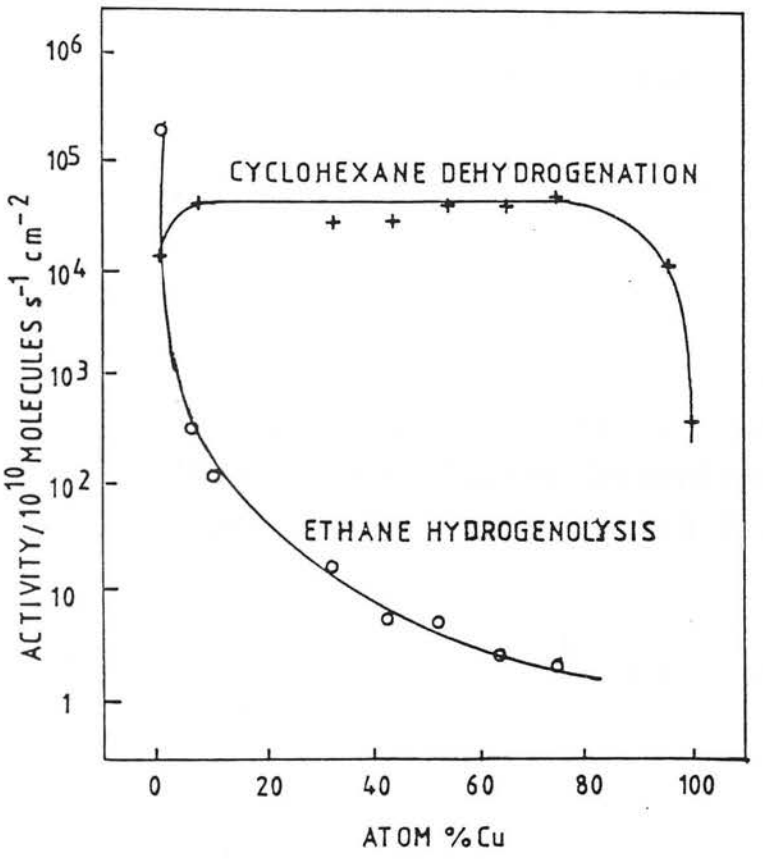

Figure 3.6 - Specific Activities of Ni - Cu Alloy Catalysts for Ethane Hydrogenolysis and Cyclohexane Dehydrogenation at 589 K[14]

Thus, for example, van Schaik and coworkers have found that SiO_2 supported Pt - Au alloys containing 12.5% Pt produce approximately equal amounts of cyclization and isomerization products from n-hexane while alloys with ca. 2% Pt produce only isomerization products[131]. With Pt/SiO_2, the selectivity for isomerization is again much larger than the selectivity for cyclization. These results were explained by assuming that isomerization may proceed through both one-site (highly diluted Pt in Au) and multiple site (Pt rich catalysts) mechanisms, while cyclization requires a multiple site[131].

The large predominance of isomerization over cyclization on Pt/SiO_2 probably arises from the fact that C_5 cyclic products initially formed on the surface suffer ring-opening in another position before desorption to yield isomerization products via the so-called cyclic route for isomerization[133].

Anderson subdivides the ensemble required for a given reaction in two parts[134]:

1 - The critical site, which is required to bind the chemisorbed species to the surface;

2 - The secondary site, which is required to maintain the flow of hydrogen to and from the critical reaction site during hydrogenation - dehydrogenation steps.

Anderson believes that isomerization and hydrogenolysis may proceed through a common intermediate in some cases, but hydrogenolysis products are formed when the supply of hydrogen around the critical site is large. The increase in selectivity for isomerization upon alloying a group VIII metal with an "inactive"metal is then thought to be caused by suppression of the supply of hydrogen to the critical site.

With alloys of group VIII elements with Cu

it has been found that the selectivity for hydrogenolysis increases with Cu addition[135-139], which is contrary to what is generally observed with other group VIII - group IB alloys. Nevertheless, the activity of highly diluted alloys of group VIII elements in Cu is considerably larger than the activity of Cu alone. It is believed that mixed ensembles containing both group VIII and Cu atoms are active in hydrogenolysis with an activity smaller than that of ensembles containing only group VIII metals but larger than that of pure Cu ensembles[135-139]. Mixed metal ensembles are likely to play an even more important role in alloys between two "active" metals[57,114].

3.4.3 - The structural effect

As mentioned in chapter 1, recent studies of hydrocarbon reactions on well-characterized surfaces suggest that metal atoms of low coordination play a very important role and different reactions appear to have different requirements in terms of the geometry of the active site[42,129]. Since group IB metals, which are commonly used as the "inactive" component in studies of bimetallic catalysts, are also generally more volatile than group VIII metals, they are expected to segregate to these positions of low coordination (cf. 3.3.3a). Furthermore, alloys may have a tendency to expose a crystal face different than that exposed preferentially by the pure metal[90]. It is thus perhaps surprising that the structural factor has been considered less often than ensemble and ligand effects in alloy catalysis.

Clarke and Rafter studied the decomposition of formic acid on Pd - Au alloy films annealed at 723 K[90]. The energy of activation for the reaction fell linearly upon addition of Pd to Au up to a Pd content of about 50% followed by a sharp increase between 60 and 80% Pd, at which point an activation energy close to that of 100% Pd

was reached. It was observed that the Au rich alloys presented a strong (111) texture while Pd rich films had a (110) texture. When the Pd film was evaporated at 75 K and sintered so as to remove the preferred orientation, an activation energy close to the value obtained for the 50% Pd film was obtained. It was concluded that a textural effect was responsible for the increase in activation energy between 60 and 80% Pd.

Hagen and Somorjai studied the reactions of several hydrocarbons on Pt - Au and Ir - Au foils[87]. It was observed that the rate of isomerization of isobutane per Pt surface atom was independent of Au coverage while hydrogenolysis and dehydrocyclization activity decreased markedly with Au addition. It was proposed that isomerization on one hand and hydrogenolysis and dehydrocyclization on the other occur on separate sites (low index planes for isomerization and defect sites for the other reactions) and that Au atoms become preferentially located at defect sites.

Clarke and coworkers observed that a SiO_2 supported Pt 10% - Au catalyst showed no sign of activity for n-pentane cyclization while dilute Pt in Au films were active for this reaction[88]. It was proposed that absence of 1,5 - cyclization on the supported catalyst is a result of the severe heat treatment used during preparation and blocking by Au of the remaining low - coordinated Pt sites thought to be suitable for cyclization.

De Jong and coworkers noticed a sharp decrease in the capacity of Pt for N_2 adsorption upon addition of Ag[89]. Poisoning by Ag of special sites required for N_2 adsorption was proposed to account for the results.

3.5 - REFERENCES

1 - B. C. Gates, J. R. Katzer, G.C.A. Schuit, Chemistry of Catalytic Processes, Mc Graw-Hill, N. York, 1979, chapter 3, p. 184.

2 - J. H. Sinfelt, in Catalysis: Science and Technology, J. R. Anderson and M. Boudart eds., Springer - Verlag, Berlin, 1981, p. 257.

3 - D.A. Dowden, in Catalysis, The Chemical Society, London, 1978, v.2, p. 1.

4 - D. A. Dowden, J. Chem. Soc., 1950, - , 242.

5 - D. A. Dowden, P. W. Reynolds, Disc. Faraday Soc., 1950, 81,184.

6 - D. A. Dowden, Ind. Eng. Chem., 1952, 44, 977.

7 - A. Couper, D.D. Eley, Disc. Faraday Soc., 1950, 8, 105.

8 - G. M. Schwab, Disc. Faraday Soc., 1950, 8, 166.

9 - N. F. Mott, H. Jones, The Theory of the Properties of Metals and Alloys, Clarendon, Oxford, 1936.

10 - W. M. H. Sachtler, G. J. H. Dorgelo, J. Catalysis, 1965, 4, 654.

11 - P. van der Plank, W. M. H. Sachtler, J. Catalysis, 1968, 12, 35.

12 - W. M. H. Sachtler, P. van der Plank, Surf. Sci, 1969, 18, 62.

13 - V. Ponec, W. M. H. Sachtler, J. Catalysis, 1972, 24, 250.

14 - J. H. Sinfelt, J. L. Carter, D. J. C. Yates, J. Catalysis, 1972, 24, 283.

15 - J. H. Sinfelt, J. Catalysis, 1973, 29, 308.

16 - H. G. Rushford, D. A. Whan, Trans. Faraday Soc., 1971, 67, 3577.

17 - W. M. H. Sachtler, R.A. van Santen, Adv. Catalysis,1977, 26, 69.

18 - R. Burch, Acc. Chem. Res., 1982, 15, 24.

19 - J. H. Sinfelt, Adv. Catalysis, 1973, 23, 91.

20 - G. Maire, G. Plouidy, J. C. Prudhomme, F. G. Gault, J. Catalysis, 1965, 4, 556.

21 - J. R. Anderson, N. R. Avery, J. Catalysis, 1966, 5, 446.

22 - M. Boudart, A. W. Aldag, L. D. Ptak, J. E. Benson, J. Catalysis, 1968, 11, 35.

23 - V. Ponec, W. M. H. Sachtler, in Proceedings of the Fifth International Congress on Catalysis, J. H. Hightower ed., North-Holland, Amsterdam, 1973, v.1, p. 645.

24 - V. Ponec, in The Chemical Physics of Solid Surfaces and Heterogeneous Catalysis, D. A. King, D. P. Woodruff eds., Elsevier, Amsterdam, 1982, v. 4,p.365.

25 - W. H. M. Sachtler,in Chemistry and Chemical Engineering of Catalytic Processes, R. Prins, G.C.A. Schuit eds., Sijthoff and Noordhoff, Alphen aan den Rijn, 1980, p. 317.

26 - R. A. Swalin, Thermodynamics of Solids, John Wiley, N. York, 2nd ed., 1972.

27 - M. Hansen, K. Anderko, Constitution of Binary Alloys, M. Graw-Hill, N. York, 2nd ed., 1958.

28 - W. M. H. Sachtler, R. Jongepier, J. Catalysis, 1965, 4, 665.

29 - R. L. Moss, H. R. Gibbens, D. H. Thomas, J. Catalysis, 1970, 16, 117.

30 - D. F. Ollis, J. Catalysis, 1971, 23, 131.

31 - D. W. Hoffman, J. Catalysis, 1972, 27, 374.

32 - F. Garbassi, A. Marzi, G.R. Tauszik, J. Catalysis, 1981, 69, 283.

33 - F. J. Kuyers, R. P. Dessing, W. M. H. Sachtler,

J. Catalysis, 1974, 33, 316.

34 - A. J. Rouco, G. L. Haller, J. Catalysis, 1981, 72, 246.

35 - J. H. Sinfelt, Y. L. Lam, J. A. Cusumano, A. E. Barnett, J. Catalysis, 1976, 42, 227.

36 - E. B. Prestridge, G. H. Via, J. H. Sinfelt, J. Catalysis, 1977, 50, 115.

37 - E. Raub, W. Platte, Z. Metallkunde, 1956, 47, 688.

38 - R. L. Moss, H. R. Gibbens, J. Catalysis, 1972, 24, 48.

39 - J. R. Anderson, K. Foger, R. J. Breakspere, J. Catalysis, 1979, 57, 458.

40 - G. A. Somorjai, Chemistry in Two Dimensions: Surfaces, Cornell University, Ithaca, 1981.

41 - J. J. Burton, E. Hyman, D. G. Fedak, J. Catalysis, 1975, 37, 106.

42 - G. A. Somorjai, Adv. Catalysis, 1977, 26, 1.

43 - Y. S. Ng, S. B. McLane, T. T. Tsong, J. Vac. Sci Technol., 1980, 17, 154.

44 - M. P. Seah, J. Catalysis, 1979, 57, 450.

45 - F. L. Williams, D. Nason , Surf. Sci.,1974, 45, 377.

46 - M. Kelley, J. Catalysis, 1979, 57, 113.

47 - P. Wynblatt, R. C. Ku, J. Catalysis, 1977, 65, 511.

48 - J. J. Burton, R. S. Polizzotti, Surf. Sci., 1977, 66, 1.

49 - D. F. Ollis, J. Catalysis, 1979, 59, 430.

50 - N. H. Tsai, G. M. Pound, F. F. Abraham, J. Catalysis, 1977, 50, 200.

51 - J. H. Anderson, Jr., P. J. Conn, S. G. Brandenberger, J. Catalysis, 1970, 16, 404.

52 - C. R. Helms, J. H. Sinfelt, Surf. Sci., 1978, 72, 229.

53 - K. Christmann, G. Ertl, H. Shimizu, J. Catalysis, 1980, 61, 397.

54 - R. A. Van Santen, W. M. H. Sachtler, J. Catalysis, 1974, 33, 202.

55 - H. Verbeek, W. M. H. Sachtler, J. Catalysis, 1976, 42, 257.

56 - M. Nakamura, B. J. Wood, P. Y. Hou, H. Wise, in Proceedings of the Seventh International Congress on Catalysis, T. Seyama, K. Tanabe eds., Elsevier, Amsterdam, 1981, v.1, p. 432.

57 - I. H. B. Haining, C. Kemball, G. L. Haller, J. Chem. Soc. Faraday Trans. I, 1981, 77, 519.

58 - J. H. Anderson, Jr.,P. J. Conn, S. G. Brandenberger, J. Catalysis, 1970, 16, 326.

59 - R. Bowmann, G. J. M. Lippits, W. M. H. Sachtler, J. Catalysis, 1972, 25, 300.

60 - T. Wang, L. D. Schmidt, J. Catalysis, 1981, 71, 411.

61 - V. Mintsa - Eya, L. Hilaire, R. Touroude, F. G. Gault, B. Moraweck, A. Renouprez, J. Catalysis, 1982, 76, 169.

62 - H. Miura, R. D. Gonzalez, J. Catalysis, 1982, 74, 216.

63 - J. R. Anderson, Structure of Metallic Catalysts, Academic, London, 1975, p. 446.

64 - S. Galvagno, J. Schwank, G. Parravano, J. Catalysis, 1980, 61, 223.

65 - I. W. Bassi, F. Garbassi, G. Vlaic, A. Marzi, G. R. Tauszik, G. Cocco, S. Galvagno, G. Parravano, J. Catalysis, 1980, 64, 405.

66 - D. E. Resasco, G. L. Haller, Appl. Catalysis, 1983, 8, 99.

67 - R. L. Moss, L. Whalley, Adv. Catalysis, 1972, 22,115.

68 - H. C. de Jongste, F. J. Kuijers, V. Ponec, in

Preparation of Catalysts, B. Delmon, P. A. Jacobs, G. Poncelet eds., Elsevier, Amsterdam, 1976, p.207.

69 - R. L. Moss, D. Pope, B. J. Davis, J. Catalysis, 1980, 61, 57.

70 - W. K. Shiflett, J. A. Dumesic, J. Catalysis, 1982,77, 57.

71 - K. Foger, H. Jaeger, J. Catalysis, 1981, 70, 53.

72 - W. N. Delgass, G. L. Haller, R. Kellerman, J. H. Lunsford, Spectroscopy in Heterogeneous Catalysis, Academic, N. York, 1979.

73 - Y. L. Lam, Ph.D. Thesis, Stanford, 1978.

74 - R. L. Garten, J. H. Sinfelt, J. Catalysis, 1980, 62, 127.

75 - J. H. Sinfelt, G. H. Via, F. W. Lytle, J. Chem. Phys., 1980, 72, 4832.

76 - R. L. Moss, in Catalysis, The Chemical Society, London, 1977, v. 1, p. 37.

77 - F. J. Kuijers, V. Ponec, Appl. Surf. Sci., 1978, 2, 43.

78 - P - C. Liao, T. H. Fleisch, E. E. Wolf, J. Catalysis, 1982, 75, 396.

79 - T. C. Wong, L. F. Brown, G. L. Haller, C. Kemball, J. Chem. Soc. Faraday Trans. I, 1981, 71, 519.

80 - H. R. Gerberich, N. W. Cant, K. W. Hall, J.Catalysis, 1970, 16, 204.

81 - W. M. H. Sachtler, Catalysis Rev., 1976, 14, 193.

82 - H. Shimizu, K. Christmann, G. Ertl, J. Catalysis, 1980, 61, 412.

83 - H. Miura, R. D. Gonzalez, J. Catalysis, 1982, 74,216.

84 - R. Gomez, G. Corro, G. Diaz, A. Maubert, F. Figueras, Nouv. J. Chim., 1980, 4, 677.

85 - D. A. Dowden, in Proceedings of the Fifth International Congress on Catalysis, J. W. Hightower ed., North - Holland, Amsterdam, 1973, v.1, p. 621.

86 - J. A. Dalmon, G. A. Martin, in Proceedings of the Seventh International Congress on Catalysis, T. Seiyama and K. Tanabe eds., Kodansha, Tokyo, 1981, p. 402.

87 - D. I. Hagen, G. A. Somorjai, J. Catalysis, 1976, 41, 466.

88 - J. K. A. Clarke,A. F. Kane, T. Baird, J. Catalysis, 1980, 64, 200.

89 - K. P. de Jong, B. E. Bongenaar - Schleuter , G. R. Meima, R. C. Verbeek, M. J. J. Lammers, J. W. Geus, J. Catalysis, 1983, 81, 67.

90 - J. K. A. Clarke, E. A. Rafter, Z. Phys. Chem., 1969, 67, 169.

91 - N. W. Ashcroft, N. D. Mermin, Solid State Physics, Holt, Rinehart and Winston, N. York, 1976.

92 - D. J. Sellmyer, Solid State Physics, 1978, 33, 83.

93 - W. E. Spicer, in Band Structure Spectroscopy of Metals and Alloys, D. J. Fabian and L. M. Watson eds., Academic, London, 1973, p. 7.

94 - P. Soven, Phys. Rev., 1969, 178, 1136.

95 - G. M. Stocks, R. W. Williams, J. S. Faulkner, Phys. Rev. B, 1971, 4, 4390.

96 - G. M. Stocks, R. W. Williams, J. S. Faulkner, J.Phys. F, 1973, 3, 1688.

97 - S. Hüfner, G. C. Wertheim, J. H. Wernick, Phys. Rev. B, 1973, 8, 4511.

98 - P. O. Nilsson, I. Lindau, J. Phys. F, 1971, 1, 854.

99 - C. Benndorf, K. H. Gressman, J. Kessler, W. Kirstein, F. Thieme, Surf. Sci., 1979, 85, 389.

100 - J. C. M. Herberts, A. F. Bourgonje, J. J. Stephan, V. Ponec, J. Catalysis, 1977, 47, 92.

101 - J. J. Stephan, V. Ponec, W. M. H. Sachtler, Surf. Sci., 1975, 47, 403.

102 - K. Foger, J. R. Anderson, J. Catalysis, 1980, 64, 448.

103 - J. W. A. Sachtler, G. A. Somorjai, J. Catalysis, 1983, 81, 77.

104 - Y. Soma - Noto, W. M. H. Sachtler, J. Catalysis, 1974, 32, 315.

105 - M. Primet, M. V. Mathieu, W. H. M. Sachthler, J. Catalysis, 1976, 44, 324.

106 - J. A. Dalmon, M. Primet, G. A. Martin, B. Imelik, Surf. Sci., 1975, 50, 95.

107 - E. L. Kluger, M. Boudart, J. Catalysis, 1979, 59, 201.

108 - F. J. C. M. Toolenaar, F. Stoop, V. Ponec, J. Catalysis, 1983, 82, 1.

109 - C. M. Grill, M. L. McLaughlin, J. M. Stevenson, R.D. Gonzalez, J. Catalysis, 1981, 69, 454.

110 - A Palazov, CH. Bonev, G. Kadinov, D. Shopov, J. Catalysis, 1981, 71, 1.

111 - T. J. Gray, N. G. Masse, H. G. Oswin, in Actes du Deuxième Congrès International de Catalyse, Technip, Paris, 1961, v. 2, p. 1697.

112 - G. C. Bond, D. E. Webster, Ann. New York Acad. Sci., 1969, 158, 540.

113 - J. P. Brunelle, R. E. Montarnal, A. A. Sugier, in Proceedings of the Sixth International Congress on Catalysis, G. C. Bond, P. B. Wells, F. C. Tompkins eds., The Chemical Society, London, 1977, v. 2, p. 844.

114 - G. Leclercq,H. Charcosset, R. Maurel, C. Bertizeau, C. Bolivar, R. Frety, D. Jaunay, H. Mendez, L. Tournayan, Bull. Soc. Chim. Belg., 1979, 88, 577.

115 - M. Nakamura, H. Wise, ref. 113, v. 2, p. 881.

116 - A. J. Renouprez, B. Moraweck, B. Imelik, V. Perrichon, J. M. Dominguez - Esquivel, J. Jablonski, ref. 56, v. 1, p. 173.

117 - D. W. McKee, J. Phys. Chem., 1966, 70, 525.

118 - Z. Karpinski, J. Catalysis, 1982, 77, 118.

119 - A. O'Cinneide and J. K. A. Clarke, J. Catalysis, 1972, 26, 233.

120 - V. Ponec., ref. 25, p. 257.

121 - M. Boudart, ref. 113, v. 1, p.1.

122 - G. A. Martin, J. A. Dalmon, J. Catalysis, 1982, 75, 233.

123 - J. Völter, G. Lietz, M. Uhlemann, M. Hermann, J. Catalysis, 1981, 68, 42.

124 - R. L. Moss, D. Pope, H. R. Gibbens, J. Catalysis, 1977, 46, 204.

125 - J. K. A. Clarke, J. F. Taylor, J. Chem. Soc. Faraday Trans. I, 1976, 72, 917.

126 - E. G. Allison, G. C. Bond, Catalysis Rev., 1972, 7, 233.

127 - R. Bacaud, P. Bussière, F. Figueras, J. Catalysis, 1981, 69, 399.

128 - J. A. Dalmon, G. A. Martin, J. Catalysis, 1980, 66, 214.

129 - S. M. Davis, G. A. Somorjai, ref. 24, p. 217.

130 - J. R. Anderson, E. E. Mainwaring, Ind. Eng. Chem. Prod. Res. Dev., 1978, 17, 202.

131 - J. R. H. van Schaik, R. P. Dessing, V. Ponec, J. Catalysis, 1975, 38, 273.

132 - A. Péter, J. K. A. Clarke, J. Chem. Soc. Faraday Trans. I, 1976, 72, 1201.

133 - F. Garin, F. G. Gault, ref. 25, p. 351.

134 - J. R. Anderson, Am. Chem. Soc. Div. Petr. Chem. Prepr., 1981, 26, 361.

135 - H. C. de Jongste, F. J. Kuijers, V. Ponec, ref. 113, v. 2, p. 915.

136 - H. C. de Jongste, V. Ponec, ref. 56, v. 1, p. 186.

137 - H. C. de Jongste, V. Ponec, J. Catalysis, 1980, 63, 389.

138 - H. C. Jongste, V. Ponec, F. G. Gault, J. Catalysis, 1980, 63, 395.

139 - P. Botman, H. C. de Jongste, V. Ponec. J. Catalysis, 1981, 68, 9.

CHAPTER 4

EXPERIMENTAL METHODS

CHAPTER 4

EXPERIMENTAL METHODS

4.1 INTRODUCTION

It is the object of the present chapter to describe the apparatus, procedure and data handling methods used in the study of hydrocarbon reactions on the several catalysts selected for investigation. Other techniques were used in individual parts of the present work mainly for catalyst characterization (temperature programmed reduction, pulse chemisorption/titration techniques) and experimental details are given in the relevant chapters. Catalyst preparation methods are also described in individual chapters. Chapter 6 deals mainly with a study of cyclopentane exchange with deuterium using deuterium-n.m.r. spectroscopy and experimental details relating to this technique are presented therein.

4.2 APPARATUS

All reactions were carried-out in static glass reactors of approximately 200 cm^3 volume attached to conventional gas-handling lines[1,2]. Analysis of the isotopic products during exchange reactions were performed by means of a mass-spectrometer directly connected to the reactor via a capillary leak. In reactions carried-out in the presence of hydrogen, samples were drawn from the reaction vessel and injected into a gas chromatograph for analysis of the products.

4.2.1 - The vacuum lines, reactor and sampling systems

Three separate vacuum lines were used in the present work. Line 1 was used in exchange reactions. Line 2 was used in reactions of small hydrocarbon molecules (isobutane, isopentane and neopentane). Line 3 was used in

the reactions of C_6 hydrocarbons (n-hexane, methylcyclopentane).

A schematic drawing of line 1 is shown in figure 4.1. All lines were of similar design and differred only in small details, the main one being thatgreaseless taps (Springham Ltd) were used in lines 1 and 3 and conventional ground glass stopcocks lubricated with Apiezon L vacuum grease were used in line 2.

All lines were equipped with two pumping systems each comprised of an Edwards ED50 "Speedivac" rotary pump and an electrically heated mercury diffusion pump made of glass. One of the pumping systems (pumping system 1) was used to evacuate exclusively the reactor volume while the rest of the line was evacuated by means of the second pumping system (pumping system 2). The ultimate vacuum attainable with these systems was of ca. 10^{-3} Pa. The residual pressure in the lines was measured by means of McLeod gauges and was frequently checked to ensure that after pretreatment and before the start of each experiment the catalysts were in contact only with the best possible vacuum. Cold traps cooled in liquid nitrogen baths were inserted between each pumping system and the lines in order to prevent contamination with mercury vapours.

Hydrogen and deuterium used in preparing reaction mixtures were purified by diffusion through electrically heated Pd-Ag thimbles (TH in figure 4.1) During purification, hydrogen or deuterium flowed from a bulb containing the "impure" gas (B1), through the Pd-Ag thimble, then through a cold trap immersed in liquid nitrogen (CT1), into a storage bulb permanently attached to the line (B2). The remaining reactants were introduced via the ground glass joints (J1, J2, J3) from glass bottles equipped with teflon Rotaflo taps (liquid reactants) or from gas cylinders (gaseous reactants)

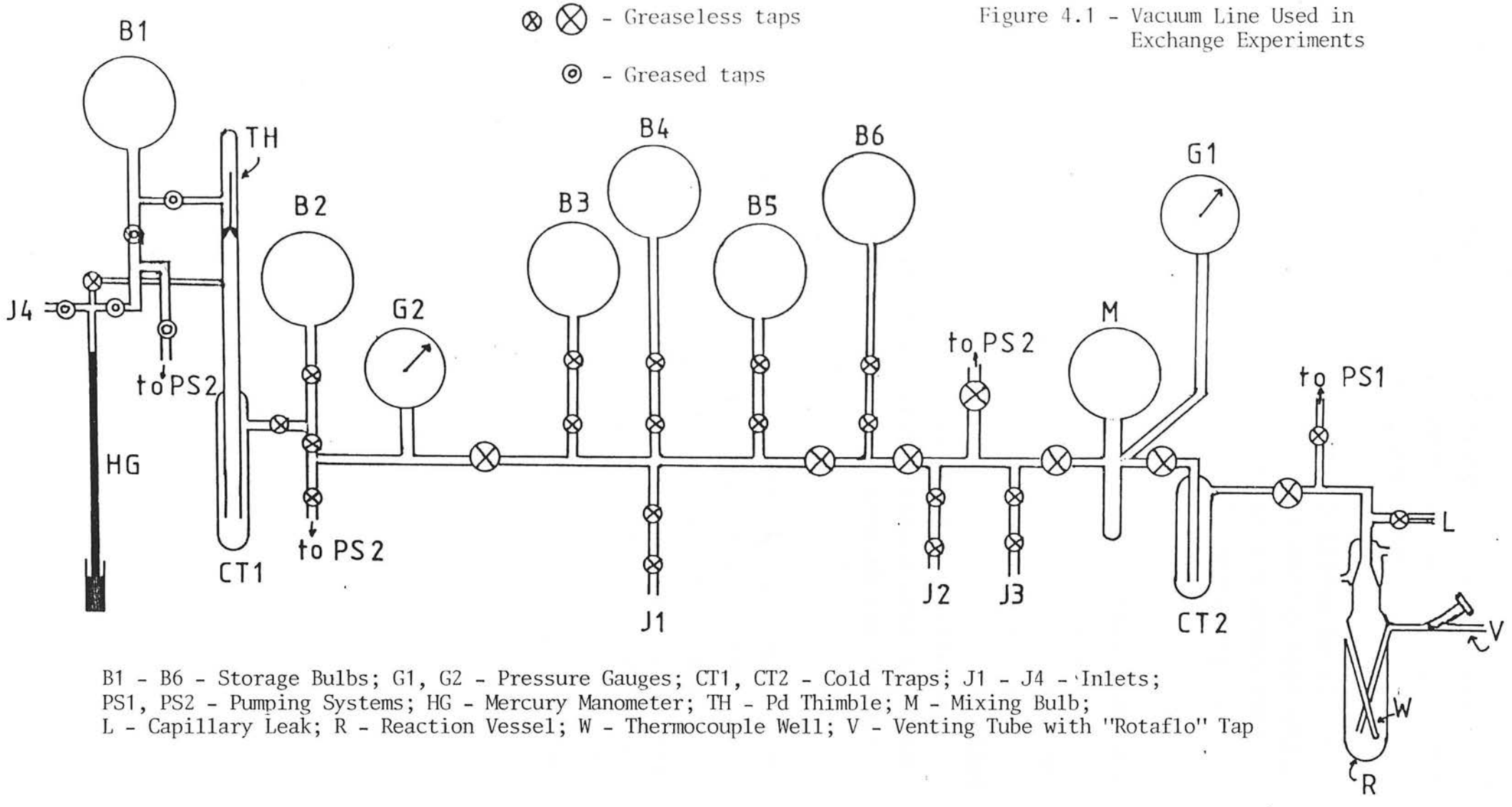

Figure 4.1 - Vacuum Line Used in Exchange Experiments

B1 - B6 - Storage Bulbs; G1, G2 - Pressure Gauges; CT1, CT2 - Cold Traps; J1 - J4 - Inlets;
PS1, PS2 - Pumping Systems; HG - Mercury Manometer; TH - Pd Thimble; M - Mixing Bulb;
L - Capillary Leak; R - Reaction Vessel; W - Thermocouple Well; V - Venting Tube with "Rotaflo" Tap

according to the procedure described in a subsequent section. After purification gaseous reactants were stored in bulbs permanently attached to the lines.

Reaction mixtures were prepared by placing known pressures of each reactant into a mixing bulb (M). The pressures were measured by means of a Bourdon type gauge (Leybold model 16044 or similar) previously calibrated against a mercury manometer (HG).

The hydrogen used in catalyst reduction was fed from a gas cylinder and was purified by passage through a "Deoxo" unit (Engelhard) to remove oxygen, then through a 4A molecular sieve trap to remove water and finally through a cold trap packed with 4A molecular sieve cooled in liquid nitrogen to complete condensation of water. After purification, hydrogen flowed into the line via one of the ground glass joints, through the reactor and out via the venting tube V.

In lines 1 and 3 (where grealess taps were used) the reactor was attached to the line through a water-cooled greaseless joint (size B24) and vacuum sealing was achieved by means of a Viton ring. Whith line 2 the reactor was attached via a B24 water-cooled ground glass joint lubricated with Apiezon L grease. The design of the reactor also included a thermocouple well (W) that extended down to the bottom of the reactor.

The reactor was heated using an externally placed close fitting tubular furnace consisting of a silica tube around which a resistance wire was wound. A chromel-alumel thermocouple was strapped to the outside of the reaction vessel and was connected to an "Eurotherm" proportional temperature controller (model PID-SCR or similar). The temperature inside the reactor was monitored by means of a chromel-alumel thermocouple inserted into the thermocouple well W and connected to a "Comark"

digital voltmeter (model 300). In all experiments the temperature was held constant to within $\pm 1^{o}$. Some reactions were carried-out at below room temperature. In these experiments the reactor was cooled using a "slush" bath prepared by stirring a substance of adequate melting point with liquid nitrogen. Carbon tetrachloride was used for reactions carried-out at 250 K and aniline for experiments at 263 K.

In isotopic exchange experiments (line 1) the reaction vessel was connected to the mass spectrometer via a capillary leak which allowed about 2% per hour of the reaction mixture to be drawn continuously into the mass spectrometer.

Figure 4.2 shows a schematic drawing of the sampling system used in line 2. The glass parts of the sampling system were built using capillary tubing so that only about 2% of the reaction mixture were drawn for each sample. With three-way tap S1 in the position shown in figure 4.2 the evacuated sampling system was filled with a sample from the reaction vessel. By turning S1 60^{o} counterclockwise the sampling system was isolated from the reactor. The sample contained in the sampling loop L (0.5 cm^3) was then injected into the gas chromatograph by means of the six-way sampling valve S3. After the injection, valve S3 was returned to the sampling position and tap S1 was turned further 60^{o} conterclockwise to evacuate the sampling system in preparation for the next sampling. The sampling system used in line 3 was similar to the one shown in figure 4.2, except that the three-way greased tap S1 was replaced by two greaseless Springham taps and two separate sampling valves were connected to the system since two chromatographic columns were used in parallel for analysis of the reaction products (see below).

4.2.2 - Mass spectrometer

A fast scanning 90^{o} magnetic sector

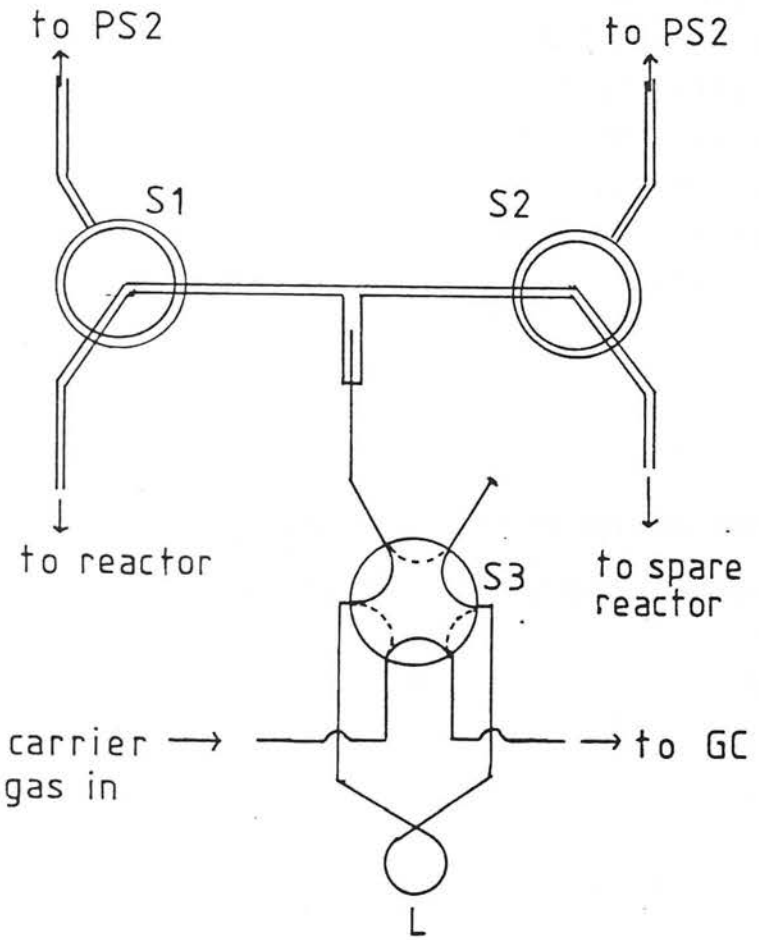

Figure 4.2 - Sampling System for Chromatographic Analysis:
PS2 - Pumping System
S1, S2 - Three - way Greased Taps
S3 - Six - way Sampling Valve
L - Sample Loop

instrument manufactured by Micromass (model MM-601) was used for isotopic analysis of the products in exchange experiments.

The molecules inside the ion source were ionized by electron impact. Different ionizing voltages were used for different exchange reactions so as to obtain a good compromise between adequate sensitivity and minimum mass spectral fragmentation. Although the spectra were corrected for peaks arising from loss of hydrogen or deuterium from the parent ions the errors in evaluating the spectra were minimized by keeping fragmentation to a minimum. The conditions selected for the different experiments are summarized in table 4.1.

TABLE 4.1

IONIZING VOLTAGES AND MASS RANGES USED IN OBTAING MASS SPECTRA

REACTANTS	IONIZING VOLTAGE/V	MASS RANGE
Methane + D_2	16	12 - 20
Neopentane + D_2	70	53 - 66
Cyclopentane + D_2	20	65 - 80
Benzene + D_2	16	76 - 96

The mass region around the parent ion of each hydrocarbon and their respective deuteriated derivatives was scanned by varying the magnetic field strength while keeping the ion accelerating voltage fixed. The neopentane molecule does not produce a measurable parent ion with electron impact ionization so that in this case the region corresponding to the loss of a methyl radical from the parent ion was scanned. Benzene exchange with deuterium was accompanied by a minor amount of deuteration and the mass range was extended to include ions of composition C_6D_{12}.

The ions were detected by means of a Faraday cup collector and the spectra were recorded using a fast response potentiometric recorder. Peak heights were

measured manually to the nearest 0.5 mm. The dynamic range attained (ratio of the largest intensity to the smallest intensity measured) was in the order of 10^4. The time necessary to record one spectrum was between 1 and 3 min.

4.2.3 - Gas chromatographs

Analysis of the reaction mixtures in experiments with $C_{<6}$ hydrocarbons (line 2) were performed with a Hewlett-Packard model F33 gas chromatograph equipped with a flame ionization detector. A 3m column with 1/8 in (3.18 mm) external diameter containing n-octane deposited on 80-100 mesh "Porasil-C" was installed in the gas chromatograph and was operated at room temperature with nitrogen at 50 psig (~450 kPa) as the carrier gas. Under these conditions, all alkanes from methane to n-pentane plus cyclopentane were completely separated in about 20 minutes. As no cyclopentane was observed as a reaction product in these experiments, our chromatograms were completed in about 15 minutes, or less when isobutane was the reactant.

Analysis of the products in experiments with C_6 molecules posed some special problems. The hydrocarbon mixtures obtained were rather complex containing 14 main components (alkanes + benzene) plus some olefins. There were practical limitations to the time that could be consumed in each analysis so that a sufficient number of samples could be analysed in the course of one experiment. By using two chromatographic systems working in parallel we achieved complete separation of all main components of the mixture in about 20 minutes.

Column A was a 50 m stainless steel capillary tube internally coated with squalane. This column was operated at room temperature with helium at 10 psig (170 kPa) pressure as the carrier gas and was installed in an F-11 gas chromatograph equipped with a flame ionization

detector. Figure 4.3 shows the chromatogram for a synthetic mixture of hydrocarbons containing the main components produced in the reactions of C_6 molecules. Isobutane was not present in this synthetic mixture but it eluted between propane and n-butane and was well separated from these components. As is clear from figure 4.3, the methane-ethane pair and the n-butane-neopentane pair were incompletely separated. Neopentane, however, was not detected as a product in the reactions studied so that it did not interfere with the n-butane peak. When methylcyclopentane was used as the reactant the benzene peak was superimposed on the tail of the methylcyclopentane peak. Since benzene was always a minor (but important) reaction product this caused considerable error in evaluating the benzene area from the chromatograms obtained with column A.

The second chromatographic system was comprised of two columns connected in series via a four-way back-flush valve. The arrangement is shown schematically in figure 4.4. Column B in this system was 2m long (3.18 mm outside diameter) and was packed with n-octane deposited on 80-100 mesh "Porasil-C". Column C was 0.3 m long (3.18 mm outside diameter) and was packed with 10% TCEP deposited on 80-100 mesh "Chromosorb-P". Column B was used for the separation of ethane from methane. Saturated hydrocarbons passed almost undisturbed through column C but benzene was retained. The samples were injected first into column B via one of the inlets of the back-flush valve. Methane, ethane and propane eluted separately from this column and flowed into column C which did not retain these hydrocarbons. After these three components eluted from column C, the position of the back-flush valve was changed, which caused the flow of carrier-gas in colunm B to be inverted. This caused the hydrocarbons that were partially separated but had not eluted from column B to be recombined into a single pulse that flowed into column C.

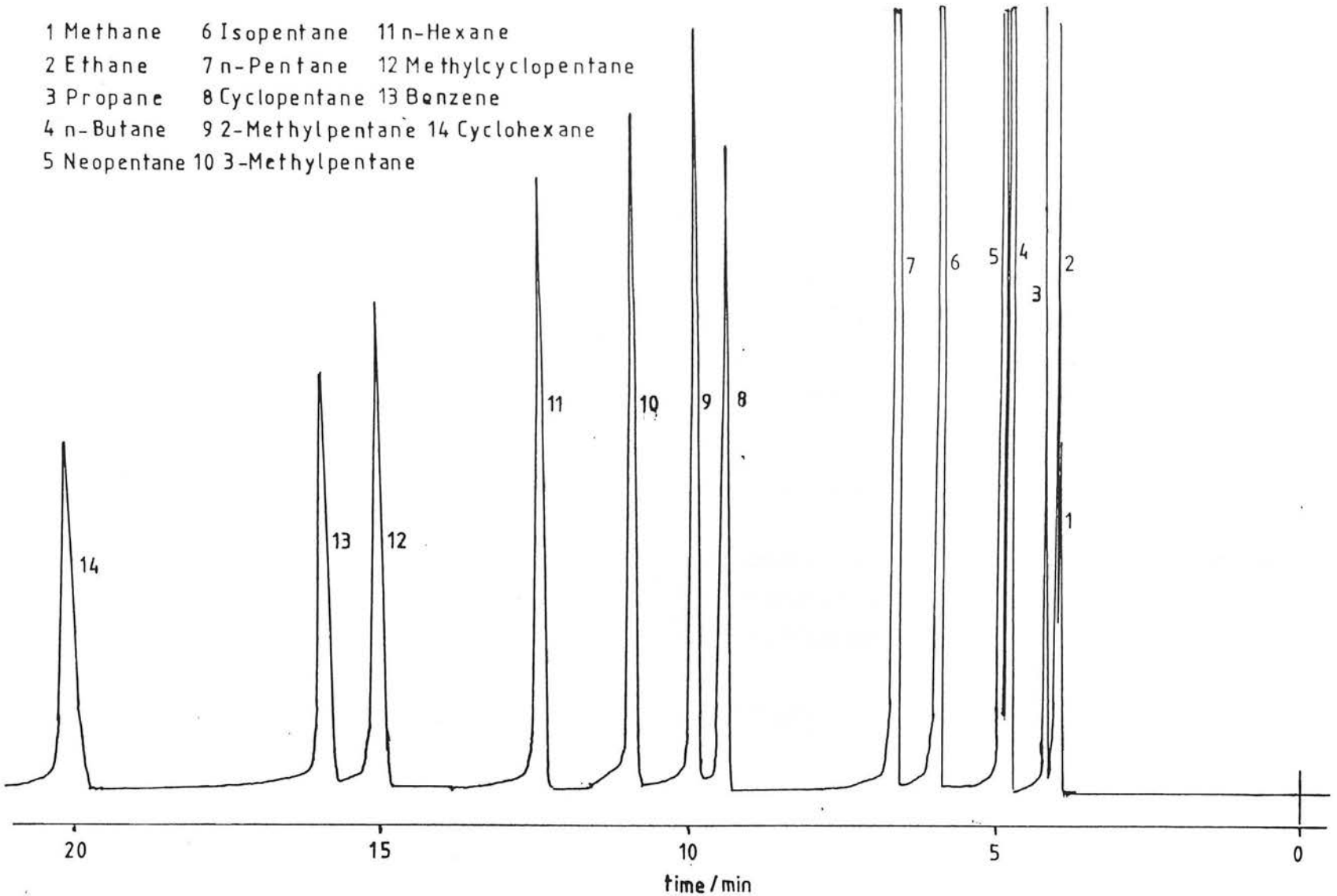

Figure 4.3 - Chromatographic Separation of Hydrocarbons up to C_6 in a 50m Capillary Collumn Coated with Squalane (room temperature, 170 kPa He)

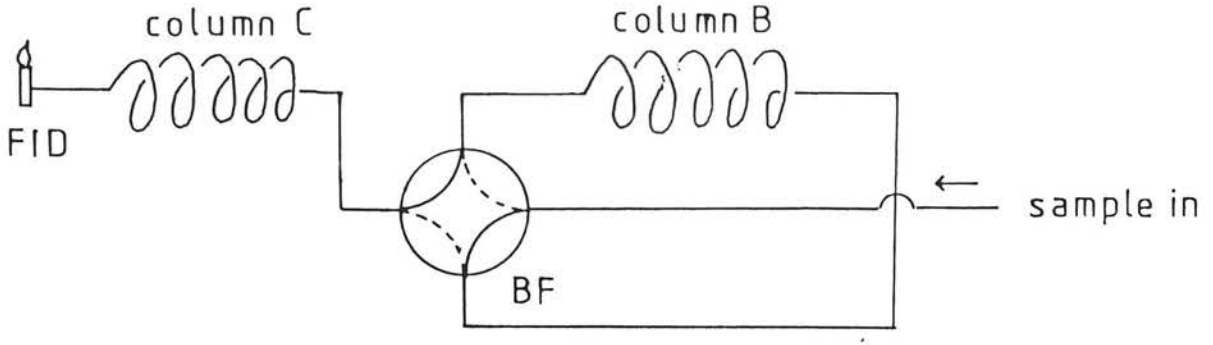

Figure 4.4 - Chromatographic System for Analysis of Light Gases and Benzene;
Column B - 2m n-octane on "Porasil - C".
Column C - 0.3 m 10% TCEP on "Chromosorb - P".
BF - Backflush valve
FID - Flame Ionization Detector.

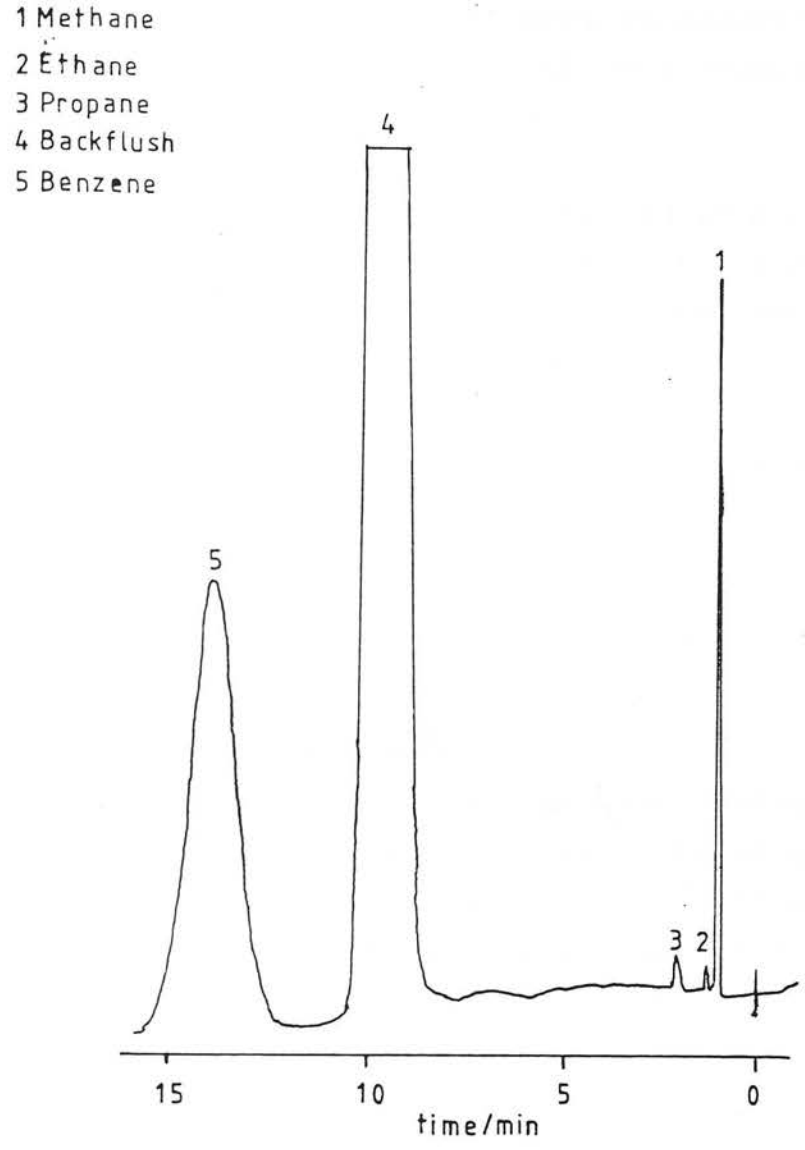

Figure 4,5 - Chromatographic Separation Obtained in System from Figure 4,4

Saturated hydrocarbons were not retained by this column and eluted as a single back-flush peak. Benzene, however, was retained and eluted from column C as a separate peak. The recorder trace resulting from this type of operation is illustrated in figure 4.5. This allowed an accurate area to be obtained for the benzene peak without interference from methylcyclopentane.

Columns B and C were installed in a Perkin-Elmer F-11 gas chromatograph equipped with a flame ionization detector and were operated at room temperature with nitrogen at 35 psig (~340 kPa) as the carrier gas.

Chromatographic peak areas were measured in all cases using electronic integrators.

4.3 PROCEDURE

4.3.1 - Volume calibrations

The volumes in the vacuum lines relevant to the preparation of reaction mixtures were the volume V_M of the mixing bulb M, the total volume V_E of the portion of the line comprising the mixing bulb, the reactor and any piping between these two parts of the system (e.g. trap CT2 in figure 4.1) and the volume V_R of the reactor. These volumes were calibrated by attaching a bulb of known volume containing a known pressure of helium and expanding the helium into evacuated parts of the system. Knowing the volume of the standard bulb, the initial pressure of helium and the pressure after expansion the volume of any selected parts of the system could be determined using Boyle's law ($P_1V_1 = P_2V_2$). The volumes determined with this method are listed in table 4.2. The volume of the standard bulb was determined by filling with distilled water and weighting.

TABLE 4.2

RELEVANT VOLUMES IN THE VACUUM LINES AT 298 K

LINE	V_M/cm^3 (1)	V_E/cm^3 (2)	V_R/cm^3 (3)
1	743	1042	207
2	317	702	193
3	622	890	190

(1) Mixing volume

(2) Expanded volume (see text)

(3) Reactor volume

4.3.2 - Catalyst pretreatment

The reaction vessel containing the desired amount of catalyst was attached to the line and evacuated for about 15 minutes using pumping system 1 (see 4.2.1). Hydrogen was admitted into the gas handling part of the apparatus and the increase in pressure was monitored using the mercury manometer HG. When the pressure was near to 1 atmosphere, the reactor was isolated from pumping system 1 and opened to the gas-handling line. Hydrogen flowed into the reactor and when the pressure in the system was just above 1 atmosphere the "Rotaflo" tap in the venting tube V was opened to allow hydrogen to flow continuously over the catalyst. The temperature and length of catalyst reduction varied according to the type of experiment performed and details are given in the relevant chapters. In general, following reduction the flow of hydrogen was interrupted by closing the appropriate taps in the hydrogen inlet (joints J2 or J3 in figure 4.1), the tap in the venting tube was closed, the reactor was isolated from the gas-handling line and evacuated at the reduction temperature using pumping system 1 for about 15 min. While the reaction mixture was prepared in the gas handling line, the reactor was cooled to reaction temperature and kept under vacuum until the start of the experiment.

4.3.3 - Purification of the hydrocarbons

Neopentane or isobutane from lecture bottles were expanded into one of the evacuated storage bulbs (e.g. B3 to B6 in figure 4.1) available in the gas-handling lines up to atmospheric pressure. A glass tube was attached to one of the inlets to the gas-handling line (e.g. J1, J2 or J3 in figure 4.1) and was evacuated. By opening the appropriate taps and placing a liquid nitrogen bath around the glass tube, the hydrocarbon contained in the storage bulb was condensed. Several freeze-pump-thaw cycles were performed in order to degas the hydrocarbon until no residual pressure could be read with gauge G1 after freezing the hydrocarbon. A glass storage tube equipped with a "Rotaflo" tap was attached to a second inlet and was evacuated. About one third of the hydrocarbon contained in the glass tube was removed by evacuation, the middle third was condensed into the storage tube and the final third was rejected. The purified hydrocarbon from the storage tube was used subsequently in preparing the reaction mixtures.

Hydrocarbons which are liquid at ambient conditions (benzene, cyclopentane, methylcyclopentane, n-hexane) were simply degassed with several freeze-pump-thaw cycles immediately before preparation of the reaction mixtures.

Methane from a lecture botlle was expanded into one of the storage bulbs available in line 1. A glass tube was attached to one of the inlets to the line and was evacuated. As much as possible of the methane from the storage bulb was condensed into the glass tube at liquid nitrogen temperature (methane does not condense completely at sub-atmospheric pressures even at the temperature of liquid nitrogen). A portion of the methane was removed by evacuation and another portion was expanded back into the storage bulb by momentarily removing the liquid nitrogen bath from around the glass tube. The remaining methane,

probably containing condensible impurities was discarded. The purified methane was stored in the storage bulb for subsequent preparation of the reaction mixtures.

4.3.4 - Preparation of reaction mixtures

The storage tube containing the hydrocarbon was attached to the gas-handling line. The hydrocarbon was degassed by repeated freeze-pump-thaw cycles to remove any air that could have leaked into the storage tube. A desired pressure of the hydrocarbon was expanded into the evacuated mixing bulb M which was then isolated from the rest of the system. A liquid nitrogen bath was placed around the cold finger located at the bottom of the mixing bulb (see figure 4.1) in order to condense the hydrocarbon. A desired pressure of purified hydrogen or deuterium (see 4.2.1) was then allowed into the mixing bulb. The bulb was again isolated from the rest of the system and the liquid nitrogen bath was removed from around the cold finger.

When methane was the reactant, a desired pressure of the hydrocarbon was allowed into the mixing bulb followed by admission of deuterium to give the selected total pressure. The admission of deuterium was as fast as possible in order to avoid diffusion of methane out of the mixing bulb.

The reaction mixtures were left standing for about 2 hours before the start of the experiments so that good homogeneization of the gas could be achieved. After this period the mixtures were expanded into the reactor which was already at the reaction temperature as described under 4.3.2.

Standard pressures of hydrocarbon or deuterium were generally used for each reaction and only in a few experiments the initial pressures of the reactants were varied.

From the pressure P_o of reactant admitted into the mixing bulb and from the relevant volumes in the vacuum lines (see 4.3.1), the pressure P of reactant in the reactor at the reaction temperature was calculated by solving equation (4.1) below which is based on the ideal gas law:

$$\frac{P\ V_R}{T_R} + \frac{P(V_E - V_R)}{T_A} = \frac{P_o V_M}{T_A} \qquad (4.1)$$

where the volumes V_M, V_E and V_R were defined in section 4.3.1, T_R is the temperature of the reactor and T_A is room temperature.

Solving equation (4.1) for P yields:

$$P = \frac{P_o V_M}{(V_E - V_R + V_R \frac{T_A}{T_R})} \qquad (4.2)$$

By substituting appropriate numerical values into expression (4.2) it is easy to see that the pressure inside the reactor was nearly independent of reaction temperature. For example, for experiments performed in line 2 an increase in reaction temperature from 298 K to 573 K caused only a 16% increase in reactant pressure. The concentrations of the reactants inside the reactor, however,which are relevant for the calculation of reaction rates varied markedly with reaction temperature. The number of molecules N_R inside the reaction vessel was calculated using expression (4.3) below:

$$N_R = \frac{PV_R}{R_G\ T_R} \times 6.02 \times 10^{23} \qquad (4.3)$$

where R_G is the ideal gas constant.

Standard initial reactant pressures used in

the different types of experiment are listed in table 4.3 and were calculated for a reaction temperature of 298 K. These pressures correspond to approximately 2×10^{19} molecules of hydrocarbon and 2×10^{20} molecules of hydrogen or deuterium admitted to the reaction vessel, except in the case of cyclopentane exchange with deuterium where a 20:1 deuterium to hydrocarbon ratio was used.

TABLE 4.3

INITIAL REACTANT PRESSURES USED IN THE DIFFERENT TYPES OF EXPERIMENTS(1)

REACTION	LINE	P_o/kPa(2)		P/kPa(3)	
		H_2 or D_2	HYDROCARBON	H_2 or D_2	HYDROCARBON
Cyclopentane + D_2	1	13.6	0.68	9.7	0.48
Other hydrocarbons + D_2	1	8.1	0.81	5.8	0.58
$C_{<6}$ molecules + H_2	2	8.5	1.13	3.8	0.51
C_6 molecules + H_2	3	9.0	1.36	6.3	0.95

(1) Calculated for a reaction temperature of 298 K
(2) Pressure in the mixing bulb
(3) Pressure in the reaction vessel

4.3.5 - Performing the experiments

In exchange experiments, the first mass spectrum was generally obtained two minutes after the reactants were admitted into the reactor. After the first spectrum, the mass range of interest was scanned every five minutes until completion of the experiment. A mass spectrum was obtained immediately before admission of the reactants in order to check for background peaks. It was generally found that the conversion of light hydrocarbon measured two minutes after admission of the reactants was negligible. This spectrum was therefore taken as representative of the fragmentation pattern of the light hydrocarbon.

In the experiments performed in lines 2 and 3, samples were drawn for injection into the gas chromatograph every 15 (line 2) or 20 minutes (line 3). The first sample was generally drawn 8 minutes after the start of the experiment.

In performing the experiments we were interested mainly in obtaining data relating to initial rates of reaction and initial product distributions. For this purpose, it was generally sufficient to analyse 8 samples for each experiment performed in lines 2 and 3 so that the duration of the experiments was between 2 and 2.5 hours. Exchange experiments were carried-out for one hour and about 12 spectra were recorded in each experiment.

With few exceptions, each experiment was performed with a fresh catalyst sample. The amount of catalyst used varied between 5 and 250 mg. Reaction conditions and catalyst amounts were selected so that the rates of reactant conversion were smaller than 1.5% min^{-1} in exchange reactions and less than 0.5% min^{-1} in other experiments in order to obtain good accuracy in determining initial reaction rates and initial product distributions. The lowest conversion rates measured were of ca 0.1% min^{-1} in exchange experiments and 0.02% min^{-1} in the other experiments.

Therefore, specific reaction rates (rate of conversion per gram of catalyst) differring by factors of as much as 10^3 could be measured at any reaction temperature.

4.4 TREATMENT OF THE DATA

4.4.1 - Reactions of hydrocarbons with hydrogen

From the chromatographic peak areas A_i, the fraction X_i of the reactant converted to substance i was

calculated using expression (4.4):

$$X_i = \frac{\frac{C_i}{C_R} \cdot \frac{A_i}{f_i}}{\sum_i \frac{C_i}{C_R} \cdot \frac{A_i}{f_i}} \qquad (4.4)$$

where C_i and C_R are the number of carbon atoms in substance i and in the reactant, respectively, and f_i is a sensitivity factor which converts the peak areas A_i into a number proportional to the number of molecules of substance i in the reactor.

If we define n_i as the number of molecules of substance i in the reactor per molecule of reactant initially present in the system, n_i values may be calculated from X_i fractions using expression (4.5):

$$n_i = \frac{C_R}{C_i} X_i \qquad (4.5)$$

Expression (4.5) is actually an approximation, since no account was taken of the fact that the number of molecules of reactant decreases with time not only because they are converted into products but also because samples are periodically drawn for chromatographic analysis. Expression (4.5) also does not take into account that some reactant molecules may be converted to species that remain adsorbed on the catalyst surface and do not appear in the gas phase. When these approximations are accepted, the rate of formation of substance i, R_i, may be calculated, in terms of the number of molecules of i produced per unit time, from expression (4.6) below:

$$R_i = \frac{dn_i}{dt} \cdot N_R \qquad (4.6)$$

where N_R is the number of molecules of reactant initially present in the reaction vessel.

The peak areas obtained from flame ionization detectors are approximately proportional to the weight of hydrocarbon injected into the gas chromatograph. If the f_i factor for methane is defined as 1, f_i values for other hydrocarbons may be approximately calculated from expression (4.7):

$$f_i = \frac{W_i}{16} \qquad (4.7)$$

where W_i is the molecular weight of substance i.

Sensitivity factors were also determined experimentally for a number of hydrocarbons by constructing calibration curves of chromatographic peak area against hydrocarbon pressure in the sampling loop. Straight lines were obtained for a wide range of pressures and the slopes of these lines are proportional to the f_i factors. Table 4.4 summarizes f_i values for a number of substances determined both experimentally and from expression (4.7). The sensitivity factors for hydrocarbons for which no calibration was available could be estimated with confidence from expression (4.7).

TABLE 4.4

THEORETICAL AND EXPERIMENTALLY DETERMINED SENSITIVITY FACTORS FOR GC ANALYSIS

Hydrocarbon	f_E (1)	f_T (2)
Methane	1.00	1.00
Ethane	1.72	1.81
Propane	2.81	2.75
i-Butane	3.52	3.63
n-Butane	3.70	3.63
n-Pentane	4.60	4.50
i-Pentane	4.67	4.50
Neopentane	4.89	4.50
Cyclopentane	4.51	4.38

(1) Experimental

(2) Calculated from expression (4.7)

Initial rates of conversion, r_o, were determined by plotting reactant concentrations, calculated from expression (4.4), against time and taking the initial slopes of the curves obtained.

Methods were used to estimate the number of surface metal atoms per gram of catalyst, n_s, as described in subsequent chapters. Turnover frequencies ν, defined as the number of reactant molecules converted per unit time per surface metal atom, were then calculated from expression (4.8):

$$\nu = \frac{r_o \cdot N_R}{m \cdot n_S} \qquad (4.8)$$

where m is the mass of catalyst used in the experiment.

Initial product distributions were obtained by plotting product concentrations calculated from expression (4.5) against conversion. The initial slopes of these curves represent the selectivity for product i, S_i,

defined as the number of molecules of i produced per molecules of reactant converted at time 0.

4.4.2 - Exchange reactions

Mass spectral intensities corrected for the presence of background peaks were fed to a computer program that further corrected the spectra for the contribution of natural isotopes and of fragments arising from loss of hydrogen or deuterium atoms from the parent ions[3]. The program takes into account that deuteriated molecules have a smaller tendency for fragmentation and that there is a greater chance of loss of hydrogen as compared to deuterium from parent ions containing both types of atoms[3]. The reliability of the fragmentation corrections was assessed by comparing the fragment peak intensities in the corrected spectra with those in the raw spectra. After correction, fragment peak intensities should be reduced to values close to zero but residual values corresponding to less than 10% of the fragment intensities in the raw spectra were considered acceptable.

For each corrected spectrum, the program calculated a percentage d_n vs. n distribution, where d_n refers to an isotopic species containing n deuterium atoms.

The product distributions obtained in each experiment were treated by the methods outlined by Kemball[4] which are briefly described in the following paragraphs.

In the absence of catalyst deactivation, the rate of disappearance r of light hydrocarbon is given at any stage of the exchange reaction by expression (4.9) below:

$$r = k\,(x_0 - {}^{e}x_0) \qquad (4.9)$$

where x_o is the fractional concentration of light hydrocarbon at any time t and $^e x_o$ is the fractional equilibrium concentration of light hydrocarbon.

Integration of expression (4.9) gives:

$$\ell n\ (x_o - {}^e x_o) = \ell n({}^o x_o - x_o{}^e) - kt \qquad (4.10)$$

where $^o x_o$ is the fractional concentration of light hydrocarbon at time 0 (generally equal to 1).

Thus in the absence of catalyst deactivation, a plot of $\ell n(x_o - {}^e x_o)$ vs. t (first-order plot) yields a straight line of slope -k, where k is the initial rate of disappearance of light hydrocarbon expressed in terms of the fraction of light hydrocarbon consumed per unit time. The equilibrium concentration of light hydrocarbon may be estimated from statistical considerations using expression 4.11):

$$^e x_o = \left(\frac{m}{m + 2R}\right)^m \qquad (4.11)$$

where m is the number of "hydrogen"(*) atoms in the reactant molecule and R is the molar D_2 to hydrocarbon ratio used in the experiments. In practice, expression (4.11) somewhat overestimates experimental $^e x_o$ values due to the bias towards more deuterated species that is generally found in exchange experiments taken to equilibrium but the error introduced by using $^e x_o$ values calculated from expression (4.11) in expression (4.10) for the calculation of initial reaction rates is negligible.

(*) Expressions such as "hydrogen" or "hydrocarbon" are used to denote that no distinction is made between isotopic species.

At any stage of the exchange reaction, the average deuterium content ϕ of the "hydrocarbon", i.e., the average number of deuterium atoms incorporated per molecule of "hydrocarbon" in the reaction mixture, may be calculated from expression (4.12):

$$\phi = \sum_{n-1}^{m} n x_n \qquad (4.12)$$

where x_n is the fractional concentration of a species containing n deuterium atoms in the isotopic mixture.

The rate of deuterium incorporation r_ϕ follows a first order law of the type:

$$r_\phi = k_\phi \left(1 - \frac{\phi}{\phi_e}\right) \qquad (.413)$$

where ϕ_e is the average deuterium content at equilibrium. Integration of expression (4.13) gives:

$$\ell n(\phi_e - \phi) = \ell n(\phi_e - \phi_o) - \frac{k}{\phi_e} t \qquad (4.14)$$

where ϕ_o is the average deuterium content at time 0 (generally 0).

Therefore, in the absence of catalyst deactivation, a plot of $\ell n(\phi_e - \phi)$ vs. t yields a straight line of slope $-k_\phi/\phi_e$, where k_ϕ is the initial rate of deuterium incorporation into the "hydrocarbon" in terms of the number of deuterium atoms introduced per molecule of "hydrocarbon" per unit time. The equilibrium deuterium content ϕ_e may be calculated from statistical considerations using expression (4.15):

$$\phi_e = \frac{2\ m\ R}{m + 2R} \qquad (4.15)$$

The ratio k_ϕ/k gives the average number of

deuterium atoms incorporated into the light hydrocarbon per molecule reacting at time 0 and is called the multiplicity of the exchange reaction M_d.

Initial product distributions were obtained from plots of x_m against the fractional conversion of light hydrocarbon $(1 - x_o)$ by measuring the initial slopes of the resulting curves. If we call d_n the fractional contribution of a species containing n deuterium atoms to the initial product distribution(**), an alternative way of calculating the multiplicity of the exchange is given by expression (4.16):

$$M_d = \sum_{n=1}^{m} n\, d_n \qquad (4.16)$$

Values of M_d close to one indicate that only one "hydrogen" is exchanged per adsorption-desorption cycle and the exchange reaction is termed stepwise. Multiple exchange is characterized by M_d values greater than 1. With molecules that exchange all of their "hydrogens" at the same rate (such as in the case of the symmetrical hydrocarbons studied here) stepwise exchange may also be recognized from product distributions obtained at any stage of the reaction, since fractional concentrations x_n should conform to the binomial distribution, given by expression (4.17):

$$x_n = \left(\frac{\phi}{m}\right)^n \cdot \left(1 - \frac{\phi}{m}\right)^{m-n} \cdot \frac{m!}{n!\,(n-n)!} \qquad (4.17)$$

(**) Throughout this work the notation d_n is used indistinctly in referring to an isotopic species containing n deuterium atoms and to its fractional contribution to initial product distributions.

4.5 SOURCE AND PURITY OF REAGENTS

Table 4.5 lists the source, grade and purity of the reagents used in the present work. Further purification of these reagents was already described in previous sections.

TABLE 4.5

SOURCE AND PURITY OF THE REAGENTS

Reagents	Source	Grade	% Purity
Hydrogen	BOC	-	-
Deuterium	Matheson	CP	99.5
Methane	G.T.Baker	U.H.P.	>99.9
Neopentane	Matheson	CP	99.5
Cyclopentane	BDH	Research	99.9
Methylcyclopentane	Koch-Light	Puriss.	99.9

4.6 REFERENCES

1. C.Kemball, Proc.Roy.Soc.A, 1951, 207, 539
2. R.S.Dowie, C.Kemball, J.C.Kempling, D.A.Whan, Proc. Roy.Soc.A, 1972, 327, 491.
3. R.S.Dowie, D.A.Whan, C.Kemball, J.Chem.Soc.Faraday Trans.I, 1972, 68, 2150
4. C.Kemball, Adv.Catalysis, 1959, 11, 223

CHAPTER 5

SIMULATION OF CYCLOPENTANE EXCHANGE PATTERNS USING A MONTE CARLO METHOD

CHAPTER 5

SIMULATION OF CYCLOPENTANE EXCHANGE PATTERNS USING A MONTE CARLO METHOD

5.1. INTRODUCTION

The exchange reactions of saturated hydrocarbons with deuterium provide an important tool in the identification of adsorbed species on the surface of metal catalysts.[1-3]

It is generally accepted that the first step in these reactions involves the dissociation of an alkane C-H bond, leading to the formation of an adsorbed alkyl species. This species may either desorb to the gas phase by acquiring a "hydrogen" atom from the surface pool (the expression "hydrogen" is used to denote that no distinction is made between isotopic species), or it may undergo a number of multipoint adsorption processes before desorption, with the result that, in the initial product distribution of the exchange reaction, products containing more than one deuterium atom may appear.

An observation of the initial product distributions obtained from carefully selected molecules may provide important clues to the nature of the adsorbed species participating in the exchange process.

Thus, work with open chain hydrocarbons highlighted the importance of α, β- diadsorbed species in low temperature exchange and the participation α,γ- and α, α - diadsorbed species at higher temperatures.

In work with cycloalkanes, additional paths were identified, since it is known that two main processes contribute to the exchange of these molecules, one responsible for the exchange of the hydrogens located

on the side of the ring where chemisorption first occurs (one-set exchange) and the other leading to propagation of the exchange to the opposite side of the ring (two-set exchange).[4-6]

A deeper insight into the mechanism of exchange reactions may be gained when appropriate theoretical models are available for comparison with experimental patterns. This type of approach is not only an important method of validating proposed mechanisms, but it also provides information about the relative rates of interconversion of adsorbed species.

Anderson and Kemball[7] devised a general method for prediction of exchange patterns for a given exchange mechanism, that is, for a given set of surface intermediates and their relative probabilities of interconversion. This method was successfully applied in the interpretation of the exchange patterns of simple alkanes such as ethane[7] and propane[8] but could only be applied to the case of cycloalkanes at the cost of some oversimplification.

This is because Anderson and Kemball's method requires the solution of a system of N simultaneous equations, where N is the number of deuterated surface intermediates involved in a given mechanism. As will be shown subsequently, the number of distinguishable intermediates involved in cyclopentane exchange is well above one hundred, even for the simple two-set exchange mechanisms considered in the present work.

The solution of such a formidable system of equations necessarily implies the use of approximate matrix inversion methods, whose accuracy is difficult to guarantee, since the coefficients of the equations will change according to the parameters of a given simulation and problems of ill-conditioning are likely

to arise.

Under those circumstances, the use of direct simulation methods, generally known as Monte Carlo methods, become an interesting alternative.

The term Monte Carlo method refers to the evaluation of a function F by using a set of random numbers to simulate the outcome of probabilistic events which determine the value of F[9].

The application of this approach to the problem of hydrocarbon exchange reactions requires the use of appropriate algorithms which numerically simulate the exchange processes occurring on a catalyst surface. Each "molecule" fed to the algorithm will emerge as a "product" containing a number n of deuterium atoms. Averaging of this process for a sufficiently large number of "molecules" will result in a d_n vs. n distribution, where d_n is the probability of formation of a product containing n deuterium atoms from an initially unexchanged molecule.

The present chapter describes simulation algorithms for the exchange of cyclopentane by some of the mechanisms proposed in the literature and discusses their application in the interpretation of real exchange patterns.

5.2. THE MECHANISMS OF CYCLOALKANE EXCHANGE

5.2.1 - One-set exchange

There seems to be general agreement[1-3] that the process responsible for one-set exchange in cycloalkanes is the same proposed to explain the exchange of open chain hydrocarbons and involves interconversion between mono - and vicinal diadsorbed species (α, β

exchange process).

This process is closely related to the Horiuti-Polanyi mechanism for olefin hydrogenation, which is shown in the scheme below.

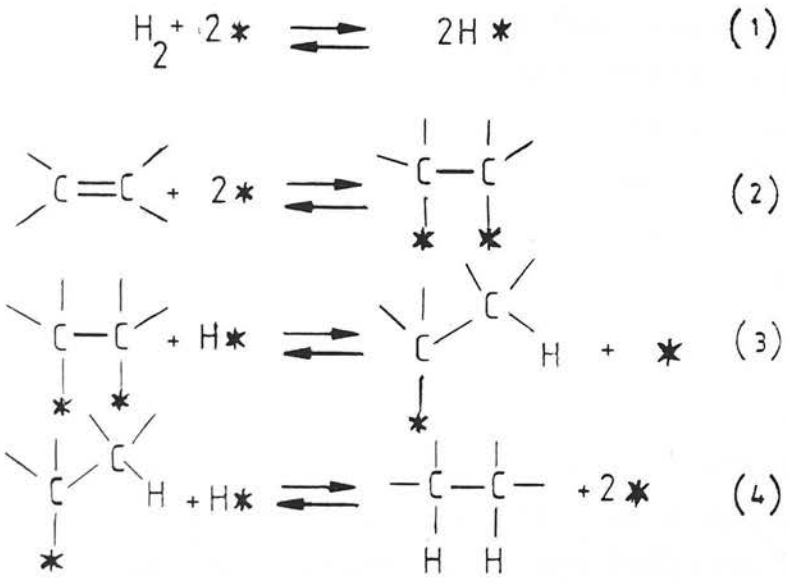

SCHEME 5.1

In this scheme, the use of an asterisk to represent an active site does not necessarily imply that two separate surface atoms are involved in this process and the nature of the diadsorbed intermediate in equations (2) and (3), shown here as diadsorbed alkane, is left open to question, since it might be better represented as a π -adsorbed olefinic species[3].

The exchange of open chain saturated hydrocarbons may be largely explained by reactions (3) and (4) above.

Under the low temperatures normaly used in exchange studies, alkanes are thermodynamically strongly favoured over olefins, so that reaction -2 is immeasurably slow and no olefinic species are observed in the gas phase.

Over most catalytically active metals, "hydrogen" adsorption-desorption is much faster than "hydrocarbon" adsorption-desorption, so that reaction(1) may be considered to be in equilibrium at any stage of the exchange process. Thus, for a sufficiently large excess of deuterium over hydrogen in the gas phase, the fraction of deuterium in the adsorbed "hydrogen" pool is essentially 1. This implies that in the initial stages of an exchange reaction, when essentially no isotopic dilution of deuterium has occurred, and when a high deuterium /hydrocarbon ratio is used, nearly every hydrogen removed from a hydrocarbon species is replaced by deuterium.

From scheme 1 it is easy to see that alternation of reactions 3 and -3 may lead to exchange of several "hydrogens" in a single visit of a hydrocarbon species to the surface, depending on the relative rates of reactions -3 (r_{-3}) and 4(r_4). The ratio r_{-3}/r_4, commonly referred to as ρ in the literature[7], represents the chance of a surface alkyl species suffering a second point adsorption relative to that of its desorbing to the gas phase. In the limit where ρ is very large, all hydrogens in the alkyl species will be exchanged before desorption to the gas phase, since unhindered rotation of alkyl groups about the carbon-carbon bond axis is faster than second point adsorption. When ρ is near to zero, only one "hydrogen" will be replaced by deuterium per visit to the surface and a so called stepwise exchange process will arise.

The α, β -exchange process may easily propagate across an open chain of carbon atoms, but is blocked at position where a quaternary centre is found, since second point adsorption involving a quaternary carbon is impossible.

For the exchange of cycloparaffins, only

cis elimination and addition of "hydrogen" is predicted by the α, β - exchange mechanism, since rotation about the carbon-carbon bond axis, necessary for trans elimination-addition, is impossible, at least for rings containing less than 7 or 8 carbon atoms[10].

Experimental findings in general agree with the predictions of the α, β exchange mechanism. Thus, in the exchange of molecules such as ethane[7], propane[8], n-butane[11], i-butane[12], n-hexane[13], etc..., which do not contain any quarternary centres, substantial amounts of perdeuterated molecules are found in the initial product distributions, specially when palladium is used as a catalyst. In gem-disubstituted alkanes, such as 3,3-dimethylpentane[14] and 2,2,3-trimethylpentane[15] little initial exchange is observed beyond 5 and 7 deuterium atoms, respectively. The initial product distributions obtained from cyclopentane and cyclohexane present maxima or pronounced breaks respectively at d_5 and d_6 (the notation d_n refers to a product containing n deuterium atoms), consistent with the cis elimination-addition character of the α, β -exchange process predicted for these molecules[11,5].

For larger ring systems, breaks in the exchange patterns become less pronounced, indicating that the flexibility of these rings is large enough to allow trans α, β-diadsorption[10].

The detailed nature of the intermediate responsible for α, β exchange is subject to some dispute. Burwell sustains that the necessary condition for α, β exchange to occur is that two neighbouring CH groups may attain an eclipsed conformation[2]. This is based on the fact that in molecules such as adamantane, where such configuration cannot occur, only stepwise exchange is observed.[5]

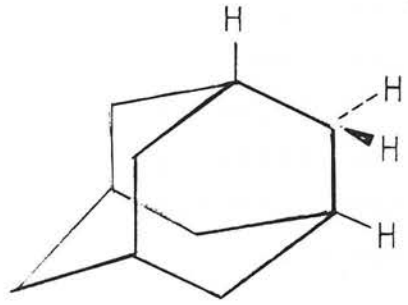

SCHEME 5.2

Also, in the exchange of bicyclo- 3.3.1 - nonane (SCHEME 5.3) over Pd[14] a maximum at d_8 is proeminent indicating that propagation of the exchange across the bridge-head is easy. While the bridge-head may easily assume an eclipsed conformation, a bridge-head bicyclononene was considered to be too strained to be important in the exchange process.

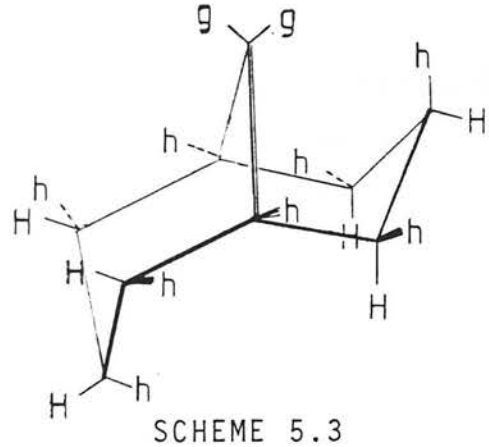

SCHEME 5.3

Burwell, therefore, favours an eclipsed 1,2 diadsorbed alkane species as the intermediate responsible for α, β exchange.

Rooney and coworkers, on the other hand, argue that the structure of a π -adsorbed olefinic species may be considerably distorted and resemble that of a 1,2-diadsorbed alkane[16].

Over Pd, experiments with caged compounds, such as the heptacyclotetradecane shown in scheme 5.4, where pairs of CH groups are firmly held in an eclipsed conformation, but where the chance of formation of a π -adsorbed complex is very remote, evidenced only stepwise exchange, and therefore supported the idea of π -adsorbed olefinic complexes as responsible for α, β -exchange[17].

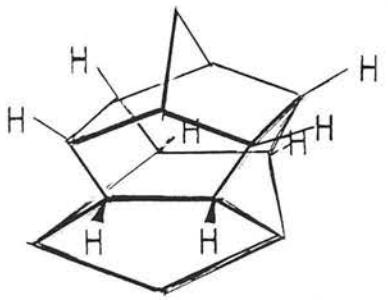

SCHEME 5.4

It should be emphasized that the α, β process is not the only one involved in saturated hydrocarbon exchange, even when only open chain compounds are considered. It has been known for a long time that a multiple exchange process is important in the reaction of methane with deuterium over many metal catalysts[18], Pd being a notable exception.

In neopentane exchange, where no α, β process can occur, products with up to three deuterium atoms are found at relatively low temperatures and, at higher temperatures, perdeuterated products are often observed[19,20].

In order to explain multiple exchange in methane, the formation of intermediates multiply bonded to the surface by one carbon atom (adsorbed carbene and carbine species) is generally accepted and in the

formation of $d_{n>3}$ products in neopentane exchange, interconversion between mono-and 1,3 di- or polyadsorbed species is postulated.

These processes, however, normally occur at temperatures considerably higher than those where α,β exchange is observed on a given catalyst. Nevertheless, whenever exchange experiments are performed at temperatures near to those where neopentane or methane multiple exchange occur, some participation of those processes has to be considered.

It should also be noticed that other exchange processes may be postulated, which show some of the characteristics of α,β exchange. For example, Kemball and Woodward[8] have analysed theoretically the possible role of adsorbed allyl species in propane exchange, using Anderson and Kemball's method[7].

These authors found that some experimental propane exchange patterns, which could not be reproduced by a single α,β process involving only one value of ρ, could be explained by assuming interconversion between 1,2-diadsorbed and 1,2,3-triadsorbed species, using a single set of parameters ρ and X, where ρ has the same meaning as before and X represents the chance of an α,β- diadsorbed species suffering a third point adsorption relative to that of reverting to a monoadsorbed state. Similarly to 1,2-diadsorbed intermediates, species bonded to the surface by three or more consecutive carbon atoms would also lead to propagation of exchange across a chain of carbon atoms and blocking of the exchange at quaternary centres.

5.2.2 - Two-set exchange

Several intermediates have been proposed to explain the mechanism of two-set exchange.

Anderson & Kemball, based on the fact that a multiple exchange process is important in the exchange of methane with deuterium over many metal catalysts, suggested that an α, α-diadsorbed species is the intermediate responsible for two-set exchange[11], as shown in the scheme below:

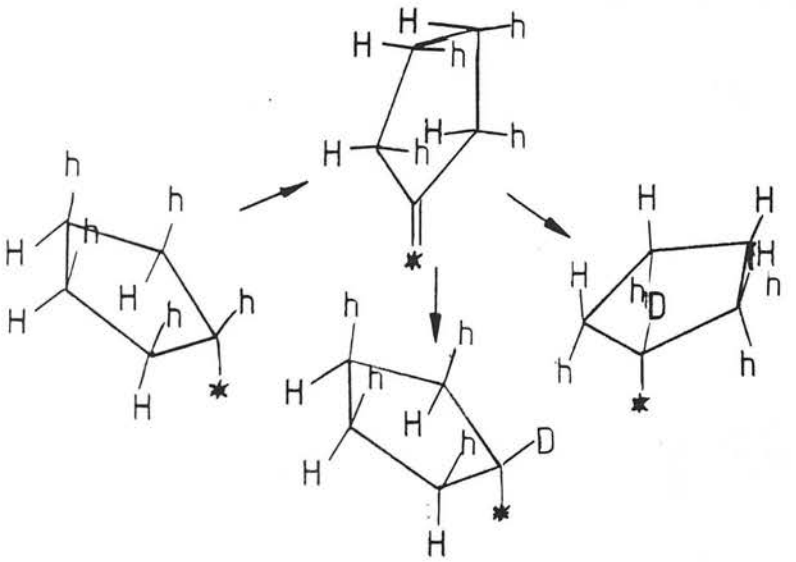

SCHEME 5.5

In this scheme, a "H" represents a "hydrogen" atom on the side of the molecule where adsorption originally occurs, a "h" represents a "hydrogen" atom on the opposite side of the molecule and a "D" represents a newly introduced deuterium atom. It is easy to see that the α, α -diadsorbed species has a 50% chance of "falling-over" to the h-side of the molecule, thereby propagating the exchange to the h-set.

This α, α-turnover mechanism, however, failed to account for some results obtained mainly over Pd catalysts. The α, α-turnover mechanism does not predict any restrictions for two-set exchange in isolated dimethylene units, such as that of 1,1,3,3 - tetramethylcyclopentane, whereas over Pd catalysts propagation of the exchange beyond a d_2 species is not observed[6]. Also in isolated trimethylene units, such as

that of 1,1,3,3-tetramethylcyclohexane[21], exchange over Pd is limited to 5 hydrogen atoms, whereas exchange of all 6 hydrogen atoms would be predicted by the α, α - turnover mechanism.

Rooney and coworkers[6] proposed a mechanism involving the formation of adsorbed π -allyl species which accounts for these facts, as shown in scheme 5.6.

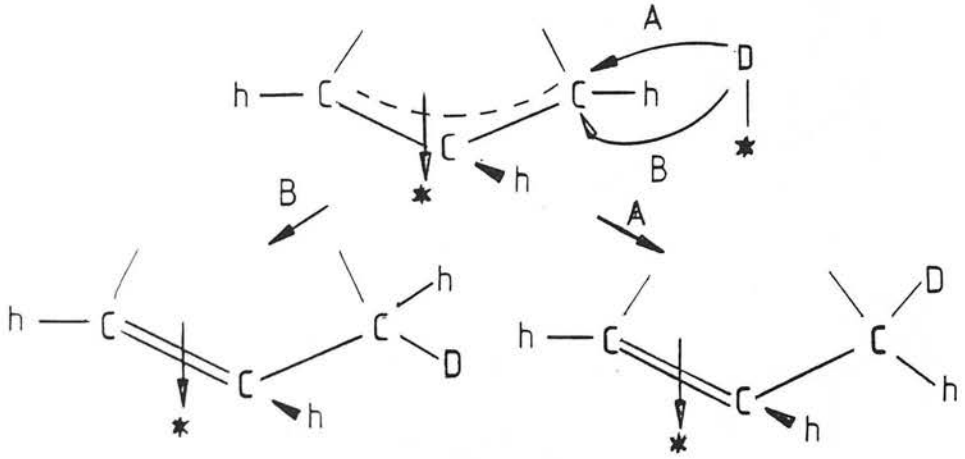

SCHEME 5.6

This mechanism envisages two separate paths for "hydrogen" attack on the π -allyl species, respectively on the far side (path A) and on the near side (path B) relative to the catalyst surface. These paths can only involve the two carbon atoms in the extremities of the π -allyl species, since attack on the central atom would lead to the formation of a disfavoured 1,3-diadsorbed species. Therefore, the central hydrogen atom of the h-set of an isolated trimethylene unit cannot be exchanged, thus explaining the observed d_5 maximum in the exchange of 1,1,3,3-tetramethylcyclohexane over Pd. Since, according to this mechanism, the formation of an adsorbed π-allyl species is necessary for two-set exchange, such process cannot occur in isolated dimethylene units, as observed in the exchange of 1,1,3,3-tetramethylcyclopentane on Pd.

Another mechanism which satisfactorily explains the experimental facts of cycloalkane two-set exchange over Pd was proposed by Burwell[5] and is generally known as the rollover nechanism (scheme 5.7).

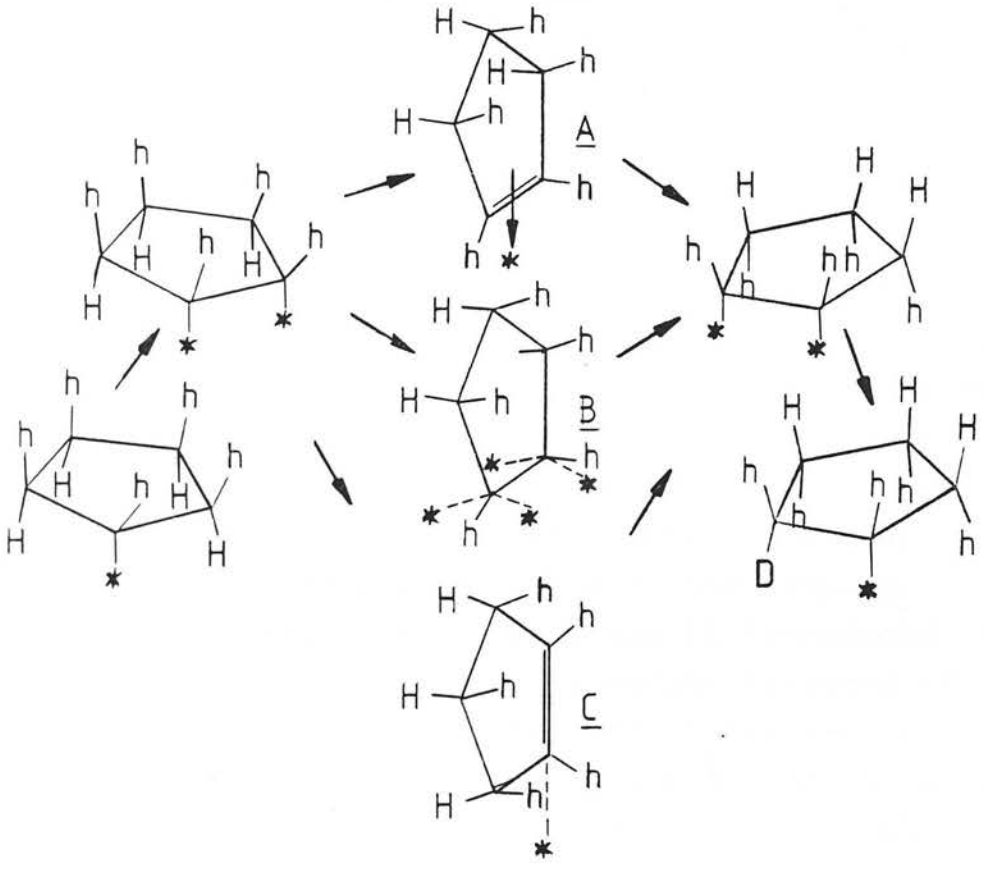

SCHEME 5.7

It can be easily verified that the predictions of the rollover mechanism are identical to those of the π-allyl mechanism, as far as exchange of isolated dimethylene and trimethylene units are concerned. A distinction between the two mechanisms was only possible by studying the exchange reactions of carefully selected policyclic ring systems.

One such system is bicyclo- 3.3.0 -octane (scheme 5.8) which over Pd exchanges all of it's 14 hydrogen atoms[14], indicating that the two trimethylene units are not isolated.

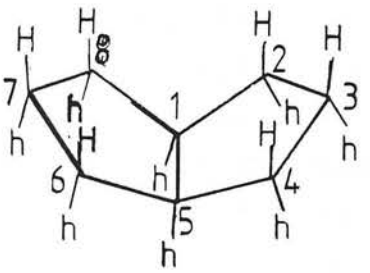

SCHEME 5,8

If the rollover mechanism is accepted, this implies, for steric reasons, that an intermediate similar to C in scheme 5.7 (end-on rollover) is involved, with the double bond between carbons 1 and 5 of the bicyclo compound. If the π-allyl mechanism is accepted, the implication is that an allyl species involving carbons 1,2 and 3 must participate in the exchange process. Therefore, if a methyl group is introduced in carbon 1, the trimethylene groups become isolated if a rollover mechanism operates, but not if the π-allyl mechanism is responsible for two-set exchange. Quinn and coworkers[22] studied the exchange of 1-methylbicyclo- - 3.3.0 - octane over Pd and found that only 11 of the 23 hydrogen atoms of the ring system are exchangeable, indicating that the trimethylene units have become isolated and therefore a rollover mechanism is operating.

It is important to note that clear-cut evidence for the rollover mechanism, as opposed to the α, α-turnover mechanism, could only be obtained in the case of Pd catalysts.

Burwell and coworkers[14] studied the exchange reactions of a number of model compounds over Pd, Pt, Ni and Rh catalysts and only on Pd could the maxima predicted by the rollover mechanism be clearly

observed. This was attributed to the small tendency of Pt, Ni and Rh to promote two-set exchange, thus obscuring such maxima. However, in bicyclo- 3.3.1 - nonane exchange over Rh a clear maximum at d_{14} is observed, whereas the rollover mechanism predicts no exchange beyond d_{12}, as found with Pd. Thus, at least in this case, a mechanism other than rollover must be responsible for two-set exchange, probably an α,α-turnover mechanism.

5.3 - THE SIMULATION ALGORITHMS

5.3.1 - Assumptions of the model

From the discussion presented in the previous section it is clear that the mechanism currently favoured in the literature to explain cycloalkane exchange over Pd involves interconversion between mono-and α,β-diadsorbed intermediates, combined with a rollover process responsible for two-set exchange. For other metals, the mechanism of turnover is uncertain and α,α-diadsorption may play an important role.

Therefore, both α,α-diadsorption and rollover processes were considered as possible turnover mechanism in the present work, with α,β-diadsorption responsible for one-set exchange, although it is recognized that other intermediates, such as adsorbed allyl species, may be important in this last process[8].

For the purposes of the model described in this chapter, the formation of an initial product containing n deuterium atoms in an exchange reaction is assumed to be the result of the following steps:

(1) Dissociative adsorption of reactant, to produce an unexchanged monoadsorbed species by removal of one hydrogen atom.

(2) A series of events ocurring on the

surface, leading eventually to the formation of a monoadsorbed intermediate containing n-1 deuterium atoms. For simplicity, this intermediate will be referred to as a d_n intermediate.

(3) Desorption of the d_n intermediate to form a product with n deuterium aoms.

An event on the surface is defined here as a series of reaction steps leading from one monoadsorbed species to another. The types of event considered are the ones shown is schemes 5.7 (rollover) and 5.5 (α, α-diadsorption), plus the α, β-diadsorption event illustrated below:

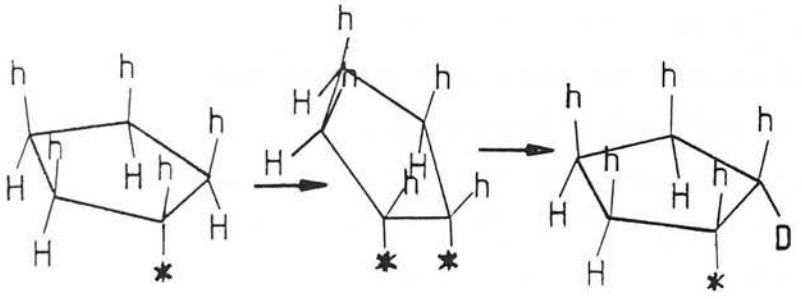

SCHEME 5.9

α, β-diadsorption event

Only one two-set exchange mechanism is considered in a given simulation, that is, a catalyst is assumed to behave either as an α, α-diadsorption or as a rollover promoter.

An infinite deuterium pool and instantaneous H + D recombination are assumed, so that the probability of hydrogen backsubstitution is negligible.

No kinetic isotope effects are considered. The probability of exchanging one hydrogen for a deuterium is assumed to be the same as that of exchanging a deuterium for another deuterium.

Differential conversions and steady-state are assumed, that is, the possibility of product readsorption is ignored and no accumulation of material on the surface is allowed, meaning that every intermediate must, eventually, either produce another intermediate or desorb to the gas phase.

It is also assumed that the observed initial product distributions are determined by a single set of probabilities per surface event that a monoadsorbed intermediate either goes to the gas phase (P_G), suffers an α,β-diadsorption event (P_B) or undergoes an α,α - diadsorption or rollover event (P_A), so that $P_G + P_A + P_B = 1$.

As a matter of programming convenience, there is a difference in the definition of P_A according to the turnover mechanism. In the case of the rollover mechanism, P_A refers to the probability that a rollover intermediate actually turns over on the surface, whereas in the α,α-turnover mechanism P_A refers to the formation of an α,α-diadsorbed intermediate. This is because, in the case of the rollover mechanism, there is a 50% chance that a rollover intermediate (A, B or C in scheme 7) falls back on the surface without actually turning-over to the opposite side, the outcome of the event being the same as that of a simple α,β-diadsorption event, whereas an α,α-turnover event is distinguishable from α,β-diadsorption, even when the α,α-intermediate falls back on the surface.

As a consequence, the maximum value for P_A is $(1 - P_G)/2$ when the rollover mechanism is considered.

Whithin the assumptions of the model, two parameters are necessary to define a given simulation. In the present case, the probability of desorption P_G

and the ratio P_A/P_B were arbitrarily chosen.

5.3.2 - The Simulation Program

The simulation program is comprised of three self-contained subroutines. The first subroutine (CPE1S) uses a numerical code related to the deuterium distribution in adsorbed cyclopentyl radicals (structural codes) and numerical simulations of the different types of surface event in order to determine the intermediates involved in a given two-set exchange mechanism.

CPE1S generates two arrays, IPREC (I) and IADR (I,J), which contain, respectively, the structural codes for all cyclopentyl radicals involved in a mechanism and for the intermediates which can be formed from each intermediate in IPREC(I) in a single surface event.

The structural code used in CPE1S consists of two sets of five binary digits (bits), one digit for each position in a cyclopentyl radical, where 0's stand for hydrogen and 1's stand for deuterium atoms. An example of the relationship between radical structure and structural code is shown in scheme 10.

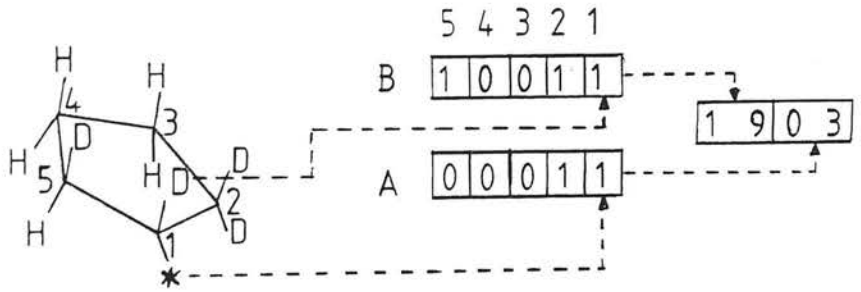

SCHEME 5.10

The position of adsorption is always the rightmost digit of set A (bit 1A) and a 1 is always placed in this position. For programming convenience, the structural codes are manipulated in the compacted

form shown at the right of scheme 10, where the two leftmost digits represent the decimal equivalent of the binary number in set B and the two rightmost digits the decimal equivalent for set A.

Using the structural code described above, simulation of surface events is straightforward. For example, α,β-diadsorption events, which have four possible outcomes, are simulated as follows:

Outcome 1: a 1 is placed in bit 2A.
Outcome 2: a 1 is placed in bit 2A and sets A and B are rotated to the right (i.e., a bit in position n goes to position n-1, except for bits 1A and 1B, which go, respectively, to positions 5A and 5B).
Outcome 3: a 1 is placed in bit 5A.
Outcome 4: a 1 is placed in bit 5A and sets A and B are rotated to the left.

Bit manipulation using decimal equivalents is easy when concepts of integer arithmetics are applied. Thus, placing a 1 in bit 5 of a binary number, for example, is equivalent to the following decimal integer operation:

$$y = x - (x/16) \cdot 16 + 16$$

The logic of subroutine CPE1S is briefly as follows:

1. An array IPREC is defined, which at the end of the run will contain the structural codes (in compacted form) of all intermediates involved in a given turnover mechanism. The first entry into this array is the code for the unexchanged cyclopentyl radical (0001).
2. Structural codes for all possible products

from this entry are generated by the event simulation routines and placed into an array IADR (I,J).

3. Each structural code generated in step 2 is checked for distinguishability against all previous entries in array IPREC and stacked onto this array if it is a new intermediate.

The word "distinguishable" is used here instead of "identical", since enantiomeric radicals produce different structural codes but are indistinguishable in the present context. Therefore, in checking for distinguishability, a reflection stage is included, which consists simply in exchanging bits 2A, 3A, 2B and 3B with bits 5A, 4A, 5B and 4B, respectively.

4. Steps 2 and 3 are repeated for every entry. Termination occurs when no new intermediates are produced from an entry which is also the topmost entry in array IPREC.

An example showing the first 10 lines of IPREC and IADR for the rollover mechanism is shown in table 5.1. The J values from 1 to 4 represent the outcomes from α,β-diadsorption events and from 5 to 8, the outcomes from rollover events.

The second subroutine, CPE2S, simply substitutes the structural codes in array IADR (I,J) for their position, I, in array IPREC (I) and generates an array ND(I) containing the number of deuterium atoms in the product of desorption from each intermediate I in array IPREC. This is easily calculated by adding the ones in the binary code for intermediate I.

TABLE 5.1

FIRST 10 OUTPUT LINES FROM CPE1S FOR THE ROLLOVER MECHANISM

I	IPREC(I)	IADR(I,J)							
		J=1	2	3	4	5	6	7	8
1	0001	0003	0003	0003	0003	0003	0003	0003	0003
2	0003	0003	0003	0007	0019	0003	0003	0403	1603
3	0007	0019	0007	0015	0027	1603	0403	1203	2403
4	0019	0007	0019	0007	0019	0403	1603	0403	1603
5	0403	1603	0403	0807	0819	0019	0007	0411	1611
6	1603	0403	1603	0107	0219	0007	0019	0503	1803
7	0015	0027	0015	0031	0031	2403	1203	1417	1417
8	0027	0015	0027	0027	0027	1203	2403	2003	2003
9	1203	2403	1203	0625	1219	0027	0015	0823	0229
10	2403	1203	2403	0325	2419	0015	0027	0919	1825

An example showing the first four lines from arrays ND and IADR, as generated by CPE2S, is shown in Table 5.2 for the rollover mechanism.

TABLE 5.2

FIRST 4 OUTPUT LINES FROM CPE2S FOR THE ROLLOVER MECHANISM

I	ND(I)	IADR(I,J)							
		J=1	2	3	4	5	6	7	8
1	1	2	2	2	2	2	2	2	2
2	2	2	2	3	4	2	2	5	6
3	3	4	3	7	8	6	5	9	10
4	3	3	4	3	4	5	6	5	6

The third subroutine, CPE3S, contains the main simulation algorithm.

The program works briefly as follows:

1. The parameters of the simulation are read into the computer memory. These are:
   PG - The probability of desorption P_G
   PAPB - The ratio P_A/P_B as defined in section 3.1
   NMOL - The number of "molecules" to be fed to the algorithm.
2. A set of 10 counters ID(K) is defined, which at the end of the simulation will each contain the number of "molecules" desorbed with K deuterium atoms.
3. A pointer I is given initial value 1, corresponding to the unexchanged cyclopentyl radical.
4. The interval [0,1] is divided into 9 regions of length proportional to PB*

W(I,J) (J=1 to 4), PA* W(I,J)(J=5 to 8) and PG (J=9).

W(I,J) is the probability per surface event of a given type for the reaction I → IADR(I,J). For α, β-diadsorption and rollover events there are four possible outcomes and, therefore, W(I,J) = 1/4. Although there are only two possible outcomes for an α, α-diadsorption event, the mechanics of subroutine IAB in program CEPlS (see appendix A1) are such that four outcomes are generated for this type of event, outcome 1 being identical to 2 and 3 identical to 4. Therefore, W(I,J) = 1/4 even when α, α-diadsorption events are considered.

The outcome of an event is frequently the precursor radical itself. This corresponds essentially to a non-event situation and has the effect of increasing the probability of all other events. Therefore, whenever IADR(I,J)= I, W(I,J) is given a value of 0, i.e, regions corresponding to a surface reaction I → I have length equal to 0.

5. A random number RN in the interval [0,1] is generated using a standard subroutine[23] and matched against the 9 regions. If the J number for which matching obtains is smaller than 9, a surface event occurs and pointer I is replaced by IADR (I,J). Steps 4 and 5 are repeated, until a RN in the 9th region is sorted (desorption event).

6. A normalized initial product distribution (exchange pattern) is finally obtained by dividing each ID(K)

by NMOL.
A complete listing of program CPE is shown in appendix A1.

5.3.3 - The "regular pentagon" molecule

The hypothetical case of the exchange of a regular pentagon molecule, C_5H_5, provides an important check to the models developed in this chapter, since it represents the limiting case in cyclopentane exchange where $P_A = 0$, i.e., where cyclopentane exchange is limited to one set of "hydrogens". This case has been analysed by Anderson and Kemball[4], using the general method described by the same authors[7].

Anderson & Kemball[7] derived a relationship between the chance, Q_m, of an adsorbed intermediate m desorbing to the gas phase to produce a hydrocarbon molecule containing N deuterium atoms and ρ (see section 2.1), as shown in expression (5.1) below:

$$Q_m(1 + \sum_n \mu_{mn}) = a_m + \sum_l \mu_{lm} Q_l \qquad (5.1)$$

where Q_l has a meaning analogous to Q_m, for intermediate l;
a_m represents the chance of forming intermediate m directly by adsorption of a reactant molecule - in the present case $a_m = 1$ for the undeuterated mono-adsorbed regular pentagon and $a_m = 0$ for any deuterated regular pentagon;
$\mu_{ij} = \rho g_{ij}$, where g_{ij} is a statistical weighting factor with the same meaning as W(I,J) as defined in sections 5.3, i.e., it represents the chance of intermediate i producing intermediate j in a single surface event.

Expressions analogous to 5.1 for every intermediate involved in a given exchange mechanism define a system of M simultaneous equations where M is the number of intermediates involved.

In the case of the regular pentagon, there are seven distinguishable mono-adsorbed intermediates involved. If the same convention is used for subscript m as the one described in scheme 5.10 (section 5.3.2) in defining compacted structural codes (except that only set A is used), solution of equations 5.1 yields the following values for Q_m:

$$Q_{01} = \frac{1}{1+\rho} \qquad (C_5H_4)$$

$$Q_{03} = \frac{2\rho}{(1+\rho)(2+\rho)} \qquad (C_5H_3D)$$

$$Q_{07} = Q_{19} = \frac{2\rho^2}{(1+\rho)(2+\rho)(4+\rho)} \qquad (C_5H_2D_2) \quad (5.2)$$

$$Q_{15} = \frac{2\rho^3}{(1+\rho)(4+\rho)(\rho^2+8\rho+8)} \qquad (C_5HD_3)$$

$$Q_{23} = \frac{4\rho^3}{(2+\rho)(4+\rho)(\rho^2+8\rho+8)} \qquad (C_5HD_3)$$

$$Q_{31} = \frac{\rho^4}{(1+\rho)(4+\rho)(\rho^2+8\rho+8)} \qquad (C_5D_4)$$

It should be noticed that the expression reported here for Q_{23} is different from the corresponding one reported by Anderson and Kemball[4] ($_2Q_{11110} + {}_3Q_{11110}$ in Anderson and Kemball's notation). The correctness of the present derivation may be assessed by adding the different Q_m' s, which should amount to 1.

From equations (5.2), a theoretical exchange pattern may be obtained, using equation (5.3):

$$
\begin{aligned}
d_1 &= Q_{01} \\
d_2 &= Q_{03} \\
d_3 &= Q_{07} + Q_{19} \\
d_4 &= Q_{15} + Q_{23} \\
d_5 &= Q_{31}
\end{aligned}
\qquad (5.3)
$$

5.4. RESULTS

5.4.1 - Precision and accuracy

Since Monte Carlo methods rely on a sequence of random numbers and since the random number generator used in subroutine CPE3S generates a different set of random numbers for every simulation run (based on date and time of the day), there will be some variance associated with the results.

The standart error of a simulation is related to the number of samples (NMOL in the present case) by a square root law, so that in order to improve the precision of the results by one order of magnitude it is necessary to increase the number of samples by a factor of 10^2.

A compromise has to be found, therefore, between number of samples (directly related to computing time) and precision of the results.

In the present case, a reasonable compromise was found for NMOL = 10000, which afforded a computing time in the order of tens of seconds (in the Edinburgh Regional Computer Center - EMAS 2972 system instalation) for slow simulation (P_G in the order of 0.01).

An assessment of the accuracy and precision of the simulations may be obtained by comparing results from the Monte Carlo method for $P_A = 0$ with those from Anderson and Kemball's exact method for the regular pentagon case.

Such comparison is shown in figure 5.1, where % d_n values are plotted against the probability of desorption P_G. The solid lines indicate the predictions of Anderson and Kemball's method and the points represent the predictions of the Monte Carlo simulation. The agreement between the two methods is seen to be excelent. Table 5.3 shows the standard error of the estimate for each deuterated product and for the overall distribution.

TABLE 5.3

STANDARD ERRORS FOR THE MONTE CARLO SIMULATION FOR THE REGULAR PENTAGON CASE

n	1	2	3	4	5	Overall[2]
S.E.[1]	0.4	0.4	0.35	0.1	0.3	0.3

(1) $$S.E. = \sum_{i=1}^{N} \frac{(d_{ni} - b_{ni})^2}{N}$$

d_{ni} = Monte Carlo result for product n in simulation i (expressed in %)

b_{ni} = Exact result for product n in simulation i (expressed in %)

N = Number of simulations

(2) $$S.E. = \sum_{n=1}^{5} \sum_{i=1}^{N} \frac{(d_{ni} - b_{ni})^2}{5N}$$

5.4.2 - The rollover mechanism

175 intermediates were generated by program CPE1S for the rollover mechanism.

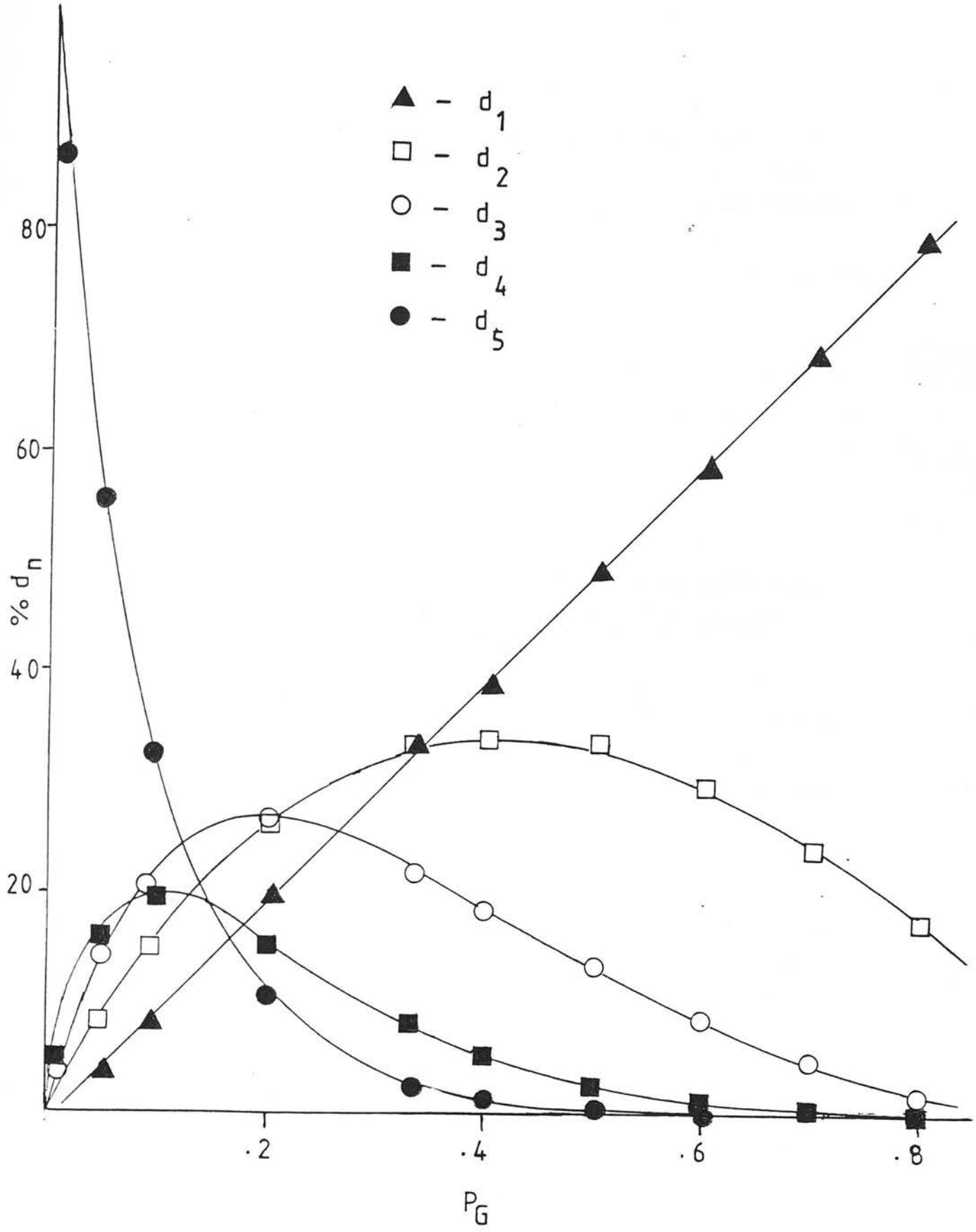

FIG. 5.1 - THEORETICAL EXCHANGE PATTERNS FOR
"REGULAR PENTAGON" MOLECULE
POINTS - MONTE CARLO METHOD
LINES - ANDERSON AND KEMBALL'S METHOD[7]

A table containing exchange patterns covering a wide range of the simulation parameters is shown in Appendix A2.

The essential features of cyclopentane exchange reported in the literature[1-3] are reproduced in the simulated patterns, namely the existence of maxima at d_5 and d_{10} under certain conditions. The most characteristic feature of the rollover mechanism,however, is the existence of a small maximum at d_8.

Low values of P_A/P_B (<0.05) tend to favour the maximum at d_8, for a range of P_G values. When P_G is higher than 5%, the maximum at d_8 disappears due to the increased proportion of d_6 and d_7 products in the distribution.

On the other hand, when P_G becomes very small, the amount of d_9 and d_{10} products increases and the maximum at d_8 again disappears.

It is of relevance to the interpretation of real exchange patterns that, as d_{10} increases relatively to d_5 and d_8, d_9 also increases in the same direction, so that, when the ratio d_{10}/d_9 is large, the ratio between d_9 and less deuterated products is also large. This is because for a d_{10} product to be formed, repetition of the rollover process is necessary. Since the most abundant d_8 intermediate (i.e., an intermediate that in desorbing will produce a d_8 molecule) contains three neighbouring D atoms and two neighbouring H atoms on the side of the ring facing away from the surface, the chance that one of the hydrogen atoms is left behind on repetition of the rollover process (giving rise to a d_9 product) is equal to that of both hydrogens passing to the side facing the surface (giving rise to a d_{10} product). A large d_{10}/d_9 ratio only obtains, therefore, when the lifetime of the adsorbed species on the surface

is large enough for several rollover events to occur, in which case the probability of desorption of less deuterated species is very small.

5.4.3 - The α,α-turnover mechanism

152 intermediates were generated by program CPEIS for the α,α-turnover mechanism.

A complete listing of exchange patterns covering a wide range of the simulation parameters is shown in appendix A2.

Three different regions may be distinguished for parameter P_A/P_B with respect to the type of exchange pattern obtained. For low P_A/P_B (<0.1), formation of α, α-diadsorbed intermediates is an infrequent event and maxima or breaks at d_5 occur.

For P_A/P_B in the vicinity of 1, both turnover and α, β-diasorption events occur frequently and a continuous distribution of deuterated products obtains.

For large values of P_A/P_B, α, α-diadsorption is faster than α, β-diadsorption and maxima at products with even number of D atoms are observed.

The outstanding feature of the first region is the occurence of saddle-like distributions in the d_6-d_{10} range, that is, patterns where both d_6 and d_{10} are larger than d_7-d_9, with no maximum at d_8. Such distributions arise from the fact that, when α, α - diadsorption proceeds from the "one-side" d_5 intermediate (which on desorption produces a d_5 molecule), there is a 50% chance that the α, α species falls back on the surface, leaving only one D atom on the opposite side of the ring, thus giving rise to a d_6 product. If the species turns over to the opposite side, propagation of the

exchange up to d_{10} is easy and a d_{10} maximum appears, provided P_G is small enough to allow complete propagation.

The region of large P_A/P_B is characterized by maxima at even numbered d_n products. Such maxima have been observed in practice for high temperature exchange over some catalysts, as will be discussed subsequently.

5.4.4 - Comparison with real patterns

In the present section real exchange patterns are compared with model distributions for several metal catalysts. Most of the examples were chosen to illustrate the good consistency that can be obtained in hydrocarbon exchange studies over widely different preparations of a given metal. Data for both films and supported catalysts are included. Also results obtained under both continuous flow and static conditions are discussed. This ensures that the patterns presented are characteristic of each metal and substantially free from complicating factors, such as diffusion limitations or product readsorption effects.

Attempts to adjust the simulation parameters in order to match simulated to real patterns were fruitless. This is not surprising, since it has been known for a long time that parallel exchange processes occur on the surface of metal catalysts, so that a single set of reaction probabilities, which would conceivably apply in the case of a homogenous surface, does not apply to the case of real surfaces[4]. Burwell in fact suggests that at least five separate processes, occurring on distinct types of site, contribute to the exchange of cyclopentane on Pd[26].

Nevertheless, it was found that in most cases the d_3 - d_8 region of real patterns could be reasonably well reproduced using a single set of

parameters, but additional processes had to be postulated in order to explain the regions d_1 - d_2 and d_9 - d_{10}. Thus, in the discussion that follows, real patterns are discussed in terms of three separate processes, giving rise to light (process I), intermediate (process II) and heavy (process III) products of exchange.

5.4.4a - Rhodium catalysts

Some examples of Rh patterns are shown in table 5.4. Example numbers followed by letter E refer to experimental patterns. Numbers followed by letters R and A refer, respectively, to model patterns obtained for the rollover mechanism and for the α, α-turnover mechanism. Patterns are normalized to the d_5 product, but for the experimental results, distributions normalized to 100% are also presented.

The most characteristic feature of Rh exchange patterns, as reported by several authors[14,20], is the existence of a pronounced maximum at d_2, followed by a minor maximum or break at d_5. Maxima at d_2 have also been reported in the exchange of other hydrocarbons (n-pentane, n-hexane) over Rh[13].

This large Rh d_2 component is interesting from a mechanistic point of view, since it cannot be reproduced in model distributions, even when superposition of patterns is considered, unless the participation of an α, α-turnover mechanism with very large P_A/P_B is postulated. Examples 1E to 3E in table 5.4 display d_2/d_3 ratios in the order of 3, while d_1 is smaller than d_2. Figure 5.1 indicates that a maximum at d_2 exists only for P_G values between 20 and 33% and that this maximum is rather shallow if only one-set exchange is considered. This prediction is also valid (see tables in appendix A2) for two-set exchange, except for the α, α-mechanism when P_A/P_B is much larger than 1. This corresponds to a case

TABLE 5.4

Rh EXCHANGE PATTERNS

Example	Catalyst	T/K	P_G	P_A/P_B	d_1	d_2	d_3	d_4	d_5	d_6	d_7	d_8	d_9	d_{10}	Reference
1R	–	–	0.2	0.1	2.18	2.87	2.73	1.58	1.00	0.32	0.13	0.05	0.01	0	
1E	2% Rh/SiO_2	250	–	–	6.10	7.70	2.80	1.80	1.00	0.30	0.22	0.08	0.02	0	(20)
					(30.5)	(38.5)	(14.0)	(9.0)	(5.0)	(1.5)	(1.1)	(0.4)	(0.1)	(0)	
1A	–	–	0.2	0.05	2.03	2.58	2.44	1.48	1.00	0.30	0.13	0.08	0.03	0.02	
2R	–	–	0.1	0.05	0.47	0.79	1.05	0.83	1.00	0.28	0.19	0.12	0.04	0.01	
2E	0.5% Rh/Al_2O_3	339	–	–	2.46	2.62	1.03	0.73	1.00	0.22	0.19	0.13	0.09	0.13	(14)
					(28.6)	(30.4)	(12.0)	(8.5)	(11.6)	(2.6)	(2.2)	(1.5)	(1.1)	(1.5)	
2A	–	–	0.1	0.02	0.41	0.67	0.89	0.73	1.00	0.20	0.07	0.07	0.03	0.03	
3R	–	–	0.07	0.005	0.17	0.32	0.46	0.46	1.00	0.03	0.03	0.03	0	0	
3E	0.5% Rh/TiO_2	291	–	–	1.22	2.22	0.81	0.52	1.00	0.03	0	0	0	0	chapter 7
					(21.0)	(38.2)	(13.9)	(8.9)	(17.2)	(0.6)	(0)	(0)	(0)	(0)	
3A	–	–	0.07	0.002	0.18	0.30	0.45	0.46	1.00	0.03	0.01	0.01	0	0.01	
4A	–	–	0.05	0.01	0.11	0.22	0.33	0.37	1.00	0.07	0.07	0.09	0.01	0.01	
4E	0.02%Rh/SiO_2	359	–	–	0.15	0.45	0.40	0.40	1.00	0.10	0.10	0.12	0.12	0.12	(14)
					(5.0)	(14.6)	(13.0)	(13.0)	(32.8)	(3.4)	(3.3)	(3.8)	(3.9)	(7.1)	
4A	–	–	0.05	0.01	0.11	0.21	0.35	0.37	1.00	0.14	0.04	0.04	0.04	0.06	

where α, α-diadsorbed species are efficiently formed on the surface, but are reluctant to participate in α, β-exchange processes.

If α, α-diadsorbed species are responsible for the Rh d_2 maximum, a parallel process with small P_A/P_B has to be postulated in order to explain the subsidiary maximum at d_5, since such maximum is not predicted for large P_A/P_B values. Also if this hypothesis is correct, cyclopentane-1,1-d_2 should be outstanding among the products of cyclopentane exchange over Rh. An attempt to observe this species was one of the main aims of the work described in chapter 6 of this dissertation.

Comparison of model with experimental patterns in table 5.4 shows that reasonable fits may be obtained for the intermediate (d_3 - d_8) region of the distributions. In examples 1E and 3E, both rollover and α, α-turnover model patterns are adequate to reproduce experimental patterns in the range d_3 to d_{10}. In example 2E, the rollover pattern probably provides a better representation, but some contribution of process III must be postulated.

Pattern 4E provides an example of a pattern which differs substantially from the previous ones. Roth et al[14] report other patterns similar to 4E. Pattern 4R reasonably reproduces 4E from d_1 to d_8, but again some contribution of a process III has to be postulated.

It is interesting that P_A/P_B values derived from the intermediate region of exchange patterns 1E to 3E vary over a factor of 20 despite the broad similarity of these distributions. On the other hand, 4E differs appreciably from 1E to 3E despite the fact that the corresponding P_G and P_A/P_B are within the range of variation of those parameters for examples 1E to 3E. It

seems, therefore, that the main characteristic features of these exchange patterns are primarily determined by the extent to which processes I, II and III contribute to the overall distributions, rather than by differences in the probabilities of desorption, α, β-diadsorption and turnover within each process.

Table 5.5 lists approximate percent contributions of the different processes for examples 1E to 4E, derived from comparison of experimental with model patterns. Process I is considered to give rise mainly to d_1 and d_2 products and its contribution is corrected for the amount of d_1 and d_2 that would be expected ro arise from process II.

Process III is considered to result mainly in d_9 and d_{10} products and its contribution is similarly corrected for the presence of process II.

TABLE 5.5

% CONTRIBUTION OF DIFFERENT PROCESSES TO CYCLOPENTANE EXCHANGE OVER Rh(1)

Example(2)	Process I	Process II	Process III
1E	44	56	-
2E	44	54	2
3E	57	43	-
4E	8	82	10

(1) See text for definition of processes I, II and III.
(2) See table 5.4 for details on catalyst and conditions.

It is relevant to note that Roth et al[14] have suggested that patterns such as 1E to 3E are characteristic of exchange over small Rh particles, while patterns such as 4E arise from exchange over large Rh particles. It would appear, therefore, that α, β-diadsorption is more efficient on sites characterized by the presence of several contiguous metal atoms, while

alkane desorption, plus whatever process is responsible for the d_2 maximum, is favoured on coordinatively less saturated sites.

5.4.4b - Iridium catalysts

Exchange patterns characteristic of supported Ir catalysts are shown in table 5.6. As with dispersed Rh catalysts, there is little tendency to propagate exchange beyond d_2 products. Contrary to Rh, the ratio d_1/d_2 is large, so that it is not clear whether a separate process giving rise to a d_2 product needs to be postulated for Ir.

From example 5E, it is clear that both rollover and α,α-turnover model patterns provide a reasonable fit for the experimental results and that little contribution from process III is apparent.

Pattern 6E seems to be better reproduced by the α,α-turnover model. Only a small contribution from process III is apparent also in this case. Table 5.7 summarizes the approximate contributions of the different process to Ir exchange patterns.

TABLE 5.6

Ir EXCHANGE PATTERNS

Example	Catalyst	T/K	P_G	P_A/P_B	d_1	d_2	d_3	d_4	d_5	d_6	d_7	d_8	d_9	d_{10}	Reference
5R	–	–	0.2	0.02	1.95	2.64	2.58	1.49	1.00	0.09	0.03	0.01	0	0	
5E	2% $Ir-SiO_2$	250	–	–	9.40	6.10	1.80	1.30	1.00	0.10	0.06	0	0	0.06	(20)
					(47.0)	(30.5)	(9.0)	(6.5)	(5.0)	(0.5)	(0.3)	(0)	(0)	(0.5)	
5A	–	–	0.2	0.01	1.85	2.45	2.39	1.35	1.00	0.07	0.02	0.01	0.01	0	
6R	–	–	0.15	0.05	0.98	1.40	1.55	1.03	1.00	0.25	0.16	0.09	0.03	0.01	
6E	0.39% $Ir-Al_2O_3$	303	–	–	9.18	4.58	1.49	1.13	1.00	0.25	0.22	0.13	0.11	0.09	(24)
					(50.5)	(25.2)	(8.2)	(6.2)	(5.5)	(1.4)	(1.2)	(0.7)	(0.6)	(0.5)	
6A	–	–	0.15	0.02	0.88	1.23	1.39	0.96	1.00	0.19	0.12	0.11	0.06	0.06	

TABLE 5.7

% CONTRIBUTION OF DIFFERENT PROCESSES TO CYCLOPENTANE EXCHANGE OVER Ir

Example	Process I	Process II	Process III
5E	55	45	-
6E	64	36	-

The numbers in table 5.7 are rather similar to those obtained for dispersed Rh catalyst, with a sowewhat larger contribution of process I.

5.4.4c - Platinum catalysts

Experimental and model patterns for Pt catalysts are presented in table 5.8. Examples 7E and 8E correspond to results obtained, respectively, over highly dispersed and film catalysts at relatively low (and similar) temperatures. Both patterns are fairly well reproduced by an α, α-turnover model and little contribution from process III is apparent, as was the case with Rh and Ir. Contributions from the different processes are summarized in table 5.9.

TABLE 5.8

CYCLOPENTANE EXCHANGE PATTERNS OVER Pt CATALYSTS

Reference	Example	Catalyst	T/K	P_G	P_A/P_B	d_1	d_2	d_3	d_4	d_5	d_6	d_7	d_8	d_9	d_{10}
	7R	–	–	0.03	0.01	0.05	0.12	0.21	0.25	1.00	0.09	0.09	0.18	0.04	0.02
(24)	7E	0.5% Pt–Al_2O_3	305	–	–	0.65	0.34	0.24	0.27	1.00	0.09	0.05	0.05	0.05	0.08
						(23.2)	(12.1)	(8.4)	(9.6)	(35.5)	(3.1)	(1.9)	(1.6)	(1.7)	(3.0)
	7A	–	–	0.03	0.005	0.06	0.09	0.18	0.22	1.00	0.10	0.02	0.02	0.02	0.07
	8R	–	–	0.03	0.02	0.07	0.14	0.25	0.30	1.00	0.16	0.18	0.29	0.10	0.08
(25)	8E	Pt film	298	–	–	0.58	0.18	0.11	0.24	1.00	0.21	0.10	0.15	0.12	0.43
						(18.6)	(5.7)	(3.4)	(7.6)	(32.2)	(6.9)	(3.2)	(4.8)	(3.8)	(13.8)
	8A	–	–	0.03	0.02	0.08	0.17	0.25	0.30	1.00	0.34	0.13	0.11	0.13	0.29
(25)	9E	11% Pt–Au film	499	–	–	(27.5)	(7.0)	(4.9)	(16.9)	(1.9)	(6.3)	(1.1)	(4.2)	(3.2)	(27.0)
(25)	10E	Pt film	502	–	–	(10.1)	(5.1)	(2.6)	(5.0)	(3.1)	(2.7)	(1.6)	(1.1)	(8.3)	(61.7)

TABLE 5.9

% CONTRIBUTION OF DIFFERENT PROCESSES TO CYCLOPENTANE EXCHANGE OVER Pt

Example	Process I	Process II	Process III
7E	30	70	-
8E	17	83	-

As with Rh, there is a smaller contribution from process I on the catalyst with larger particle size. This effect is, however, less pronounced with Pt.

Table 5.8 also includes results obtained by Dessing and Ponec[25] over Pt films at high temperatures. Maxima at products containing an even number of deuterium atoms are apparent in those patterns. As discussed in section 4.3, these maxima are characteristic of large P_A/P_B, small P_G processes, that is, processes which lead to the formation of α, α- diadsorbed intermediates preferentially to α, β-diadsorbed species, whose lifetime on the surface is however sufficiently long for some α, β-diadsorption events to occur before desorption. In example 9E, however, the maximum at d_4 is too sharp, as compared to d_2 and d_6, to be accounted for by interconversion between α, α- and α, β-diadsorbed species. It is possible that α,α,β,β-tetra adsorbed intermediates play an important role in cyclopentane exchange over Pt at high temperatures.

5.4.4d - Palladium catalysts

Pd is by far the most studied catalyst with respect to cycloalkane exchange and most of the evidence for a rollover mechanism has been obtained over this metal. The patterns shown in table 5.10 clearly indicate that a much better fit between experimental and model distributions is indeed obtained when the rollover model is used, if proper allowance is made for sizeable

contributions of processes I and III.

One of the most characteristic features of exchange over Pd is the pronounced tendency shown by this metal to promote the formation of perdeuterated hydrocarbons. In the case of cyclopentane exchange, this has been attributed to a greater ease of the rollover process on Pd[27,28]. This has been correlated with the reported weakness of the olefin - Pd π bond as compared to those of other metals[14,27]. Also the decrease in contribution of the d_{10} product when Pd is alloyed with Ni has been explained by dilution of Pd ensembles responsible for the rollover mechanism, which were thought to be larger than those responsible for other surface processes[28].

In our view, this type of interpretation which attributes the Pd d_{10} maximum to a large rollover probability is not necessarily correct. P_A/P_B values which provided the "best fits" for the intermediate region of experimental exchange patterns were lower for Pd than for any other metal. This indicates that rollover is actually somewhat more difficult on Pd than on other metals. The Pd d_{10} maximum arises from a large contribution of process III, whose main requirement is the existence of sites where alkyl-alkene interconversion is much faster than alkane desorption, provided some probability of rollover exists.

Table 5.11 summarizes the contribution of the different processes to the exchange of cyclopentane over Pd. Comparison of examples 12E and 13E is particularly instructive, since these results were obtained over the same catalyst, at two different temperatures[26]. It is clear that the fourfold increase in the d_{10}/d_5 ratio when the temperature is increased by 30 K is almost solely caused by a corresponding fourfold increase in contribution of process III relative to process II.

TABLE 5.10

CYCLOPENTANE EXCHANGE PATTERNS OVER Pd CATALYSTS

Example	Catalyst	T/K	P_G	P_A/P_B	d_1	d_2	d_3	d_4	d_5	d_6	d_7	d_8	d_9	d_{10}	Reference
11R	–	–	0.03	0.005	0.05	0.10	0.17	0.21	1.00	0.04	0.05	0.11	0.01	0.01	
11E	Pd film	273	–	–	0.91	0.48	0.25	0.18	1.00	0.03	0.03	0.18	0.15	0.58	(4)
					(24.0)	(12.7)	(6.6)	(4.8)	(26.5)	(0.7)	(0.7)	(4.8)	(3.9)	(15.3)	
11A	–	–	0.03	0.002	0.05	0.08	0.16	0.21	1.00	0.04	0.01	0.01	0.01	0.02	
12R	–	–	0.03	0.005	0.05	0.10	0.17	0.21	1.00	0.04	0.05	0.11	0.01	0.01	
12E	5% Pd–Al_2O_3	313	–	–	0.44	0.71	0.26	0.20	1.00	0	0.05	0.12	0.07	1.00	(26)
					(11.5)	(18.5)	(6.8)	(5.2)	(26.0)	0	(1.3)	(3.2)	(1.7)	(26.0)	
12A		–	0.03	0.002	0.05	0.08	0.16	0.21	1.00	0.04	0.01	0.01	0.01	0.02	
13R	–	–	0.02	0.01	0.04	0.08	0.14	0.18	1.00	0.08	0.10	0.28	0.06	0.06	
13E	5% Pd–Al_2O_3	343	–	–	0.25	0.35	0.20	0.20	1.00	0.05	0.08	0.25	0.08	3.91	(26)
					(3.9)	(5.5)	(3.1)	(3.1)	(15.7)	(0.8)	(1.2)	(3.9)	(1.2)	(61.4)	
13A	–	–	0.03	0.002	0.05	0.08	0.16	0.21	1.00	0.04	0.01	0.01	0.01	0.02	

Patterns 12R and 13R in table 5.10 indicate that the amounts of d_{10} attributable to process II are small for the relevant P_G - P_A/P_B combinations. Thus, the pronounced differences in exchange patterns obtained at different temperatures are caused primarily by differences in energy of activation for adsorption-desorption for parallel processes occurring on distinct types of sites.

TABLE 5.11

% CONTRIBUTION OF DIFFERENT PROCESSES TO CYCLOPENTANE EXCHANGE OVER Pd

Example	Process I	Process II	Process III
11E	0.33	0.48	0.19
12E	0.26	0.47	0.27
13E	0.08	0.31	0.61

Exchange patterns reported by Schrage and Burwell[26] for supported Pd catalysts (examples 12E and 13E) present an important maximum at d_2 which may not be reproduced in model distributions, even when superposition of patterns is considered, similarly to what was found for supported Rh. If the d_2 maxima on Pd and Rh arise from similar mechanisms, this poses an interesting problem, since Pd is generally considered to be a poor catalyst for α, α-diadsorption[18].

5.4.4e - Nickel catalysts

Experimental and model patterns for Ni catalysts are shown in table 5.12. Reasonable fits were only obtained for the region from d_3 to d_7, probably because process III on Ni gives rise to products in the whole region from d_8 to d_{10}, in contrast with Pd, where mainly the d_{10} product seems to be formed by this process. Thus, no information may be gained from Ni exchange patterns regarding possible mechanisms of turnover.

The contribution of different processes

TABLE 5.12

CYCLOPENTANE EXCHANGE PATTERNS OVER Ni CATALYSTS

Example	Catalyst	T/K	P_G	P_A/P_B	d_1	d_2	d_3	d_4	d_5	d_6	d_7	d_8	d_9	d_{10}	Reference
14R			0.1	0.1	0.60	0.97	1.27	0.98	1.00	0.46	0.35	0.22	0.11	0.03	
14E	42% $Ni-SiO_2$	343	–	–	0.98	2.27	1.31	0.80	1.00	0.32	0.34	0.48	0.52	2.20	(14)
					(9,6)	(22.2)	(12.8)	(7.8)	(9.8)	(3.1)	(3.3)	(4.7)	(5.1)	(21.6)	
14A	–	–	0.1	0.05	0.53	0.82	1.04	0.89	1.00	0.43	0.21	0.18	0.12	0.08	
15R	–	–	0.1	0.05	0.47	0.79	1.05	0.83	1.00	0.28	0.19	0.12	0.04	0.01	
15E	73% Cu-Ni film	343	–	–	1.55	2.64	1.35	0.83	1.00	0.23	0.14	0.31	0.28	0.79	(29)
					(17.0)	(29.0)	(14.8)	(9.1)	(11.0)	(2.5)	(1.5)	(3.4)	(3.1)	(8.7)	
15A	–	–	0.1	0.035	0.47	0.75	0.97	0.81	1.00	0.32	0.14	0.13	0.08	0.06	

to cyclopentane exchange over Ni are shown in table 5.13. The values in this table are rather close to those obtained for Pd, but both the rate of alkane desorption relative to alkyl-alkene interconversion and the probability of turnover seem to be higher on Ni than on Pd, as judged from P_G and P_A/P_B values which provided the best fits for process II.

TABLE 5.13

% CONTRIBUTION OF DIFFERENT PROCESSES TO CYCLOPENTANE EXCHANGE OVER Ni

Example	Process I	Process II	Process III
14E	0.21	0.51	0.28
15E	0.34	0.55	0.11

Similarly to supported Rh and Pd, a large d_2 component is apparent in Ni exchange patterns, but both on film and supported forms in the case of Ni.

5.5. CONCLUSIONS

A Monte Carlo type method was developed, which allows the simulation of cyclopentane exchange patterns for a mechanism involving interconversion between monoadsorbed and α, β-diadsorbed species, combined with α, α-turnover or rollover processes responsible for two-set exchange.

Comparison of experimental with model patterns showed that at least three separate processes, probably occurring on distinct types of site, have to be postulated in order to explain experimental distributions:

- Process I, characterized by a large probability of alkane desorption, giving rise mainly to d_1 and d_2 products;
- Process II, responsible for the central (d_3 - d_8)

portion of the product distributions;

- Process III, characterized by low probabilities of alkane desorption, responsible for the large amounts of d_{10} products observed on some catalysts.

Satisfactory fits generally obtained for the central portion of the product distributions, using a single set of simulation parameters, which indicates that process II arises from a relatively homogeneous region of each catalyst surface.

Information regarding the probability of turnover on different catalyst can only be obtained from P_A/P_B values derived for process II, since the only requirement for process III is that the rate of alkane desorption is very small as compared to that of other surface processes, and the requirement for process I is that the probability of alkane desorption is large, so that the chance of exchange propagation beyond d_2 is small.

Thus, probabilities of turnover may ou may not be different for processes I, II and III on a given catalyst. It follows that interpretations which attribute a large d_{10} component to a greater ease of turnover may not be considered to be correct "a priori".

Differences in the exchange patterns for different metals seem to arise mainly from differences in the extent to which process I, II and III contribute to the overall distributions, rather than from differences in P_G and P_A/P_B within each process. Similarly, the effect of temperature on the exchange patterns obtained on a given catalyst may be primarily attributed to differences in activation energy for adsorption-desorption on the sites responsible for each process, rather than to changes in the relative probabilities of alkane desorption, α,β-diadsorption and turnover on each type of

site.

The extent to which processes responsible for the production of more extensively deuterated products contribute to exchange patterns decreases in the order:

Pd, Ni > Pt > Ir

At least for Pd, Ni and Pt, this order is valid for both film and supported catalyst. Rh patterns, as reported by Roth et al[14], seem to be very sensitive to catalyst preparation method, but dispersed Rh catalysts show a behaviour similar to Ir. Interestingly, this is similar to the order in which heats of vaporization of the different metals increase[30] (Pd < Ni < Pt < Rh < Ir).High energies of vapourization have been associated with high metal-carbon and metal-hydrogen binding energies[31]. It may be speculated that the sites responsible for extensive multiple exchange become deactivated, due to strong adsorption of hydrocarbon residues, on metals for which vapourization energies are higher.

Fits between model and experimental patterns were generally not good enough to allow definite conclusions to be drawn regarding possible mechanisms of turnover, except for Pd, where a rollover mechanism is clearly favoured. Pt patterns are better represented by an α, α-turnover model, as is one of the Ir patterns. Some Rh patterns are better described by a rollover model. No information in this respect could be extracted from Ni patterns.

Patterns for supported Pd, supported Rh and Ni catalysts display an important d_2 component which can only be explained, with basis on the models described in the present chapter, if there is a region on the surface of those catalysts where α, α-diadsorbed intermediates are efficiently formed, but do not readily participate in α, β-exchange processes. It is relevant, however, that

Pd is generally not considered to be a good catalyst for α,α-diadsorption[18]. A fuller discussion on the nature of this d_2 component is presented in chapter 6. Process I is probably a combination of two different mechanisms, one giving rise to most of the d_1 product (and possibly some of the d_2 product) and the other responsible for a substantial part of the d_2 product.

5.6 - REFERENCES

1. C.Kemball, Adv.Catalysis, 1959, 11, 223.

2. R.L.Burwell, Acc.Chem. Res., 1969, 2, 289

3. K.A. Clarke and J.J. Rooney, Adv.Catalysis, 1976, 25, 125.

4. J.R.Anderson and C.Kemball, Proc. Roy. Soc. A., 1954 226, 472

5. K.Schrage and R.L.Burwell, J.Am. Chem.Soc., 1965, 88, 4555.

6. F.C.Gault, J.J.Rooney and C.Kemball, J.Catalysis,1962, 1, 255.

7. J.R.Anderson and C.Kemball, Proc.Roy.Soc.A., 1954, 223, 361.

8. C.Kemball and I.Woodward, Trans.Faraday Soc., 1960, 56, 138

9. J.M.Hammersley and D.C. Handscomb, Monte Carlo Methods, Methuen, London, 1964.

10. R.L.Burwell, B.K.C. Shim and H.C.Rowlinson, J.Am.Chem. Soc., 1957, 79, 5142.

11. S.O.Thompsom, J.Turkevich and A.P.Irsa, J.Am.Chem.Soc., 1951, 73, 5213.

12. C.Kemball, Proc. Roy. Soc. A., 1954, 233, 377.

13. F.G.Gault and C.Kemball, Trans. Faraday Soc., 1961, 57, 1781.

14. J.A.Roth, B.Geller and R.L.Burwell, J.Res.Inst. Catalysis, Hokkaido Univ., 1968, 16, 221.

15. R.L.Burwell and W.S.Briggs, J.Am.Chem.Soc., 1952, 74, 5096.

16. H.A.Quinn, J.H. Graham, M.A.McKervey and J.J.Rooney, J.Catalysis, 1972, 26, 326.

17. M.A.McKervey, J.J.Rooney and N.G. Samman, J.Chem.Soc. Chem.Commun., 1972, 1185.

18. C.Kemball, Proc. Roy. Soc. A, 1953, 217, 376

19. C.Kemball, Trans.Faraday Soc., 1954, 50, 1344

20. I.H.B.Haining, C.Kemball and G.Haller, J.Chem.Soc., Faraday Trans. I, 1981, 77, 2519

21. J.J.Rooney, J.Catalysis, 1963, 2, 53

22. H.A.Quinn, J.H.Graham, N.A.Mckervey and J.J.Rooney, J.Catalysis, 1972, 22, 35.

23. The IMSL library, International Mathematical and Statistical Libraries Inc., 7th Ed., 1979

24. D.Garden, M.Phil Thesis, University of Edinburgh, 1981.

25. R.P.Dessing and V.Ponec, J.Catalysis, 1976, 44, 494.

26. K.Schrage and R.L.Burwell, J.Am.Chem. Soc., 1966, 88, 4549.

27. J.K.A. Clarke and J.F.Taylor, J.Chem. Soc., Faraday Trans.I, 1976, 72, 917.

28. J.L.Vlasveld and V.Ponec, J.Catalysis, 1972, 24, 250.

29. V.Ponec and W.M.H. Sachtler, J.Catalysis, 1972, 24, 250.

30. J.R.Anderson, Structure of Metallic Catalysts, Academic Press, London, 1975, p.446.

31. J.R. Anderson and B.G. Baker, in Chemisorption and Reactions on Metallic Films, J.R.Anderson ed., Academic Press, London, 1971, v.2, p.98.

CHAPTER 6

A DEUTERIUM N.M.R. STUDY OF CYCLOPENTANE EXCHANGE ON SUPPORTED METALS

CHAPTER 6

A DEUTERIUM - N.M.R. STUDY OF CYCLOPENTANE EXCHANGE ON SUPPORTED METALS

6.1 - INTRODUCTION

The exchange reactions of hydrocarbon with deuterium are commonly followed by mass-spectrometric analysis of the products, wherefrom initial product distributions are derived in terms of the total concentration of products containing a given number of deuterium atoms.

In some cases, inspection of the initial product distributions allows conclusions to be drawn regarding the arrangement of deuterium atoms in the products. For example, in the exchange of cyclopentane over metals, there can be little doubt that the frequently observed maximum at d_5 originates from a product containing all of the hydrogen atoms on the same side of the ring replaced by deuterium.

In other cases, however, analysis of mass spectral parent peaks does not provide such clear-cut results, nor is it possible to derive information from the isotopic distribution in fragment peaks, due to the scrambling of "hydrogen" atoms[1] (and sometimes of the carbon skeleton[2]) which frequently accompanies electron impact fragmentation.

Other spectroscopic techniques sensitive to isotopic substitution have been used to this end. Microwave Spectroscopy provides results particularly rich in detail[3,4], but its application is limited to molecules which possess a permanent electric or magnetic dipole moment[5].

Recently, Brown and coworkers[6] demonstrated the potential usefulness of deuterium - n.m.r. spectroscopy for the estimation of the possible groupings of deuterium atoms in isotopically substituted cyclopentanes. From a combination of deuterium - n.m.r. and mass-spectrometric data for the simultaneous exchange and deuteration of cyclopentane, the authors were able to demonstrate that

cyclopentene exchange on ZnO is limited to the vinylic hydrogens, without any double-bond migration, and that cyclopentene formation occurs by a simple addition process, without any further exchange or scrambling of hydrogen and deuterium atoms in the molecule.

As a result, only d_1 - to d_4 - cyclopentanes were observed as reaction products, corresponding mainly to $-CHD-CH_2-$, $-CHD-CHD-$, $-CD_2-CHD-$ and $-CD_2-CD_2-$ groupings. Resonances attributed to each of these groupings were observed in the deuterium - n.m.r. spectra for samples from the catalytic reactions. Assignment of the respective frequencies was possible from comparison of n.m.r. peak areas with the proportions of deuterated cyclopentanes estimated from mass-spectrometric analysis.

The work described in the present chapter was aimed at determining isotopic shift values for other possible deuterium groupings, by examining n.m.r. spectra for mixtures of deutero-cyclopentanes, prepared under various experimental conditions, and applying this knowledge to the study of the mechanism of cyclopentane exchange over metal catalysts. Particular importance was given to the elucidation of the nature of the large d_2 component observed in the exchange of saturated hydrocarbons, mainly on Rh, but also on Ni and Pd catalysts, for which conflicting interpretations exist in the literature[7,8].

Three different types of samples were prepared for examination. With the first type (kinetic or K series), the extent of exchange was limited to low conversions, so that initial products of the reaction comprised a large proportion of the deuterated species, and Al_2O_3, Ir/SiO_2, Ir/Al_2O_3, Rh/TiO_2 and Pt/Al_2O_3 catalysts were used in preparing samples for this series. For the second type of sample (equilibrated or E series), exchange reactions carried-out with different deuterium to hydrocarbon ratios were taken to equilibrium. The third class was comprised of a single sample of isotopically impure cyclopentane -

1,1 - d_2 prepared from cyclopentanone according to scheme 6.1[9].

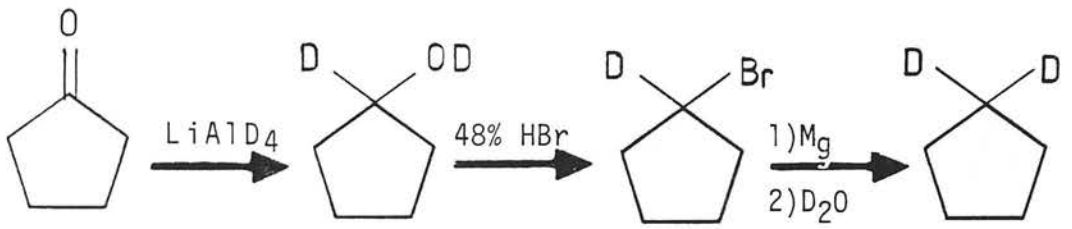

SCHEME 6.1

6.2 - EXPERIMENTAL

6.2.1 - Reagents and Materials

The source and purity of cyclopentane and deuterium were described in chapter 4.

The catalysts used were 0.51 wt % Pt/Al_2O_3[10] (see also chapter 8), 0.39 wt % Ir/Al_2O_3[10] (see also chapter 8), an Ir/SiO_2 catalyst containing 10^{-4} atom-g of Ir per gram of SiO_2, a Condea S.B.γ-alumina of high purity[12] and a 0.6 wt % Rh/TiO_2 catalyst (see chapter 7). Catalyst pre-treatment procedures were the same described in the relevant references.

Preparation of cyclopentane - 1,1 - d_2 was described in detail in reference 9. The deuterium-n.m.r. spectrum for this sample mixed with a small amount of cyclopentane - d_{10} used as an internal reference is reproduced in figure 6.1. The resonance occurring at lowest frequency corresponds to the deuterium nuclei in cyclopentane - d_{10}; the one at highest frequency occurred in the position expected for cyclopentane - d_1; the next resonance had a shift consistent with cyclopentane - 1,2-d_2 (cis + trans) and the most proeminent resonance was assigned to cyclopentane - 1,1 - d_2. The occurrence of cyclopentane - 1,2 - d_2 (32%, cis + trans), with smaller

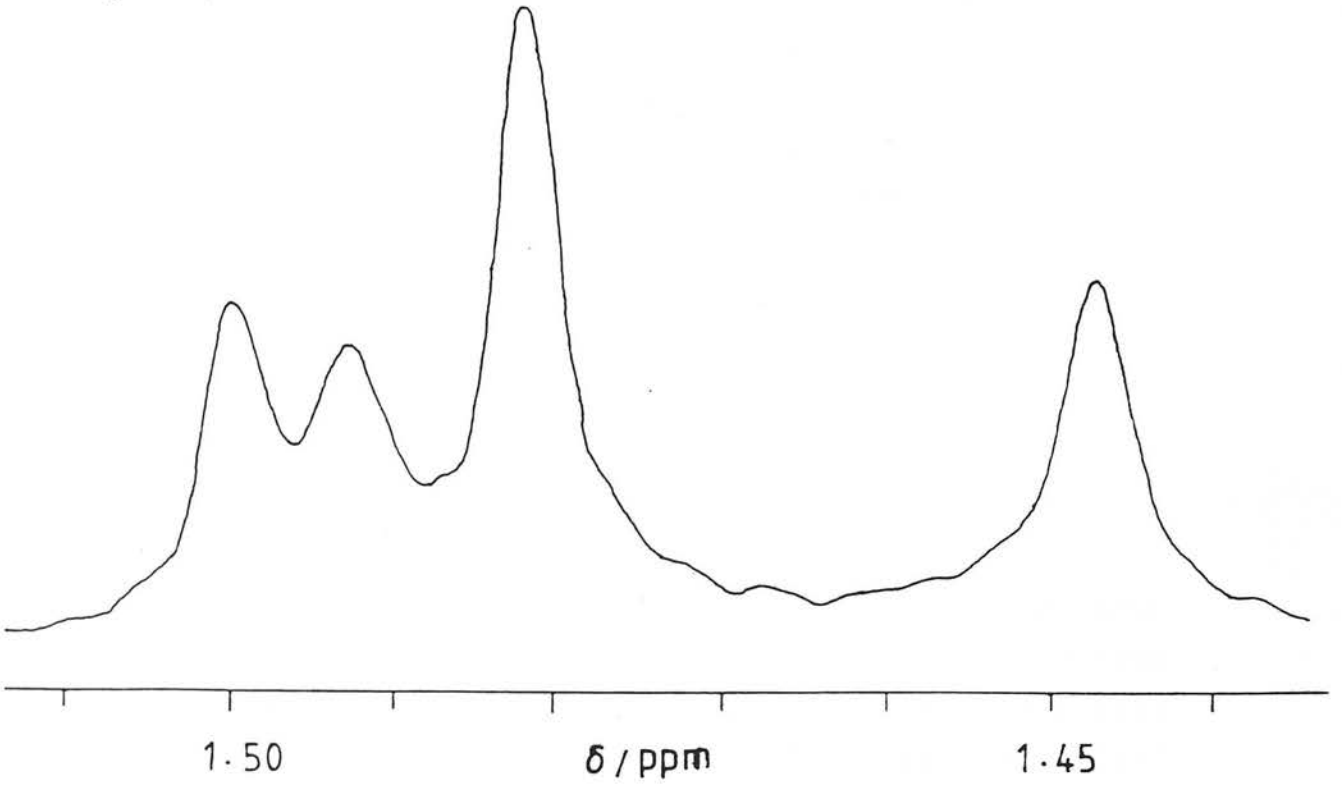

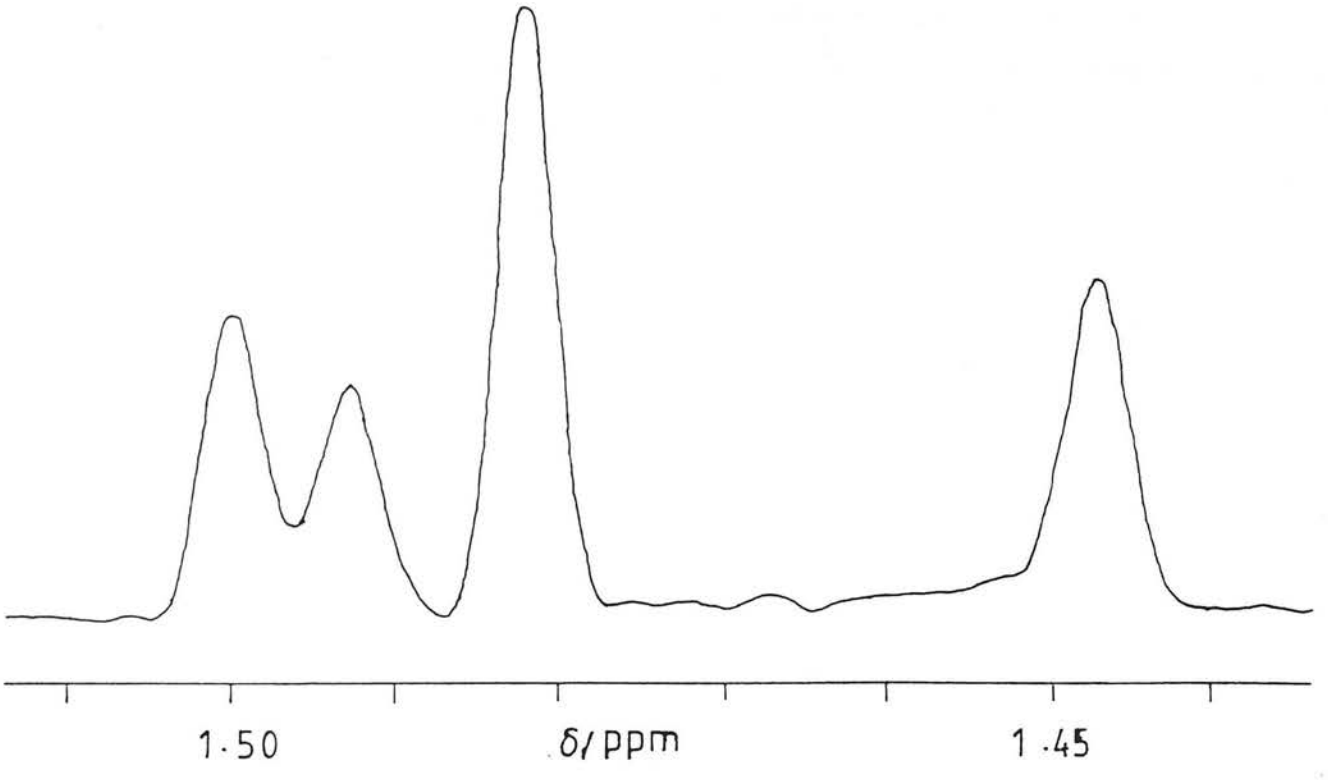

FIG. 6.1 D-N.M.R. SPECTRA FROM EXPERIMENT S1;
(a) WITHOUT LINE-NARROWING
(b) WITH LINE-NARROWING

quantities of cyclopentane - 1,3 - d_2 (11%, cis + trans) whose resonance was not observed due to overlap with other resonances, was caused by isomerization of the intermediate carbonium ion during the bromination step, as established by deuterium - n.m.r. analysis of the resulting monodeuterated bromocyclopentanes[9].

6.2.2 - Apparatus and Procedure

6.2.2a- Exchange Experiments

The apparatus used in the exchange experiments consisted of a static reactor of ca. 200 cm^3 volume coupled to a conventional gas-handling line and to a mass spectrometer via a capillary leak as described in detail in chapter 4. The procedure used for dosing the reactants and performing the experiments were also described in chapter 4. Larger amounts than usual of cyclopentane and deuterium were used so that enough deuterated material could be collected for n.m.r. analysis. Table 6.1 shows the experimental conditions for the different runs.

In experiments K2 to K5, conversions were kept at low values (5 to 12%) in order to obtain an isotopic mixture rich in initial products of reaction. In experiments E2 - E4, the reactions were taken to equilibrium, so that a mixture containing known amounts of all possible isotopic species could be obtained.

TABLE 6.1

EXPERIMENTAL CONDITIONS FOR EXCHANGE EXPERIMENTS

Experiment	Catalyst	Temperature/K	CP/10^{19}molecules(1)	D_2/CP(2)
K2	Rh/TiO_2	246	7.3	10
K3	Rh/TiO_2	247	7.3	10
K4	Ir/Al_2O_3	301	14.6	5
K5	Pt/Al_2O_3	300	14.6	5
E2	Rh/TiO_2	353	(3)	(3)
E3	Rh/TiO_2	353	14.6	5
E4	Rh/TiO_2	353	14.6	1

(1) Number of cyclopentane molecules charged to the reactor

(2) D_2/cyclopentane ratio

(3) Preparation of cyclopentane - d_{10} (see text)

Experiment E2 was designed to prepare a sample rich in cyclopentane - d_{10} and was performed in two stages. In the first stage, a 10:1 deuterium/cyclopentane mixture was equilibrated at 353 K over a Rh/TiO_2 catalyst. The reaction vessel was then immersed in liquid nitrogen until peaks arising from "cyclopentane" could be no longer observed with the mass spectrometer. The reaction vessel was then evacuated to remove the equilibrated "hydrogen" gas isotopic mixture and a new batch of deuterium was introduced. The reaction mixture was brought to reaction temperature and a new equilibration was performed. A product containing 73% cyclopentane - d_{10} was recovered.

Besides the samples from the experiments listed in table 6.1, two other samples were important in assigning isotopic shifts, namely samples K6 and E1. Sample K6 was obtained from an experiment performed over the Ir/SiO_2 catalyst at 250 K. Experiment E1 was actually a "kinetic" experiment (limited conversion) performed over Al_2O_3 but as cyclopentane exchange over alumina is strictly stepwise concentrations for each isotopic

configuration could be estimated from mass spectrometric measurements.(*)

6.2.2b- Sample Collection

The procedure for sample collection will be explained with reference to figure 4.1 in chapter 4. After the desired conversion was attained in the exchange experiment as estimated from the mass spectrometer trace, the reactor R was opened for a few seconds to the evacuated portion of the vaccuum line comprised of trap CT3, the mixing bulb M and the storage bulb B6. A liquid nitrogen bath was previously placed around trap CT2,so that as the reaction mixture flowed from the reactor into the line most of the exchanged cyclopentane condensed in CT2. Since the volume ratio of B6 + M + CT2 to R was greater than 10, this method allowed over 90% of the sample originally in the reactor to be recovered without any further significant exchange. Condensation into trap CT2 was allowed to continue for a few hours so that as much as possible of the hydrocarbon was collected. The system was then slowly evacuated using pumping system 1, which caused the gases to flow from B6 and M through the trap CT2 to the vaccuum pumps and any gas phase "cyclopentane" remaining condensed into CT2. After evacuation was completed the liquid nitrogen bath was transferred from CT2 to the cold-finger available in M and the hydrocarbon was distilled into it. The mixing bulb was isolated from the system and the hydrocarbon was allowed to expand by removing the liquid nitrogen bath in order to estimate the collection yield from the pressure reading in gauge G1. Collection yields in the order of 80% were generally obtained. The hydrocarbon was then condensed into a 5mm n.m.r. tube attached to inlet J2. The n.m.r. tube contained about 0.5 cm of 5% deuterochloroform solvent and was cooled in liquid nitrogen. After sample collection the

(*) We thank I.H.B Haining for performing experiments K6 and E1.

n.m.r. tube was sealed in a flame.

6.2.2c- N.M.R. Measurements

Deuterium - n.m.r. spectra were obtained in a Brüker WH-360 spectrometer operating at 55.28 MHz using the Aspect 2000 data system. The presence of 5 % deuterochloroform in the solvent provided an internal reference taken as δ = 7.25 p.p.m.. Spectra were obtained at 298 K and full operational details are given in reference 9. Digital resolution was 0.6 p.p.b. per point.

Since the small isotopic shifts observed were comparable with the widths of the resonance lines, it was generally difficult to determine resonance positions accurately from directly Fourier transformed spectra. Substantial improvement in resolution could be obtained by multiplying the free induction decay signal by a double exponential function of the form exp $(at - bt^2)$ where a and b are adjustable positive constants and t is time. Such function transforms the original Lorentzian form exp $(-t/T_2)$ into a Gaussian line shape exp $(-bt^2)$ which has much less extensive side wings. Careful selection of a and b was necessary in order to optimize resolution without the introduction of spurious maxima. Even with the application of this line-narrowing technique, it was not always possible to obtain complete resolution, particularly with some of the equilibrated samples. Both directly transformed and line-narrowed spectra are shown in the figures in the present chapter.

6.3 - RESULTS

6.3.1 - Mass Spectrometric Results

Product distributions derived from mass spectrometric measurements are shown in table 6.2 for the "kinetic" series of experiments, which also includes

TABLE 6.2

% COMPOSITION OF CYCLOPENTANES FROM KINETIC EXPERIMENTS DETERMINED BY MASS SPECTROMETRIC ANALYSIS

Expt.	K1[1]	K2	K3	K4[2]	K5	K6[3]
Catalyst	ZnO	Rh	Rh	Ir(I)	Pt	Ir (II)
d_o	-	94.2	87.4	91.7	93.0	70
d_1	2	2.3	4.3	5.2	2.3	9
d_2	42	1.9	3.7	1.9	1.2	7
d_3	38	0.6	1.8	0.5	0.6	4
d_4	18	0.3	1.2	0.3	0.6	3
d_5	-	0.3	0.8	0.2	1.7	3
d_6 to d_{10}	-	0.4	0.8	0.2	0.6	4
ρ[4]	-	97.0	93.4	95.7	96.4	83.2

(1) From reference 6

(2) Ir/Al_2O_3

(3) Ir/SiO_2

(4) % Contribution of primary reaction products.

results reported in reference 6 for the cyclopentane formed during simultaneous exchange and deuteration of cyclopentane on zinc oxide (experiment K1). The product distributions shown in table 6.2 correspond to the last mass spectrum obtained before sample expansion.

The objective of experiments K2 to K5 was to obtain deuterated products as representative as possible of the initial products of exchange, i.e., products corresponding to molecules which reacted only once at the catalyst surface. It may be easily shown that the fraction ρ of initial products of reaction in the product distribution may be estimated, for a given fractional conversion X from expression (6.1) below, assuming no dilution of the deuterium pool:

$$\rho = \frac{1 - x}{x} \ln \frac{1}{1 - x} \qquad (6.1)$$

Values of ρ are included in table 6.2 and were above 90% in all experiments except for K6 where as much as 16.8% secondary exchange products are expected.

The product distributions reported in table 6.2 display the characteristic features of cyclopentane exchange over Pt, Rh and Ir as described in chapter 5, i.e., a large d_2/d_3 ratio on Rh, a large contribution from stepwise exchange on Ir and a pronounced maximum at d_5 on Pt. This feature of the Pt distribution is of relevance to the assignment of deuterium - n.m.r. isotopic shifts since the d_5 maximum largely corresponds to a species with all hydrogen atoms from one side of the ring replaced by deuterium and should contribute with an intense resonance due to five identical nuclei to the deuterium - n.m.r spectrum of the sample from K5.

Table 6.3 shows mass-spectrometric results for the equilibrated series of experiments. With equilibrated samples, the deuterium number distribution (x_n vs. n distribution) should conform to the binomial

TABLE 6.3

% COMPOSITION OF CYCLOPENTANES FROM EQUILIBRATED SAMPLES

Expt.	E1	C1[1]	E2	E3	C3[1]	E4	C4[1]
d_0	68.6	69.2	-	0.3	-	11.4	11.4
d_1	27	23.4	-	0.6	0.2	27.9	27.6
d_2	4	4.4	-	1.5	1.3	30.1	30.2
d_3	0.4	0.4	-	4.7	4.8	19.2	19.5
d_4	-	-	0.3	11.4	12.1	8.2	8.3
d_5	-	-	0.3	20.1	20.9	2.5	2.4
d_6	-	-	0.4	24.6	25.0	0.6	0.5
d_7	-	-	0.4	20.7	20.6	0.1	0.07
d_8	-	-	2.8	11.5	11.1	0.02	0.01
d_9	-	-	22.7	3.8	3.5	-	-
d_{10}	-	-	73.0	0.7	0.5	-	-
ϕ[2]	0.36	0.36	9.60	5.9	5.9	1.95	1.95

(1) Calculated distribution using expression (4.17)

(2) Average deuterium content from expression (4.12)

distribution given by expression (4.17) in chapter 4. Applications of expression (4.17) are shown in colums C1, C3 and C4 of table 6.3 for experiments E1, E3 and E4, respectively. The excelent agreement between experimental and calculated distributions provides a good check both on the assumption of isotopic equilibration and on the accuracy of the mass-spectrometric measurements. Although experiment E1 was not taken to equilibrium it corresponds to a stepwise exchange process and sould conform to the binomial case.

It is worth noticing that although expression (4.17) correctly predicted isotopic concentrations for experiments E3 and E4 for the observed deuterium contents ϕ, the values of ϕ did not correspond to the equilibrium values expected on a purely statistical basis (5.0 and 1.67, respectively) for the D_2/cyclopentane ratios listed in table 6.1. This is due to the bias towards more deuterated species normally observed in equilibrated exchange experiments[13].

6.3.2 - Deuterium - n.m.r. Measurements

Figures 6.2 to 6.7 show deuterium n.m.r. spectra for the kinetic experiments both in direct and line-narrowed form. In all spectra there was an intense resonance at $\sigma = 1.501 \pm 0.007$ p.p.m., which was the resonance at highest frequency in all spectra. Since all product distributions presented a considerable amount of d_1 product, this resonance was assigned to cyclopentane - d_1 and was taken as an internal reference for the remaining resonances. The variations in absolute value for the reference line were expected on the basis of changes in "cyclopentane" concentration in the solvent from sample to sample.

The positions of the peak maxima relative to the reference line ($\Delta\sigma$ values) are shown at the top of

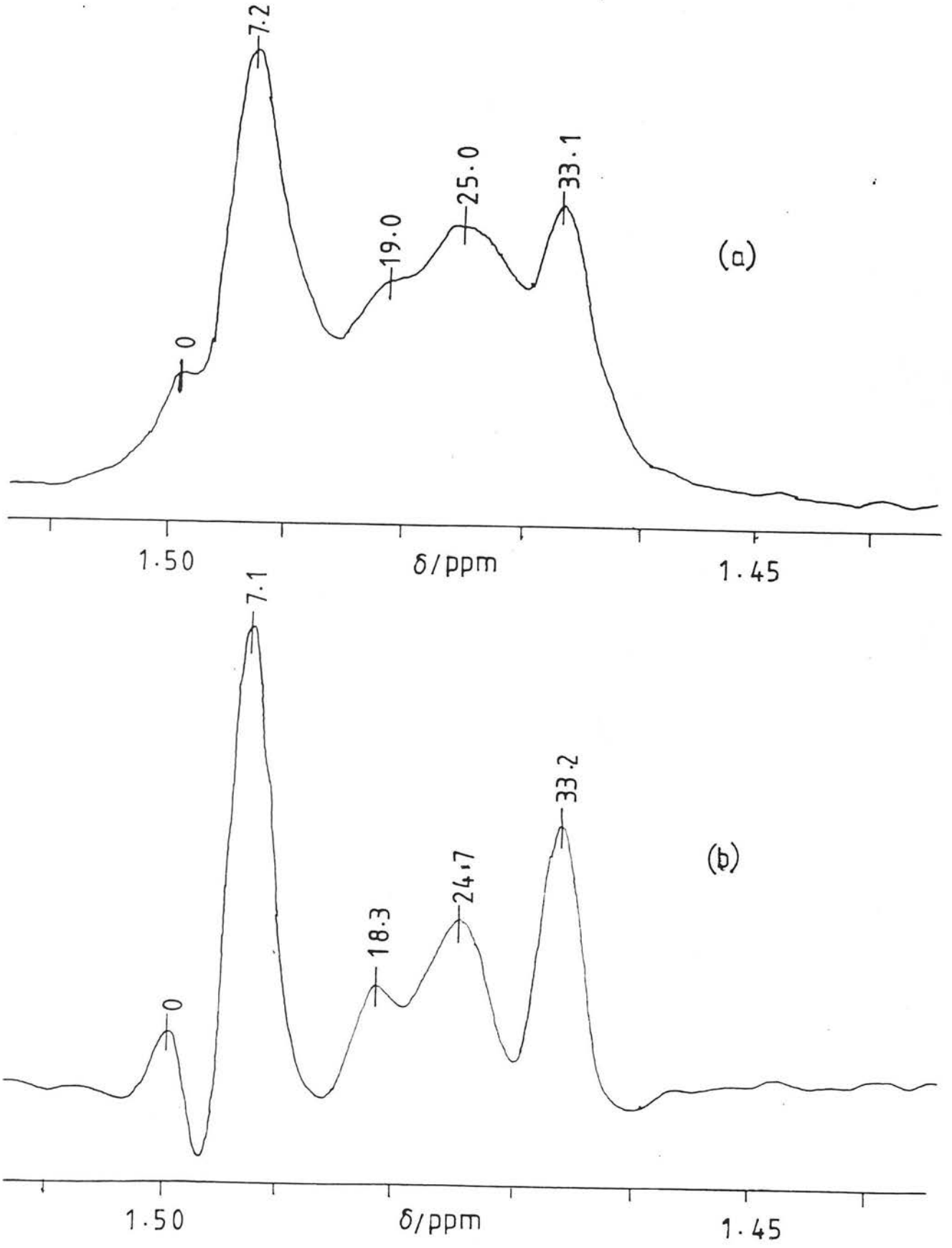

FIG. 6.2 - D-N:M.R. SPECTRUM FROM EXPERIMENT K1[6];
(a) WITHOUT LINE - NARROWING
(b) WITH LINE - NARROWING
$-\Delta\delta$ VALUES ABOVE PEAKS IN P.P.B UNITS

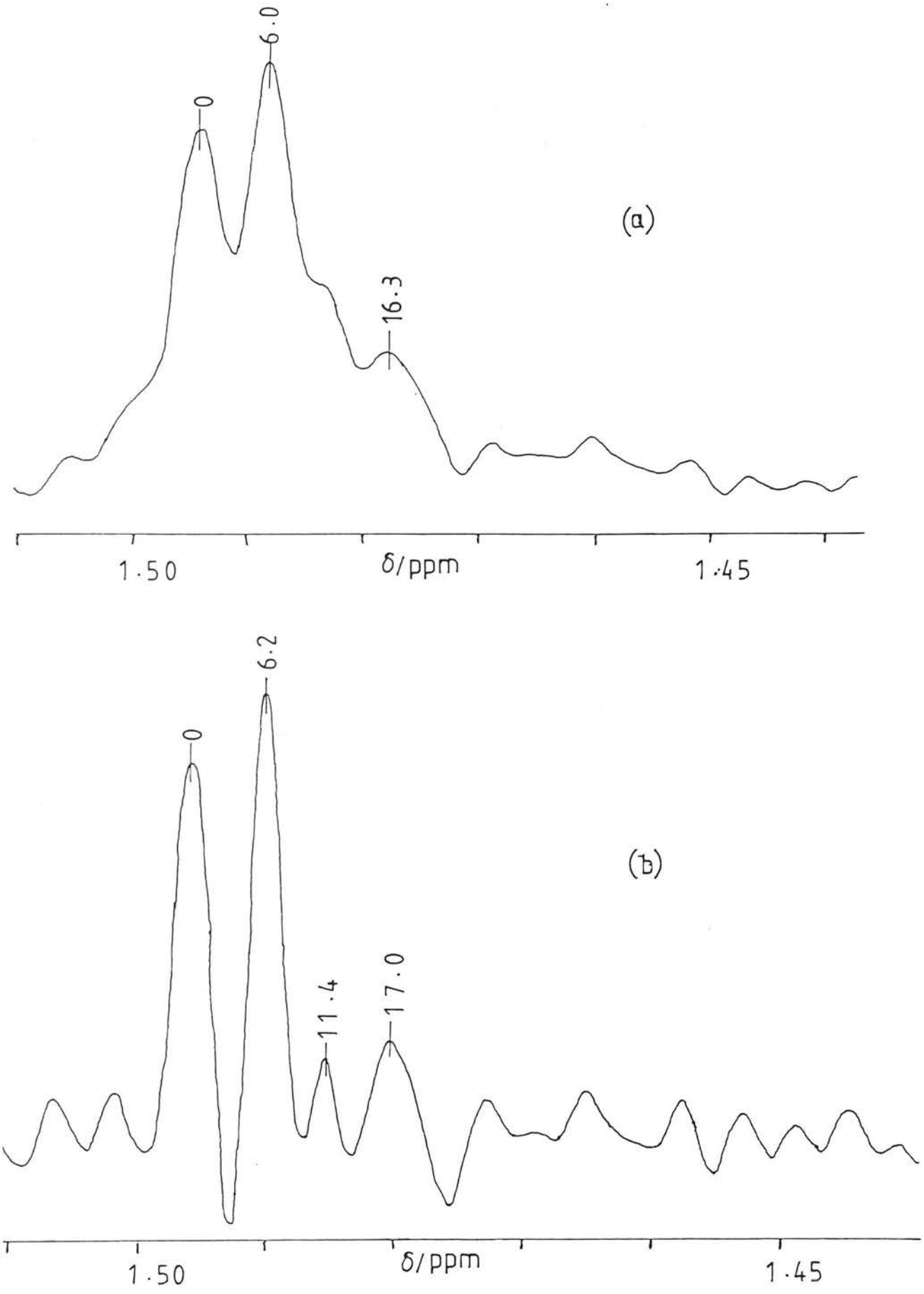

FIG.6.3 - D-N.M.R. SPECTRA FROM EXPERIMENT K2;
(a) WITHOUT LINE-NARROWING
(b) WITH LINE-NARROWING
-$\Delta\delta$ VALUES ABOVE PEAKS IN P.P.B. UNITS

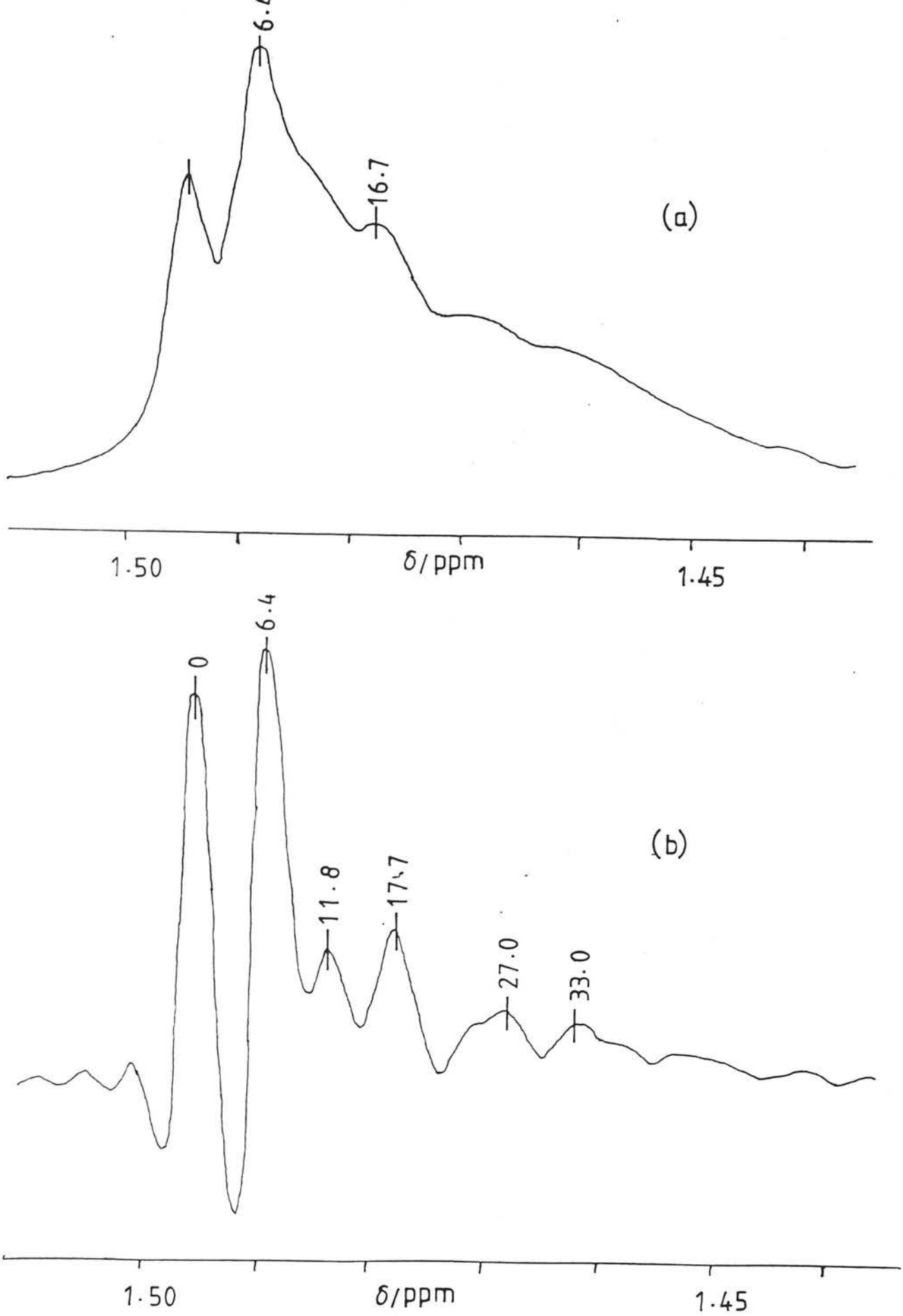

FIG. 6.4 - D-N.M.R. SPECTRA FROM EXPERIMENT K3;
(a) WITHOUT LINE-NARROWING
(b) WITH LINE - NARROWING
-$\Delta\delta$ VALUES ABOVE PEAKS IN P.P.B. UNITS

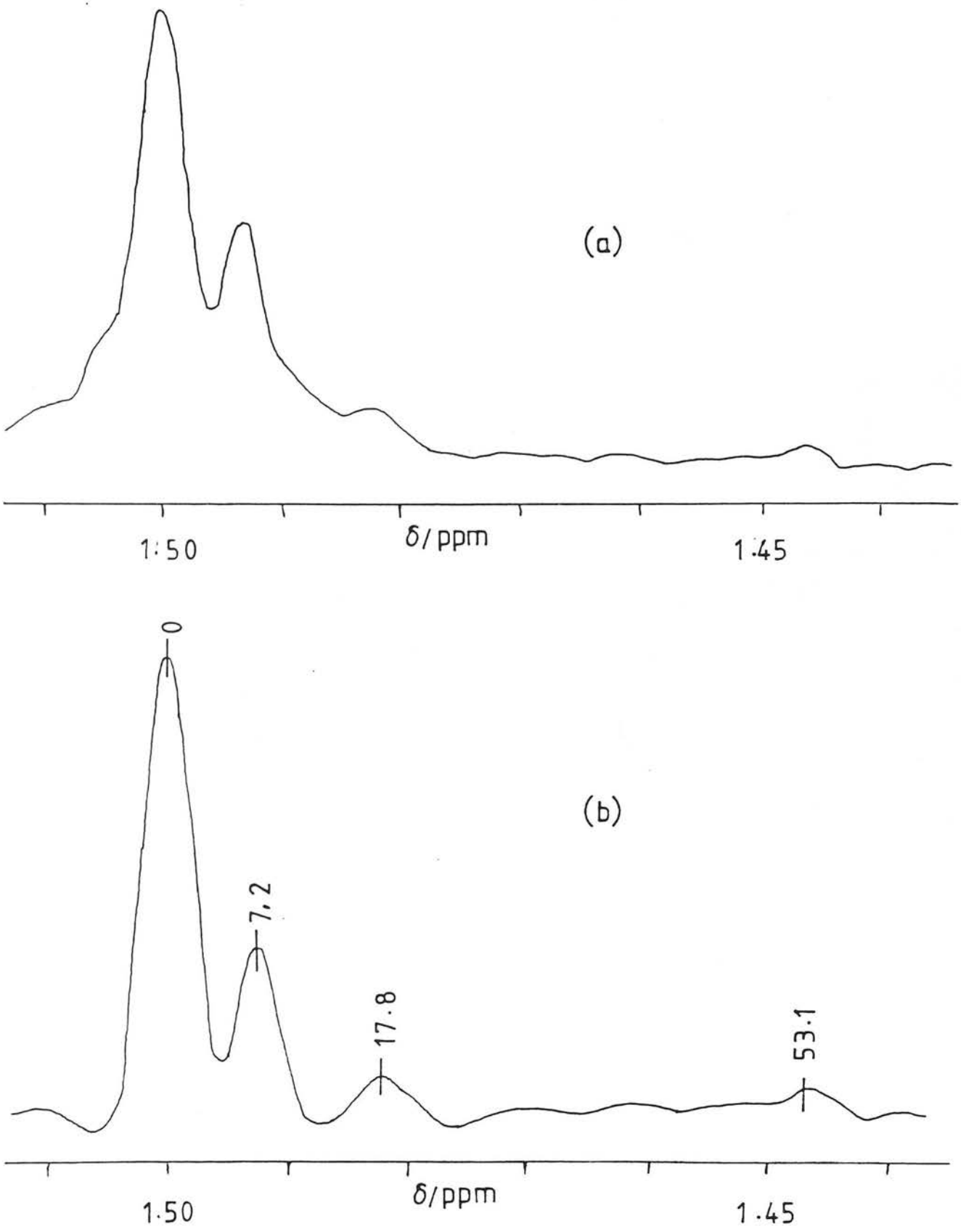

FIG. 6.5 - D-N.M.R. SPECTRA FROM EXPERIMENT K4;
(a) WITHOUT LINE-NARROWING
(b) WITH LINE - NARROWING
-$\Delta\delta$ VALUES ABOVE PEAKS IN P.P.B. UNITS

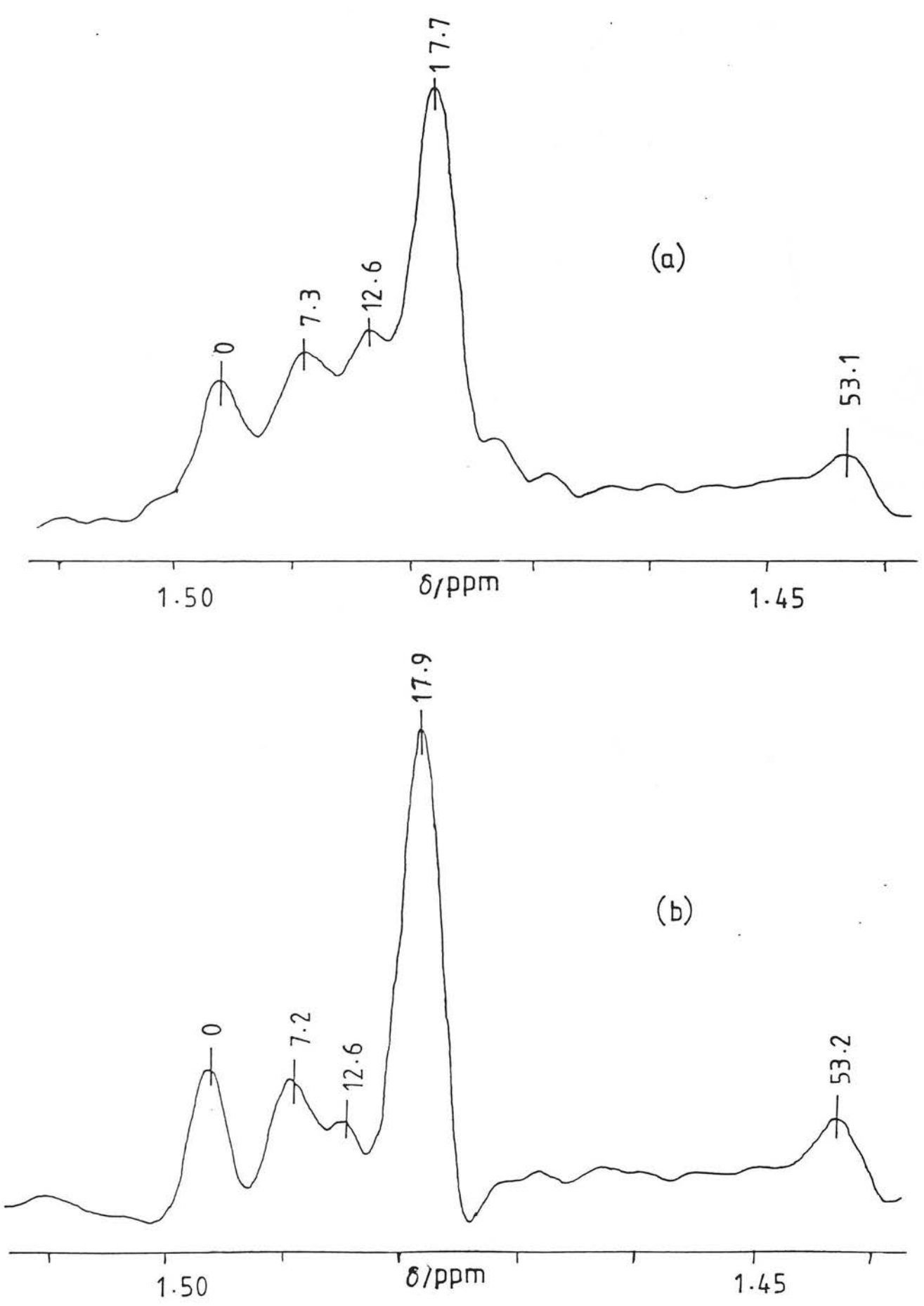

FIG. 6.6 - D-N.M.R. SPECTRA FROM EXPERIMENT K5;
(a) WITHOUT LINE - NARROWING
(b) WITH LINE - NARROWING
-$\Delta\delta$ VALUES ABOVE PEAKS IN P.P.B. UNITS

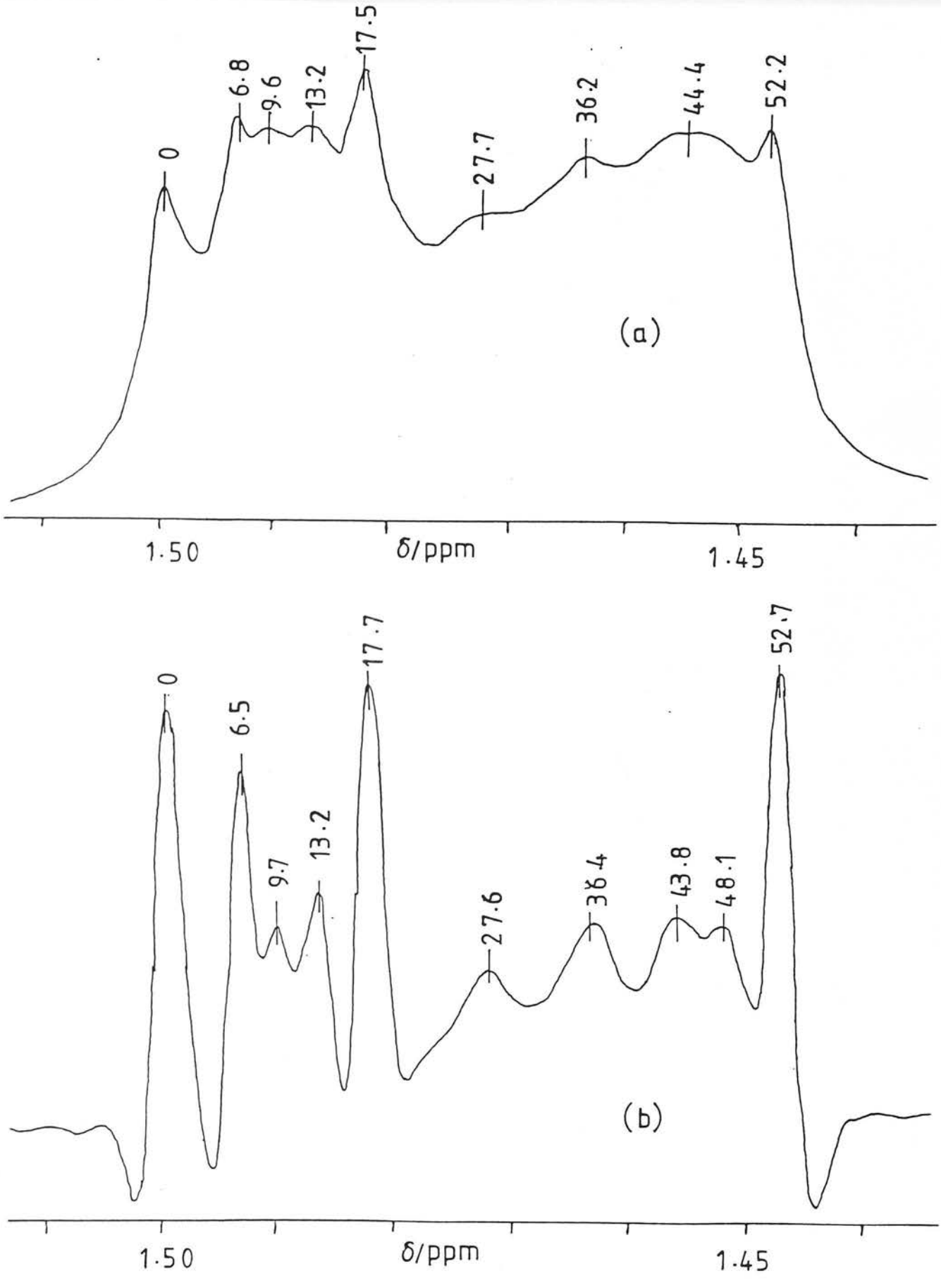

FIG. 6.7 - D- N.M.R. SPECTRA FROM EXPERIMENT K6;
(a) WITHOUT LINE - NARROWING
(b) WITH LINE - NARROWING
$\Delta\delta$ VALUES ABOVE PEAKS IN P.P.B. UNITS

each peak in the relevant figures. Substantial improvement in resolution was attained using the line - narrowing technique without causing significant displacement of the resonance lines, as the numbers in figures 6.2 to 6.7 indicate. Only for the $\Delta\sigma$ = 12.6 p.p.b. line in sample K5 and the $\Delta\sigma$ = 16.3 p.p.b. line in sample K2 could we observe displacements larger than 0.5 p.p.b.

N.m.r. spectra for the "equilibrated" series are shown in figures 6.8 to 6.11. Experiment E2 produced a single resonance at σ = 1.4425 p.p.m., corresponding to the ten equivalent deuterons in cyclopentane - d_{10}. By mixing E2 with samples from K4 and K5 it was established that the isotopic shift for this species relative to cyclopentane - d_1 was - 52.8 p.p.b. Resonances from experiments E3 and E4 were considerably broader than the ones from the kinetic series. This is due to the large number of isotopic configurations contributing to the spectra of equilibrated samples as compared to the much simpler mixtures expected for the kinetic series where products arising mostly from one-set α,β exchange processes (see chapter 5) are likely to occur.

6.4 - DISCUSSION

6.4.1 - Interpretation of Isotopic Shifts

In attempting to interpret our deuterium - n.m.r. results, two basic assumptions were made, which find support in earlier reports in the pertinent literature[14,15], namely:

1 - That the resonance frequency of a deuterium nucleus in "cyclopentane" may be influenced by other deuterium atoms located in any of the nine remaining positions in the molecule;

2 - That the effect of multiple deuterium substitution is additive, so that fixed isotopic shift contributions may be assigned to each position of substitution.

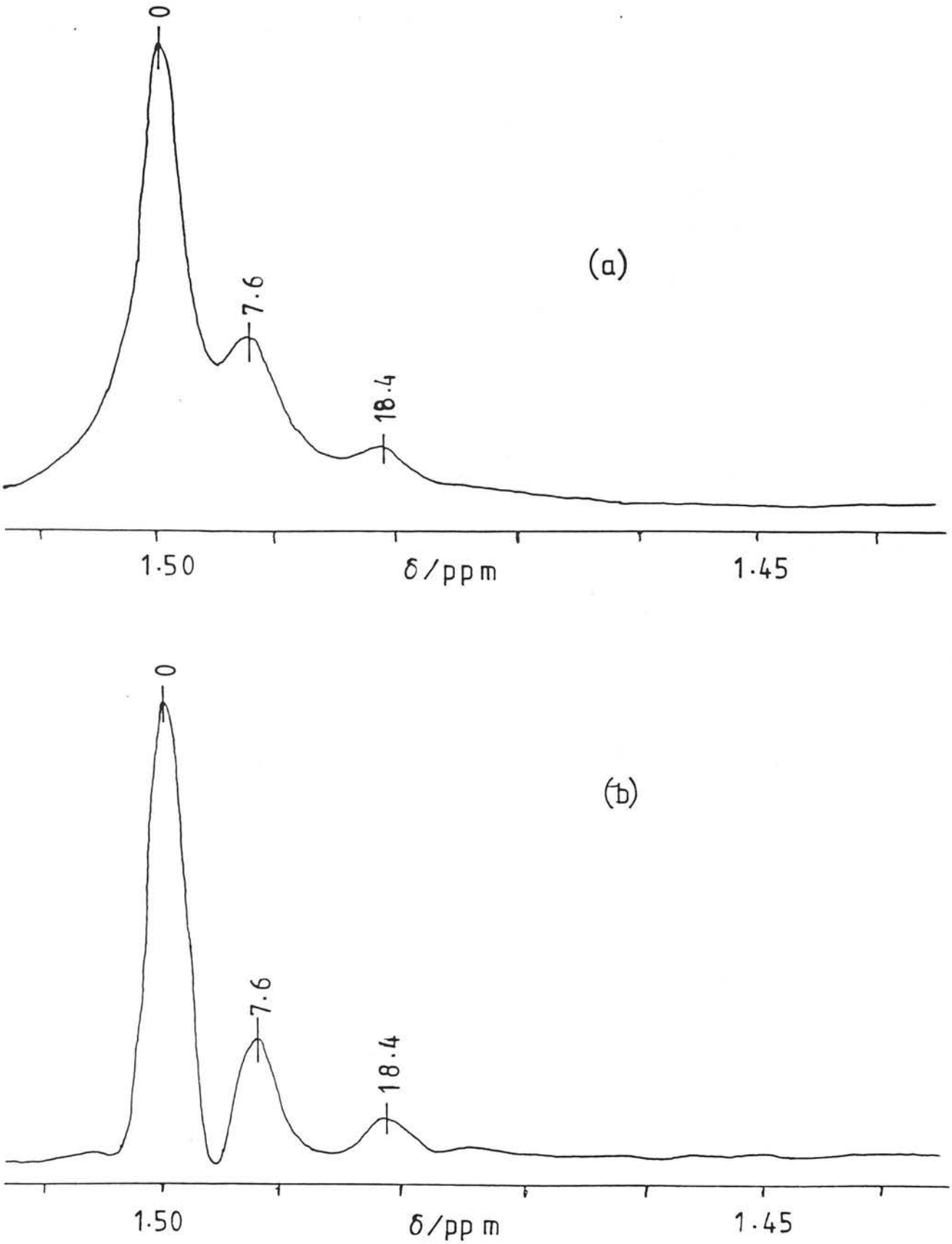

FIG. 6.8 - D - N.M.R. SPECTRA FROM EXPERIMENT E1
(a) WITHOUT LINE - NARROWING
(b) WITH LINE - NARROWING
-Δδ VALUES ABOVE PEAKS IN P.P.B. UNITS

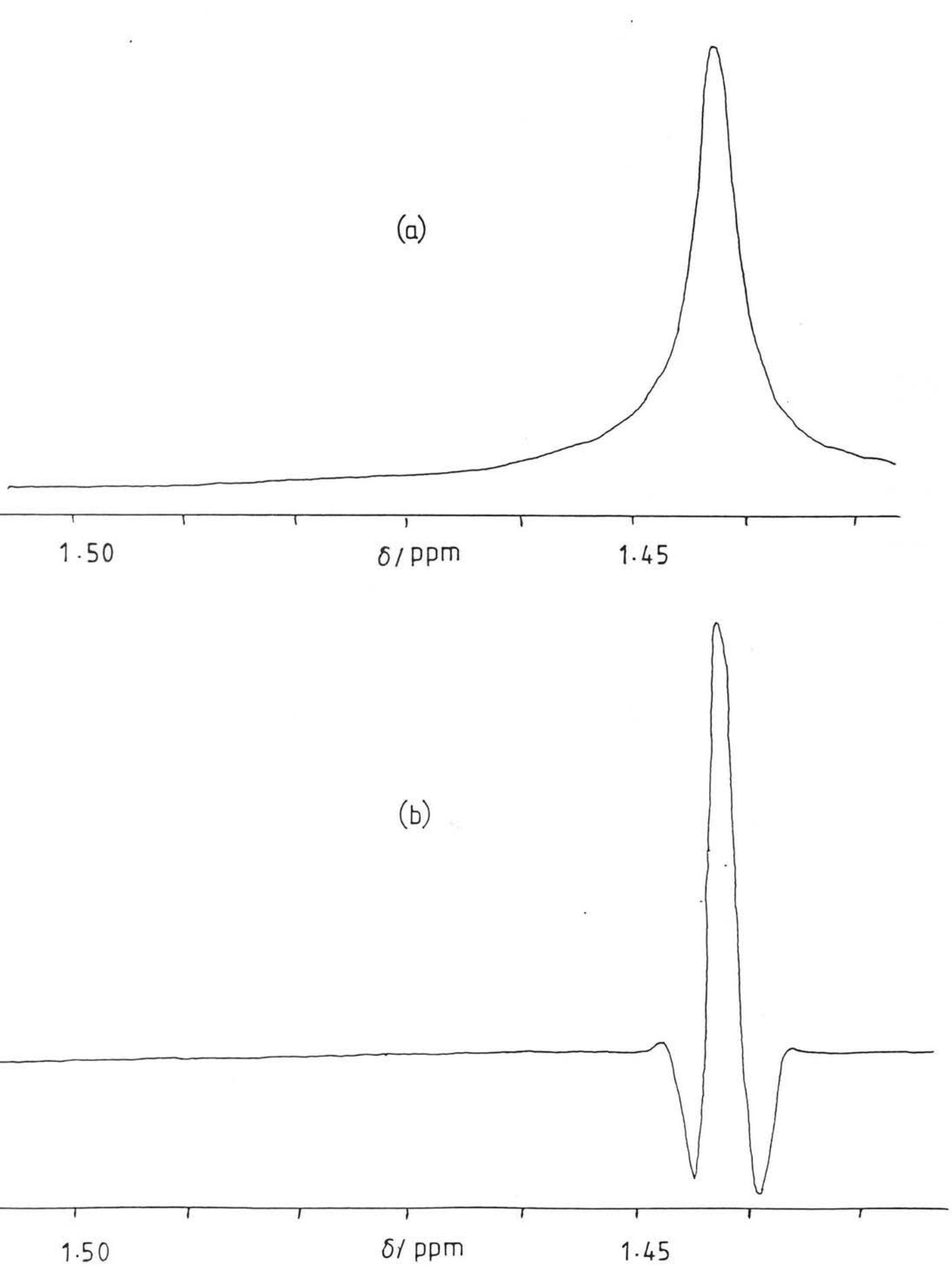

FIG. 6.9 - D- N.M.R SPECTRA FROM EXPERIMENT E2
(a) WITHOUT LINE - NARROWING
(b) WITH LINE - NARROWING
$-\Delta\delta$ VALUES ABOVE PEAKS IN P.P.B. UNITS

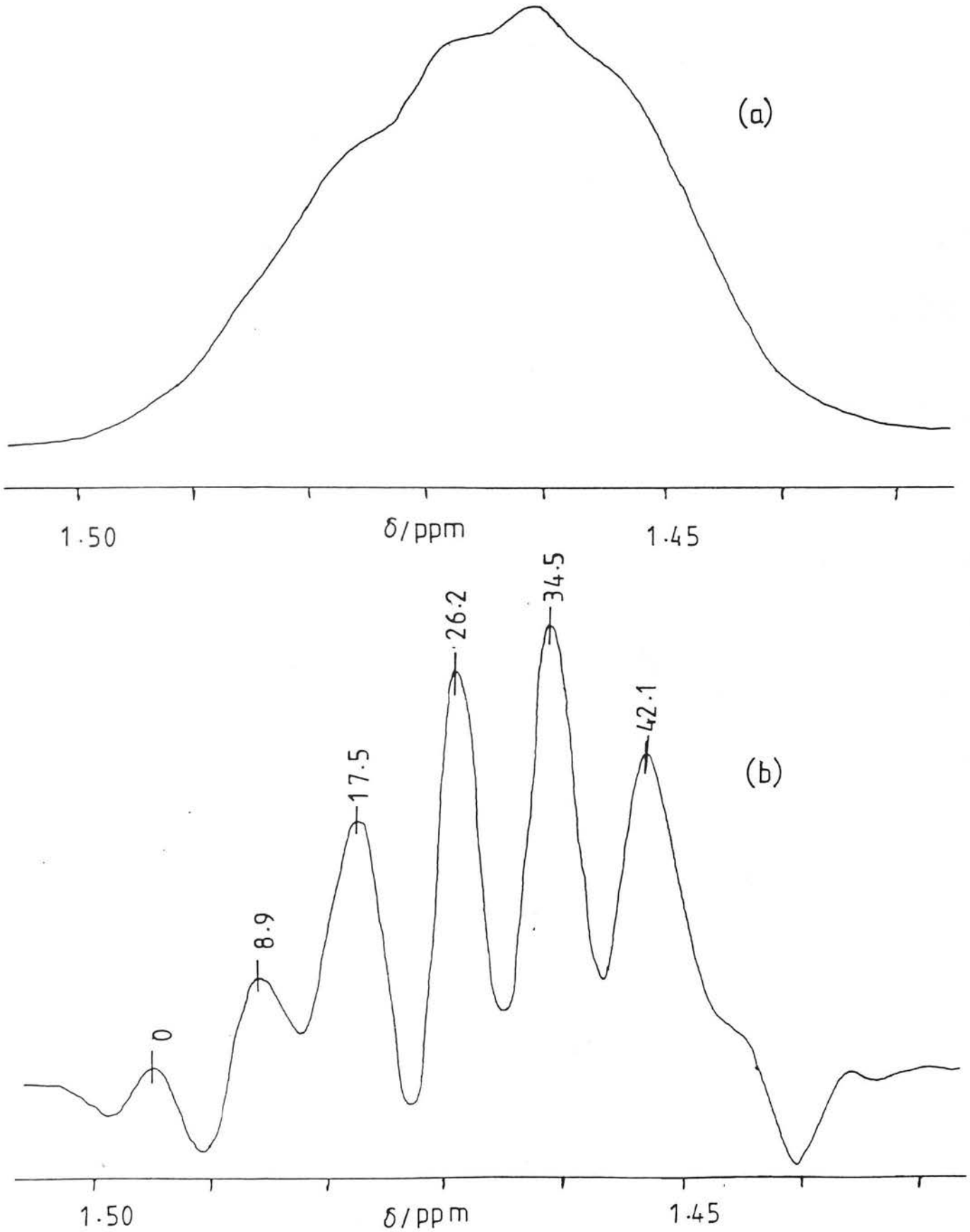

FIG. 6.10 - D - N.M.R. SPECTRA FROM EXPERIMENT E3;
(a) WITHOUT LINE-NARROWING
(b) WITH LINE - NARROWING
$-\Delta\delta$ VALUES ABOVE PEAKS IN P.P.B. UNITS

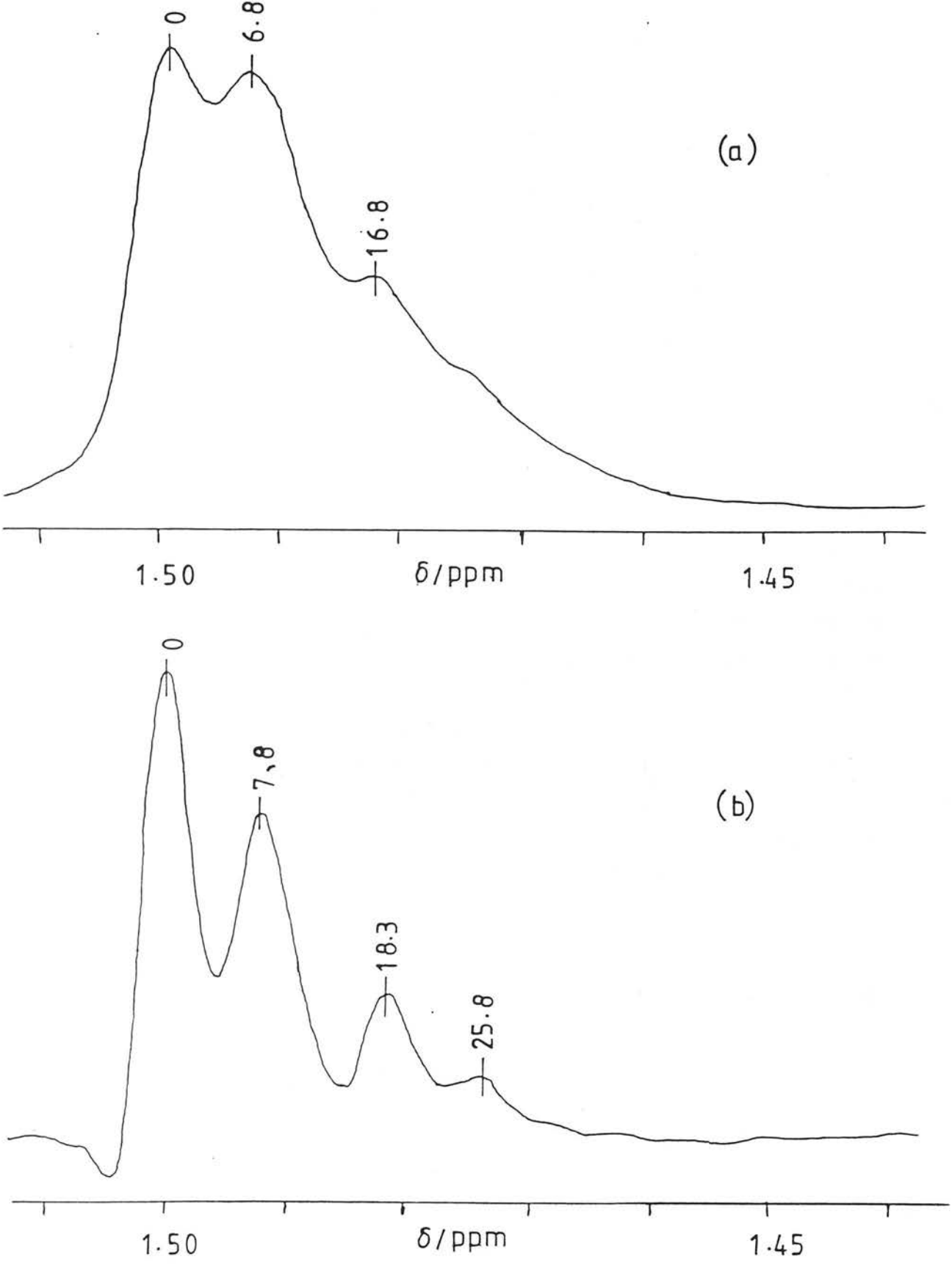

FIG. 6.11 - D- N.M.R. SPECTRA FROM EXPERIMENT E4

(a) WITH OUT LINE- NARROWING

(b) WITH LINE - NARROWING

-$\Delta\delta$ VALUES ABOVE PEAKS IN P.P.B. UNITS

In the discussion that follows, the symbols α, β_C, β_T, γ_C and γ_T refer to isotopic shift contributions for each position shown in scheme 6.2 below:

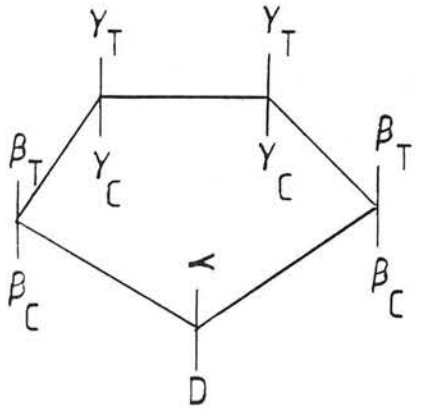

SCHEME 6.2

For maximum accuracy in the assignment of isotopic shift contributions, it is important to select as a basis - set intense, well - defined resonances not subject to ambiguous interpretations. In the present case, a basis - set of five resonances was chosen, named A to E, as shown in table 6.4. This table indicates, for each resonance, the sample on which it occurs most unambiguously (reference sample) and its probable occurrence in other samples. The corresponding isotopic shifts are given between brackets in p.p.b. units relative to the cyclopentane - d_1 resonance ($\Delta\ \sigma$ values).

TABLE 6.4

BASIS - SET FOR ASSIGNING ISOTOPIC - SHIFT CONTRIBUTIONS

RESONANCE	REFERENCE SAMPLE(1)	OCCURENCE IN OTHER SAMPLES(1)
A	S1(-17.9)	E1 (-18.4)
B	K1 (-7.2)	K3 (-6.0); K4 (-7.2); K5 (-7.3); K6 (-6.5).
C	K1(-33.2)	
D	K5(-17.8)	K3(-16.3); K6(-17.5)
E	E2(-52.9)	K5(-53.1); K6(-52.3)

(1) Shift values between brackets in p.p.b. relative to the cyclopentane - d_1 resonance.

The following comments apply to the resonances in table 6.4:

Resonance A - This was the most proeminent resonance in synthetic sample S1 and there can be little doubt that it corresponds to cyclopentane - 1,1 - d_2. Confirmation of this assignment was obtained from sample E1 (Al_2O_3 experiment), where a 1:4 cyclopentane - 1,1 - d_2 to cyclopentane - 1,2 - d_2 (cis + trans) ratio is expected on a statistical basis. This is approximately true for the ratio of areas for the peaks at - 18.4 and -7.6 p.p.b. in sample E1. An isotopic shift contribution of ca. - 18 p.p.b. may therefore be assigned to an α - substitution.

Resonance B - The arguments presented in reference 6 clearly demonstrate that this resonance arises from cyclopentane -cis-1,2-d_2 (β_C substitution). Resonances in similar positions occurred in all samples from the kinetic series, specially in the experiments with the Rh/TiO_2 catalyst (experiments K2 and K3)which also displayed a maximum at d_2 in the product distributions derived from mass-spectrometric measurements. Also in the equilibrated series, resonances occurred in this aproximate region, but consistently shifted to lower frequencies (-7.6 p.p.b. in sample E1, - 8.9 p.p.b. in sample E3 and - 7.8 p.p.b. in sample E4). This was caused by overlap with the β_T line, which is expected to occur at a slightly lower frequency and with the same intesity as the β_C line in the equilibrated series (see below).

Resonance C - Following the arguments presented in reference 6, this resonance was assigned to the four equivalent deuterons in cyclopentane - 1,1, 2,2 - d_4. According to the additivity assumption, the $\Delta\sigma$ value for resonance C equals $\alpha + \beta_C + \beta_T$ and using the value previously assigned to α and β_C a β_T value of ca.-8p.p.b. is derived.

Resonance D - This was the most proeminent resonance in the deuterium - n.m.r. spectrum from experiment K5 and this line may be safely assigned to a cyclopentane - d_5 species with all of the deuterium atoms on the same side of the ring. Thus, the value for this resonance is given by $2\beta_C + 2\gamma_C$ which allows a γ_C value of ca.-2p.p.b. to be derived. Resonance D also occurred less pronouncedly in samples K3 and K6, as might have been expected from the fact that a clear break between d_5 and d_6 was observed in the initial product distributions for these samples, indicating that the d_5 product was mostly provenient from one-set exchange.

Resonance E - This was the only resonance observed with sample E2 and must correspond to cyclopentane - d_{10}. Resonances in similar positions occurred in the spectra from samples K5 and K6 and were the lowest frequency resonances in these spectra. The expected shift for resonances E is given by $\alpha + 2\beta_C + 2\beta_T + 2\gamma_C + 2\gamma_T$, giving a γ_T value of ca. - 0.5 p.p.b..

6.4.2 - Computer Calculated Spectra

Validation of the additivity hypothesis and of the derived isotopic shift contributions should be obtained by comparing experimental n.m.r. spectra from samples whose isotopic composition is accurately known with spectra synthetized matematically from the known isotopic compositions, the assumed isotopic shift contributions and an appropriate line-shape function. Such comparison should involve only directly transformed spectra, since the line-narrowing procedure introduces distortions in the spectral line - shapes and only for directly transformed spectra does the Lorentzian line-shape apply. Spectra from the equilibrated series satisfy the criterion of known isotopic composition, but their usefulness is impaired by the large number of contributing species and consequent extensive band overlap. However, some degree

of comparison is possible from kinetic experiments, if this comparison is limited to the 0 to - 18 p.p.b. range of $\Delta\delta$ values and the simplifying assumption is made that only products arising from one-set exchange contribute to this region. This simplification is justified with basis on the pronounced maxima or breaks at d_5 in the relevant product distributions and the generally small amount of products containing more than five deuterium atoms observed in the kinetic experiments.

Figures 6.12 to 6.15 show computer calculated spectra for samples K2, K4, K5 and K6. Signal intensities $H(\nu)$ at each frequency ν were calculated assuming a Lorentzian line - shape for each espectra line using expression (6.2) below:

$$H(\nu) = \Sigma \frac{Bi}{1 + A\,(\nu - \delta_i)^2} \qquad (6.2)$$

where:
Bi is the concentration (or any number proportional to concentration) of D nuclei of type i in the isotopic mixture;

A is an adjustable linewidth parameter;

δ_i is the chemical shift (position of the peak maximum) for D nuclei of type i.

Within the assumption of α, β - exchange only, seven distinct types of deuterium nuclei contribute to the high frequency region ($\Delta\delta$ = 0 to - 18 p.p.b.) of the spectra as shown in scheme 6.3:

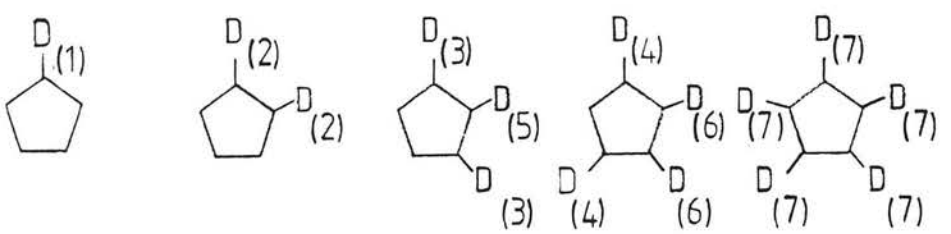

SCHEME 6.3

Bi concentrations for use in expression (6.2), where subscript i refers to the number in brackets in scheme 6.3 were estimated from mass spectral product distributions using expressions (6.3) below:

$$B_1 = x_1; \quad B_2 = 2x_2; \quad B_3 = 2x_3$$

$$B_4 = 2x_4; \quad B_5 = 2x_3; \quad B_6 = 2x_4 \qquad (6.3)$$

$$B_7 = 5x_5$$

Where x_i is the fractional contribution of products containing i deuterium atoms to the product distribution.

Curves labelled A in figures 6.12 to 6.15 correspond to spectra calculated using isotopic shift contributions directly derived from the set of reference lines (β_c = -7 p.p.b.; γ_c = - 2 p.p.b.). Comparison with the corresponding directly transformed spectra reveals some general resemblance but considerable difference in detail, particularly the lack of a clear maximum between resonances B and C in the calculated spectrum for the Pt/Al_2O_3 experiment (figure 6.12) and of the two maxima between the same resonances in the calculated spectrum for Ir/SiO_2 (figure 6.13). Although it may be argued that some discrepancy is expected due to the assumption of α, β - exchange only and the neglect of species which reacted more than once on the catalyst surface, it is relevant that all of the salient features of the experimental spectra were reproduced in the calculated spectra when a slightly modified set of isotopic shift contributions was used (β_c = - 6 p.p.b.; γ_c = - 3p.p.b.). This is clear from the curves labelled B in figures 6.12 to 6.15 which were built using the modified set of contributions and which reproduce all maxima in the $\Delta\delta$= 0 to - 18 p.p.b. region of the experimental spectra within $\pm$ 1 p.p.b.. This modified set of contributions implies a rather low $\Delta\delta$ value for the deuterons in cyclopentane - cis - 1,2 - d_2 as compared to the experimental values. We

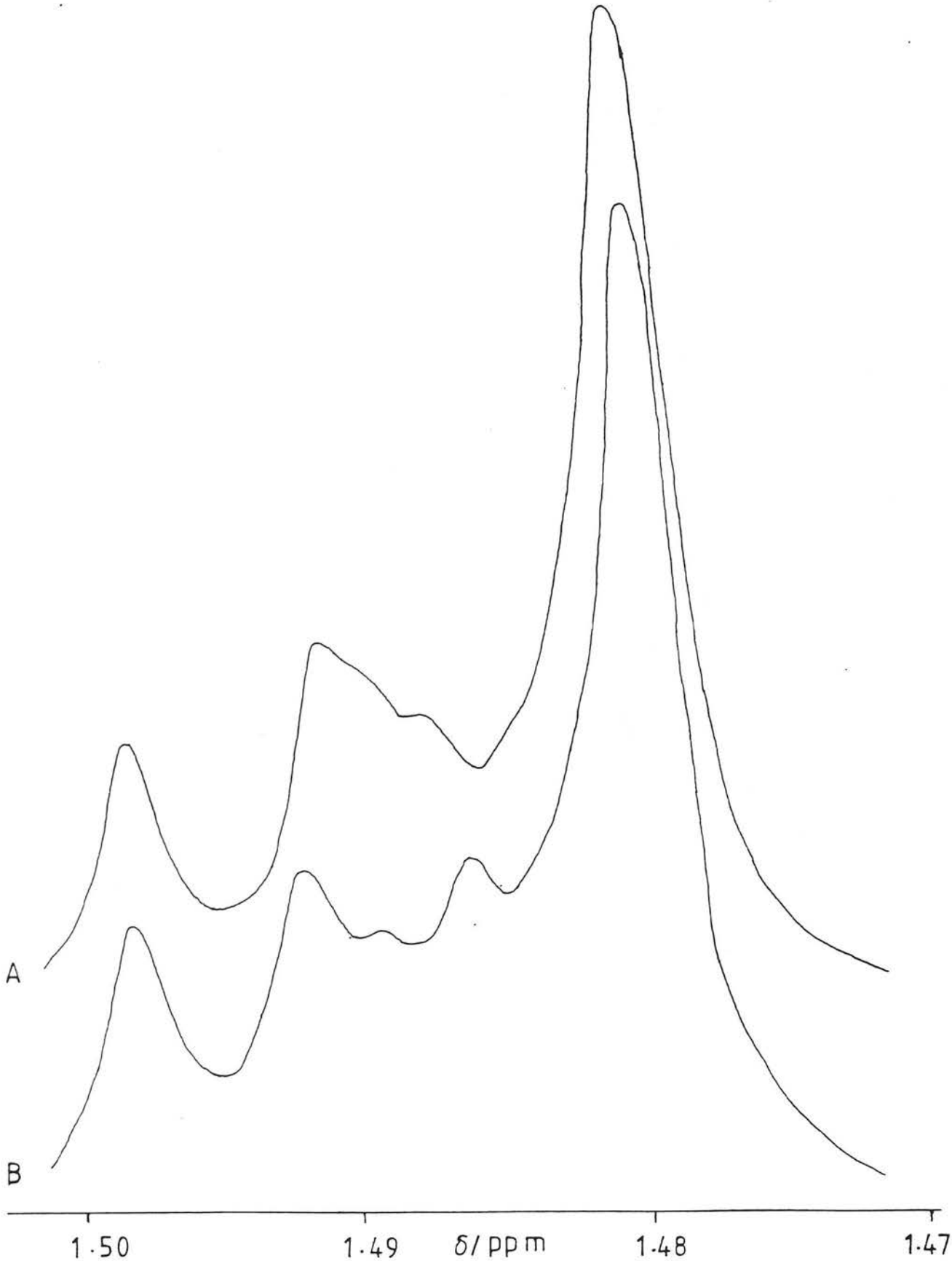

FIG. 6.12 - CALCULATED D- N.M.R. SPECTRA FOR EXPERIMENT K5;

A- β_c = -7 P.P:B.; γ_c = -2 P.P.B.; A = 4 x 10^5

B- β_c = -6 P.P.B.; γ_c = -3 P.P.B.; A = 4 x 10^5

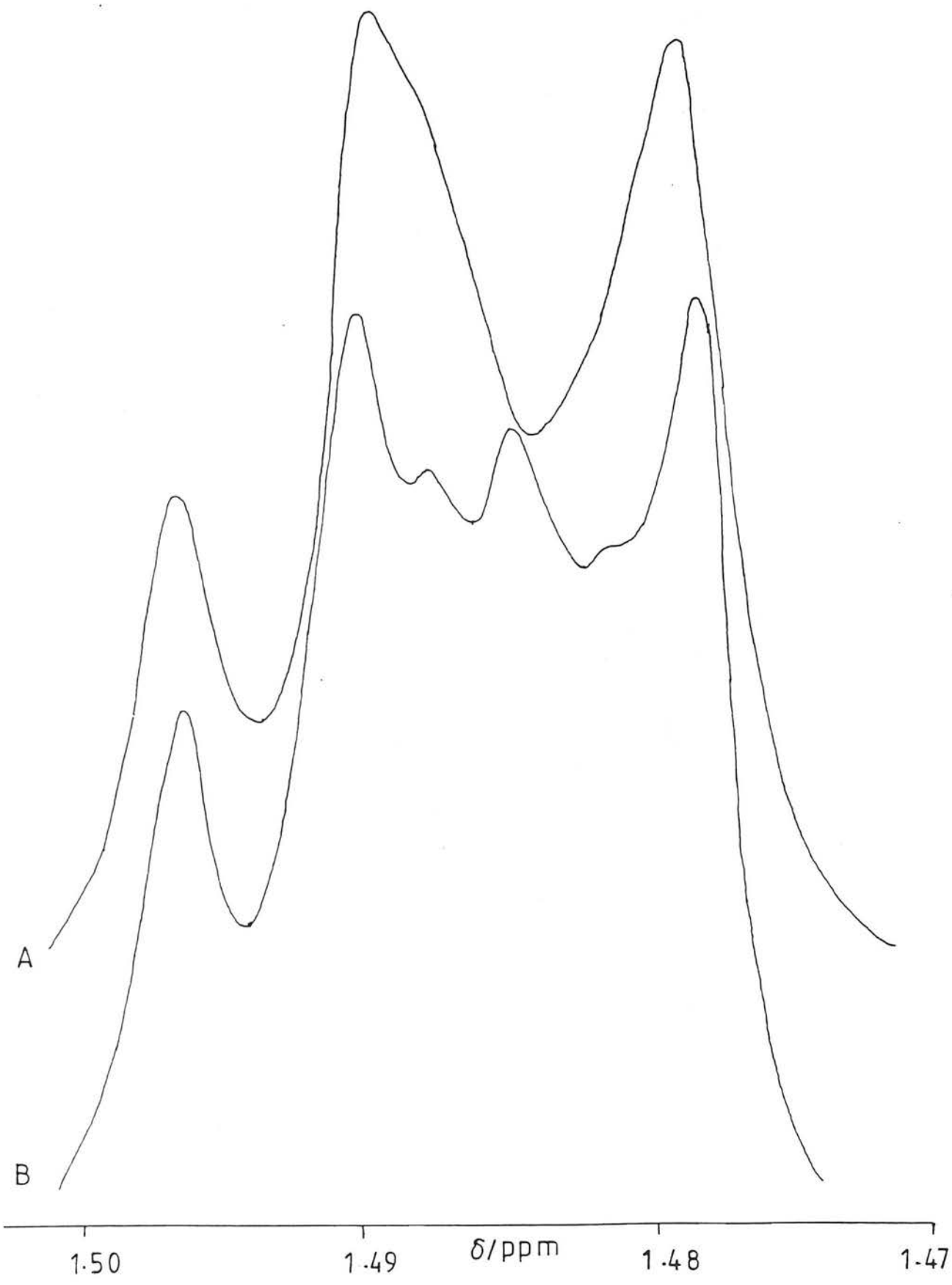

FIG. 6.13 - CALCULATED D- N.M.R. SPECTRA FOR EXPERIMENT K6;
A- β_c = -7 P.P.B.; γ_c = -2 P.P.B.; A = 3 x 10^5
B- β_c = -6 P.P.B.; γ_c = -3 P.P.B.; A = 3 x 10^5

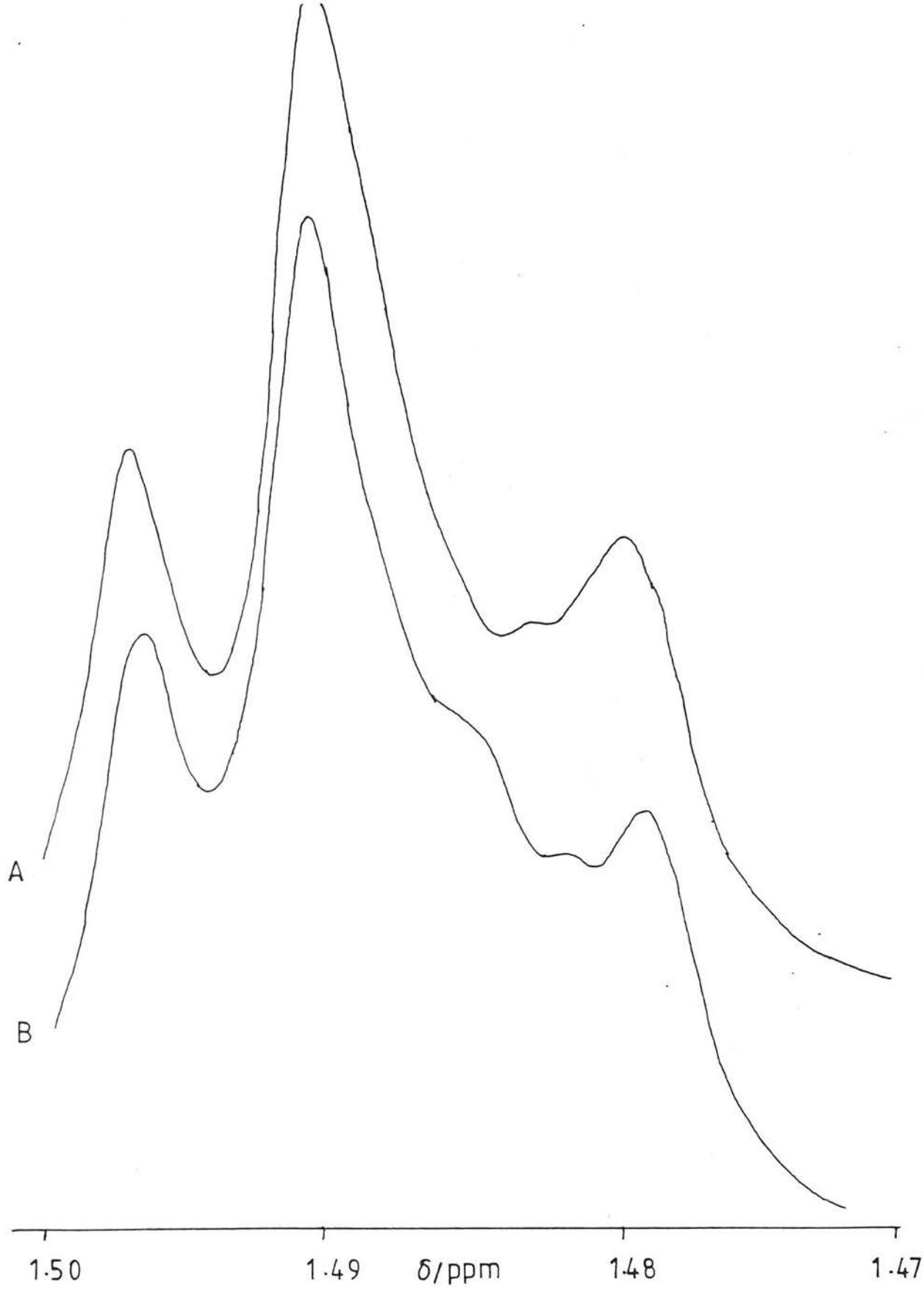

FIG. 6.14 - CALCULATED D-N.M.R. SPECTRA FOR EXPERIMENT K2;
A-β_c = -7 P.P.B.; γ_c = -2 P.P.B.; A = 2.5 x 10^5
B-β_c = -6 P.P.B.; γ_c = -3 P.P.B.; A = 2.5 x 10^5

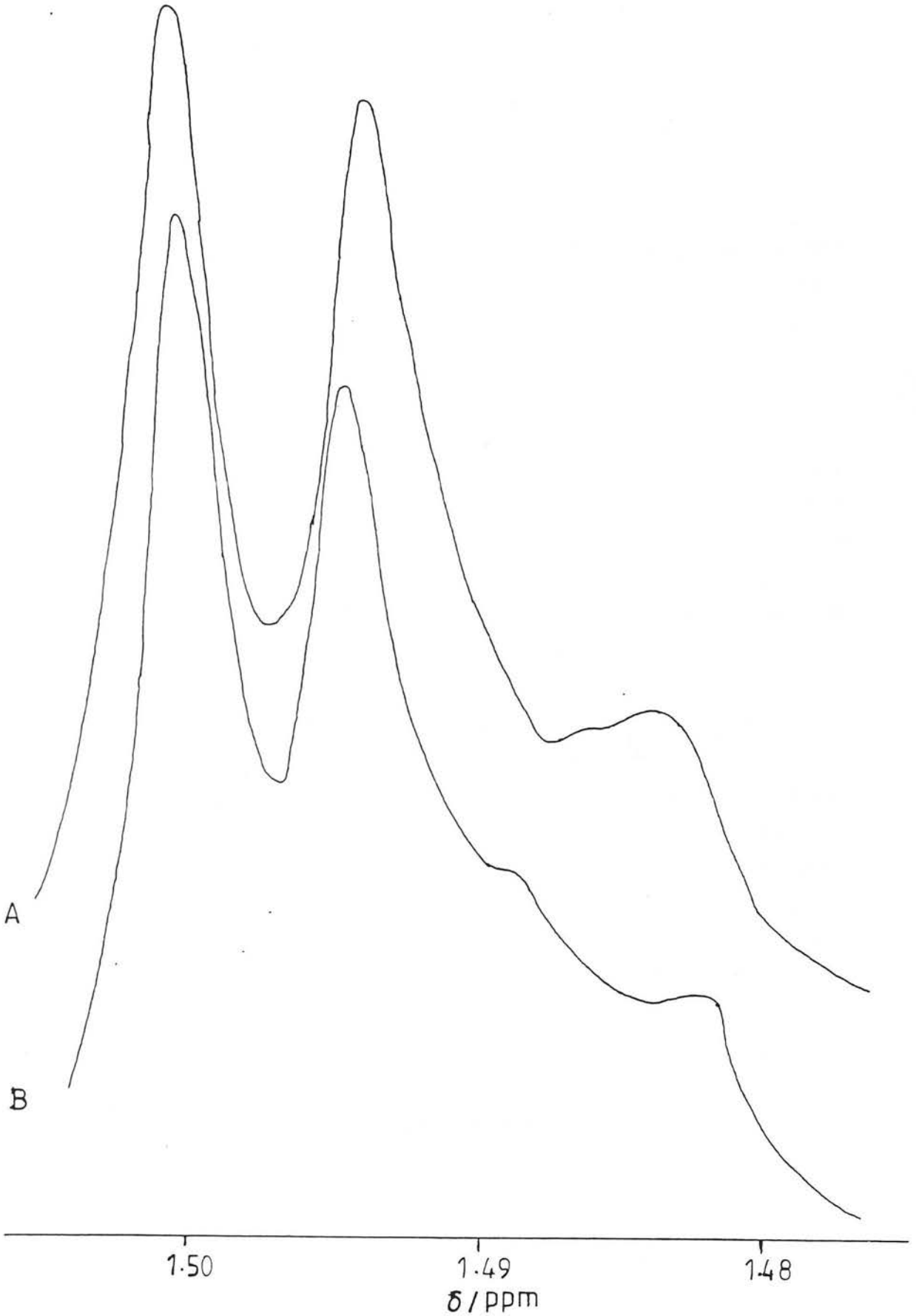

FIG. 6.15 - CALCULATED D- N.M.R. SPECTRA FOR EXPERIMENT K4;

A- β_c = -7 P.P.B; γ_c = -2 P.P.B.; A = 3 x 10^5

B- β_c = -6 P.P.B.; γ_c = -3 P.P.B.; A = 3 x 10^5

believe this reveals a lack of strict applicability of the hypothesis of additivity of isotopic shift contributions.

6.4.3 - Equilibrated Series

The difficulty in extracting detailed information from experiments E3 and E4 has been already commented. It is interesting however that the line - narrowed spectra for these samples displayed a set of well defined peaks whose positions could be reproduced assuming a simplified set of isotopic shift contributions that takes into a account only α and β substitution (ignoring differences between cis - and trans - substitution) and neglects any γ - shifts. Tables 6.5 and 6.6 show the good agreement between calculated and experimental isotopic shifts for experiments E3 and E4, respectively, using α = - 17.6 p.p.b. and β = - 8.8 p.p.b..

The chosen value for α is very near to the - 18 p.p.b. reported in section 6.4.1 and was taken as - 17.6 p.p.b. ($\alpha = 2\beta$) as a matter of convenience since lines separated by 0.4 p.p.b. only would not be resolved under the present conditions. With this simplification, ten types of deuterium nuclei may be defined according to the number of deuterium substituents in positions α and β, giving rise to seven separate lines, as shown in table 6.5. The percentage concentration, $Q_{A,B}$, of each type of deuterium in the isotopic mixtures (directly proportional to n.m.r. peak area) may be calculated for a "cyclopentane" sample with average deuterium content ϕ from expression (6.4) below:

$$Q_{A,B} = 100 \cdot \frac{4!}{B!(4-B)!} \cdot \left(\frac{\phi}{10}\right)^{A+B} \cdot \left(1 - \frac{\phi}{10}\right)^{5-A-B} \qquad (6.4)$$

TABLE 6.5

CALCULATED AND OBSERVED RESONANCES FOR SAMPLE E3

Nbr. of D atoms[1]		$-\Delta\delta$/p.p.b[2] (calc.)	$-\Delta\delta$/p.p.b (obs.)	Peak areas (calc.)[3]	Peak areas (obs.)[4]
α	β				
0	0	0	0	1.1	0.2
0	1	8.8	8.9	6.7	4.8
1	0)	17.6	17.5	16.1	15.9
0	2)				
1	1)	26.4	26.2	23.4	20.5
0	3)				
1	2)	35.2	34.1	25.7	25.7
0	4)				
1	3	44.0	42.1	19.9	23.6
1	4	52.8	(5)	7.1	(5)

(1) A - nbr. of α substituentes; B - nbr. of β substituents.

(2) α = 17.6 p.p.b.; β = -8.8 p.p.b.

(3) Calculated from expression (6.4) for Φ = 5.9

(4) Scaled to match $\Delta\delta$ = - 35.2 p.p.b. (calc.) resonance.

(5) Not sufficiently resolved from $\Delta\delta$ = 42.1 p.p.m. line.

TABLE 6.6

CALCULATED AND OBSERVED RESONANCES FOR SAMPLE E4

Nbr. of D atoms[1]		$-\Delta\delta$/p.p.b[1] (calc.)	$-\Delta\delta$/p.p.b[1] (obs.)	Peak areas[1] (calc.)	Peak areas[1] (obs)
α	β				
0	0	0	0	33.8	33.8
0	0	8.8	7.8	32.8	34.6
1	0)	17.6	18.3	20.1	
0	2)				21.6[2]
1	1)	26.4	25.8	9.8	
0	3)				

(1) See footnotes in table 6.5

(2) Resonances not sufficiently resolved to obtain individual intensities

where A and B represent, respectively, the number of α and β deuterium substituents around the type of nucleus considered. Values of $Q_{A,B}$ calculated from expression (4.5) are presented in tables 6.5 and 6.6, together with integrated n.m.r. peak areas from line-narrowed spectra, scaled to match the largest $Q_{A,B}$ in the respective samples. The agreement between calculated and observed peak areas is satisfactory, bearing in mind the uncertainties introduced by the line-narrowing procedure.

Most of the maxima in the $\Delta\delta$ = - 18 to - 53 p.p.b. region of the line-narrowed spectrum from experiment K6 (see figure 6.7) could also be reproduced reasonably accurately using the simplified treatment as shown in table 6.7.

TABLE 6.7

PEAK MAXIMA IN THE LINE-NARROWED SPECTRUM FOR SAMPLE K6 (-18 TO -53 p.p.b. REGION)

Nbr. of D atoms(1)		-Δδ/p.p.b.(1) (calc.)	-Δδ/p.p.b.(1) (obs.)
α	β		
1	1	26.4	27.6
0	3		
1	2	35.2	36.4
0	4		
1	3	44.0	43.8
			(48.1)(2)
1	4	52.8	52.7

(1) See footnotes (1) to (3) in table 6.5
(2) Not accounted for by simplified treatment

6.4.4 - Comparison With Literature Data

There have been relatively few reports in the literature on deuterium isotope effects on the resonance frequencies of other deuterium nuclei. Diehl and Leipert[17] reported isotopic shifts for geminal substitution ranging from -12 to -29 p.p.b. depending on the particular compound studied. The same authors observed that isotopic shifts are of the same order for both proton and deuteron resonances. From work by Halliday and Bindner[18] it is possible to derive and isotopic shift of ca. -18 p.p.b. for geminal substitution in deuterated methylamines (cf. figure 1 in reference 18). Haddon and Jackman[14] reported a -19 p.p.b. geminal isotopic shift for proton resonances in cyclohexane derivatives and Allred and Wilk[19] reported a -19 p.p.b. shift for the proton resonance in methane-d_1. All reported values are thus in agreement with the α - shift found in the present work and the similarity of isotopic effects on proton and deuteron resonances is substantiated.

Vicinal deuterium isotope effects on proton resonances in cyclohexane derivates are β_{ea} = -7 p.p.b., β_{ee} = -7 p.p.b. and β_{aa} = -14 p.p.b. (e = equatorial, a = axial) according to Haddon and Jackman[14]. Allred and Wilk[19] reported β isotope effects on proton resonances ranging from -1 to -9 p.p.b. per vicinal deuterium atom in simple deuterated alkanes (ethane, i - butane, neopentane).

The fact that we found $\beta_T > \beta_C$ is in line with expectations since vicinal deuterium shifts have been found to be dependent on the X - C - C - D dihedral angle (X = resonating nucleus) in a given ethane - like fragment, being largest for the larger dihedral angles[15].

Allred and Wilks[19] reported a γ - shift of -1 p.p.b. per deuterium atom for the proton resonance in neopentane - 1,1,1 - d_3, while Haddon and Jackman[14] reported γ = - 3.5 p.p.b. for proton resonances in cyclohexane

derivatives. Haddon and Jackman[14] observed a parallelism between deuterium isotope effects and coupling constants for analogously oriented protons, substantiated by earlier findings in the literature[20]. Since couplings occurring over four bonds have been found to be a maximum for a planar W path arrangement[21] such as that prevalent for cis - 1,3 - substituents in cyclopentane, a larger γ_C value is expected in comparison with γ_T, as found in the present work.

The hypothesis of additivity of isotopic shift contributions is generally found to apply at least to an approximate degree[14,15].

6.4.5 - Mechanistic Significance of the Results

In chapter 5 literature data on the exchange reactions of cyclopentane were presented and the fact was highlighted that some metals (Rh, Ni and Pd under some conditions) tend to promote the formation of large amounts of d_2 among the initial products of exchange that cannot be explained by a mechanism involving solely interconversion between monoadsorbed and α,β - diadsorbed species. A possible explanation was the existence of a region on the catalyst surface where the exchange is limited essentially to monoadsorbed - α,α - diadsorbed alkane interconversion. If this hypothesis is correct cyclopentane - 1,1 - d_2 should be outstanding among the initial products of exchange, specially on Rh which shows little tendency to promote exchange beyond d_2. An attempt to observe such species using deuterium n.m.r. spectroscopy was one of the main aims of the present work.

It is unfortunate that the value of α = -18 p.p.b. coincides with the isotopic shift for the "all-cis" cyclopentane - d_5 resonance and it is thus not possible to assess quantitatively the contribution of cyclopentane-1,1 - d_2 in the presence of the d_5 compound. Qualitatively,

however, comparison of the spectra from experiments K3, K4 and K5 with the corresponding calculated spectra (figure 6.12 to 6.15) shows that the experimental results broadly conform to an α,β - exchange model and in no case was the resonance at $\Delta\delta \sim -18$ p.p.b. larger than expected for the amount of cyclopentane - d_5 present in the mixtures. It is specially significant that the resonance for cyclopentane - d_5 predominated with the sample from the Pt/Al_2O_3 experiment, the resonance from cyclopentane-d_1 was proeminent with the sample from the Ir/Al_2O_3 experiment and the resonance corresponding to cyclopentane-cis - 1,2 - d_2 was the most important in the samples from the Rh/TiO_2 experiments. This indicates that the large amount of d_2 product formed on Rh is not due to an important α,α - diadsorption process, as might have been expected from the fact that a pronounced d_2 maximum is found under some conditions even on Pd which is a metal that shows little tendency to promote α,α - diadsorption. Also temperature dependence studies with Ni[22] and Pd[23] catalysts show that the d_2 maximum is favoured at low temperatures, whereas the contribution of α,α - diadsorbed species is expected to increase with increasing reaction temperature[24].

Quinn and coworkers[8] suggested that the Pd d_2 maximum arises from migration of olefinic species formed on the metal surface to sites which can only add two deuterium atoms but are unable to propagate the exchange. This mechanism is, however, difficult to conceive at the light of the principle of microscopic reversiblity. For a sizeable maximum at d_2 to occur it would be necessary that a substantial portion of the adsorbed olefin initially formed on the exchange propagating sites (sites A) migrates to the deuterium adding sites (sites B) before reverting to a mono-adsorbed state (adsorbed alkyl). Deuterium would then have to be rapidly added before the olefinic species migrates back to sites A. If A to B migration is fast as compared to olefin deuteration in

sites A, it is difficult to understand how olefin deuteration in sites B could be fast as compared to back-migration to sites A, since exchanged cyclopentane is the end product from the processes occurring on both types of site.

A more acceptable alternative involves the contribution of a process whereby addition and abstraction of two "hydrogen" atoms occurs in one step, i.e., without the intermediacy of monoadsorbed alkane. Some early mechanisms of olefin hydrogenation proposed in the literature involve steps of this type, such as the mechanism of Farkas and Farkas[25] which envisages a one step addition of hydrogen to adsorbed olefin or the mechanism of Jenkins and Rideal[26] which involves a reaction of gas phase or weakly adsorbed olefin with dissociatively chemisorbed hydrogen. Although it is now generally accepted that the main route for olefin hydrogenation requires the intermediacy of mono-adsorbed alkane, some contribution of a one-step addition mechanism is not denied[27,28] and in fact some evidence for its operation has been claimed[27]. Direct formation of α,β - diadsorbed alkane has also been proposed by Gault and Kemball[7] in order to explain the large maximum at d_2 found in n-pentane and n-hexane exchange on Rh.

Species of the α,α - diadsorbed type do not seem to play a predominant role in low temperature exchange even on Rh, except perhaps as an intermediate for α,α - turnover, but may become important at higher temperatures as indicated by the maxima found at products containing an even number of deuterium atoms in cyclopentane exchange on Pt[29], Pt-Au[29], Pd[30], Pd-Au[30] and Pd - Sn[30] films and also in propane exchange over sintered Ni films[31]. Examination of these high temperature exchange reactions using deuterium - n.m.r. spectroscopy should be rewarding.

6.5 - CONCLUSIONS

Mixtures of isotopic cyclopentanes were prepared by reaction of the unexchanged hydrocarbon with deuterium over several metal catalysts and were examined using deuterium - n.m.r. spectroscopy. Peak maxima in the n.m.r. spectra were interpreted in terms of isotopic shift contributions dependent on the position of substitution of a deuterium nucleus relative to the resonating nucleus. The following isotopic shift contributions were derived from a set of five well-defined resonances: α = -18 p.p.b.; β_C = -7 p.p.b; β_T = -8 p.p.b.; β_C =-2p.p.b. ; γ_T = 0 p.p.b.. Comparison of computer calculated with experimental spectra showed that the agreement between calculated and observed isotopic shifts was generally better when using a slightly different set of shift contributions, namely: α = -18 p.p.b.; β_C = -6 p.p.b. ; β_T = -9 p.p.b.; γ_C = -3 p.p.b.. The small differences between the two sets of values probably arise from a lack of strict applicability of the additivity rule used in deriving the shift contributions but both are in line with expectations as shown by a comparison with literature data.

Spectra of equilibrated samples were more complex than those obtained from the kinetic experiment due to the greater range of possible products in the former case. Nevertheless, both the positions and the areas of the peaks in the line-narrowed spectra of equilibrated samples could be satisfactorily reproduced assuming a simplified set of contributions which takes into account only α - and β - substitution ignoring differences between cis - and trans - contributions (α = -17.6 p.p.b.; β = -8.8 p.p.b).

The spectra from samples obtained from the kinetic experiments broadly conformed to those expected if only products arising from α,β - exchange were present in the mixtures. In particular, no predominant contribution of cyclopentane - 1,1 - d_2 was found in the n.m.r., spectra

obtained from the experiments performed on Rh/TiO_2 although the corresponding mass-spectral product distributions contained an important d_2 component. It is believed that a substantial portion of this d_2 component arises from a process whereby abstraction or addition of two "hydrogen" atoms occurs in one step, possibly a Rideal type mechanism involving adsorbed cyclopentene (α,β - diadsorbed cyclopentane) and gas phase or molecularly adsorbed hydrogen.

6.6 - REFERENCES

1 - B.J. Millard, D.F. Shaw, J. Chem. Soc. B, 1966, - , 664.

2 - H.M. Grubb, S. Meyerson, in Mass Spectrometry of Organic Ions, F.W. McLafferty ed., Academic Press, 1963, p. 453.

3 - T. Kondo, S. Saito, K. Tamaru, J. Am. Chem. Soc., 1974, 96, 6857.

4 - C.S. John, J.G. Williamson, L.V. F. Kennedy, J. K. Tyler, J. C. S. Faraday Trans. I, 1980, 76, 1356.

5 - S. Walker, in Spectroscopy, B.P. Straughan, S.Walker eds., Chapman and Hall, London, 1976, V. 2, p. 76.

6 - R. Brown, C. Kemball, D. Taylor, J. Chem. Research, 1982, - , (S) 232;(M) 2329.

7 - F.G. Gault, C. Kemball, Trans. Faraday Soc., 1961, 57, 1781.

8 - H. A. Quinn, J. H. Graham, M.A.McKervey, J.J. Rooney, J. Catalysis, 1972, 20, 326.

9 - A. C. Faro, Jr.,C. Kemball, R. Brown, I.H. Sadler, J. Chem. Research, 1982, -, (S) 342; (M) 3732.

10 - D. Garden, M. Phil. Thesis, Edinburgh, 1981.

11 - I.H.B. Haining, C. Kemball, G.L.Haller, J. Chem. Soc. Faraday Trans. I, 1981, 77, 2519.

12 - C.S.John, C. Kemball, E.A. Pearce, J. Chem. Res., 1979, -, 4830.

13 - C. Kemball, Adv. Catalysts, 1959, 11, 223

14 - V.R. Haddon, L. M. Jackman, Org. Magn. Res., 1973, 5, 333.

15 - J.B. Lambert, L.G. Greifenstein, J.Am. Chem. Soc., 1974, 86, 5120.

16 - T.C. Farrar, E.D. Becker, Pulse and Fourier Transform NMR, Academic Press, N.York, 1971, p. 29.

17 - Th. Leipert, P. Diehl, Helv. Chim. Acta, 1964, 47, 545.

18 - J.D. Halliday, P.E. Bindner, Can. J. Chem., 1976, 54, 3775.

19 - H. Batiz - Hernandez, R.A. Bernheim, in Progress in N.M.R. Spectroscopy, J. W. Emsley, J. Fecney, L.H. Sutcliffe eds., v.3, Pergamon Press, London, 1967, p.93.

21 - M. Barfield, J. Am. Chem. Soc., 1971, 93, 1066.

22 - V. Ponec, W.M.H. Sachtler, J. Catalysis, 1972, 24, 250.

23 - K. Schrage, R.L. Burwell, Jr., J. Am. Chem. Soc., 1966, 88, 4549.

24 - C. Kemball, Proc. Roy. Soc. A, 1953, 217, 376.

25 - A. Farkas, L. Farkas, Trans. Faraday Soc., 1939, 35, 917.

26 - G.I. Jenkins, E. K. Rideal, J. Chem. Soc., 1955, -, 2490.

27 - G.C. Bond, Trans. Faraday Soc., 1956, 52, 1235.

28 - G.C. Bond, P.B. Wells, Adv. Catalysis, 1964, 15, 91.

29 - R.P. Dessing, V. Ponec, J. Catalysis, 1976, 44, 494.

30 - J.K.A. Clarke, J. F. Taylor, J. Chem. Soc. Faraday Trans. I, 1976, 72, 917.

31 - J.R. Anderson, R.J. MacDonald, J. Catalysis, 1969, 13, 345.